

Building energy modelling to support the commissioning of holistic data centre operation

Citation for published version (APA):

Zavrel, V. (2018). *Building energy modelling to support the commissioning of holistic data centre operation*. [Phd Thesis 1 (Research TU/e / Graduation TU/e), Built Environment]. Technische Universiteit Eindhoven.

Document status and date:

Published: 16/05/2018

Document Version:

Publisher's PDF, also known as Version of Record (includes final page, issue and volume numbers)

Please check the document version of this publication:

- A submitted manuscript is the version of the article upon submission and before peer-review. There can be important differences between the submitted version and the official published version of record. People interested in the research are advised to contact the author for the final version of the publication, or visit the DOI to the publisher's website.
- The final author version and the galley proof are versions of the publication after peer review.
- The final published version features the final layout of the paper including the volume, issue and page numbers.

[Link to publication](#)

General rights

Copyright and moral rights for the publications made accessible in the public portal are retained by the authors and/or other copyright owners and it is a condition of accessing publications that users recognise and abide by the legal requirements associated with these rights.

- Users may download and print one copy of any publication from the public portal for the purpose of private study or research.
- You may not further distribute the material or use it for any profit-making activity or commercial gain
- You may freely distribute the URL identifying the publication in the public portal.

If the publication is distributed under the terms of Article 25fa of the Dutch Copyright Act, indicated by the "Taverne" license above, please follow below link for the End User Agreement:

www.tue.nl/taverne

Take down policy

If you believe that this document breaches copyright please contact us at:

openaccess@tue.nl

providing details and we will investigate your claim.



**Building energy modelling to
support the commissioning of
holistic data centre operation**

Vojtěch Zavřel

/ Department of the Built Environment

bouwstenen

243

Building energy modelling to support the commissioning of holistic data centre operation

PROEFSCHRIFT

ter verkrijging van de graad van doctor aan de Technische Universiteit Eindhoven,
op gezag van de rector magnificus prof.dr.ir. F.Baaijens, voor een commissie
aangewezen door het College voor Promoties, in het openbaar te verdedigen op
woensdag 16 mei om 13:30 uur

door

Vojtěch Zavřel

geboren te Praag, Tsjechische Republiek

Dit proefschrift is goedgekeurd door de promotoren en de samenstelling van de promotiecommissie is als volgt:

voorzitter: prof. ir. E. S. M. Nelissen

1^e promotor: prof. dr. ir. J. L. M. Hensen

copromotor: dr. J. D. Bynum (WSP USA)

leden: prof. dr. ing. D. Pesch (Cork Institute of Technology)

prof. dr. ing. D. Müller (RWTH Aachen)

prof. ir. W. Zeiler

prof. dr. ir. B. de Vries

dr. ing. J. Salom (Catalonia Institute for Energy Research)

**Building energy modelling to support the commissioning
of holistic data centre operation**

This research has received funding from the European Union's Seventh Framework Programme for research, technological development and demonstration under grant agreement no. 608826.



© Vojtěch Zavřel, 2018

All rights reserved. No part of this publication may be reproduced, distributed, or transmitted in any form or by any means, including photocopying, recording, or other electronic or mechanical methods, without the prior written permission of the author.

A catalogue record is available from the Eindhoven University of Technology Library

ISBN: 978-90-386-4463-9

NUR: 955

Published under Bouwstenen series 243 of the Department of the Built Environment, Eindhoven University of Technology.

Printed by TU/e Printservice, The Netherlands

Preface and acknowledgements

It feels like it was yesterday when I first looked at the Vertigo building with the huge logo of Eindhoven University of Technology on the top. As it was my first day, I felt a bit frightened about the four-year journey of my PhD. At that time, I was leaving my beloved girlfriend Zuzka, my family and friends. They knew that this was a unique opportunity that I must accept. They offered me constant support and gave me the strength to take the first step, even though I felt I was in a dense fog of self-doubt that prevented me from seeing the end of the journey.

Today, standing at the same place and looking to the 6th floor of this building, where I was sitting for the last four years, I realize that I am at the end of this journey and that I now trust in myself much more than before. In last four years, I experienced a transition from an engineering way of thinking “If it is not broken don’t fix it” to a research way of thinking “how do we know that it is not broken?” “If it’s not, is there chance to make it better?”. This approach sounded to me overcomplicated, but as the wisdom of our grandmothers state, the apples on top of the tree are always tastier than those we can reach from the ground. The only question is how to reach them.

Indeed, the expression “research” implies to search again and again, to be curious, to learn from previous mistakes and to gain some knowledge from them. However, the pursuit of knowledge is likely infinite, and this is the great pitfall for any researcher. Everything in our universe can always be studied at deeper abstraction, wider scale or over a longer timeframe. Therefore, as Jan Hensen taught us, we should always keep in mind the purpose of our research and define the boundaries of research accordingly. Otherwise, the fascinating iterative process of researching may be endless. Albert Einstein perfectly

addressed this pitfall in one short sentence and his quote become a mantra that I follow in my life:

“Everything should be made as simple as possible, but not simpler”

(Albert Einstein)

I would like to thank Jan Hensen for giving me the opportunity to start this PhD journey in his research group. Jan always motivated me and encourage me to think outside of the box and to see my research from different perspectives. He offered inspiring and constructive comments, which ensured that I remained on the right track.

I am also grateful to Martin Bartak for the trust that he placed in me. Without his recommendation I would likely never have started this journey.

I would also never have finished my work without the great support and patience of all my advisors and tutors. Thanks to John Bynum for all his patience in the first year of my study. He prepared me well for the following years. Thanks to Ignacio Torrens for his great advices and hard work in the Genic project. He never let me down, even in situations that appeared hopeless. Thanks to Duncan Harkness for his advice on academic style. He helped me greatly to chew through each chapter of this thesis.

In addition, results in this thesis were gathered in collaboration with a number of industry and academia partners within the Genic project. I am thankful to our partners: Atos for providing the integration framework; IBM Research for providing the workload generator and prediction modules; United Technologies Research Centre for providing the thermal management module; University College Cork (UCC) for providing the workload allocation algorithm; Cork Institute of Technology (CIT) for providing project coordination, the demonstration data centre and the integration framework; Acciona for providing the lab of renewable energy sources and the power

management module. I would especially like to thank Dirk Pesch, Thomas Scherer, Piotr Sobonski, Deepak Mehta, Diarmuid Grimes, Enric Pages Montanera, Tomás Fernandez Buckley and Luis de Juan Muñoz

I met tens of great people from places all around the world. They made a great working and living environment. They made me feel almost like at home in Eindhoven. I will miss all of the people who passed our corner of the 6th floor. Thanks to Rajesh, Christos, Roel, Isabela, Sanket, Hemshika, Luyi, Marie, Adam, Peter, Rebeca, Sai, Raul, Olga, Katarina, Zahra, Parisa, Antia, Christina, Sam, Dmitry, Tomaz, Massimo and many others. Let's meet some other Friday and enjoy the Bitterbalen taste again. I am also happy that I met all of the funny people from the Chill-Con-Comedy improvisation theatre and ChalOyna band. I cannot imagine how better to spend my leisure time here. I also never forgot old friendships from my homeland. I am grateful for my friends Šléša, Léňa, Skačer, Pokša, Křupka, Vogy, Michal (aka Meny), Jiří and Tom, who visited me often.

Now It is time to turn away, walk across the small bridge over the Dommel river heading out of the campus and leave the huge logo of Eindhoven university of technology behind.

I know where my roots are.

Thanks to my family, thanks to my mum Marcelka, dad Ludvik, little sis Verča and big bro Ondra. Thanks to my parents-in-law Růženka and Honza. thanks to you all for your unending support.

I know where my heart belongs.

Special thanks to Zuzka for all her love. Four years are over. I am coming home.

Nice memories and great friendship stay in Eindhoven

Vojtěch Zavřel

Summary

As an area of research, Building Energy Simulation (BES) has developed greatly over the last 50 years. Originally, BES tools were developed for the analysis of energy use in residential and office buildings. However, after BES tools demonstrated the ability to solve multi-domain problems and perform system-level analysis, their range of applicability has been extended to other building types. This research demonstrates the applicability of BES for the analysis of energy use in data centres (DCs) and introduces a new application of BES tools as a testing environment for external control algorithms.

As the role and size of DCs has grown in recent years, their electricity consumption has become a key concern of both DC operators and researchers. The rapid innovation of information technologies (IT) and related digital infrastructure has led to an exponential growth in global DC electricity consumption, which is estimated at 1.7-2.2% of the total world electricity consumption, and this growth is expected to continue in the near future. The continuing growth of DC energy use calls for the development of advanced energy efficiency strategies to ensure sustainability in the DC sector.

DCs typically consist of three main management pillars: IT workload management, thermal management and power supply management. In order to arrive at what is called here “holistic” DC operation, this thesis works on simulation support for the development and commissioning of the proposed operational strategy. Here, the term holistic DC operation denotes the coordination of these management fields in conjunction with system-level optimization to ensure high-level objectives such as minimizing cost or CO₂ emissions through the integration of renewable energy sources. The main obstacle to these goals is the lack of testing possibilities due to the mission critical nature of the DC environment, where any possible downtime of DC services results in financial penalties and reputation loss. Thus, the complex

multi-domain character and the mission critical nature of the DC environment makes the development of holistic DC operation very challenging.

In contrast, DC energy modelling and dynamic computational experimentation represent a “safe” virtual testing environment for novel control strategies. Successful tests in such a safe environment can accelerate the process of implementing new operational strategies in physical DCs. A virtual testing environment using BES is a feasible method to indicate the potential of tested strategies. In this research, BES models are not directly involved in any optimization procedure. However, they are used as a “virtual building laboratory”, in this case a so-called “virtual DC environment”, which enables interactive testing of external control algorithms for a given DC specification.

The successful development and application of the virtual DC environment is one of the main achievements of this work. Also, a novel workflow of simulation-based testing is proposed to support the development of advanced control strategies. This workflow introduces simulation-based closed-loop testing, where the real operational processes are simulated by using interactive communication between the virtual DC environment and external control algorithms.

In order to mimic the real system, the virtual DC environment captures the characteristic dynamic energy behaviour of the DC infrastructure, including IT, DC space, cooling, power delivery and power supply systems. Capturing the full extent of the complex dynamic energy behaviour of the DC systems requires adopting a wide scope in the modelling of the DC while addressing multiple domains acting at multiple scales.

Such a simulation-based assessment provides exhaustive information regarding the testing of several multi-domain control algorithms and their combination. The results demonstrate the importance of detailed, multi-criteria evaluation, which aids better decision making during the development phase of holistic

control strategies, and furthermore supports the commissioning of the holistic control platform for real DCs.

However, such a BES application goes beyond typical building physics and services expertise. It requires a very broad knowledge of multiple systems and processes specific for the DCs. Moreover, the virtual DC environment is designed for the interactive testing of external control algorithms developed by external experts from several different domains. As such, the virtual DC environment is necessarily part of a wider simulation tool-chain within the framework of a multi-domain team. Accordingly, the collaboration of a multi-domain team is key for the successful application of a virtual DC environment, and ultimately also for the implementation of the holistic DC operational platform in real DCs. The current research secured the required multi-domain team by embedding itself in the framework of the Genic project, funded by the Framework Programme 7 of the European Commission.

In conclusion, the main advantages of employing a virtual DC environment are that it allows interactive closed-loop testing of multiple control algorithms from different domains at the same time, and it reduces the risk of failure during commissioning. The external partners particularly appreciated the repeatability of testing of the same boundary conditions by comparing different approaches, and the ability to reduce the time required to conduct comprehensive testing in comparison with real experimentation.

The first prototype of the virtual DC environment for the testing of external control algorithms represents a new use of BES. This research is unique in that the first prototype developed here was applied in all phases of the proposed workflow: from conceptual modelling, through executable model development, to a real-world application of an existing DC. The usability of the newly developed virtual DC environment was endorsed by a wide consortium of industrial and academic partners within the Genic project

Table of Contents

Preface and acknowledgements	I
Summary.....	V
Nomenclature	X
1 Introduction.....	1
1.1 Background and motivation.....	1
1.2 Problem statement and research objective.....	5
1.3 Research methodology.....	7
1.4 Thesis outline.....	10
2 Understanding the data centre environment.....	13
2.1 Environmental impact, business strategies and future trends.....	13
2.2 Data centre infrastructure overview	23
2.3 Holistic data centre operation.....	36
3 Definition of computational experimentation	51
3.1 Testing workflow to support commissioning of holistic data centre operation	53
3.2 Conceptual modelling of data centre environment to support commissioning of holistic operation.....	62
3.3 Concluding remarks.....	75
4 Development of the virtual data centre environment	77
4.1 Methods and tools for data centre energy modelling	77
4.2 Modelling of the data centre environment.....	81
4.3 Definition of boundary conditions	112

4.4	Integration of the virtual data centre environment	114
4.5	Concluding remarks	120
5	Validation and demonstration of the virtual data centre environment	121
5.1	Technical specification of the case-study	121
5.2	Measurement uncertainties in model validation and demonstration.....	130
5.3	Validation and demonstration studies	143
5.4	Concluding remarks	166
6	Execution of computational experimentation.....	171
6.1	Computational experiment definition.....	171
6.2	Computational experiment results	193
6.3	Concluding remarks	216
7	Conclusion and future work	223
7.1	Conclusion	223
7.2	Direction for future work	230
Appendix A: Candidates for monitoring and local control in the DC environment.....		
		233
Appendix B: Server arrangement in the real and simulation setup		
		238
Appendix C: Validation and demonstration of the DC space model.....		
		242
References		
		249
Curriculum vitae		
		263
List of publications		
		264

Nomenclature

Acronyms

AC	Air-conditioning
BES	Building Energy Simulation
CBPS	Computational Building Performance Simulation
CFD	Computational Fluid Dynamics
COP	Coefficient of Performance
CPU	Central Processing Unit
CRAC	Computer Room Air-conditioning
CRAH	Computer Room Air-handling
CV	Coefficient of the Variance
DC	Data Centre
DCIE	Data Centre Infrastructure Efficiency
DCIM	Data Centre Infrastructure Management
DX	Direct Expansion
HVAC	Heating, Ventilating, Air-conditioning
IoT	Internet of Things
IT	Information Technology
ITE	Information Technology Equipment
KPI	Key Performance Indicator
LAN	Local Area Network
OEF	On-site Energy Fraction
OEM	On-site Energy Matching
ORC	Organic Rankine Cycle
PDU	Power Delivery Unit
PSU	Power Supply Unit

PUE	Power Usage Efficiency
PV	Photovoltaic
RAM	Random Access Memory
RES	Renewable Energy Source
RMSE	Root Mean Square Error
SEMO	Single Electricity Market Operator
SHI	Supply Heat Index
SLA	Service Level Agreement
UPS	Uninterrupted Power Supply
VM	Virtual Machine
WSN	Wireless Sensor Network

Organizations

ACCIONA	Spanish conglomerate group dedicated to the development and management of infrastructure
ASHRAE	American Society of Heating, Refrigerating and Air-conditioning Engineers
ASHRAE TC9.9	ASHRAE Technical Committee 9.9
ATOS	European IT services Corporation
CIT	Cork Institute of Technology
IBM	International Business Machines Corporation
IEA	International Energy Agency
TU/e	Eindhoven University of Technology
UCC	University College Cork
UTRC	United Technologies Research Center

Symbols

Δp_{i-j}	pressure drop between nodes	(pa)
Δt_{CRAC-i}	temperature difference between air node and supply air	(°C)
Δt_{i-j}	temperature difference between air nodes	(°C)
ρ	density	(kg m ⁻³).
τ	time	(s)
C	empirical permeability constant	(m s ⁻¹ pa ⁻ⁿ).
$C_{eff,eq}$	effective thermal capacitance of IT equipment	(J K ⁻¹).
$C_{eff,i}$	effective thermal capacitance of air node	(J K ⁻¹).
$c_{p,air}$	specific thermal capacitance of air	(J kg ⁻¹ K ⁻¹).
$f_{n_{ctr}}()$	control function	(-)
m_i	mass of node	(kg)
m_{i-j}	mass flow between nodes	(kg s ⁻¹).
n	power law exponent	(-)
nr	number of samples	(-)
$P_{act,eq}$	actual power load of IT equipment	(W)
$P_{idle,eq}$	idle power load of IT equipment	(W)
$P_{max,eq}$	nominal (maximal) power load of IT equipment	(W)
$Q_{diss,eq}$	heat dissipated from IT equipment	(W)
$Q_{i,conv}$	convective heat flux from/to other zones	(W)
$Q_{i,cool}$	heat flux from/to cooling devices	(W)
$Q_{i,gain}$	internal heat gain	(W)
$Q_{i,LG}$	heat flux of long-wave radiation between surfaces	(W)
$Q_{i,trans}$	heat transfer from/to node through solid construction	(W)
$Q_{loss,eq}$	heat losses of IT equipment	(W)
R	gas constant for dry air	(J kg ⁻¹ K ⁻¹).

T	thermodynamic temperature of air node	(K)
t_{eq}	representative temperature of IT equipment	(°C)
t_{in}	inlet temperature	(°C)
t_{out}	outlet temperature	(°C)
V_{CRAC-i}	volumetric flow of CRAC unit	(m ³ s ⁻¹).
V_i	volume of node	(m ³)
$V_{i,j}$	volumetric flow between nodes	(m ³ s ⁻¹).
x_{ref}	reference signal	(-)
\bar{x}_{ref}	average of reference signal	(-)
x_{sim}	simulated signal	(-)

1 Introduction

1.1 Background and motivation

As an area of research, building energy simulation (BES) has developed greatly over the last 50 years. It now offers sophisticated computational engines capable of modelling building physics, indoor environment, building services and integrated building energy systems, including renewable systems. BES allows for the modelling of heat, air, moisture, light, electricity, pollutants or control signal flows within building systems. As such, BES can capture numerous aspects of the building's behaviour and address multi-disciplinary problems of building physics and services. In so doing, BES can allow the researcher to arrive at a comprehensive understanding of the design and operation of a particular building. This knowledge can reveal the consequences to the environment of operating the building and can improve the building's performance and reduce its energy demand.

A review of the literature shows that many powerful and reliable BES tools have been developed during the past decades and that they have played an important role in all project phases. Examples of the use of BES in various phases include energy planning and district energy concepts [1]–[3], early design of overall building properties [4]–[6], design of innovative building components [7]–[9] and also commissioning and operation of buildings [10]–[12].

Originally, BES tools were developed for residential and office buildings. However, since BES tools have demonstrated the ability to solve multi-domain problems and perform system-level analysis, their range of applicability has been extended to other building types. Leading examples of research in this area come from the Computational Building Performance Simulation research

group at the Technical university of Eindhoven. These examples include the application of BES tools for greenhouses [13] and warehouses [14].

This thesis is focused on the commissioning and operation project phases, and the building type of interest is the data centre (DC). As a building type, DCs can be understood as highly complex environments that play a critical role in the digital infrastructure. The complexity of the environment arises from the vast number of systems required to effectively manage the high-density electricity demand of the housed Information Technology (IT) equipment and associated heat dissipation. The criticality of these environments arises from the fact that if a DC fails, crucial information and services will be denied to the DCs customers. Therefore, since DCs can be understood to be of a mission critical nature, any denial of services represents a severe risk in the digital world in which we live. As such, DC operators face severe penalties when their service is interrupted. To ensure the desired functioning of each data centre environment, the cooperation of IT, cooling and power delivery domains is essential.

The rapid evolution of the digital infrastructure has led to exponential growth of global DC electricity consumption, which is estimated at 1.7-2.2% of the total world electricity consumption, and this growth is expected to continue in the near future [15]. The continuing growth of DC energy use calls for the development of advanced energy efficiency strategies to improve sustainability in the DC sector. The main obstacle to this development is the lack of testing possibilities due to the mission critical nature of the DC environment, where any possible downtime of DC services is related with financial penalties and reputation loss [16]. Thus, the multi-domain character and the mission critical nature of the DC environment makes the development of next generation DCs very challenging.

Alternatively, DC energy modelling and computational experimentation represent a “safe” virtual testing environment for novel control strategies. Successful tests in such a safe environment can accelerate the process of implementing new strategies in physical DCs. Virtual DC environments using BES are a feasible alternative to indicate the potential of tested strategies.

To further describe the current research, BES is used to create a simulation model for commissioning support of “holistic” DC operation. The rationale of “holistic” DC operation is based on optimal coordination and supervisory control of multi-domain DC processes at the system level. As an advanced strategy to achieve DC efficiency, the “holistic” operation requires extensive testing support. The virtual testing environment should capture the characteristic dynamic energy behaviour within the DC. It is important to note here that capturing the full extent of the complex dynamic energy behaviour requires a wide scope of research in which expertise of IT, cooling, power delivery and power supply must be incorporated.

It is also important to note that this simulation model will not be directly involved in any control or optimization procedure; however, it will be used as a “virtual building laboratory”. This general concept of computational experimentation has been widely applied in other research areas. The “virtual building laboratory” can support the development of individual building components as well as complex and multi-domain system-level strategies. A computational experimentation framework was designed on the basis of experience gained from mentioned research projects within the Computational Building Performance Simulation research group [13],[14]. These examples demonstrate the efficacy of computational experimentation for various cases.

The “virtual building laboratory” concept is particularly suitable for problems where real experimentation may not be feasible and conventional evaluations cannot be performed, as has been noted for DCs. The “virtual building

laboratory” in the present case is the so-called “virtual DC environment”, which enables simulation-based assessments of holistic operation strategies targeting IT workload, thermal and power supply managements. The main aims of the thesis are to develop a multi-domain model of the DC environment and to demonstrate the model’s usability.

Such a BES application goes beyond typical building physics and services expertise. It requires a very broad knowledge of multiple systems and processes specific for DCs. Moreover, the virtual DC environment, presented within this thesis, is designed for the testing of external control algorithms developed by experts from several different domains. As such, the virtual DC environment is necessarily part of a wider simulation tool-chain within the framework of a multi-domain team. Accordingly, the collaboration of a multi-domain team is key for the successful application of a virtual DC environment and ultimately also for the implementation of the holistic DC operational platform in real DCs.

The current research secured the required multi-domain team by embedding itself in the framework of the Genic project funded by the European Commission [17], [18]. The Genic consortium is a partnership of leading European industry experts in the area of IT systems and services, building energy and thermal control systems, construction, and operation of data centres, as well as university partners who specialise in the areas of embedded network and system design, building modelling and simulation and constraint optimisation. The partnership brings together a unique blend of expertise in embedded wireless building monitoring (IBM, CIT), building and thermal modelling and simulation (IBM, TU/e), building systems and control (UTRC-I), IT load modelling and optimisation (ATOS, IBM, UCC), building energy management (UTRC-I, Acciona), IT system integration (ATOS, IBM), management services (UTRC-I, CIT, ATOS), and renewable energy systems

(Acciona, UTRC-I). This research utilises a wide project background, which enables the joint efforts and expertise of the multi-domain team to be exploited. The development of the “virtual DC environment” was conducted in consultation with the relevant domain experts and simulation users[17].

As mentioned, the development of the virtual DC environment requires an understanding of the physical processes from several domains governing the DC. The modelling of such a complex system is a very challenging task. Indeed, the energy modeller requires a broad overview of DC systems and processes, besides energy modelling expertise. Nevertheless, the modeller does not necessarily have to be an expert in all of the simulated systems.

At this point, it should be underlined that the thesis is written from the perspective of the energy modeller and developer of the virtual DC environment, and not from the perspective of a DC systems specialist or a control algorithm developer. Whereas the DC system specialist brings deep knowledge of the given system, and the control algorithm specialist focuses on optimal control of the DC processes, the main roles of an energy modeller in the multi-domain team are (i) to provide conceptual advice regarding energy modelling of complex systems, (ii) to develop the testing environment using knowledge of BES and from consultation with experts from neighbouring fields and, (iii) designing and executing computational experiments including guidance for results analysis.

1.2 Problem statement and research objective

1.2.1 Problem statement

The fundamental premise of the wider Genic project is that the energy consuming equipment in data centres must be supplemented with sustainable energy generation and storage equipment and operated as a complete system to achieve an optimal energy and emissions outcome. This vision is centred on

the application of hierarchical adaptive supervisory control to operate all of the primary data centre components in an optimal and coordinated manner, thereby minimizing energy use.

The advanced “holistic” DC management, which will likely play an important role in interfacing DCs with modern city infrastructures, requires advanced development and commissioning support. Reliability is the top priority in the DC, which means opportunities for testing in the DC environment are extremely limited. Any development of the advanced DC management is locked in a “trap”, since due to the absolute priority of end-user satisfaction, the functionality of any novel approach must paradoxically be proven before its deployment with only minimum or no access to the real DC facility. The development of the “holistic” DC management requires a safe testing environment to execute comprehensive functionality testing at various levels of domain acting at multiple scales. Specifically, three main domains can be identified within the DC environment: data computing, thermal conditioning and DC powering acting across the following levels of scale: chip & server, rack, room, building & system and district & cloud.

1.2.2 Aims and objective

This thesis aims to develop a testing framework for the simulation-based assessment of “holistic” DC management. The objective of this research is to develop a multi-scale and multi-domain virtual DC environment enabling comprehensive and extensive testing of external control algorithms. Specifically, the thesis will include the development of dynamic control-oriented energy models to estimate and predict the server rack temperature distribution and the overall electrical and thermal performance of data centres across all primary system components. Then, energy management and control algorithms developed by external partners will be evaluated in a simulation environment before deployment and validation at the test sites. The primary

goal is to assess the feasibility and effectiveness of the control algorithms in improving the overall efficiency of the data centre and to determine the energy saving potential expressed in terms of environmental impact and power usage effectiveness.

The novel contribution of this research is seen in the development of a multi-domain “holistic” modelling approach for the data centre building type of where a large modelling scope was required. Another area where the current research aims to advance beyond the-state-of-the-art is the new application of BES tools as a testing environment for external control algorithms.

1.3 Research methodology

The research methodology follows the general hypothesis of the modelling and simulation process (see Figure 1-1), which is adapted from Sokolowski and Banks [19], and is further discussed in chapter 3.

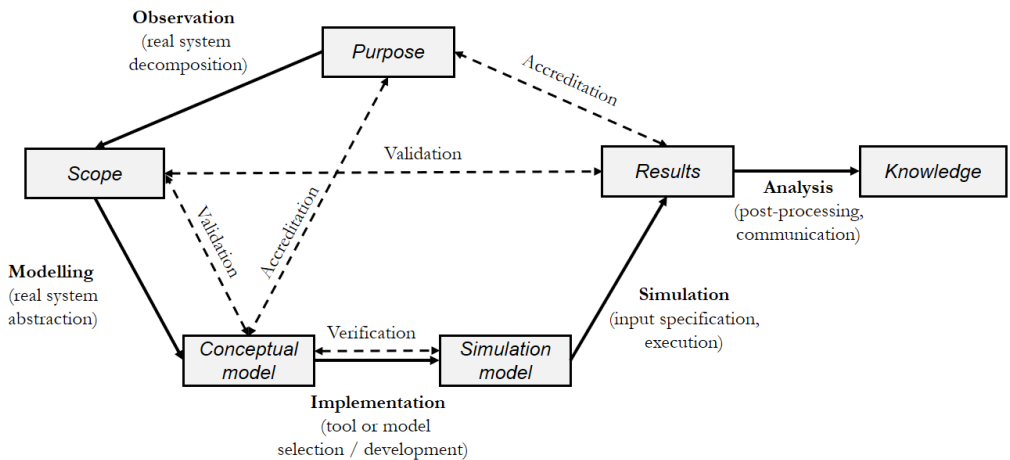


Figure 1-1 Modelling and simulation framework

The methodology is divided into individual blocks, which can be categorized as (i) purpose definition, (ii) computational experiment preparation, such as observation, abstraction and model development/selection, (iii) computational

experiment definition and (iv) execution and computational experiment evaluation. Each block contains several sub-tasks. This general framework can support various types of computational experiment. Below, each block of the methodology is identified for the specific aim of this thesis.

- (i) The purpose – the simulation-based assessment for commissioning of multi-domain “holistic” DC operation was defined based on a literature review and requirements of external control algorithm developers.
 - Firstly, the social influences, market types and research challenges are identified. The multi-disciplinary character of this work requires an understanding of various fields and systems as well as their control. This knowledge is obtained through a comprehensive literature review of relevant systems. The literature review is also necessary to later analyse the state-of-the-art of DC energy modelling approaches in order to transform the conceptual model into an executable model.
 - Secondly, the case-study used in this research is selected. The technical specification of the case study is collected in the framework of this methodology block. Based on technical specifications of a demonstration DC and Renewable Energy Source (RES) laboratory, the presented virtual DC environment is configured.
 - Last but not least, this methodology block provides a selection of the key performance indicators relevant for the purpose of this research.
- (ii) In the computational experiment preparation block the proposal of the testing procedure is established. The modelling scope is defined, and the conceptual model is developed and validated. The conceptual model is then implemented in the selected simulation environment. The process of implementation requires careful selection and development of simulation sub-models in order to satisfy all requirements of scope and levels of abstraction. The final product is the executable model of the virtual DC

environment, which can be integrated into the wider simulation tool-chain, enabling the testing of the external control algorithms.

- (iii) In the computational execution block, the first step is to specify the computational experiment (e.g. simulation inputs, requested outputs, simulation period, etc.). Once the computational experiment is fully specified, the computational experiments are executed.
- A first set of experiments must provide a validation of the proposed virtual DC environment. In order to assure the quality, the virtual DC environment is configured according to the given demonstration case-study and is simulated without any influence of the external algorithms. These results are compared against the available monitored data from the real DC system and eventually relevant standards to demonstrate the performance of the virtual DC environment. If the external algorithm developers are satisfied with the performance, the virtual DC environment can be used as a testing environment. Otherwise, the virtual DC environment needs to be calibrated or even redefined.
 - A second set of experiments incorporates the interaction of the virtual DC environment and external control algorithms. The virtual DC environment substitutes a real facility in the control-loop and thus supports the commissioning of the external algorithms. In order to enable interactive communication with these algorithms, the virtual DC environment is integrated into the wider simulation tool-chain
- (iv) The evaluation of the computational experiments consists of post-processing and analysis of results. Firstly, the computational experiment results are reported and endorsed (accredited) with the external partners (simulation users). Secondly, in addition to knowledge generated from the results, further knowledge was also derived from the novel application of

BES models within the Genic project, in which the initial prototype of the virtual DC environment was used in the multi-disciplinary pilot study.

1.4 Thesis outline

Chapter 1 describes the research background, motivation and aims

Chapter 2, provides an overview of the DC environment for readers unfamiliar with this topic. Since the thesis deals with a multi-disciplinary audience, the environmental impact, DC market and description of the overall DC system are important for understanding the holistic vision. This holistic vision is introduced both for the systems and for their control.

Chapter 3 proposes a new application of building energy models as a testing environment. This chapter introduces the concept of simulation-based closed-loop testing of the externally developed algorithms. Furthermore, conceptual modelling of the virtual DC environment, which enables the simulation-based closed-loop testing, is discussed here.

Chapter 4 deals with selected modelling approaches, required inputs for the model and also specifies the wider simulation tool chain. Special interest is paid to DC space modelling, since BES rarely supports this modelling at the required level of resolution (i.e. 1/3rd of rack). The multi-zonal airflow network method is proposed in order to capture the required resolution of the DC space modelling.

Chapter 5 deals with validation and demonstration of the virtual DC environment. The previously presented simulation models are configured based on a case-study conducted with a demonstration DC and RES laboratory. The model performance is validated and demonstrated using measured data from both sites of the case-study and from relevant standards. Again, since DC space modelling is a relatively new topic for BES research, the study emphasises the validation of the DC space model.

Chapter 6 demonstrates the usability of the virtual DC environment for the given application, where the virtual DC environment is used for the testing of externally developed algorithms. Thus, the virtual DC environment is under the influence of the tested external algorithms. The virtual DC environment is connected to the wider simulation tool-chain to enable the interactive communication with the external algorithms, where the simulated outputs are provided as “virtual monitoring”. While the tested multi-domain algorithms operate the virtual DC environment, the performance data, generated by the virtual DC environment, are collected. The recorded results from these experiments are analysed and discussed in this chapter.

Chapter 7 provides evaluation of the usability of the virtual DC environment, conclusions from the current research and recommendations for future research.

2 Understanding the data centre environment

Chapter 2 provides an overview of the data centre (DC) environment for readers unfamiliar with this topic. Since the thesis deals with a multi-disciplinary audience, the description of the overall DC system is important for understanding the holistic vision. The holistic vision is introduced both for the systems and for their control.

2.1 Environmental impact, business strategies and future trends

2.1.1 Data processing environmental impact

The rapid innovation of information and communication technologies has brought about a new digital era of information transfer. Within this new paradigm digital information is playing an increasingly important role in both the public and business domains. End-users of data centre services comprise a broad group of individuals, companies, universities and other educational institutions, research laboratories, banks, government installations, etc. [20, Ch. 1]. In fact, some business sectors can now be described as fully digitalized. This ongoing process of dematerialization and virtualization may ultimately lead to reductions in total global primary energy use [21]. A key facet of this digital revolution is the role of data centres, sometimes referred to as server farms, which enable the data processing necessary to run internet-based services. The importance of DCs has grown significantly in recent years with the emergence of cloud computing, which has enabled a wide range of new services for both individuals and businesses. As a result, DCs now routinely have to manage numerous services and deal with huge computational demands.

The electricity consumption related to data processing represents a significant share of global energy consumption. However, many users of digital services

have little understanding of the relation between energy consumption and using every-day services such as email, social networking, picture sharing, web applications or multi-media streaming. In other words, there is a general lack of understanding of the link between data processing and electricity consumption.

In fact, in 2015, global electricity consumption related to data processing, including the local computing of end-user devices, data transfer and remote computing in DCs, was estimated to be around 4% of the total world electricity consumption [22]. It is also estimated that more than half of this electricity consumption is accounted for by computing at the end-user side. The recent shift to cloud computing not only offers very convenient services for end-users, but also transfers the computing demand from end-user devices to DCs. Therefore, there is a real need for more efficient DCs, where the data can be processed in a professional and sustainable manner.

Currently, DC electricity consumption is estimated to represent between 1.7-2.2% of total world electricity consumption [15]. Although DC electricity consumption has grown exponentially over the last two decades, it has been stagnating in the last 5 years, partially due to the adoption of energy-efficiency measures on the DC side and partially due to slowing growth of client demand, which is largely related to the saturation of internet coverage in developed countries (Europe 79% and North America 74% coverage) [23]. In fact, there is a strong correlation between the internet host count and the growth of DC energy consumption, which can be observed in literature [15], [24].

Since worldwide internet coverage is still only around 47% [23], the continuing growth of data processing demand can be expected as internet coverage rises in developing countries. Moreover, an increasing number of user devices per person in developed countries and the expansion of the internet of things (IoT)

in the near future will require additional computing demand, which suggests that the environmental impact will likely grow further still.

2.1.2 Data centre business classification

DCs come in various sizes ranging from small server closets to small and mid-sized datacentres up to hyper-scale internet data centres providing services such as those of Google, Facebook or Amazon. The hyper-scale DC architecture has experienced recent growth in large part due to the rise of cloud computing, as is shown in Figure 2-1. However, as can be seen, although their use is decreasing, server closets and small-sized DCs, usually with lower energy efficiency than larger DCs, still account for a considerable share (around 25%) of the data processing market.

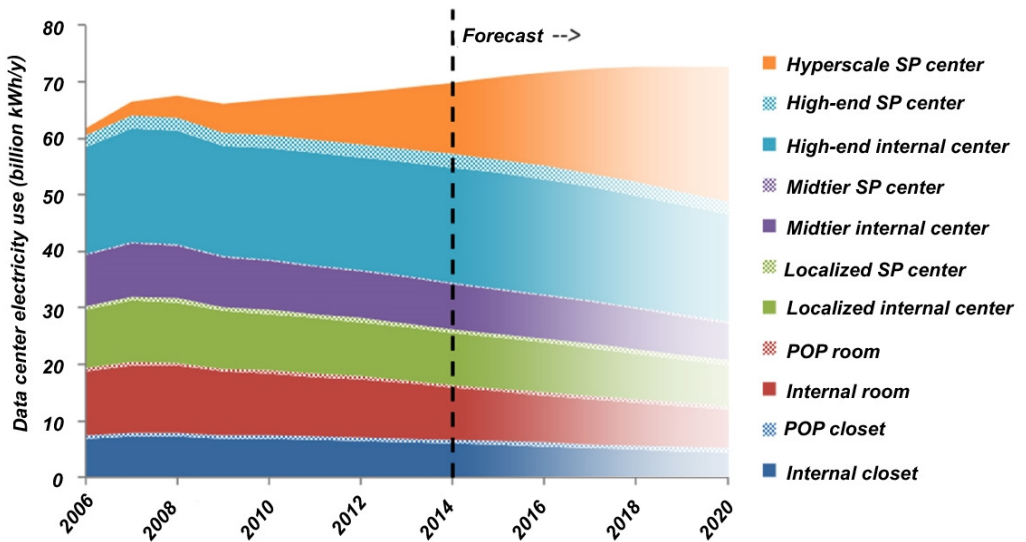


Figure 2-1 Total electricity consumption by space type adopted [15]

The size of DCs is also related to the main business models in the DC environment. These business strategies are briefly introduced because they may

influence the applicability of some technical solutions (e.g. cooling) mentioned in Section 2.3.

Three distinct business strategies or a combination of the three can be used to obtain data processing services:

- a) ownership of IT hardware and related infrastructure,
- b) colocation of IT hardware,
- c) multitenancy of IT hardware related with cloud computing,
- d) combination.

Three general actors can also be identified: the DC owner or operator, the provider of data processing services and the end-user. The role of each actor differs in each business strategy. Figure 2-2 depicts the relationship amongst these actors.

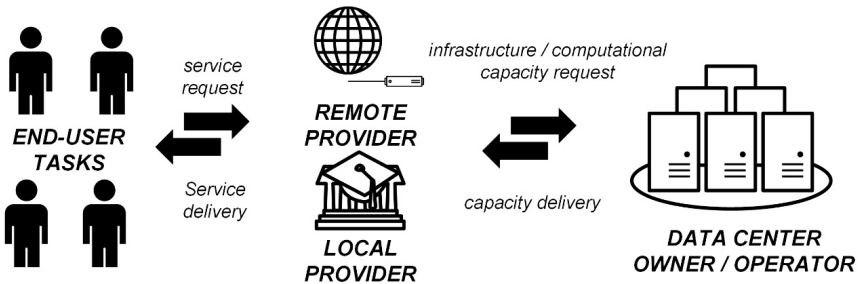


Figure 2-2 General actors in the data processing field

- a) **The ownership business strategy** includes IT hardware, software, network connections and other necessary facilities such as uninterrupted power supply, cooling, security and fire safety systems, etc. This business model is typically applicable for small server closets and server rooms providing non-critical data processing services, such as a shared company data repository. In this case, all three actors usually belong to one enterprise. This type of DC rarely reaches high levels of reliability and

energy efficiency due to the high investment required for DC infrastructure.

- b) **The colocation DC business strategy** is a type of DC strategy where uninterrupted power supply, cooling capacity, and network connections are provided by the DC owner or operator. The colocation business model is usually associated with mid and large size DCs and was widely used in the previous few decades. The DC owner or operator rents the physical space in racks to several data processing providers, which deliver their own Information Technology Equipment (ITE) with installed data processing services for end-users. This solution allows the spreading of the investment cost related to the reliability of the services among several enterprises, which makes high quality data processing affordable. The DC space is divided into smaller clusters with different owners, data processing services, and utilization of ITE. Each DC owner must consider the need to increase the amount of physical space and cooling capacity over the lifetime as their business grows. The easy and secure access to ITE and convenient manipulation of racks is an important aspect of running the colocation DC. Therefore, colocation DCs usually exploit air-based cooling, which allows this flexibility. The main drawback of colocation DCs is that their configuration usually limits the capability of modern IT management techniques, which are discussed in section 2.3. The ITE capacity needs to be able to manage peaks. This configuration leads to low computation productivity with an average utilization of ITE up to 20% [25], J. Glanz stated in the New York Times an even lower range of between 6 to 12% [26]. Therefore, this business model is on the decline due to the rise of cloud computing, which allows increased productivity of ITE. In addition, many colocated DCs began to struggle with physical space and lack of power and cooling capacity related to inefficient

utilization of IT resources and problems associated with the necessity of DCs to be located in urban areas. These problems accelerated the adoption of virtualization technologies, and together with the growth of network bandwidth, cloud computing has experienced a boom in the last 5 years [27].

- c) **The internet-based (cloud) DC business strategy** is a type of DC strategy that allows for the multi-tenancy of ITE. Multi-tenancy is essentially the sharing of IT capacity among several providers. The Internet-based DC is usually associated with mid, large and hyper-scale sized DCs. The basic cloud service is Infrastructure as a Service (IaaS). The DC owner or operator owns the entire DC infrastructure, including ITE, and offers virtualized IT machines in the form of computational capacity via the internet to the provider or directly to the end-users. Nowadays, DC operators have extended their services and they are able to provide the full infrastructure including OS platforms. The end-user or service provider can develop their own applications using an OS, programming languages, libraries and tools supported by the DC operator (Platform as a Service) or use some existing software applications (Software as a Service). This business model gives more freedom to the DC owners or operators in terms of data manipulation within the DC. It allows the full application of modern ITE management techniques such as ITE virtualization and workload consolidation, described further in section 2.3. Furthermore, the multitenancy of the ITE leads to a significant increase of ITE productivity. While the average utilization of an individual server may be between 20-40% in the co-located DCs, here the utilization of the server is significantly higher at around 60-80% of the nominal computational capacity [28]. The service provider or end-user directly rents computational resources but no longer requires access to the physical hardware. It may open opportunities

for wider application of technically complex solutions because providers no longer require access to individual hardware (e.g. liquid cooling solution).

As a concluding note, cloud computing and global internet coverage afford the end-user greater reach in terms of data processing services, even though the physical infrastructure is housed in remote areas in large scale DCs.

2.1.3 Current trends in data centre environments

In the recent past, the majority of DCs were small-scale and were located in-house in computer rooms or closets. Nowadays, however, it is common for businesses to outsource their data processing needs to computer warehouses, which are buildings containing all necessary facilities from several domains [29]. The traditional DC framework is being significantly extended in order to integrate the DC environment into modern cities and district infrastructures, while the IT management must follow the trend of rising cloud computing. Two key factors, modern IT management and sustainability goals and policies, are widening the scope of the DC environment, making it even more sophisticated and complicated. The extension of the traditional DC framework is depicted in Figure 2-3

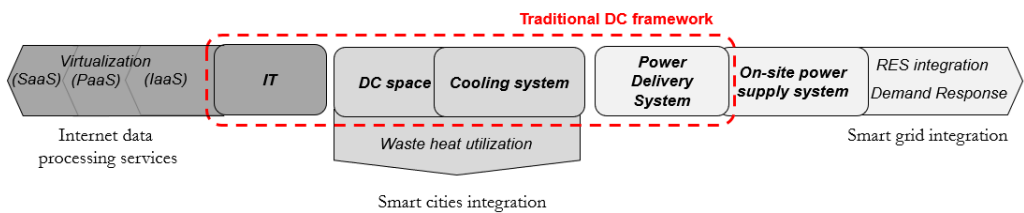


Figure 2-3 Trends in the three main data centre systems

The continued rise of “cloud computing”, and the wider application of advanced IT workload management such as virtualization techniques, offers better services for clients (service provider or directly end-user) and improves

the utilization of computational capacity. DC operators guarantee the computational capacity and offer their infrastructure for computation (Infrastructure as a service) or other additional services such as Platform as a Service (PaaS) or Software as a service (SaaS) [30].

The virtualization of IT equipment (ITE) driving cloud computation is also beneficial for DC operation. The predictive data allocation and workload consolidation may allow unnecessary servers to be turned off and idle power to be saved [31]. The easier and faster data manipulation via the internet may open the possibility of multi-data centre processing. The multi-data centre operation may migrate IT workload into regions with a higher ratio of renewable energy in the grid [32].

The whole process of data computing can also become more efficient and sustainable through the meaningful utilization of waste heat. Even though the DC can produce an enormous amount of heat, this heat is of low quality. In particular, the temperature potential of conventional air-based cooling systems is very low. The return air may be gathered in the range of 27 to 40°C. Despite the enormous amounts of heat dissipation generated in DCs, it is very difficult to deliver this heat to waste heat consumers. In fact, the low-quality heat makes utilization of waste a heat very challenging task [33].

The vision for future generation DCs relies on the higher integration of renewable energy sources (RES) in order to reduce the carbon footprint resulting from the electricity consumption of global data processing. Considering the high-density power demand and the high penalty costs associated with power outages, the integration of on-site RES systems will again be a very challenging process for the DC environment. Moreover, investment in RES power supply has not yet made business sense for regular DC operators [34]. Only leading companies like Google or Facebook could afford to invest in renewable energy, but it could be argued that this investment

is largely for the sake of corporate social responsibility and the resulting company image. At this point, the possible cost related with DC downtime is a much more pressing problem than reducing the cost of energy consumption because energy still plays a relatively minor role in the DC's operating expenses. Although the energy cost is continuously increasing, it is still a considerably lower expense than the upgrading of servers, server management, and administration costs, as shown in Figure 2-4.

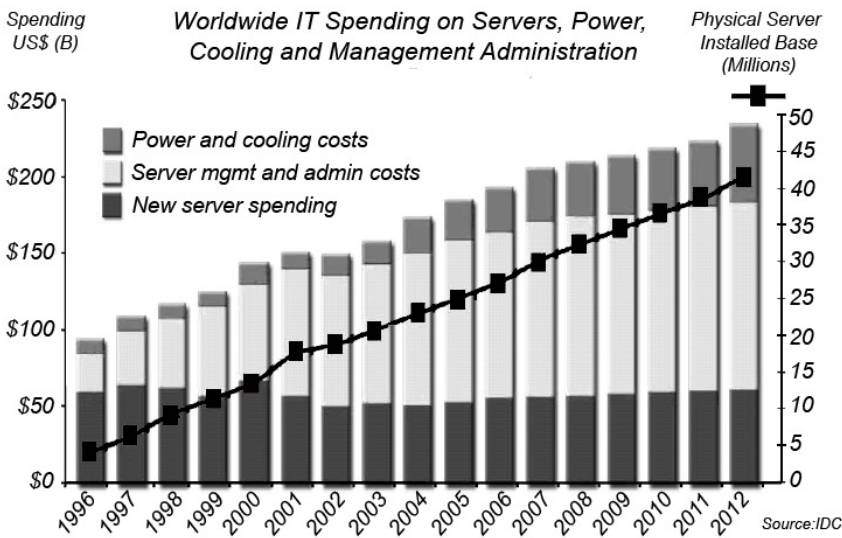


Figure 2-4 The worldwide IT spending on Server, Power, Cooling, and Management Administration adopted [27]

In the current situation, DC operators are poorly motivated to invest in renewable solutions. However, the situation may soon change because end-users are increasingly concerned with their own sustainability goals and policies. The computational price does not have to be the only criteria in market competition. Also, related CO2 emissions may play an important role in the business decision making. Therefore, there is a need to develop cost-

effective renewable energy supply, including storage management that can be safely integrated into DCs.

Another pressing challenge is to integrate the complex DC infrastructure into smart cities infrastructures while respecting all of the core DC's processes. The integration into the infrastructure of smart cities requires demand response from actors in the district heating networks and especially electrical grids. The DC infrastructure may have good potential for demand flexibility because it consists of large electrical uninterrupted power supply (UPS) storage, and often also thermal storage, and if a service level agreement (SLA) permits, the possibility of postponing or migrating non-urgent IT tasks to other DCs [35]. The coordination of workload management with thermal and power supply management is under-researched. The model-based operation may open the way toward multi-domain holistic cooperation and may build the necessary interface for smart city infrastructures in the future. At this stage, there are strategies such as thermal and power supply aware computation [36]–[38], which show promising potential in terms of facilitating coordination of DC processes. However, these strategies have only been tested in a very limited fashion in real DC facilities and their potential has not yet been proven. The main barrier is their need for extensive and comprehensive training, which conflicts with satisfying all of the reliability and availability requirements of DCs.

The first commercial data centre infrastructure management (DCIM) platforms have also been developed, which are mainly focused on visualization and business planning aspects [39]. However, system coordination and holistic energy management including RES are largely not addressed by commercial DCIM platforms. Moreover, the uptime institute survey for 2015 [25] reveals that the commissioning time of commercial DCIM platforms has been longer than 6 months in 74% of installed cases. Seemingly, there are several serious

obstacles prolonging their realization, such as the cost of advanced technologies or licenses, communication difficulties among several experts and a lack of testing potential at this level of complexity.

To conclude, next generation DCs require solutions which go beyond the component level. Indeed, there is a need for a holistic DC operational platform considering the system level optimization. However, testing and commissioning of any advanced control strategy or any novel design concept are often slowed down if not even discarded. This is generally due to a lack of access caused by the mission critical nature of the DC environment.

2.2 Data centre infrastructure overview

The primary functions of the data centre are computing, storing, routing or other manipulation of data. Specifically, the services hosted by DCs are web and mail services, multi-media streaming, social networking, high-performance computation, bank transfers, big data storing and other data processing. Nowadays, any activity on the internet is inherently related to data processing. The term “data processing services” is used further in the text as a general term for all of the aforementioned services provided for end-users.

In most cases, the service must be satisfied 24 hours a day, all throughout the year. Any violation of a SLA, such as denial or delay of the service, may lead to significant financial penalties and reputation loss for the DC owner or operator. Therefore, it is absolutely key to understand that reliability and availability of the data processing services are the most important aspects to consider because the downtime cost is very expensive. The issue is that the cost is not only related to failure detection, diagnostics, and repair. Actually, these are the minor expenses. The downtime cost is mainly related to business disruption, lost revenue and end-user productivity [16]. Therefore the requirements for a trouble-free data centre operation are very strict. [40, Ch. 14].

Table 2-1 Description of DC tier levels adopted [41]

tier level	requirements
1	<ul style="list-style-type: none"> • single non-redundant distribution path serving the ITE • non-redundant site infrastructure capacity components • basic site infrastructure with expected availability of 99.671%
2	<ul style="list-style-type: none"> • meets or exceeds all Tier 1 requirements • redundant site infrastructure capacity components with expected availability of 99.741%
3	<ul style="list-style-type: none"> • meets or exceeds all Tier 2 requirements • multiple independent distribution paths serving the ITE • all ITE must be dual-powered and fully compatible with the topology of a site's architecture • concurrently maintainable site infrastructure with expected availability of 99.982%
4	<ul style="list-style-type: none"> • meets or exceeds all Tier 3 requirements • all cooling equipment is independently dual-powered, including chillers and HVAC systems • fault-tolerant site infrastructure with electrical power storage and distribution facilities with expected availability of 99.995%

The Uptime Institute, a well-known advisory organization on improving the performance, efficiency and reliability of business critical infrastructure, defined a 4-tier level certification standard for DC reliability and availability [41]. According to this standard, DC services must be available between 99.671% - 99.995% per year with various levels of DC component redundancy depending on the tier level, which is briefly described in Table 2-1. To imagine 99.995% availability and the high requirements for the DC facility (tier 4), the DC down time cannot be longer than 26 minutes per year in order to satisfy the highest tier level. The reliability of the DC always has top priority and any novel solution must respect this.

In order to satisfy the high standards, the secondary function of the data centre is to ensure the reliability of the DC services and to satisfy the required operational conditions of the Information technology equipment (ITE) in terms of uninterrupted power delivery and required indoor environment secured by thermal conditioning of the DC space.

The primary data processing and the two secondary processes of thermal conditioning and data center powering are depicted in Figure 2-5. This figure also shows the source and product of each process and components related with these processes.

Monitoring and visualization of the aforementioned DC processes are crucial for effective management of the DC system. The following sections introduce the process in detail while possible candidates for monitoring categorized according to scale and domain/process are presented in Appendix A.

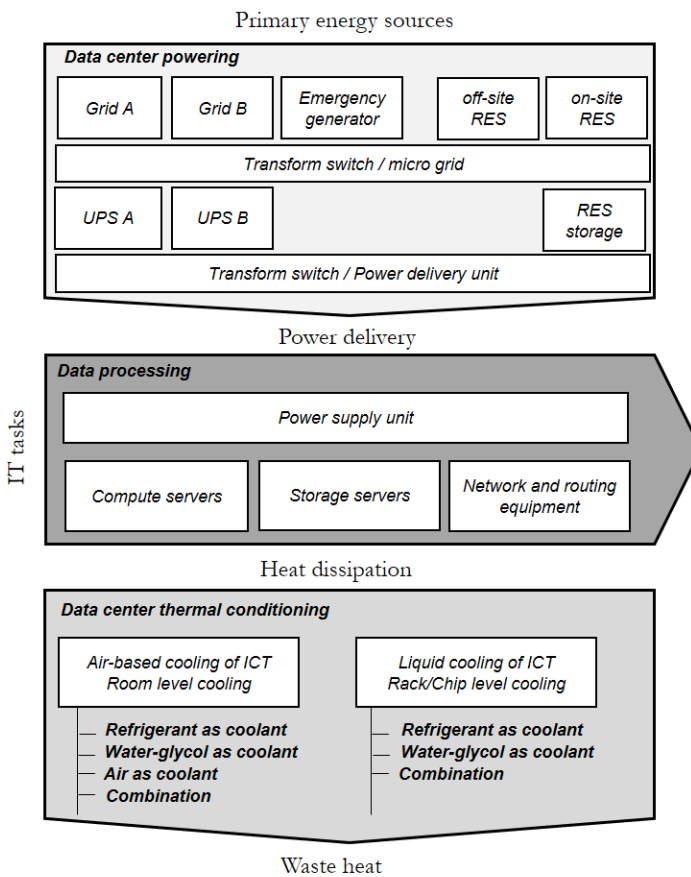


Figure 2-5 Key processes and related components within DC environments

2.2.1 Data processing and IT equipment characteristics

In general, it should be understood that the given chip technology and related ITE architecture may significantly influence the electrical energy performance of the server required for a single switch, and thus the overall efficiency of data processing [42]. The utilized processor usually consumes 30 to 40% of total server electricity demand. Thus, the CPU utilization can in most cases indicate the useful work done by the hardware.

Further, the non-utilized server consumes relatively high idle power for auxiliary server components (Fans, Memory etc.), which may account for 20 to 60% of total server electricity demand [43]. To reiterate, average ITE utilization using conventional ITE workload management is only around 6 to 12% [26]. In other words, much of the time, the servers consume idle energy while waiting for a peak. The server architectures and their innovation are a separate discipline requiring deep knowledge of electronics and computer engineering, and therefore the chip scale is out of the scope of this thesis. Since this research aims to achieve global DC energy management, the characterization of ITE described in this section is understood as a given design aspect.

As energy engineers, our interest usually starts at the server or rack scale. The ITE is stored in cabinets or racks with standardized sizes [44], [45]. From a physics perspective, 99,9% of the electric energy consumed by the server, which is required for the computing - changing low voltage states at chip level - is dissipated as heat [46, Ch. 2].

The ITE can be categorized as classes according their function as (high-) computing servers, storage servers and network equipment. The computational performance and related heat dissipation vary significantly with respect to server configuration, manufacturer or year of release. An example of the performance variance for enterprise servers is shown in Figure 2-6. The idle power and the standby power levels are also shown in this figure.

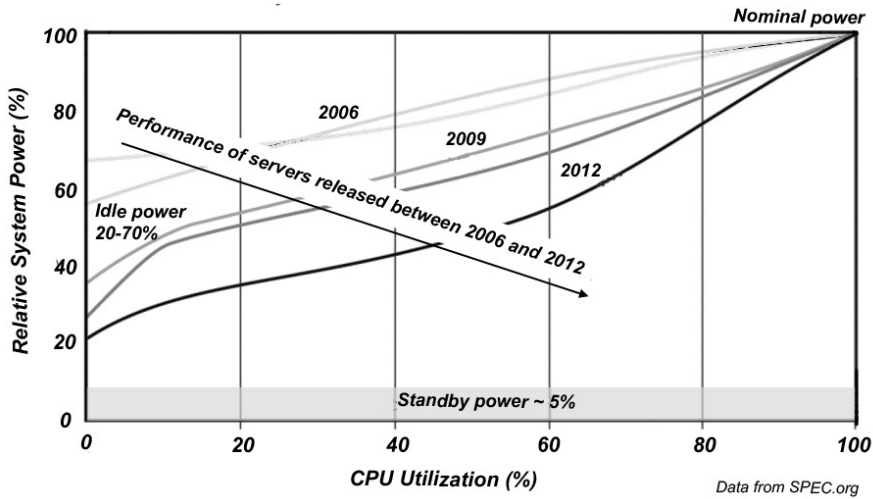


Figure 2-6 The compute servers' variance with respect to year of release adopted [43]

Since the focus of this thesis is on the commissioning and operation phase, the DC space arrangement is considered as a given design aspect in this study. The performance levels represented by nominal power density per DC floor area are listed here in order to understand the range of performance levels and related heat dissipation. Nowadays, computing servers may dissipate between 0.9 to 5 kW per m² of floor area (up to 10kW per rack), while storage servers dissipate about 0.3 to 0.4 kW per m² of floor area [47]. The dissipation of network and routing equipment may be neglected because of its very low power density.

2.2.2 Data centre thermal conditioning

Over the last decades, the computing efficiency of ITE has significantly increased, which correlates to respective increases in the power density per floor area and related heat dissipation in DCs. As mentioned above, the heat dissipation to the DC space is 10kW per rack on average. However, in the high-populated racks, it may even reach up to 40kW per rack [48]. This enormous

non-uniform heat gain must be removed from the DC space by a cooling system in order to ensure the required ITE operational conditions.

Traditionally, the ITE has been cooled down by air, which is usually conditioned for the whole DC room. The air-based solution is popular especially since it allows easy access to and physical manipulation of racks, in which the hardware is situated. However, air as a cooling medium has physical limitations and may not be sufficient for cooling of the high-performance electronics that are expected in the near future. The trend towards higher computational efficiency has led to the recent rise of liquid-based cooling of the ITE or even of individual electronics [50]

Liquid based cooling offers higher heat removal efficiency due to better physical properties of the coolant entering each rack, server or even chip. As a coolant, a water glycol mix, refrigerant or oil may be used. Liquid-based cooling has been mainly used in research until now due to its technical complexity. Nevertheless, its application can already be seen in a limited number of industry experiments and demonstration sites [49]

Although liquid-based cooling may have good potential in the future for use with high-performance electronics, its usability is currently limited only to specific types of data processing services. In the current situation, the market is still dominated by air-based cooling, which is sufficient for most of the current needs. Liquid-based cooling covers only 11% of the market [51]. Therefore, this thesis is focused only on the more common air-based cooling configuration.

Air-based cooling configuration

ASHRAE TC9.9 [47] introduces allowable operational conditions for standardized classes A1-A4 for volume and storage servers in tightly controlled environments, class B for office and home environments and class C for a factory environment. Allowable operational conditions are conditions declared

by ITE manufacturers. This is not a statement of reliability range, but a testing range of performance by ITE manufacturers prior to the official ITE release. Therefore, TC 9.9 specifies recommended environmental ranges to ensure the reliable environmental conditions valid for classes A1-A4. The recommended environmental range is similar to the allowable range defined by intake dry-bulb air temperature, humidity or maximum dew point or maximum temperature rate of change. The recommended environmental ranges to note here are the dry-bulb temperature range of 18 to 27 °C, and relative humidity range of 30% to 60% [47]. The typical air-based cooling configuration contains: DC space air distribution, computer room air-conditioning (CRAC) unit, heat rejection circuit, and roof mounted chiller or dry-cooler. The typical cooling configuration is shown in Figure 2-7

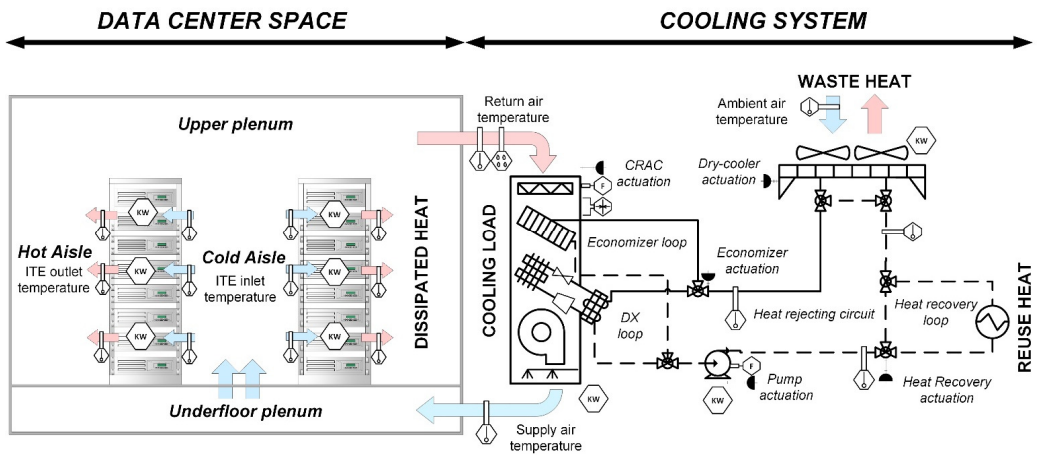


Figure 2-7 Typical air-based system configuration including monitoring candidates and actuation spots

Air distribution in the DC space has been extensively studied in the last few years using measurements or high-resolution simulation [52]. The key finding is that it is beneficial to zone the DC space into a cold and hot aisle arrangement. The conditioned supply air is delivered to the cold aisle. The most

common configuration is air distribution under an elevated floor with perforated tiles, which is called under floor air distribution. However, various configurations of DC spaces can be found (e.g. overhead air distribution) which all follow the cold and hot aisle arrangement [20, Ch. 1]. The conditioned air is taken from cold aisle zones by the internal fans of the ITE in order to cool down internal electronics. The used warm air is rejected to the hot aisle and returned to the CRAC unit, usually via an overhead plenum.

Since ITE deployment is heterogeneous and supply air distribution is rarely controlled, there is a risk of used air recirculation and of the so-called supply air bypass phenomena. The recirculation of used air causes dangerous local hot spots when the cold aisle temperature rises locally due to infiltration of the warm air from the hot aisle. A less dangerous bypass is achieved when supply air does not enter the ITE and it is mixed with return air. However, this decreases the return air temperature to the CRAC unit and thus reduces the cooling efficiency. Both of these phenomena have a negative effect on the efficiency of DC cooling. This problem can be solved by design-related solutions, such as building a physical barrier between the aisles, known as cold and hot aisle containment [53]. In the operation phase, the hot spots can be eliminated by so-called thermal-aware computing, described in section 2.3.

Moving from the room scale to the building & system scale of the cooling process, there are many system variants for rejecting the waste heat to the outdoor environment. Basically, The CRAC recirculates and adjusts the indoor air in the DC space. The heat from the DC space is removed via several heat exchangers in the heat rejecting circuit before it is rejected to the ambient environment. The heat is transferred to the coolant distribution system and is rejected by an external dry-cooler or chiller.

The air-based cooling system can be further divided according to the coolant used in the heat rejection circuit

- refrigerant cooling system (mechanical cooling)
- water-glycol cooling system
- air handling cooling system
- combined (air-side or water-side economizer)

Economizer function

The function of an economizer is to bypass the costly and energy-hungry operation of the compressor unit (refrigerant circuit) in periods when the outside temperature is below the required supply temperature and therefore the outside temperature can be directly used for cooling. The economizer utilization hours differ according to climate and type of economizer. A review of economizer system typologies can be found in literature [54]

The water-side economizer is implemented in the heat rejection circuit, which consists of the combined refrigerant and water-glycol distribution system. The CRAC unit usually accommodates a second cooling coil for air. When possible, it is desirable to exploit air-to-water cooling, as it is more economical than the alternative air to-refrigerant cooling. The economizer piping bypasses the refrigerant unit and is connected to the rest of the rejection circuit. Then, the heat is released in a cooling tower or drycooler to the ambient environment. The series of heat exchanges limits the applicable range of outside temperature. Typically, the water side economizer is actuated by an outside temperature below 13°C [40] and operational hours depend on climate conditions. The advantages of such a system are (i) easy implementation in the conventional refrigeration system, (ii) no direct influence of outside conditions, and (iii) relatively small size of piping and distribution system elements in comparison with an air-side economizer.

An air-side economizer bypasses the entire heat rejection circuit and directly supplies the unconditioned outside air via a computer room air handling unit (CRAH). Since the air is directly injected from the ambient environment without any additional exchange, the applicable range of outside temperature is below 20°C [40]. This range allows more operational hours of the air-side economizer in comparison with the water-side economizer. For colder climates, the economizer can totally bypass the refrigeration unit throughout the year. Therefore, the air-side economizer can significantly reduce the cooling system consumption up to 90% compared to conventional systems using refrigeration [55]. However, it should be noted that with the use of outside air, strict control of temperature, humidity levels and pollution particles is necessary to avoid their infiltration into the DC space. This solution is also rarely applicable for a DC placed within the wider building complex because the enormous duct size of the air distribution system, which is required to cover the high cooling load, is difficult to implement.

Generally, the current trend for air-based cooling of ITE is to design non-mechanical cooling of DCs to maximize the operational hours of economizers if given climatic conditions permit. Mechanical cooling is still installed as back-up cooling, or the DC operator may allow the indoor temperature to exceed the recommended temperature range and operate in the allowable range for a short period of time. In order to utilize non-mechanical cooling even for southern climatic zones, the fluctuating external air is not sufficient as a heat sink. The ideal source should be stable over the year with a temperature below the lower bound of the recommended range (i.e., 13°C and 20°C for water-side and air-side economizers, respectively). For instance, water or ground sources can be used instead of external air.

2.2.3 Data centre powering

An UPS is required for all mission critical equipment in the DC. To ensure reliable powering, many DCs are connected to two separate grid sectors in order to minimize the risk of a power outage. Moreover, the power supply is usually backed up by electric energy storage (i.e. battery arrays) to overcome shorter periods of power outage from the grid. Larger DC systems may be equipped with an on-site power plant, usually diesel generators, to overcome a longer period of outage from the grid.

In this thesis, the power system is divided into two sub-systems: power delivery and power supply systems. Examples of typical power lines can be found in the literature [57] and are shown in Figure 2-8.

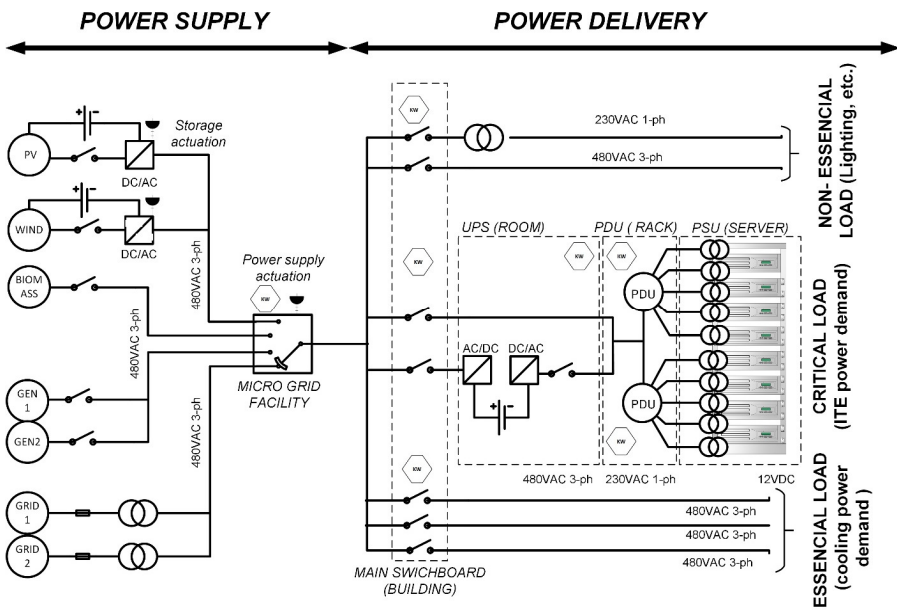


Figure 2-8 The typical power line scheme adapted [57]

The power delivery system is defined as all devices required to transform the electric energy from the main DC switchboard to individual electronics, cooling devices etc. The power delivery system includes all devices handling

quality of power, such as transformers, inverters, etc. The related losses of the power delivery system are always accounted for as DC energy demand in the DC energy balance. The power supply system is defined as all components supplying power for the data centre, which may consist of any combination of grid supply, off and on-site RES systems owned by the data centre operator or owner, emergency diesel generators, etc. The power supply is accounted for as DC energy production in the DC energy balance.

As a side note, the role of some components (e.g. electric energy storage or grid) may be changed from the perspective of the DC energy balance. For instance, the idle UPS battery array and related power loss can be counted as part of the power delivery system. However, in emergency situations the UPS battery array acts as part of the power supply system. Similar changes relating to the grid may apply when the on-site RES system delivers a surplus. In this case, the energy flux is reversed, and energy is exported to the grid.

Power delivery system

The data processing and thermal conditioning demand a significant amount of electricity in the DC. The third largest part of DC energy consumption (after IT and cooling consumption) is power loss related with power delivery and UPS system. Another demand is related with lighting and powering of auxiliary (e.g. safety and security) systems. The power usage efficiency (PUE), defined by a ratio of total DC demand to ITE demand, indicates the efficiency of secondary systems required for running primary data processing. The typical energy breakdown for conventional (PUE ~ 2), best practice (PUE ~ 1.5) and state of the art (PUE ~ 1.2) data centres are shown in Figure 2-9 [56].

While powering individual components, the three-phase power of alternative-current with 480V, usually supplied from the grid, has to be transformed several times in order to reach the required power of direct-current of 12V for electronic applications. The power delivery losses related to the electric energy

manipulation are usually in the range of 21% to 32% of total DC power consumption [43]. The power delivery efficiency is given by the type and configuration of the power delivery line.

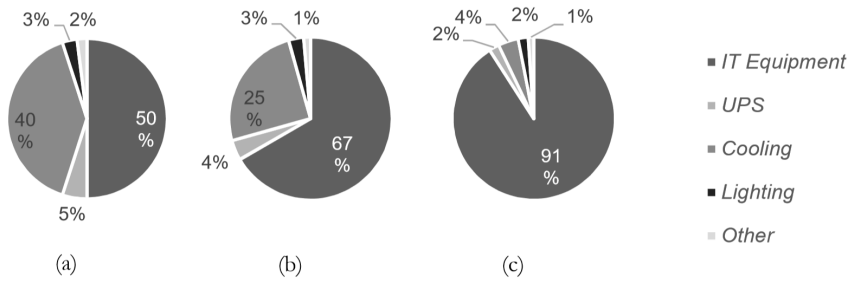


Figure 2-9 (a) Conventional DC breakdown, (b) Best-practice DC breakdown, (c) State-of-the-art DC breakdown

The power delivery system supplies critical, essential and non-essential loads. The critical loads are backed up by UPS systems. The IT devices require power transformation by power delivery units (PDU) and Power Supply units (PSU). The power delivery efficiency decreases rapidly for partially utilized DCs. The nameplate values of individual components significantly influence the part-load efficiency curve, which is further discussed in section 4.2.5 as a modeling aspect of the power delivery system. All in all, the power delivery system essentially cannot be actively operated, and its efficiency largely depends on the design choices. Since this work is mainly interested in the commission and operational phases, the dynamic behavior of the power delivery system is taken into consideration, but the assessment of power delivery systems is out of scope in this work.

Power supply system

The power supply is generally doubled or tripled in order to satisfy the required reliability of the DC. The most reliable DCs (tier IV) are usually connected to two independent grid circuits. To reiterate, the power supply is usually backed

up by several alternative power sources, such as UPS battery facilities for short-term outages and on-site diesel power generators for long-term outages. As mentioned, the main challenge for next generation DCs is to introduce renewable energy systems into already complex and sophisticated infrastructure. In fact, Google, the current leader in data processing, has committed to power their DCs by 100% renewable energy by the end of 2017 [58], and other hyper-scale firms such as Facebook, Microsoft or Amazon will follow in cutting their consumption of fossil fuels for reasons of good publicity and independence from the electricity providers. Seemingly, carbon neutral DCs are technically possible. The question remains if the powering by on-site renewable sources is also cost-effective and reasonable for small and mid-sized DCs, which still amount to around 45% of DC stock [15]. This work is mainly focused on current or best practice renewable technologies, which are expected to be competitive with fossil fuels in the near future, and to be compatible with power grid supply. More specifically, the work is focused on the integration support of photovoltaic (PV) systems, wind turbines and biomass electricity generation and their combination with electricity storage. The on-site renewable system specification is further discussed again in section 4.2.5 as a modeling aspect.

2.3 Holistic data centre operation

As stated earlier, future DC operation strategies aim at system-level optimization. System-level optimization means automated optimization and synchronization of setpoints for all components in the DC. The holistic operation goes even further and aims to automatically synchronize individual domain management via supervisory policies in order to reach high-level objectives such as minimizing cost, maximizing on-site RES utilization or reducing CO₂ emissions.

Holistically optimized DC operation is defined as an integrated management and control platform for DC wide optimization of energy consumption by integrating monitoring and control of computation, communication, data storage, cooling, on-site renewable power generation, energy storage, and waste heat management.

The fundamental premise of holistic optimized operation is that the energy consuming equipment in the DC must be operated as a complete system, where all domains are coordinated to achieve both DC reliability as well as high energy efficiency. The DC is preferably supplemented with renewable energy from the grid or from its own RES generation facilities to achieve optimal energy use. The goal of holistic optimization is to minimize energy use through optimal manipulation of local equipment controller setpoints and the provision of coordinated control of computing load, cooling distribution, and on-site power supply coverage to minimize cost and CO₂ emission outcomes [59]. The vision of the holistically operated DC is centred on the hierarchal architecture of the control platform. The architecture can be divided into individual control levels, where the control is delegated from higher-level policy, through system level setpoints, to individual component actuation signal. The hierarchal architecture is depicted in Figure 2-10.

The holistic architecture introduces a hierarchy of 4 levels of control: (I) monitoring and local control, (II) single-domain management, (III) multi-domain management and (IV) collaborative management. The hierarchical holistic operation aims to achieve optimal coordination of all processes and components belonging to level (O).

The main controlling flow begins with the monitoring of a controlled system (processed signal). The individual components are actuated by local controllers based on a given setpoint. Based on the monitoring, the management of single-domains enables the generation of a prediction and allows setpoints to be

varied to reach an optimum at system-level. The prediction is also provided to the supervisory management level, which is able to co-ordinate and synchronize the domains in order to achieve optimal energy use or emissions outcomes.

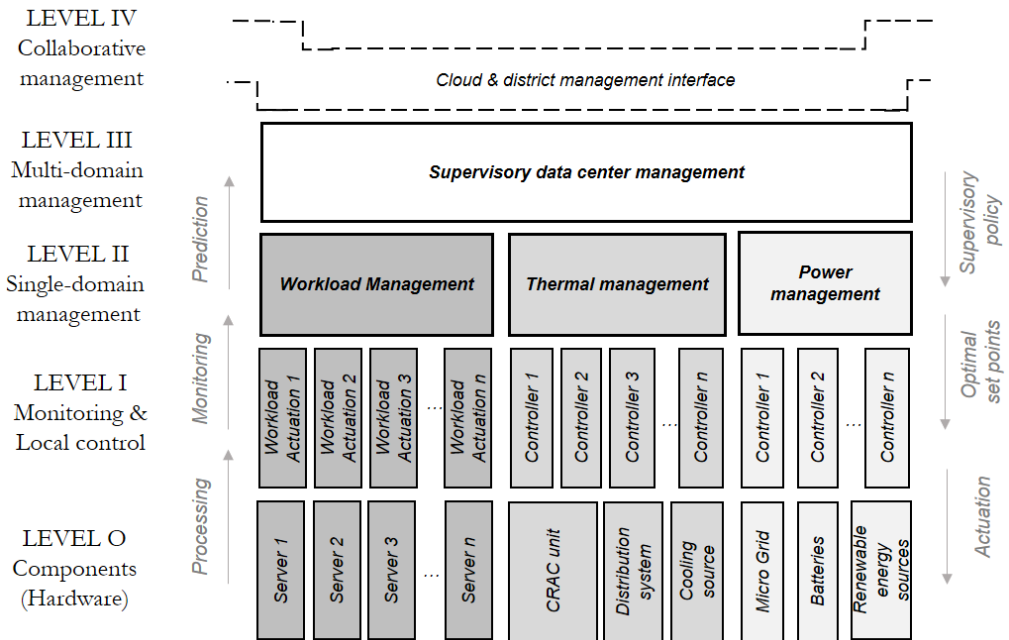


Figure 2-10 Hierarchical architecture of holistic operation adapted [59]

The supervisory management provides policies, which are additional constraints considered in the system-level optimization. The optimal setpoints given by single domain management consider the supervisory policies, and finally the individual controller generates the actuated signal, which results in the components/devices being actuated in a holistic manner.

The Genic project, briefly introduced in Chapter 1, aimed to develop and implement such an integrated management and control platform for DC wide optimization. The development of control platforms consists of the following elements: monitoring, individual domain management, supervision, fault

detection and diagnostics, integration framework, graphical user interface and also platform development tools such as the virtual testing environment, which is the main subject of this work [60]. Further, this section is mainly focused on the modules necessary for regular DC operation, which will be later tested via a virtual DC environment.

To reiterate, the holistic DC control platform requires a multidisciplinary approach. Several expert groups are necessary for the development of the wide or holistic DC optimization and coordination. Besides the limited testing possibilities discussed in detail in chapter 3, a multidisciplinary team is crucial for the successful platform development. However, the foundation of such a team often fails in practice. Usually, the vendors provide control algorithms for individual components, but rarely for individual domain management at the system level. The DC components are often controlled by independent controllers without any coordination of control processes [61].

The architecture must deal with the multiple domains acting at various scales of the DC environment. The communication among multiple services developed by these expert groups is absolutely crucial for setting up the entire holistic control platform. For that purpose, internet-based communication with a modular structure is proposed. A module can be understood here as an encapsulated service or algorithm, which is prepared to be deployed to the internet-based communication middleware (e.g. monitoring, prediction models, actuation, etc.). In this modular structure, individual modules can be easily replaced or removed by alternative or updated control modules. The modules communicate via a message-oriented communication middleware, RabbitMQ [62], with a predefined I/O structure. The communication middleware allows message exchange between various software entities from geographically dispersed developers via the internet. Thus, the individual

modules can exchange required information to achieve coordinated operation, while the confidentiality of each expert group is guaranteed.

Such a modular structure offers high platform flexibility (e.g. support of various coding languages, easy integration of already developed algorithms, etc.). Each module is identified by application topic name, functions (measures, control, log, model, test, etc.) and available input and required outputs. The data exchange frequency also needs to be specified for each module. The modules can communicate with each other based on time or an event. The time-based communication is a data exchange where the data are provided with a given periodicity (e.g. 5 min). The event-based communication is a data exchange where data are provided based on predefined event, which can be initiated randomly in time (e.g. new update of data)

The wide optimization process relies on prediction models. Each management contains prediction models of related DC processes. In general, the prediction models must satisfy the required outputs of decision-making modules (actuation or supervision) and provide these outputs in limited computational time given by execution time. Thus short-term (i) and long-term (ii) prediction models can be identified for holistic operation application.

The scheme in Figure 2-11 shows the use cases of the short and long-term prediction and also the communication data flow between single and multi-domain (supervisory) managements.

The flows of information presented in Figure 2-11 consist of the following elements:

1. The monitoring senses processed signal feedback for the next execution time. The states of the individual DC process are measured, and the monitoring data are provided to the holistic platform with given periodicity. For instance, the Genic platform works with a sensing periodicity of 5 minutes.

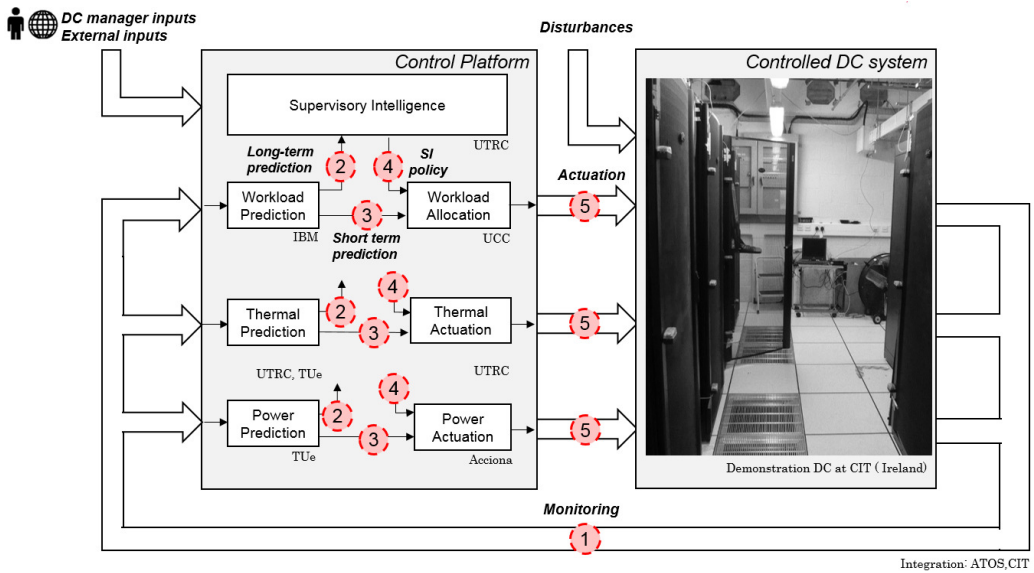


Figure 2-11 Use-case of prediction models for holistic DC operation

2. The long-term prediction models provide trends for every execution time of supervisory control (e.g. 1 hour) with a long-term prediction horizon (e.g. 24hours) and support high-level optimization and coordination.
3. The short-term prediction models provide profiles for every execution time of system level actuation (e.g. 5 min) with a short-term prediction horizon (e.g. 1 hour)
4. The supervision decision making provides the optimal policy for the next execution period to system level actuation in order to reach high-level objectives in the long-term horizon.
5. The system-level actuation provides optimal setpoints for the next execution period to local controllers in order to reach the system level objectives in the short-term horizon.

2.3.1 Monitoring and local control

All system and processes presented in Section 2.2 such as data processing, thermal conditioning and powering are monitored for control, fault detection,

and visualization purposes. The typical candidates for the monitoring are shown in Appendix A. Briefly, the data processing is usually measured based on server performance. Nowadays, virtual machine (VM) software offers online monitoring of server performance via an internet network. In terms of thermal conditioning, the majority of the modern cooling systems have an option for an open interface via a local area network (LAN), or another specialized network protocol such as Building Automation and Control network (BACnet) [63], which can be connected to the internet. Similarly, the measurements of the electricity consumption or generation can be done by smart meters or smart switchgear, which can provide information regarding current, voltage, and power via a LAN.

The system monitoring is crucial for both lower-level control (i.e. local control logic of individual components) and higher-level algorithms (i.e. system-level control of overall domain). The local control is very often inseparably embedded within individual components (e.g. internal control of compressor units, thermostatic valves, server fans, etc.) and therefore it is denoted here as lower-level control. The characteristics of the local controllers/actuators needs to be taken into account in the higher-level control.

There are a large variety of controllers such as on-off, programmable logic, PID, or advanced model predictive control, which actuate individual components (see more in [64]). The internal component actuation can significantly influence the behaviour of the overall controlled system and it can introduce irregularity into the system behaviour. In the worst case, the actuation of the local controller can even disturb the higher-level control. However, delegating the actuation to local controllers is often necessary, since the development of system level controls already deals with a wide range of complexity of the controlled system. The higher-level control usually

recommends the optimal set points and delegates the control of components to the individual local controller actuators.

In this research, the local controllers are considered an inseparable part of the DC facilities and their energy behaviour, which later in this thesis will be represented by a virtual DC environment.

2.3.2 Single domain management level

Each single domain management typically belongs to a different level of scale. For instance, the IT workload management mainly operates at the server or rack scale, while the conventional thermal and power management operates more at the room and building scale. When RES or waste heat utilization are considered, the scope can be extended even further to the district scale. The holistic approach aims to bridge the individual managements. This section describes concepts of individual single domain management and the possibility for interaction.

IT workload management

First, the term IT workload should be clarified. The energy engineers often confuse IT workload with IT power load, which is in the end related with dissipated heat. It is important to understand that for the same IT workload (i.e. the same amount of IT tasks), the IT power outcome may dramatically differ based on the given IT workload management strategy (workload allocation). The IT workload management determines the final assignment of the IT tasks to individual servers with various energy performance. In this thesis, the IT workload is always related with end-user's IT tasks. The schema in Figure 2-12 shows the IT workload in relation with end-user tasks, IT power load and dissipated heat

The IT workload management is responsible for monitoring, predicting and ensuring the optimal operation of IT workload within the DC (at the server or rack scale). Modern IT workload management, such as IT workload

virtualization and consolidation, allows the decoupling of IT hardware from software applications. The IT tasks can be numerically represented by VMs, which contain an estimate of the computational capacity. Thus, incoming IT tasks can be analyzed and consolidated with other IT tasks before their allocation to the hardware. Hardware requirements e.g. CPU (Central Processing Unit), RAM (Random Access Memory) or Hard Drive utilization can be predicted in advance. In other words, the application (e.g. web-service, file-service, etc.) is not associated with the specific hardware, and the IT workload can be migrated and allocated to any server within the virtualized cluster. The virtualization provides operational flexibility and leads to higher utilization of the individual hardware [28].

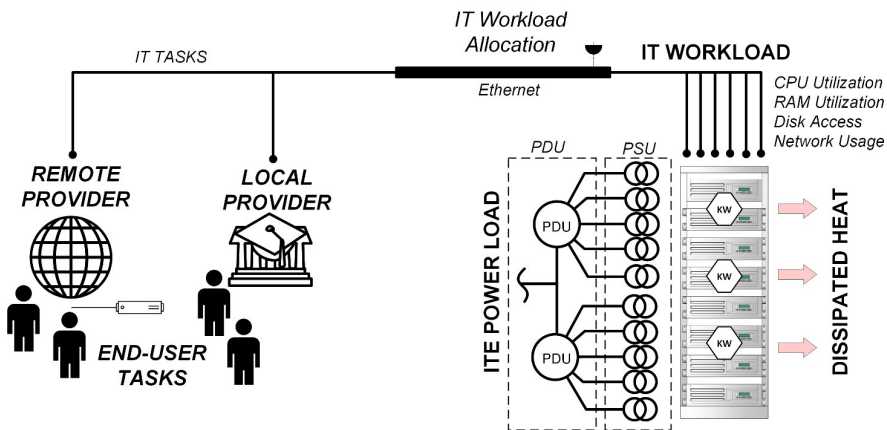


Figure 2-12 IT workload management versus ITE power load

Data centers typically include thousands of physical servers hosting numerous VMs for each application or customer. Despite the possibility of consolidation leading to the utilization at server and rack scale, the DC electricity attributed to the performance of productive computation is still very low from the overall DC perspective [25]. The energy aspect of the computing is rarely considered in the workload allocation process. The priority of the workload allocation is mainly concentrated around satisfying all SLAs of each VM without any

disruption, regardless of the energy outcome. Although many VMs can be consolidated into a single server, a number of resources used by VMs can vary significantly over time and thus all resources are usually active to be able to manage possible peaks without any SLA disruption. Therefore, the energy-aware consolidation and allocation of the IT workload to the individual servers is still very challenging. The following energy-aware workload strategies can be found in literature.

- The first strategy of energy-aware workload allocation is to prioritize the most efficient servers for workload allocation. This solution requires the complete mapping of parameters related to server performance, such as maximal and idle power consumption. It should be noted that this strategy is not valid for a theoretical case when the DC is occupied by identical server types. More information about this strategy can be found in literature [31],[65].
- The second strategy of energy-aware workload allocation is the “power nap” strategy, which saves the idle energy of non-utilized servers by setting them to standby mode. Accurate IT workload prediction is necessary to activate the servers in advance of a peak to avoid any SLA violation. More information about this strategy can be found in literature [31],[65].
- The third strategy of energy-aware workload allocation, the so-called thermal-aware workload allocation, aims to support the cooling performance by the distributing of the workload and related heat dissipation based on priorities given by thermal management. This strategy aims to avoid dangerous hotspots and to reduce the cooling consumption by achieving optimal air temperature distribution across the DC. More information about this strategy can be found in literature [37], [66]–[68].
- The last energy-aware workload strategy evaluates the available primary energy sources. The strategy is based on postponing the workload

processing until RES generation is available. This strategy is often in conflict with SLA agreement because only very limited types of IT tasks can be shifted in time without any SLA violation. More information about this strategy can be found in the literature [38],[69].

Thermal management

Thermal management is responsible for monitoring of the thermal DC environment and cooling systems, prediction of temperatures and cooling power demand, and prediction of the potential for the reuse of waste heat. The thermal management optimally coordinates and operates the cooling system's components to reach the recommended operational conditions for the housed ITE. This section is focused on thermal operation strategies for conventional air-based cooling systems, introduced in the section above.

The optimal system-level operation cannot usually be provided by simple controllers (e.g. rule-based control) and the wider optimization and coordination of setpoints requires model-based control. The thermal management can be divided into management of the cooling system components (the room and building scale) and supply air management within the DC space (the rack and room scale).

- Each component such as the CRAC/CRAH unit, pumps, valves, chiller, economizer, cooling tower or dry-cooler, usually operates with constant setpoints, which leads to a significant decrease of part-load efficiency. The cooling system cannot properly adapt to the part-load IT power demand and related heat dissipation. The coordination of the components' setpoints and wide system-level optimization aims to improve the part-load efficiency. This management assumes variable temperature setpoints for the DC inlet temperature and economizer actuation and also actuation with variable speed of all fans and pumps in the system. The system-level thermal management considers the waste heat utilization. The decision-

making process is influenced by supervisory management policies such as maximum DC inlet temperature, desired heating demand for waste heat utilization, and recommended charge/discharge thermal storage profiles for long term horizons (e.g. 24 hours). The algorithm seeks optimal component setpoints to minimize the HVAC power while meeting all supervisory policies.

- The scope of the thermal management usually ends at the CRAC/CRAH unit settings. These temperature or airflow setpoints are constant for the related DC section or overall DC space. The controller usually operates based on a single temperature, which is taken as a reference for the whole related DC space. In current practice, the return air temperature or an average of multiple sensors in the DC space is used for the unit control. On the other hand, nowadays racks or even IT devices are often equipped with embedded temperature sensors, which can be integrated into the DC sensor network and communicate with the control platform [19]. Such a sensor network offers high-resolution monitoring of temperatures in the DC space. However, the potential of such high-resolution monitoring is not fully utilized due to the lack of actuation of thermal management at the rack or server level. In other words, thermal air management has very limited ability to adjust conditions for individual racks or even servers. Despite this, the thermal management is able to analyze the high-resolution monitoring data and generate thermal preferences for IT workload management allowing for so-called thermal-aware computation explained above. By migrating virtual machines (representative of IT workload) to thermally preferable hardware, the distribution of dissipated heat can be controlled. Thermal-aware computation allows thermal management to act at the rack or server level, avoids hot spots and potentially increase the

temperature difference and thus also the part-load (operating) efficiency of the CRAC/CRAH unit.

Power supply management

The power management is responsible for monitoring and prediction of on-site RES power generation and DC power delivery losses. The power management actuates micro-grid devices, on-site controllable power plants and electricity storage. The decision-making process is influenced by supervisory management policies such as the desired renewable ratio and recommended charge/discharge battery profile for long term horizons (e.g. 24 hours). The algorithm seeks optimal component setpoints to minimize the energy demand from the grid while meeting all supervisory policies.

2.3.3 Multi-domain management level

The multi-domain management can be categorized into two types: (i) supervisory management focusing on the coordination of the internal domains within the DC environment (e.g. IT workload, thermal and power domains), (ii) collaborative management aiming to coordinate the entire DC with external domains (e.g. electrical grid). The coordinated DC operation, where data exchange amongst the domains is enabled, can improve the overall DC efficiency achieving high-level objectives such as minimizing DC energy use, cost and CO₂ emissions. Furthermore, it can support the integration of the DC environment into the modern urban infrastructures.

At this level, information from the levels below (e.g. monitoring, prediction etc.) or external information (e.g. weather forecast, day-ahead market price) is collected and processed by a multi-domain management, which provides policies for the lower levels to reach the coordinated operation. For example, the multi-domain management, which collects information across the domains (including external data sources) can be beneficial for automatized decision making with long-term prediction horizons (e.g. 24 hours ahead). Such decision

making can support both electrical and thermal storage management, heat recovery management as well as demand response management using energy flexibility of all DC domains.

Supervisory management

The supervisory management is responsible for the domain coordination. The coordination is provided via optimal IT workload, and thermal and power supply policies. The supervisory management generates policies based on (i) external data input (e.g. day-ahead grid price service, contribution of RES in the grid, heating demand of the waste heat consumer, etc.) and (ii) internal long-term energy prediction of individual sub-systems. The supervisory management matches the long-term demand and power generation predictions of the electricity or heat fluxes and then optimizes the policies in order to achieve the desired economic or environmental DC outcome. The decision-making follows the user-defined settings such as (i) minimization of operating cost, or (ii) minimization of total carbon emissions, or (iii) maximization of the use of the on-site RES. The algorithm seeks policies which satisfy the user-defined settings. The high-level policies are sent to each single-domain management as additional requirements and constraints on the optimization process at the domain-level. If the policies are followed, the overall DC is operated in line with supervisory management following the high-level goals (minimizing energy use, cost and related CO₂ emissions).[36], [59]. As an example, the supervisory level can read predictions of DC demand, on-site energy and day-ahead market price. After doing so, the supervisory algorithm generates policies for the single-management level, which may recommend postponing workload processing, relaxing temperature setpoints to allowable temperature limits for a short period of time, or recommend a utilization profile of energy storage for the following 24hours.

Collaborative management

In the near future, supervisory management may have an additional purpose, such as being an interface for the infrastructure of modern “smart cities”. This vision is centered on workload operation of DC clusters diversely spread around the world (e.g. the concept of RES Aware Service Migration [32]) and integration of DCs to smart grids and district heating infrastructures. The rising concept of the IoT promises easy information exchange between individual physical devices, vehicles, plants and buildings. If the IoT is realised, the supervisory interface, which will provide relevant performance indicators on behalf of the overall DC system, will be necessary for integration and coordination of processes at the larger district level. However, this work aims solely at the testing of the operation of an individual DC and this district level integration and coordination is not the focus of the current research. The collaborative management is considered in the hierarchical architecture in order to provide a complete vision, including future trends.

3 Definition of computational experimentation for commissioning of holistic data centre operation

Chapter 3 proposes a new application of building energy models as a testing environment for multi-domain control algorithms developed externally by other entities, which were briefly presented in the previous chapter. In addition, the requirements and concepts for the modelling of a virtual data centre (DC) environment, enabling such a testing, are also discussed in this chapter.

To summarize the previous chapters, next generation DCs require solutions going beyond the component level and coordination of individual DC processes. The holistic operation of next generation DCs will likely play an important role in satisfying sustainability goals and allow the integration of DC infrastructure into the wider framework of smart cities in the future. To reiterate, the holistic data centre operation platform is a type of supervisory energy management, which aims at system-level control and multi-domain coordination.

Due to lack of testing possibilities related with the stringent requirements for trouble-free DC operation, the current DC supervisory management or integrated management is usually still restricted only to centralized monitoring or data visualization. These requirements complicate the implementation of advanced operation strategies. Actually, the survey conducted by the Uptime institute in 2015 [24] reveals that the current DC supervisory management or integrated management experiences a long installation process of the platform.

This process can take longer than 6 months in 74% of cases. So far, purchasing of such a DC supervisory management or integrated management provides minimal or no return on investment [25]. Thus, most DC operators still rely on basic local controllers at the component level, whose installation usually requires less effort, even though the performance provided by such control is often inefficient and the DC facility cannot adequately adapt to the part-load utilization, which results in lower energy efficiency. Moreover, the individual DC systems work independently without any coordination.

Indeed, the current supervisory management and integrated management can be extended by adding holistic DC optimization (e.g. the one proposed by the Genic project), which aims to achieve cost-effective and sustainable operation. However, the challenges are not only in development of the supervisory management, which requires significant effort and skills, mentioned by [64], but presently a significant challenge also exists in the commissioning process.

The typical constraints for the commissioning of any advanced building operation strategy, identified by [70], are (i) the difficulties in testing performance in extreme plant conditions, and (ii) the requirement of a very broad knowledge of multiple systems and controller types to carry out tests and interpret results.

These general constraints can be fully applied to the DC case. Actually, the situation here is even more difficult. The DC facility consists of multiple systems from various domains of expertise. Moreover, the availability of the DC facility for any testing is generally very problematic due to the mission critical nature of the DC environment. As such, the development and commissioning of novel control strategies are often slowed down if not even discarded. Therefore, an alternative testing approach is being researched in order to support the implementation of modern control strategies.

3.1 Testing workflow to support commissioning of holistic data centre operation

3.1.1 Concept of simulation-based closed-loop testing

In contrast to real experimentation, computational experimentation offers a “safe” testing environment. Such a testing environment enables a detailed evaluation of the algorithm performance in terms of energy saving potential as well as extensive and multi-domain testing possibilities for the supervisory platform prior to its commissioning. The simulation-based testing of the control strategies is centred on the development of the virtual DC testbed, the so-called virtual DC environment, which provides the required feedback for the testing of the advanced DC operational platform. The closed-loop testing concept plays a very important role in the development of modern control algorithms, which usually require feedback from the controlled plant. Contrary to stand-alone testing, the simulation-based closed-loop testing ensures similar testing conditions to real operation since it considers the controlled plant dynamics and emulates external disturbances. Moreover, the virtual DC environment allows evaluation of various multi-domain aspects and it thus captures the energy consequences of tested control actions to multiple domains. Figure 3-1 depicts the virtual DC testbed within a typical closed-loop arrangement, where the virtual DC testbed sits in place of a controlled plant which is usually used in control theory to denote the real facility – the DC system in this case.

Computational experimentation can be a very powerful tool for evaluating different control strategies. The application of computational experiments for development and commissioning purposes is relatively rare in practice due to difficulties in developing a virtual environment, which requires energy modelling expertise. Such testing using a virtual testbed is mainly beneficial for the supervisory control platform operating at system-level, where real

experiments are rarely possible. The DC environment is an example of where computational experiments can find wide application due to the mission critical nature and limited possibility of real experimentation. Moreover, the test subject – the holistic operational platform - aims at several domains and systems, which makes real experimentation even more complicated.

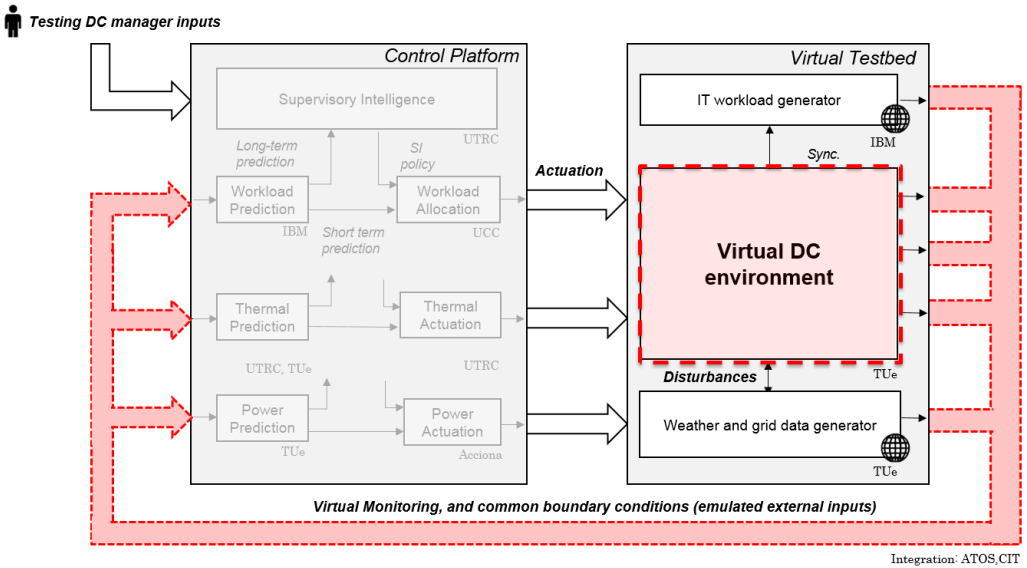


Figure 3-1 Concept of simulation-based closed-loop testing

A similar concept of operational platform development and commissioning application from different fields has been recently applied in several projects such as [71], [72]. In our case, the simulation-based closed-loop testing can be applied in two main use-cases: simulation-based development support and simulation-based commissioning support. Two new use cases are introduced as phases which bridge enhanced operational platform development and commissioning to a real facility. Figure 3-2 depicts the new phases.

The phase of the simulation-based development support offers the possibility to assess the DC operational platform in a closed-loop with the virtual DC testbed. The process can be understood as a virtual operation. At this stage of

development, the numerical representation of a general DC typology is usually sufficient for the testing of an initial algorithm prototype. Moreover, the specific DC configuration may not be available at this stage of development. The initial platform prototype is tested in the closed-loop fashion for a given testing period and set of boundary conditions. The quality of the control is assessed based on the virtual processed signal or on higher-level performance indicators relevant to global DC performance. The evaluation is provided to the algorithm developer for further tuning or as an independent and advanced evaluation of the algorithm performance.

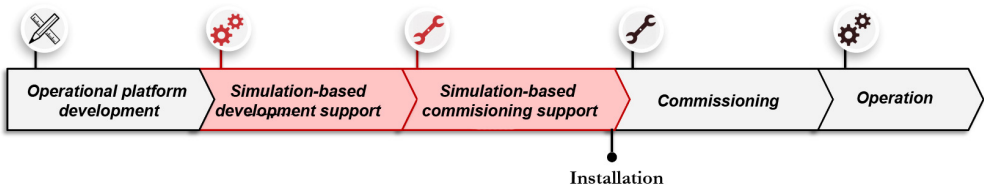


Figure 3-2 New phases: functionality testing, and virtual commissioning

The main advantages of the closed-loop testing are; that the virtual DC environment simulates the feedback as virtual monitoring while receiving the tested control signal; the closed-loop testing allows variability of testing configurations (e.g. testing various configuration of algorithms at once, testing under extreme boundary conditions, etc.); and it allows for repeatability and comparability of the testing results (possibility of replication of boundary conditions). Moreover, the virtual DC environment using building energy simulation tools can be composed from various physics-based sub-models, which in most cases can be configured based solely on technical sheets. Such an example of building simulation model offers higher autonomy of the virtual DC environment because it is not driven by any data, and thus a larger range of validity of the model can be expected. In addition, the novel operational platforms are often implemented together with a retrofit of the DC facility.

The detailed assessment of DC retrofit alternatives or energy efficient measures (e.g. cooling system variants, installation of on-site RES) can also be conducted in this phase.

The phase of the simulation-based commissioning support aims at the preparation of the operational platform for installation to the real DC facility. The process can be understood as virtual commissioning. At this stage of development, the specific DC configuration is known, and initial sets of measurements are often available for calibration of the virtual DC testbed. The numerical model simulates the real monitoring system. The functionality testing and the extensive training of the platform can be virtually executed for the specific DC case. Once the virtual DC environment follows the agreed data format of the real monitoring system, the virtual DC environment can be easily removed and substituted by real facilities in a “plug & play” fashion. Similarly, as in the previous use case, the final platform prototype is tested in the closed-loop fashion for a given testing period and boundary condition. The quality of the control is assessed based on virtual processed signal feedback and higher-level performance indicators regarding global DC performance. The virtual DC environment may also provide more extensive analysis in this phase. For instance, it provides the opportunity for risk assessment of the operational platform, such as the testing of missing or faulty inputs, or sensitivity of the platform to a predefined uncertainty range of the “virtual monitoring”. The setting of the risk assessment (e.g. definition of missing data, or range of virtual monitoring error) is determined together with the developer of the external algorithm. Thus, the critical or abnormal behaviour of the platform can be detected before its installation.

Besides the above mentioned advantages of the simulation-based testing, the added value of virtual commissioning is proper training of the advanced operational platforms. Practically speaking, the functionality testing and initial

training is performed in a virtual environment before platform installation. The virtual commissioning functions to reduce the commissioning time and minimize the risk of failure during the commissioning phase.

3.1.2 Workflow of simulation-based closed-loop testing

This section describes the main steps required for virtual closed loop testing. The proposed workflow is stated based on experience from our main case-study, the Genic project. The workflow is related with the computational experiment preparation block presented in chapter 1, and it specifies the steps necessary for the setup of the simulation tool chain and provides guidance for the execution of the computational experiment. The workflow can be briefly summarized in the following steps:

1. Data collection and computational experiment definition
2. Virtual testbed development and quality assurance
3. Stand-alone (open-loop) testing of individual algorithms
4. Simulation-based (closed-loop) functionality testing of individual algorithms
5. Simulation-based (closed-loop) functionality testing of the overall platform (combination of partner algorithms)

Each of these five steps is presented in detail in Figure 3-3 and Figure 3-4 below. The workflow also shows the roles of computational experimenter and control algorithm developer.

Data collection and computational experiment definition

Data collection is common for all actors. It is necessary to collect the technical specifications consisting of housed servers, DC space geometry and arrangement, cooling systems, power delivery and power supply systems, Also, initial measurements of the DC system are collected if they are available. The experiment definition needs to be agreed by all actors. The testing use case, key

performance indicator, baseline setting for benchmark simulation and testing scenario definition (boundary condition setup) are usually defined in this step.

Virtual testbed validation and demonstration

The virtual testbed development is elaborated in detail in chapter 4. Since the main purpose of the computational experiment is to evaluate the performance of control algorithms developed by external partner(s), the validation and demonstration study (executed in chapter 5) is very important in order to build trust between computational experiment executor and external algorithm developer. Due to the large scope of this study, the validation and demonstration study needs to be decomposed into individual sub-models representing the parts of the system. In this case, the model was compared with measured data wherever the measured data were available. If there was not enough data, the performance of sub-models was demonstrated and compared with relevant standards. In the end, all assumptions regarding validation and demonstration must be documented and the results must be provided to the algorithm developer.

Initial algorithm training (stand-alone testing)

This step is done by the external algorithm developers. The stand-alone (open-loop) testing is standard current practice in the testing of control algorithms, and remains the starting point of the workflow. The open-loop testing requires training data. Training data can be gathered from previously measured data of any DC facility with a similar topology, or this data can be measured directly at the particular DC facility. During this measurement process, the DC is controlled by the default settings of all local controllers.

The virtual DC testbed can also support the stand-alone testing by providing a set of training data according of the developer's needs (e.g. data for different boundary conditions, behaviour of the system for step response of control signal, extreme conditions, etc.).

In open-loop testing, the control algorithm is not connected to any actuators (real or virtual). The performance of the individual control algorithm is assessed based on the quality of the control signal. This is generally sufficient for simple controllers. However, more complex control platforms with multiple inputs and outputs from several domains are problematic to assess based on individual control signal traces. Nevertheless, the stand-alone testing still needs to be executed. In this phase, initial information regarding control signal variables such as expected variable range, data format, etc. are gathered for the next steps.

Simulation-based closed-loop testing of an individual algorithm

The enhanced operational platform usually consists of various modules and “managements”, as depicted in section 2.3 above. In this step, the operational platform is decomposed into individual modules or managements and they are connected one by one to the virtual actuators of the virtual DC testbed. The virtual actuators receive the control signal and the numerical model of the virtual DC provides a simulation of the processed signals of the controlled system. The algorithm performance is assessed based on the virtual processed signal. The assessment takes into consideration sampled disturbances and dynamic behaviour of the controlled system, including local control of individual devices (usually given by the manufacturer).

The closed-loop testing reveals the algorithm performance from a complex system-level perspective and indicates consequences to other domains. This assessment may detect potential limits or errors of the particular tested algorithm. Additionally, the simulation-based testing can provide a comparative analysis of competitive algorithms. Competitive algorithms are algorithms targeting the same objective in a single domain which but use a different approach to reach the objective. The comparative analysis of their performance can support a decision-making process.

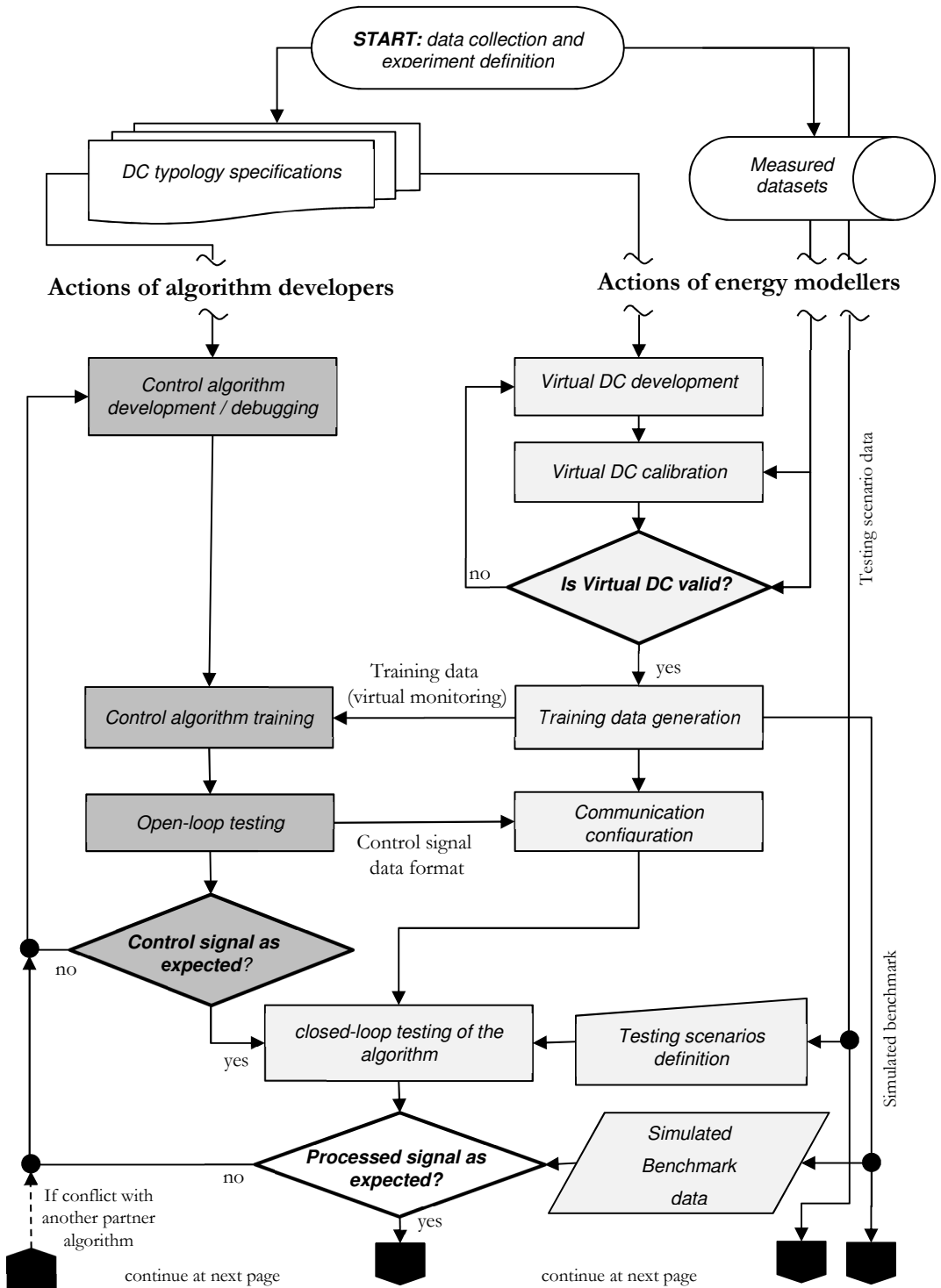


Figure 3-3 Workflow of simulation-based closed-loop testing - part I: single algorithm testing

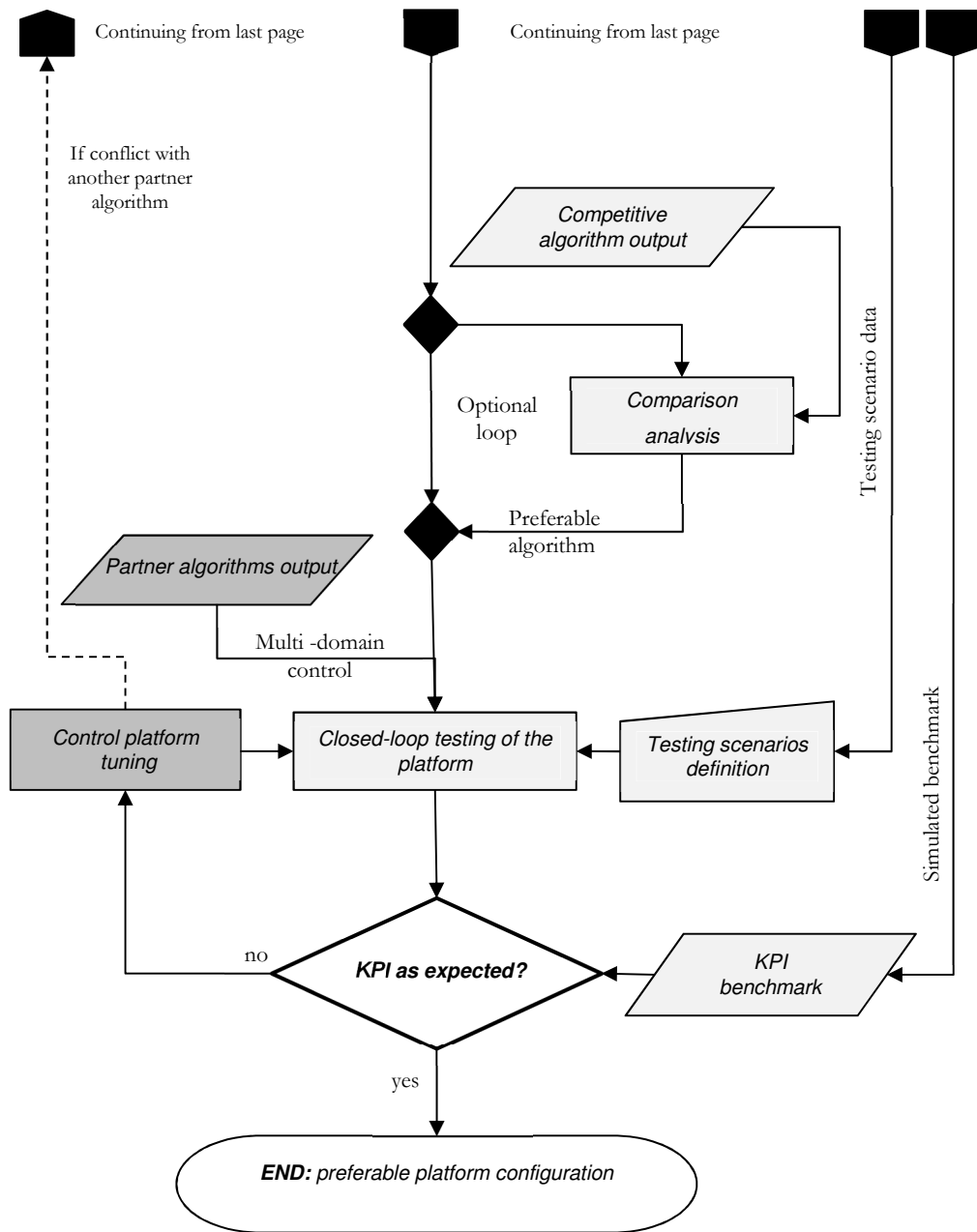


Figure 3-4 Workflow of simulation-based closed-loop testing - part II: multiple algorithm testing

Simulation-based closed-loop testing of an overall platform

The final step of the workflow is the closed-loop testing of the overall operational platform. This step requires the testing of multiple partner algorithms against the virtual testbed at the same time. The partner algorithms are algorithms that cooperate and actuate the multi-domain system. Each algorithm targets its own objective and optimizes its domain of interest (e.g. IT workload management or thermal management).

The holistic control platform acts at several domains and actuates various devices. The evaluation based on the processed signal (e.g. energy demand, temperature traces) is not sufficient at this level of complexity. In order to assess such an enhanced operation, the predetermined key performance indicators addressing the performance of the overall system are evaluated. The multi-criteria assessment reveals possible conflicts between the actuation of partner algorithms and assesses the operational performance of the platform as whole.

3.2 Conceptual modelling of data centre environment to support commissioning of holistic operation

3.2.1 Conceptual modelling within the modelling and simulation process

As stated earlier, the intention behind the development of a virtual DC testbed is to realistically quantify the impact of control algorithms on the DC infrastructure behaviour and to prepare the ground for their smooth installation in a real DC infrastructure. Undoubtedly, the virtual DC testbed as a simulation model for development support of advanced holistic operation must cover the multi-domain nature of the real DC infrastructure. Since the simulated DC system should address the wide scope inherent in the real DC system, and because these systems are complex, attention should be paid to

conceptual modelling. Moreover, the recent development of simulation tools and coding languages allows the use of various libraries of simulation models. Nowadays, advanced modelling approaches are available via user-friendly interfaces for a wide user group and are not restricted to computer science experts. In addition to the continuous increase of computational performance, the modelling of complex systems crossing established fields and domains has become feasible in the last decade. As Cook [73] concludes, these days, the coding of any simulation model is not really a problem, the problem is actually what we should simulate. The importance of solid architecture of the conceptual model has risen with the current trend of complex multi-domain approaches working at several scales of the overall system. The conceptual model is defined as a preliminary system representation by either graphical diagram, flow chart or simplified pseudo-code [74]. The conceptual model represents a studied system or process for communication purposes. According to Pace [75], the conceptual model describes how a simulation-model developer intends to implement the simulation model to satisfy the requirements of the simulation user. Therefore, the computational model is often used as an agreement between simulation developers and simulation users. The conceptual model formulation is always case-dependent.

The conceptual model formulation can be also understood as a process of seeking the optimal conceptual model complexity, which is strongly related with purpose definition and problem analysis. Robinson states that “[t]he issue in conceptual modelling is to abstract an appropriate simplification of reality... The overarching requirement is the need to avoid the development of an overly complex model. The aim should be to keep the model as simple as possible to meet the objectives of the simulation study” [76]. A good illustration of this point can be found in, Hensen and Trcka [77, Ch. 1] who related the model complexity with potential error in performance prediction and model input

uncertainties in their so-called fit-for-purpose modelling concept. Working from a slightly different perspective, Zeigler et al. proposed a definition of model complexity as a composition of scope and resolution [78, Ch. 13].

$$\textit{model complexity} \leftrightarrow \textit{scope} + \textit{resolution} \quad (3.1)$$

The scope refers to how much of the real system (real DC infrastructure) is going to be represented. The scope is defined as the number of independent sub-systems, which need to be modelled to satisfy the purpose. The scope is related with the domain and scale of the real system. The dynamic simulation also requires the definition of temporal scope, which means defining a time horizon of evaluation (e.g. week, month or year evaluation).

The resolution is defined as number of variables per sub-system. Generally, the resolution can be further divided as resolution of physical abstraction (e.g. energy balance, temperature, massflow), spatial resolution (e.g. number of temperature nodes per room) and temporal resolution (time discretization).

The model complexity has often been understood as the “only” level of resolution, especially for single domain or component-level oriented studies where the scale is relatively narrow. The studies regarding DC energy modelling are no exception and they are mostly associated with high-resolution modelling of DC space, as is further discussed in section 4.1. Our multi-domain purpose requires a dynamic system which considers modelling complexity in both “dimensions” of scope and resolution. Finally, equation 3.1 also indicates that the highest resolution does not necessarily mean the highest modelling complexity in total.

While the previous flow chart in section 3.1.2 presented the workflow of the proposed computational experiment including information exchange between algorithm developer and modeller, the schema in Figure 3-5 is focused more on modelling and simulation process. The schema is adapted from Sokolowski

and Banks [19] and shows the individual stages of modelling and simulation processes and the interaction among these stages. This general framework is widely accepted as a fundamental principle of modelling and simulation. Moreover, their usability was proven by experience gained in several projects of the research group of Computational Building Performance Simulation at Eindhoven University of Technology. Based on these experiences, a new block entitled “knowledge” was added, as can be seen in the presented schema. The rationale behind this addition is that the purpose definition may not necessarily lead to new knowledge generation from a scientific point of view. Since the modelling and simulation methods are currently commonly used for practical purposes without scientific aims, purpose and knowledge generation should be distinguished.

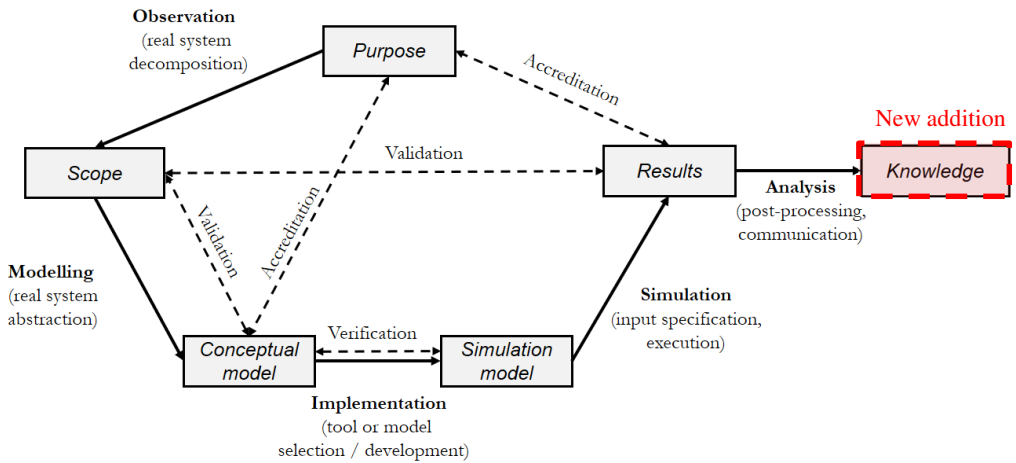


Figure 3-5 Modelling and simulation process adapted [19]

As mentioned in the research methodology in Chapter 1, the modelling and simulation process starts with the analysis of purpose definition. At this point, the necessity of the application of the simulation techniques needs to be justified (available guidelines can be found in literature [79], [80]). As discussed in the beginning of this chapter, real DC systems must be numerically

represented to enable computational experimentation of external algorithms prior to their installation. Once the purpose is clarified, the modelling and simulation process can take place.

Generally, the modelling and simulation process can be described in 5 steps, which are related to the research methodology stated in section 1.3, and are compatible with the testing workflow presented in section 3.1.2.

- (i) The first step is to observe the real-world system and then to decompose the system into individual domains, scales and system dynamics. The scope of the modelling is defined according to the purpose definition and real system observation. The scope can be understood as the real-world items of interest and is related with Zeigler's [78] definition of complexity.
- (ii) The second step is modelling of the real-world items of interest, which means real system abstraction. The resolution is defined as a complementary part of the scope in the complexity definition and is analysed and defined in terms of level of abstraction, and spatial and temporal discretization. The product of the real system abstraction is the conceptual model. Once the conceptual model is defined and the interactions between individual domains, scales, evaluation period and model resolution are specified, the model can be validated against the scope definition. Before the next step, the conceptual model is accredited by the simulation user (external algorithm developers in our case).
- (iii) The third step is implementation of the conceptual model and development of the simulation (executable) model. The implementation includes existing tools and simulation model selection. This step may include simulation model development, if necessary. The simulation model is verified against the conceptual model.
- (iv) The fourth step is the execution of the simulation and the reporting of results. This step includes the simulation input specification, such as

definition of simulation scenarios and specification of boundary conditions. The simulated results are validated against the behaviour of the real system within the scope of the conceptual model. Then, the results are provided to the simulation user as a solution for the desired purpose, who then provides the so-called accreditation.

- (v) The last step is the overall modelling and simulation process evaluation including post-processing and analysis of the results obtained from experimentation, which leads to knowledge generation.

In addition, the two types of model complexity should be distinguished (i) conceptual complexity, related with the purpose definition and conceptual modelling, and (ii) computational complexity, related with computational resources and simulation model development. The conceptual and computational complexity do not have to necessarily correlate; however, they need to be balanced in such a way that both purpose and technical requirements are satisfied. Therefore, the modelling process is always an iterative process, where technical requirements given by the simulation model must meet the purpose definition related to the conceptual model, and vice versa.

3.2.2 Conceptual modelling of data centre environment

Despite the wealth of previous studies regarding DC energy modelling, few have gone further than single domain problems. However, at present, the multi-domain nature of the support of advanced holistic DC operation development requires wide modelling scope addressing several domains at various scales. The wide scope will likely compromise the model resolution in order to accomplish the simulation in the limited computational time given by the closed-loop concept described in section 3.1. In order to efficiently apply the closed-loop concept, a transient and interactive response in a reasonable time is required.

The real DC system is decomposed into individual sub-systems and sub-processes related with the DC system. They are: IT equipment (ITE), cooling system, power supply system, power delivery system, building and DC space, electric grid, waste heat utilization, IT workload processing, outdoor climate impact, DC control impact, other ancillary systems (e.g. security and safety systems)

Figure 3-6 shows the DC system decomposition based on simulation objective, modelling scope and boundary conditions. In this example, simulation objective is the tested holistic operational platform. The testing of the given algorithms requires a processed signal feedback from most of the energy systems within the DC. Therefore, the modelling scope is relatively large and needs to represent the energy behaviour of the IT, DC space, cooling, and power supply and power delivery systems.

The boundary conditions of these dynamic models (e.g. end-user workload demand, power grid status, and weather condition, heat demand to heat recovery system) are represented by sample data (e.g. real end-user traces, grid CO₂ equivalent, historical or statistical data). The same boundary conditions that affect the virtual DC environment must be provided to the tested algorithms during the proposed testing procedure in order to ensure consistency of the decision-making when using the virtual testing environment. As an example, some of the tested algorithms may require a weather forecast for their decision-making. The data of the real weather forecast must be substituted by a synthetic weather forecast based on sampled weather data, which is shared by the entire wider simulation framework. To do so, all tested algorithms and the virtual DC environment work under common boundary conditions, which ensures repeatability and comparability of the simulated results.

Systems which are not considered to be controlled by the tested algorithms, or those whose contribution to the total energy use is minor, can be neglected (e.g. ancillary systems). Figure 3-6 also shows the relation of individual domains/systems mentioned above and indicates the scales of the DC system. Server/rack, DC room, building and district scales can be identified within the DC environment.

The next step is the identification of possible model resolution. For each sub-model the resolution in terms of level of abstraction, spatial and temporal discretization needs to be identified in line with the purpose. The resolutions vary for each sub-model.

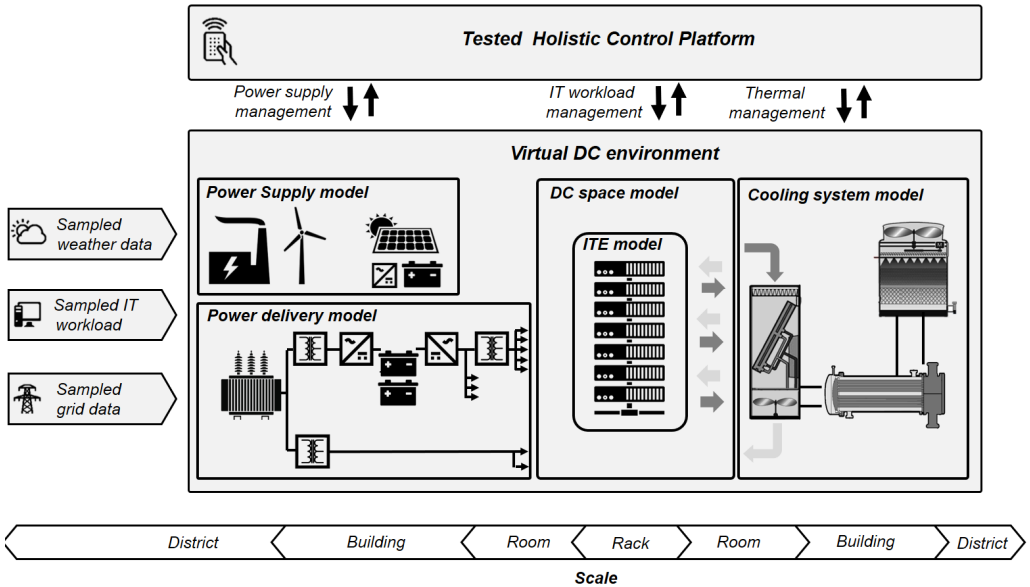


Figure 3-6 Conceptual model: virtual DC environment decomposition

Modelling resolution of IT equipment

Firstly, it is worth restating the distinction between IT workload versus IT power load in this work. These terms are often confused as they are used differently in different fields. While IT workload is understood as the technical

characterization of requested IT tasks in terms of CPU utilization, RAM utilization, Network utilization, etc., the IT power load is the electrical power load consumed by the servers, which is dissipated as heat in the space. This section solely describes the modelling of IT power load and related heat dissipation into the DC space. The models of IT workload, the so-called “virtual machines”, which are often used in modern IT workload management, are not the subject of this thesis.

The range of resolution of ITE model varies in terms of level of abstraction and level of spatial discretization. The level of discretization is usually linked with the spatial discretization of the DC space model, described in the section below. The ITE can be represented for the entire DC space or can be represented per section of DC space. More detailed resolution requires spatial discretization at the level of a group of servers or at level of an individual server.

The range of abstraction starts from low level abstraction, where ITE are represented in space as IT power load and related heat dissipation. The nominal heat dissipation is usually part of the technical specification of any IT equipment. The typical values can be found in ASHREA thermal guidelines [47]. The nominal heat dissipation can be modulated using a utilization profile in order to represent part-load performance. The heat dissipation acts at the DC room temperature node as additional heat gain of the room.

Continuing in the resolution range, the mid-level of abstraction assumes that DC space is represented by multiple thermal/air nodes. Thus, the heat dissipation related with ITE acts at specific thermal/air nodes in the DC space which represents the node of a rack. As such, the heat dissipation is assigned in the geometry of the DC space and the heat gain acts at these specific thermal/air nodes. This level of abstraction allows the modelling of the arrangement of the ITE in the space (e.g. effect of hot and cold aisles arrangement). The ITE is represented by nominal power load, idle power load,

standby power load or maximal airflow through rack. A utilization profile is used to represent the part-load performance of an individual group of servers. Examples of such a mode can be found in [43] and further description can be found here in Chapter 4.

The models with the highest level of abstraction extend to the mid-level ITE model by representing each individual server and their internal thermal/air nodes, such as chip temperature, case temperatures, internal fan speed etc. These models operate at such a level that the information from the virtual machines can be combined with the thermal performance of the server. Examples of these complex models can be found in literature [20] [81]

Modelling resolution of datacentre space

Similarly, the modelling resolution of the DC space can be understood in terms of levels of abstraction and in terms of levels of spatial discretization. When modelling DC space, opting for low spatial discretization generally implies a low level of abstraction, and, similarly, opting for high spatial discretization implies a high level of abstraction. The range starts from low level of abstraction with single zone discretization, where the states are represented by enthalpy, temperature and relative humidity. Air distribution is represented by an efficiency factor. The range progresses to mid-level of abstraction with multi-zonal discretization, where an additional state is relative pressure, which is calculated using an airflow network method. The range ends with DC space defined by mesh and uses a high-resolution modelling method such as Computational Fluid Dynamic (CFD). A review of mentioned building modelling methods for “regular” building types is elaborated in detail in [82].

Modelling resolution of cooling system

The resolution of the cooling system model at the system level can differ in terms of level of abstraction. The spatial discretization is usually irrelevant for the modelling of cooling devices at system level. It is only relevant for a detailed

analysis of individual components. However, to some extent, the model decomposition, which is necessary for the representation of individual cooling system components, can be understood as “spatial discretization”, although, this designation would be misleading since the discretization here cannot be seen as spatial in the same sense as it is in DC space modelling. Similarly, as for the DC space, a resolution range can be found for cooling devices or for HVAC systems in general. The resolution range can vary in terms of level of abstraction (simulated states) and level of decomposition (number of sub-models)

The range starts with a representation of the overall system as one piece. The overall system can be represented by an efficiency curve (e.g. curve of COP factor), where efficiency varies based on the model’s input (e.g. amount of rejected heat), return air temperature and outside air temperature. The next level of this range is that the HVAC model is decomposed into the individual components (e.g. fans, pumps, heat exchangers, etc.) and then each component is represented by an individual model. The simulated states are usually inlet and outlet temperature as well as power demand from each component. The range ends with a detailed system (e.g. the refrigerant circuit) that is decomposed into compressor, evaporator, condenser and expansion valve. The model at high-level of resolution usually includes a hydraulic calculation. The simulated states are then inlet and outlet temperature, power demand and also inlet and outlet pressure.

Modelling resolution of power system

Like the previously mentioned models, power delivery and supply models exist in a range of resolution. These models can also vary in terms of level of abstraction and level of system decomposition. The lower level of resolution is generally restricted to the level of energy fluxes, and the performance (e.g. electrical losses) of individual components is modelled based on their efficiency

curve. The higher level of power system modelling includes states such as current and voltage, and the efficiency is defined based on component properties such as resistance, impedance and capacitance. The levels of resolution for the overall model of the virtual DC environment are further summarized in tables below.

Table 3-1 Conceptual modelling: low-level of modelling resolution

LOW-LEVEL OF RESOLUTION	<p>Data Centre Model</p>
	<ul style="list-style-type: none"> • model using known DC efficiency profile → decomposition/spatial discretization is not possible → temporal discretization without limits → control strategy cannot be evaluated
	<p>Data Centre Model</p>
<ul style="list-style-type: none"> • energy conservation equation, • simplified single-zone model of the DC space, simplified efficiency-based system models → decomposition/spatial discretization of the system's sub-models is not possible → temporal discretization without limits 	

Table 3-2 Conceptual modelling: mid-level of modelling resolution

MID-LEVEL OF RESOLUTION	
	<ul style="list-style-type: none"> • energy conservation equation, momentum conservation • multi-zonal modelling with possibility of simplified air distribution model • system decomposition, simplified models at component level <p>→ spatial discretization for individual zones of the DC space with similar temperatures</p> <p>→ temporal discretization without limits suitable for long term evaluation</p>
MID-LEVEL OF RESOLUTION	
	<ul style="list-style-type: none"> • energy conservation, momentum conservation, Ohm's law • multi-zonal modelling with airflow network <p>→ course spatial discretization for given DC layout</p> <p>→ system decomposition, detailed models at component level</p> <p>→ the evaluation period can be limited by selected temporal discretization</p>

Table 3-3 Conceptual modelling: high-level of modelling resolution

HIGH-LEVEL OF RESOLUTION	
	<ul style="list-style-type: none"> • finite volume method using Navier-Stokes equations. • limited co-simulation with other systems <p>→ fine spatial discretization for given DC layout</p> <p>→ limited possibility of transient simulation, usually steady-state</p>

3.3 Concluding remarks

In summary, the algorithm developers require the testing of IT workload, thermal and power management, and their co-operation and coordination with each other. The numerical model must cover a wide range of scope and dynamic interaction between each domain. The proposed closed-loop concept that enables comprehensive testing requires a numerical model, which can be integrated into a wider simulation-tool chain and can provide an “online” interactive response in a reasonable time. The wide scope and time constraints likely compromise the resolution of selected sub-models.

The highest resolution class is hardly applicable in our case, because it does not support an interactive multi-domain aspect and analysis at system level. The operational phase of this project and multi-scale aspect require analysis at the component level for most of the systems; therefore, the lowest class can also be disqualified for these domains.

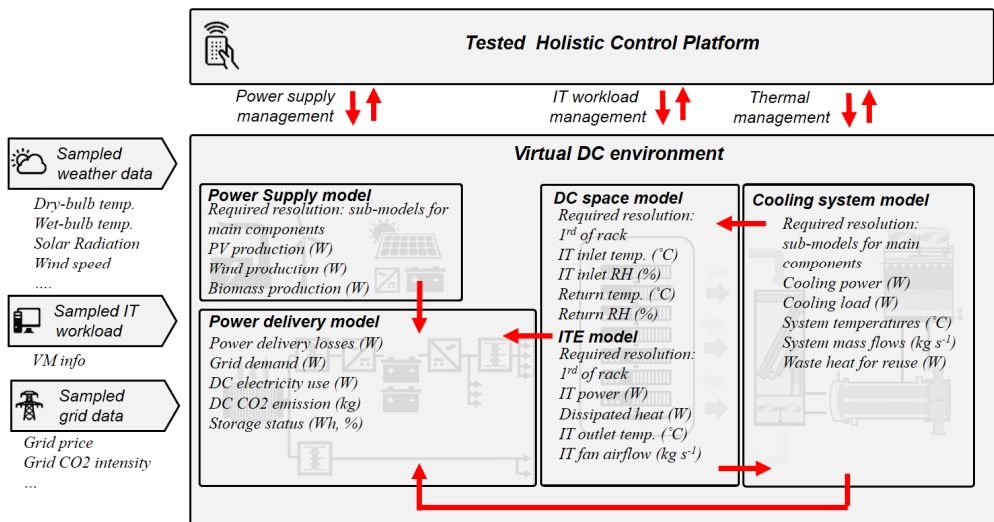


Figure 3-7 Conceptual model: outputs and internal communication of sub-models of the virtual DC environment

Indeed, the selection of resolution level may vary for each sub-model. For instance, the power and thermal systems need to be decomposed and represented at the level of individual components to provide full control capability of the system. However, the holistic energy management does not actuate these components directly but delegates setpoints to the local control layer, which is part of the virtual DC environment. Therefore, the power and thermal systems can be simplified in some situations (e.g. modelling of the hydronic system is usually not required for the representation of cooling system). In general, these systems can be modelled at mid-lower level of resolution.

On the other hand, the modern thermal management and in particular the thermal aware computation strategy require high resolution temperature monitoring of the DC space at the level of 1/3rd of each rack. In order to connect the server/rack scale with room/building scale, the DC space model requires a mid-higher level of resolution of this domain, which allows for the simulation of the DC space for the given geometry and with relatively high spatial resolution (1/3rd of rack). Figure 3-7 depicts the final conceptual model, considering modelling scope and resolution and indicates the main information exchange between each sub-system and required inputs from external data.

4 Development of the virtual data centre environment

Chapter 4 presents possible modelling approaches that can be suitable for the presented conceptual model of the virtual data centre (DC) environment. As described in the previous chapter, the five main systems: IT equipment, DC environment, cooling system, power delivery and power supply systems, must be numerically represented. This chapter mainly deals with selection and development of simulation models. In addition, the required inputs for these models are discussed in this chapter.

4.1 Methods and tools for data centre energy modelling

As mentioned, the conceptual model is also used for communication between simulation developer and simulation user. After agreement on the conceptual model, the process of implementation can start to create the simulation (executable) model. This section discusses currently available tools which are used for data centre or building modelling.

Although dynamic energy simulation of DC applications appears to have great potential, this potential is underutilized due to a lack of awareness across the DC community. Typically, DC energy modelling has been focused on component-level studies, specifically on DC air-distribution using high-resolution models such as Computational Fluid Dynamics (CFD). [52]. The requirement to understand the DC infrastructure at system-level presents the opportunity for an application of other tools.

The testing and commissioning of a novel operational platform requires reasonable computational time. On the other hand, new generation sensor networks allow higher resolution monitoring, which is necessary for advanced airflow assessments and indoor environment control in modern DCs [20]. In order to satisfy the limited computational time, a minimum number of temperature nodes should represent the virtual DC environment. This number is related to the spatial resolution of the DC space, where larger numbers of computational nodes lead to more demanding computation. An optimal level of resolution and corresponding simulation approach need to balance the requirements of transient behaviour on one hand and on the other hand enable assessment of advanced airflow management driven by high resolution monitoring (e.g. indoor temperature monitoring of 1/3rd of a rack). High-resolution models such as CFD models are commonly used to analyse the design of the DC space arrangement in academia as well as in industry. As mentioned, numerous research studies have covered high resolution modelling of DC airflows and heat transfer [52]. The main outcome of these studies is that the arrangement of DC space benefits from the separation of cold and hot aisles. In fact, several specialized CFD software programs for DCs are currently available for the evaluation of DC space configurations. However, high resolution models are solely used for the design of the DC space and mainly for steady-state simulation of a few critical cases [83]. This does not match the multi-domain scope, nor the operational phase of the current purpose definition. The requirements such as transient response and possibility to integrate models of different domains (e.g. IT equipment, cooling or power supply) are difficult to satisfy with high-resolution models.

At the other end of the resolution spectrum of the simulation model, there are modelling approaches that cover the overall complexity of DC systems from the chip to the cooling tower levels [84]–[86] based on approximate or

empirical relationships and simplified models. These empirical approaches are usually valid only for specific cases and the models are rarely transferable to other DC configurations. Therefore, this approach is not compatible with our understanding of the virtual DC environment, because the virtual DC laboratory would prevent easy adaptation to other DC specifications. Moreover, these models are not able to sufficiently represent the temperature distribution in the DC space, which is crucial for modern control strategies such as thermal-aware workload allocation [37]. Transient white box modelling approaches fulfil the requirements to create a virtual DC environment for the testing of novel enhanced operational strategies. This virtual DC environment should be a “stand alone” model with minimum need for preliminary measurements. Building Energy Simulation (BES) tools, developed over the last 50 years, offer sophisticated computational engines for modelling building physics and building services systems. BES tools allow simulation of transient behaviours of buildings and HVAC systems, as well as advanced systems such as on-site renewable energy systems. In addition to this, there is usually sufficient support for co-simulation or integration of user models [6], [77].

Even though a BES approach satisfies most of the requirements, BES tools have rarely been used for DCs. Whilst BES tools are unknown to the majority of the DC community, the BES community is aware of their potential. This can be demonstrated by the addition of special energy models for data centres in Energyplus (version 8.3, released 2015) [87] or the DC library now available for Transient System Simulation Tool (TRNSYS, renewIT library, 2016) [88]. Concerning the application of BES for DC modelling in the past, Phan and Lin [89] investigated a multi-zone representation of a DC with cold and hot aisle arrangement in Energy Plus. Also, the modelling of airflow in DC space using Modelica was recently addressed [90]. Similarly, Salom, Oro et al. [91], introduced simplified dynamic modelling of DC space. In addition, the same

team [92] also investigated DC modelling to support the integration of renewables into the DC using TRNSYS [93].

As shown, there are several BES tools that can be used for the defined purpose. All of these tools are capable of providing sufficient support for the modelling of the virtual DC environment. TRNSYS was selected because it is a well-established tool that allows the modelling of various type of energy systems including building physics, HVAC, electrical and control systems. In addition, TRNSYS is compatible with many other simulation environments (e.g. Matlab, CONTAM, etc.), where user-defined models or scripts can be co-simulated.

Modelica could offer similar modelling support. However, many Modelica libraries related with building physics and HVAC are still under development. Therefore, TRNSYS was found to be the most suitable option. Even though energy plus is a well-known tool in building physics modelling, there are some limitations in its ability to model systems adequately because the predefined configuration of the system often have to be followed. In contrast, TRNSYS offers higher flexibility in terms of system modelling.

Although BES was found to be a suitable approach for testing and commissioning of novel control strategies because it allows dynamic energy simulation of various systems, the typical discretization of rooms is one temperature node per room (zone). This spatial resolution is not sufficient for the DC case due to the cold and hot aisle containments and strict temperature zoning. The other issue is with representation of bypass and recirculation phenomena related with the heterogeneous heat gain profiles across the space as a result of IT utilization. Therefore, a DC space model needs to be represented by several temperature nodes. A multi-nodal method capable of representing the required level of resolution needed to be investigated. Existing models of IT, cooling and power supply devices including renewables can be

used. The main challenge using BES tools is to achieve accurate representation of the temperature distribution in DC space.

4.2 Modelling of the data centre environment

4.2.1 Specifics of data centre energy modelling

The previous section discussed the reasoning and benefits of using BES. BES tools were predominantly developed to investigate office and residential buildings, but the scope of BES tools has recently been extended for use in other building types. While the DC has similar physical phenomena as other building types, there are several specific phenomena which must be taken into account in DC modelling. Before the individual models are described, the key differences between modelling “regular” building types and DCs are elaborated.

Primarily, the DC space is not designed for human occupancy. The DC space is mainly occupied by IT equipment; therefore, the indoor environment quality requirements differ considerably from houses and office buildings. For instance, there is no need for daylight or specific levels of fresh air, thus window opening, glazing properties, shading, and window solar gains do not need to be considered in the model. Similarly, particle pollution levels are not of interest in this study. The pollution level is of course an important aspect of DC indoor quality since polluted air can cause serious damage to IT equipment. However, assuming proper maintenance, this aspect has minimal consequences for DC energy demand, especially in the studied cooling system with air recirculation. For the system-level energy modelling presented in this study, the pollution level is assumed to always be satisfactory.

The indoor environment quality for “holistic” system modelling is largely determined by the required operational conditions of individual IT equipment (ITE) in terms of temperature and humidity ranges, which are to some extent

similar to thermal comfort requirements for human occupancy [94]. The ASHRAE guideline mentioned in section 2.2 specifies that the recommended operational conditions are in the range of 18-27°C for temperature, and in the range of 30-60% for relative humidity for all classes of ITE [47].

In contrast to “regular” building types, the temperature distribution is very different in the DC. While a relatively homogenous temperature distribution is required across the whole living or working space, the DC space is strictly divided into cold and hot aisle regions by rack arrangement, as also mentioned in section 2.2. The temperature difference between these cold and hot regions can differ in the range of 5-10°C [53]. Therefore, the DC space cannot be truly represented by one temperature node with an assumption of well-mixed air in the zone. The DC space must be represented by multiple zones according the cold and hot aisle regions.

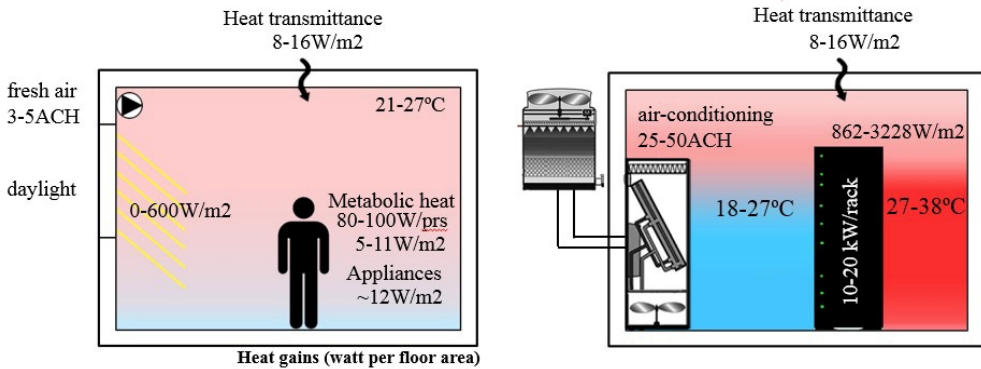


Figure 4-1 Office versus DC indoor environment

The DC space houses numerous IT equipment. The ITE dissipates an enormous amount of heat in comparison with typical office heat gains. For instance, the typical office space has internal heat gains in the range of 5.4 to 21.5 W m⁻², intermittent solar gains of up to 600 W m⁻² and related air change of up to 4 h⁻¹ [14], where heat transfer is mainly driven by natural convection with buoyancy effects.

Contrary to typical office spaces, the internal heat gains of DC space are relatively constant and in the range of 862-3228 W m⁻² [40]. The heat dissipation is concentrated around the chip, which is an area of a few centimetres, and the heat needs to be mechanically ventilated from the servers. The internal airflow of each piece of ITE is usually in the range of 190 - 290 kg h⁻¹ per kW of heat gain [95]. This heat is rejected from ITE to the DC space, where the cooling system must ensure the required operational conditions. Thus, the typical air change rate in the DC space is approximately 10 times higher than in an office (25-50ACH). The mechanical ventilation of individual ITE and the huge air-change rate in the DC room achieved by Computer Room Air-conditioning (CRAC) units indicates that the heat transfer is mainly driven by forced convection.

Table 4-1 Main difference between “regular” building and data centre [94], [96],[97]

parameters	“regular” building	data centre
indoor quality requirements <ul style="list-style-type: none"> • temperature range (°C) • relative Humidity (%) 	thermal comfort 21-27 (°C) 30-60 (%)	operational conditions 18-27 (°C) 30-60 (%)
heat gain characteristic <ul style="list-style-type: none"> • solar heat gains (windows) • occupancy (human) • appliances • heat transition (walls) 	mixed load 0 - 600 W m ⁻² 5 - 11 W m ⁻² 8 - 12 W m ⁻² ~ 8-16 W m ⁻²	appliances dominated load NAN NAN 862 - 3228 W m ⁻² ~ 8-16 W m ⁻²
air distribution characteristic <ul style="list-style-type: none"> • convection • cooling system • air change (ACH) 	mixed natural/forced mixed natural/mechanical 2-5 (h ⁻¹)	forced mechanical 25-50 (h ⁻¹)
internal thermal capacitance characteristic <ul style="list-style-type: none"> • max. imposed weight • estimated additional internal thermal capacitance 	190-230 (kg m ⁻²) 175-210 (kJ K ⁻¹ m ⁻²)	479 - 958 (kg m ⁻²) 300-600 (kJ K ⁻¹ m ⁻²)

Another important characteristic for dynamic simulation is the imposed weight and related thermal capacitance. While the maximum imposed load in an office is usually 239 kg m^{-2} , the imposed load in a data centre can range from 479 to 958 kg m^{-2} . The related thermal capacitance is estimated based on the imposed load and the thermal material properties of housed objects (furniture or IT equipment). The differences discussed above are summarized in Table 4-1.

4.2.2 IT equipment modelling

One of the main sources for the characterization of the dynamic behaviour were measurements conducted in the wider framework of the Genic project. The measurements were conducted by one of the partner of the Genic project, T.Scherer, (Courtesy of IBM Research, Zurich). Two types of servers, namely the IBM System x3250 M4 and the IBM System x3650 M4, were measured. The presented measurements illustrate the processes to be modelled. The experiment was performed for the IBM System x3650 M4, where the CPU load was increased from idle to full load in steps of 20 % CPU utilization and then returned to the original idle state in a single step. The inlet air temperature remained constant at 18°C during the whole experiment and the CPU frequency was fixed at 3200 MHz.

The first plot presented in Figure 4-2 shows the relationship between CPU utilization and IT power. The average CPU utilization is plotted with a dark blue line, while the maximum and minimum values of the individual cores are plotted with light blue lines.

The second plot focuses on system temperatures. The average CPU temperature is plotted with red lines, while the minimum and maximum temperatures of the individual cores are plotted with orange lines. The data from 3 nodes at system outlets are plotted with purple lines and inlet temperature is plotted with a blue line.

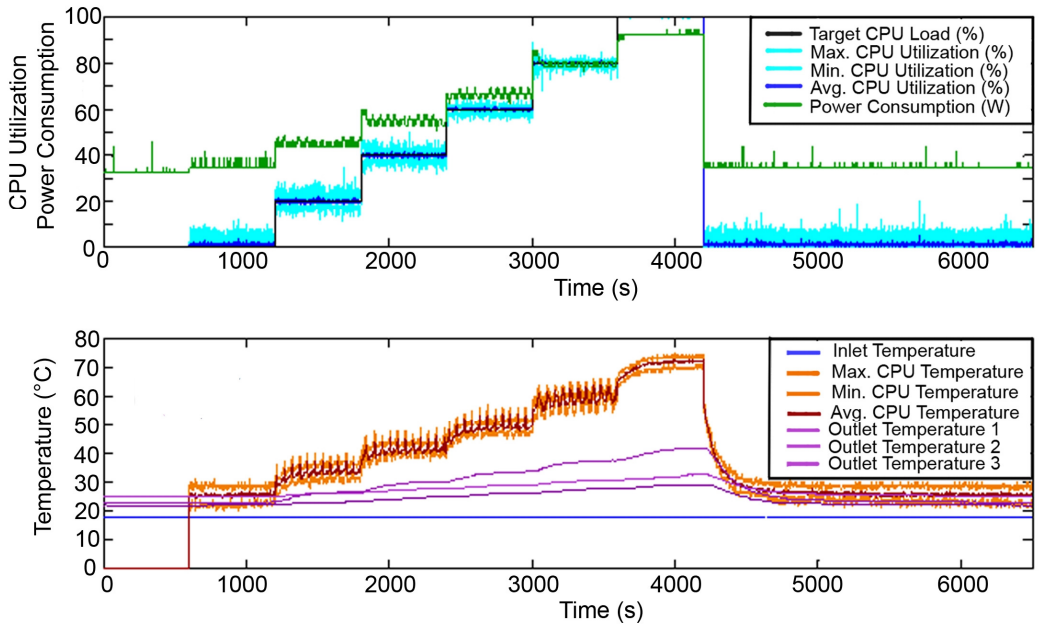


Figure 4-2 Step response of power and temperature to varying CPU utilization for the IBM System x3250.

While a linear relation can be observed between CPU utilization and electrical power, a delayed response is likely caused by the thermal capacitance of the server, which is observed in the outlet temperature measurements. Figure 4-3 shows the measured average power consumption for different levels of CPU utilization at steady state. For the two considered systems, the power consumption increases linearly with the CPU utilization. The linear approximation is depicted with a green line. The fan power consumption of 0.7 W for the x3250 server and 2.0 W for the x3650 server, respectively, is included in the idle power consumption.

The fan speed is controlled based on the measured inlet air temperature. At higher inlet air temperatures, the fan speed and consequently the power consumption (proportional to the fan speed cubed) increase significantly, as illustrated in Figure 4-4. With a constant inlet air temperature of 18 °C,

however, the fan speed remains constant over the whole CPU operating range, i.e. it is independent of the CPU utilization.

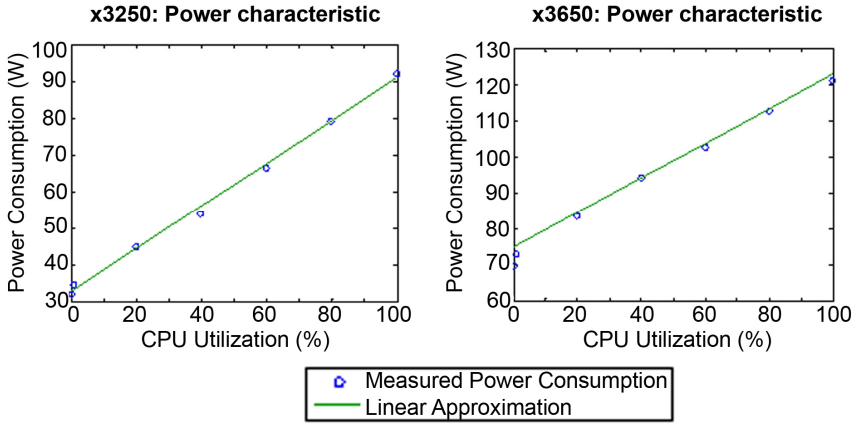


Figure 4-3 Power consumption versus CPU utilization

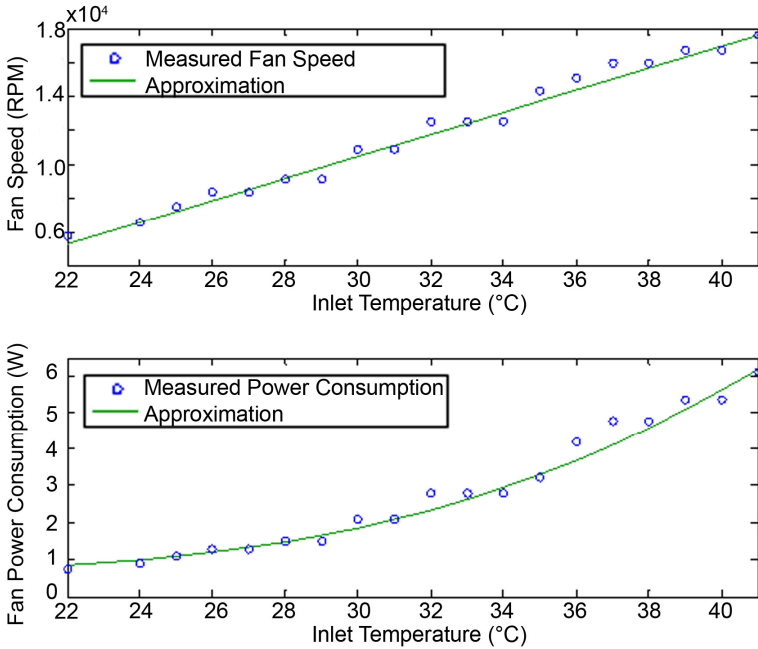


Figure 4-4: Fan speed and fan power consumption as a function of the inlet air temperature.

It should be noted that for safety reasons, the internal controller would run the fans at maximum speed if a defined CPU threshold temperature were exceeded. However, at low inlet air temperatures this is not relevant, as the CPU temperature remains well below the threshold temperature, even if the server continuously runs at maximum load.

The ITE model is defended based on observed processes and literature [43], [98]. A server or even a group of servers, called a “box”, can be represented by a model such as that depicted in Figure 4-5. The ITE model can be scaled according to discretization requirements of the DC space model.

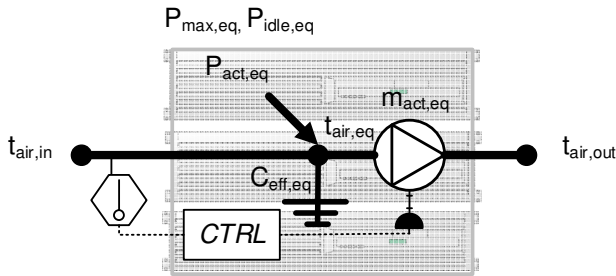


Figure 4-5 Schema of ITE model

The model requires parameters such as nominal (maximal) power load $P_{max,eq}$, idle power load $P_{idle,eq}$, effective thermal capacitance of ITE $C_{eff,eq}$ and definition of control function of the internal fan. The model inputs are utilization or actual power $P_{act,eq}$ of represented servers and inlet temperature. The outlet temperature and airflow are calculated as the main output.

In the recommended inlet temperature range, the actual workload and associated heat dissipation can be approximated linearly as a function of CPU utilization ut (-). The linear behaviour observed in Figure 4-3 can be described by equation 4.1.

This relation can also be found in literature [43],[86].

$$(4.1) \quad Q_{diss,eq} \approx P_{act,eq} = (P_{max,eq} - P_{idle,eq}) \cdot ut + P_{idle,eq}$$

The nominal load $P_{max,eq}$ can be found in the technical specification of each device. The idle load $P_{idle,eq}$ is not always specified, but it can be estimated at 20 - 40% of nominal power [43] based on server type and year of release. As described in literature [98], the speed and related electricity consumption of internal server fans can vary depending on the increase of the inlet temperature. Despite this effect, power consumption of internal fans is assumed to be constant and in the recommended range of inlet temperature. This item is included in idle load. If the inlet temperature exceeds the upper bound of recommend range of inlet temperature, the assumption of constant power consumption of the fan is not valid due to quadratic growth. shown in Figure 4-4. The actual power needs to be corrected accordingly.

In the description of each box model, the outlet temperature can be assumed to be the temperature of the equipment $t_{eq} \approx t_{out}$. Further, when the box is integrated into the DC space model, these temperature nodes can vary.

The temperature behaviour shown in Figure 4-2 can be represented by an energy balance described by equation 4.2).

$$(4.2) \quad C_{eff,eq} \frac{dt_{eq}}{dt} = Q_{diss,eq} + \dot{m}_a \cdot c_a (t_{in} - t_{eq}) + Q_{loss,eq} + \dots$$

The temperature delays on step change of utilization and actual power load are modelled using the effective thermal capacitance $C_{eff,eq}$ (J K⁻¹). This parameter can be estimated based on the weight of the box and specific heat capacity of the server. The specific heat capacity of the server can be deduced from the material decomposition of a typical server shown in Figure 4-6 [99]. The specific heat capacity of the server can be assumed to be between 580-630 J kg⁻¹ K⁻¹ based on the weighted average of material properties.

Again, the server is cooled down by forced convection. The airflow is controlled based on the inlet temperature in order to ensure suitable operating conditions for the CPU and other embedded electronics. The control logic can differ according to type and manufacturer of the IT equipment. Basically, there are two typologies of the internal fan control: constant speed and variable speed. While control of a constant speed fan is set by the manufacturer of individual server, the variable speed is dependent on inlet temperature and settings of the internal control function $\dot{m}_{i-j} = f_{n_{ctrl}}(t_{in})$. In general, the internal airflow is in the range of 190 - 290 kg h⁻¹ per kW of heat gain from ITE [95]. In both cases, the internal fan control has an emergency stage, where the internal controller runs the fans at maximum speed if a defined CPU threshold temperature, which is usually 80°C [100], is exceeded.

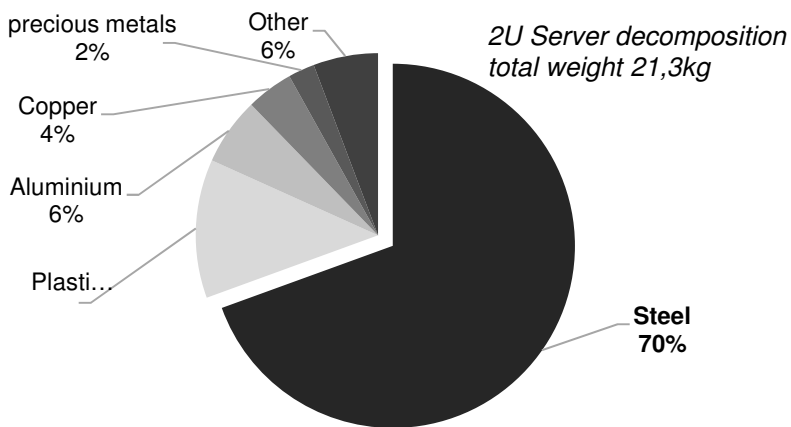


Figure 4-6 server material decomposition (based on [99])

In summary, the ITE model is integrated into the DC space model, which includes not only the described convective heat transfer, but also additional conduction and radiation transfers to the DC space. The energy model of the dynamic ITE must pay close attention to two characteristics of the modelled process: (i) the ITE brings additional heat capacitance into the space, which

causes the delayed change of the temperature in time, and (ii) the ITE often has autonomous control mechanisms for temperature regulation related with internal airflows. The estimate of internal airflow and its control is important for capturing bypass and recirculation phenomena in the DC space.

4.2.3 Data centre space modelling

The representation of the DC space is essential for the modelling of widely used air-based cooling of IT equipment. Basically, the DC space model provides a necessary bridge between the ITE model and the cooling devices and power delivery models. This bridging is essential in order to capture a higher level of complexity at multiple scales, as discussed in the previous chapter. Here, the dynamic DC space model represents the level of the room and provides the necessary link between the rack-to-chip levels represented by the ITE model, and the models related with the building level such as the cooling devices model and power delivery model.

The efficiency of air distribution in the DC room and the presence of bypass and recirculation phenomena significantly influence the efficiency of the cooling system and DC as whole. The mixing of the return air with the supply air can decrease the cooling efficiency, which may lead to an increase of cooling electricity consumption in the range of 20 - 40%, which may in turn result in up to a 15% increase in total DC electricity demand [101]–[103]. According to literature [101]–[103], the air distribution phenomena have a relatively high impact on DC efficiency, and thus the DC space model is also very important in the modelling of overall DC processes.

The efficiency of air distribution in DCs has been extensively studied with CFD in the last decade. The findings from several CFD studies have been expertly summarized by Rambo and Yogendra [52]. Two key findings of these studies are of particular relevance to the present work. First, air distribution within a DC space is best managed via a cold and hot aisle arrangement. Second, and

related to the first, is that air distribution can be improved by imposing physical barriers between the cold and hot regions in the DC space, which is referred to as cold and hot aisle containment. These and other findings resulting from CFD analysis are now routinely applied in practice.

However, the application of these high-resolution models is limited by their large computational demand. The results from these simulations usually capture only one steady-state step in time and do not take into account the changes in thermal conditions resulting from other DC systems (e.g. dynamic behaviour of IT equipment, variable supply temperature from cooling system etc.). Such simulations are commonly used to predict only a few selected scenarios in given conditions (e.g. a different layout of the DC), which are compared to find the best DC arrangement [83]

These high resolution models can be simplified due to the forced convection environment, which is typical to the DC environment, by using the so-called potential flow modelling [104], [105]. This simplified method makes the dynamic high-resolution simulation of DC space affordable in terms of computation demand. However, this method, and related tools, are still mainly focused on air distribution and ITE arrangement, and thus do not typically allow dynamic co-simulation with other DC systems, which is necessary in order to fulfil the given requirements for the virtual DC environment.

In contrast to the high-resolution modelling mentioned above, BES tools can capture processes and interactions between the multi-domain systems. In terms of DC space modelling, BES tools remain on the opposite side of the resolution spectrum. While the CFD tools represent the DC space using thousands of computation nodes, the typical resolution of BES tools is one computational node per room/zone. To reiterate, this resolution is not sufficient for the representation of bypass and recirculation phenomena in the DC space.

A simplified modelling approach representing bypass and recirculation phenomena has recently been introduced by Oro and Salom [91]. This approach relies on single-zonal representation of the DC space, but the supply and return temperature of cooling devices is corrected by constant efficiency factors of air distribution (bypass and recirculation mass flow ratio) [106].

Since the publication of CFD results, it is known that the DC space should be divided into cold and hot regions which have considerable temperature differences. Furthermore, the supply and return temperatures of the CRAC units may differ from the inlet and outlet temperatures of ITE due to ineffective DC arrangements and the associated lack of air distribution efficiency. Thus, the multi-zonal representation of the DC space is a necessary condition for the current research. The cold and hot aisle zoning was first applied in BES research in a study by Phan and Lin (2014) [89]. However, this study assumes containment of aisles without air mixing, and it does not capture wanted recirculation and bypass phenomena related with air distribution efficiency.

This research investigates two different levels of resolution for the DC space modelling, which both belong to the category of medium level of resolution. Both models use a multi-zonal airflow network approach in order to predict the airflow distribution. The multi-zonal airflow network is described in detail below:

- The DC space model with lower mid-level resolution, which is referred to hereafter as low-resolution model, is essentially a combination of the simplified multi zonal approach presented by Phan and Lin [89] and air distribution efficiency approach for a single zone presented by Oro [91]. The DC space is sorted into zones according to the temperature potential. The zones are defined by volumes, but the exact DC geometry is not followed. For this resolution, the DC room is divided into the following 5

zones: underfloor plenum, cold aisle, racks, hot aisle and overhead plenum space. The zones are connected to an airflow network to predict the bypass phenomena. The recirculation cannot be captured by the airflow network at this level of resolution. Therefore, the recirculation is given by empirical corrections regarding air distribution efficiency. This resolution can provide a sufficient representation of the DC space for most of the system-level applications, such as annual energy analysis of the overall DC system. However, this model cannot predict spatial temperature distribution in the DC space based on DC geometry and rack arrangement. A greater level of detail may be required for the testing of some of the modern DC control algorithms.

- The DC space model with higher mid-level resolution, which is referred to as the high-resolution model in this section, represents the DC space at the level of 1/3rd of rack. This resolution is in agreement with the resolution of modern DC space monitoring, while still allowing for co-simulation with other DC systems and external algorithms. This DC space model uses the higher spatial discretization of the multi-zonal airflow network method [107], enabling characterization of the DC space arrangement. This method is inspired by the potential flow approach and works with a similar assumption to that of the forced convection pattern in the DC space.

Both low- and high-resolution models and an application of the multi-zonal airflow network method are further described in this section.

There have been attempts to use the airflow network method for multi-nodal office rooms in the past. These attempts concluded that the standard definition of the airflow network is not able to fully cover the natural convection phenomena for a multi-nodal resolution level. Thus, additional functionalities based on empirical data were added [108], [109]. However, again, the

characteristics of the DC space differ considerably from those of typical office spaces (see in Figure 4-7).

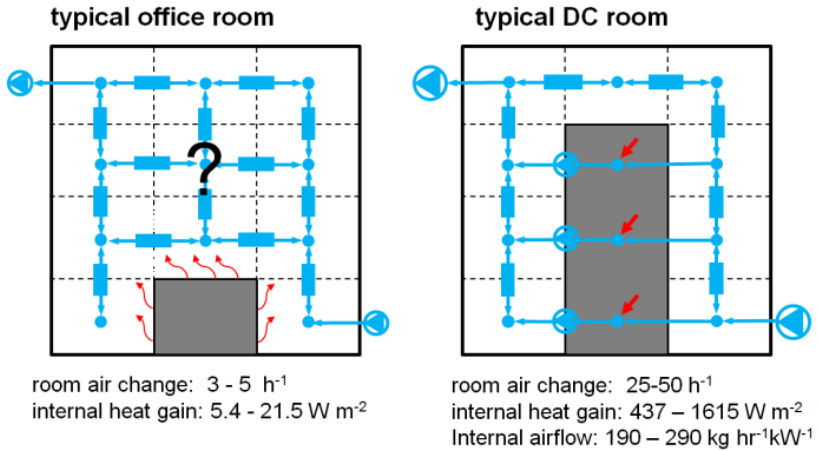


Figure 4-7 Multi-zonal airflow definition: “regular” building versus data centre

Contrary to typical office spaces, the DC case can take advantage of a multi nodal airflow network approach. CRAC units ensure air change approximately 10 times higher than in an office. Moreover, to reiterate, heat dissipation from IT devices placed in racks needs to be mechanically ventilated from servers. Ultimately, these observations demonstrate that the DC space is strongly driven by forced convection. This conclusion allows for the definition of multi-zonal airflow networks, where numerous nodal connections are already known and given by the ITE or the cooling system models. The potential airflows can be predicted even when buoyancy effects are neglected because for such a rough spatial discretization there are still enough defined airflow connections for each node, and it is possible to estimate unknown bulk airflows based on the law of continuity. The method can be divided into two parts: Airflow modelling and Energy modelling, which are coupled together. Regarding the tools used, airflow modelling is carried out in CONTAM and linked to energy

simulation in the TRNSYS environment [93], [110]. The overall concept will be explained using simplified examples for both low- and mid-level models.

In the lower mid-resolution modelling, the zones are represented with nodes with volumes in tens of m^3 . These zones are grouped according to DC environment conditions (e.g. cold aisles, hot aisles etc.), so they don't necessarily follow the DC layout and geometry. In contrast, in the higher mid-resolution model, the typical volume of nodes is 1 m^3 or higher. In the ideal case, at least two surfaces (e.g. an external wall and internal surface of a rack) should be assigned to each temperature node in order to avoid a large number of unknown airflow connections for the airflow network solver.

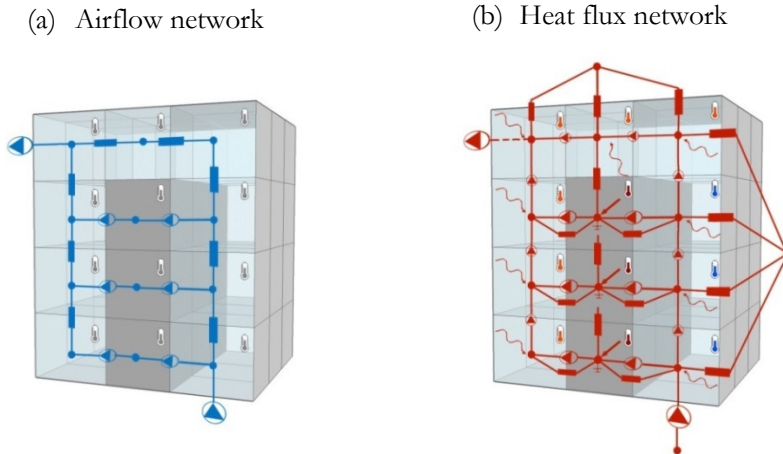


Figure 4-8: Typical (a) airflow network modelling and (b) heat flux network for multi-zonal

Let us imagine a DC with one row of racks. A section of the example DC with typical airflow and heat flux network is shown in Figure 4-8. In order to capture the room geometry, the networks must be extended to the 3rd dimension. However, this multi-zonal method still leads to relatively rough irregular spatial discretization with respect to the specific layout of the DC. This means each

node (zone) may have a different volume of air depending on the specific geometry and arrangement of the DC space.

Airflow modelling

The effect of the previously mentioned rough discretization can be demonstrated by the example DC section of the airflow network, where the airflow network has enough defined connections by internal airflow through the IT devices and CRAC unit and all unknown airflows can be calculated based solely on the mass continuity formula.

If the airflow network is extended across the whole space, additional unknown connections are added, and an iterative process is necessary to arrive at a numerical solution. Each unknown connection between air nodes is defined as a specific airflow crack or opening (representing floor tiles), or as a specific power law with the same parameters for “free space connection” [6, Ch. 5].

The specific power law is shown in equation 4.3 as a generalized formula for the connection description within the airflow network:

$$(4.3) \quad \dot{V}_{i \rightarrow j} = C(\Delta P_{i \rightarrow j})^n$$

Where $\dot{V}_{i \rightarrow j}$ ($m^3 s^{-1}$) is volumetric flow between nodes, $\Delta P_{i \rightarrow j}$ (pa) is the pressure drop, C ($m s^{-1} Pa^{-n}$) is an empirical “permeability” constant and n is the power law exponent. The recommended setting for “free connection” is $C = 0.83$ and $n = 0.5$ [108]. By using equal parameters of the power law for each connection, a forced airflow pattern driven by known airflows in the space is guaranteed.

Regarding the preliminary assumptions that the airflow pattern is strongly forced and the buoyancy effect is neglected for the given spatial discretization, the airflow pattern is calculated for each step as isothermal.

The ideal gas law is used for each node in the network to yield equation 4.4

$$m_i = \rho V_i = \rho \frac{P_i V_i}{RT} \quad (4.4)$$

Where m_i (kg) is the mass of the air in zone i , V_i (m^3) volume of air zone i , P_i (pa) pressure in zone i , T (K)~const. zone temperature, and $R=287.005$ (J $kg^{-1}K^{-1}$) is the gas constant for dry air.

The quasi-steady state airflow between zones has to satisfy the conservation of mass (as shown in equation 4.5), which implies that air can neither be created nor destroyed within a zone.

$$\sum m_{i,j} = 0 \quad (4.5)$$

When considering multiple zones, the solution leads to a system of nonlinear algebraic equations. The Newton-Raphson method [111] is used to numerically solve a defined system in the Contam tool. In 1989 Walton laid the foundations for the development of the Contam solver and airflow network analysis [112]. The last update of the Contam tool was completed in 2005 [113].

To summarize, in this use-case, an airflow network method is used to estimate the isothermal air distribution. This calculation is based on the pressure potential given by the massive CRAC airflow and also on the internal airflows through IT devices. This airflow pattern is passed to the energy model, which calculates the temperature distribution for a given time-step.

The low-resolution model requires a correction for recirculated air. This correction is needed due to the averaging of the pressure over the large volume of a zone. For instance, the cold aisle zone, where the air is supplied, is always over pressurized compared to the average pressure of the other zones at this level of resolution. The resolution is not detailed enough to represent the DC geometry and related local pressure conditions. Thus, low-resolution does not allow the airflow network to capture the recirculation effect. The modelling of

recirculation is simplified, and it uses an air distribution efficiency factor. Factors such as recirculation mass flow ratio [106] or Supply Heat Index (SHI) factor [114] can be used for the correction. Similarly, Oro applied these factors for single zone representation [91]. The recirculation factors can be stated based on empirical measurements, CFD simulations or values in the literature. The depicted airflow network in c for the high-resolution model already has sufficient resolution to address the bypass and recirculation phenomena based on the given geometrical arrangement. The resolution of 1/3rd of rack is detailed enough to represent the pressure level surrounding each rack and the potential air flow in the DC space. On the other hand, zones related with 1/3rd of rack are still rough enough to predict bulk airflow transfers between zones while neglecting buoyancy and stream effects. The multi-zonal airflow network does not support as fine a discretization as is possible in CFD analysis, for example. At this level of resolution, the airflow network solver does not typically contain a computational engine to represent the buoyancy, stream or turbulence effects at play.

Energy modelling of the data centre space

The energy modelling is similar for both low- and high-resolution models. The temperature distribution across the DC space is influenced by several energy fluxes. Different characteristics of heat transfer are indicated, which can be drawn as an energy flux map, shown in Figure 4-8.

Below, the individual heat transfer characteristics are briefly described.

- The heat transfer between DC space and the ambient environment is primarily via conduction through external walls. The conductive heat transfer is represented by red rectangles in Figure 4-8. In cases where the ambient environment is conditioned in a similar temperature range as the DC space (e.g. neighbourhood office room), the assumption of an

adiabatic boundary condition (i.e. no heat transfer between ambient) can be made.

- The convective heat transfer within the internal zones of the DC space is defined by an airflow pattern and difference of air temperatures among internal zones. The airflow pattern is calculated using the airflow network method described above. The convective heat transfer between internal zones is represented by the fan symbol in Figure 4-8.
- The significant heat dissipation from IT devices may cause larger differences in surface temperatures between the racks and external walls. The surface temperatures and radiative heat transfer between rack and wall surfaces are also calculated within all internal zones. The DC space is characterised by longwave radiation and this heat transfer is represented by thin wavy arrows in Figure 4-8.
- Internal heat gain from the heat dissipation of IT (i.e. thick straight arrow in Figure 4-8) is applied to the rack nodes. These zones are occupied by a large amount of IT devices. Therefore, additional thermal mass (i.e. grounding symbol in Figure 4-8) needs to be added to these nodes.

The fundamental heat balance for each node can be expressed mathematically as in equation 4.6. The most significant heat fluxes are included; however, the terms of the equation are slightly different for each node.

$$C_{eff,i} \frac{dt_i}{d\tau} = \dot{Q}_{i,trans} + \dot{Q}_{i,conv} + \dot{Q}_{i,LGrad} + \dot{Q}_{i,gain} + \dot{Q}_{i,cool} + \dots \quad (4.6)$$

Where $C_{eff,i}$ ($J K^{-1}$) is the thermal capacitance of zone i , t_i ($^{\circ}C$) temperature of zone i , τ (s) is time, and $\frac{dt_i}{d\tau}$ is the derivation of zone temperature in time.

$\dot{Q}_{i,trans}$ (W) is heat transfer through solid constructions. One of the types of heat transfer is conduction, which is calculated by the transfer function coefficient method [115].

$\dot{Q}_{i,\text{conv}}(\text{W}) = \rho \dot{V}_{j \rightarrow i} c_{p,\text{air}} \Delta t_{j-i}$ is the convective heat flux from other zones, where $\dot{V}_{j \rightarrow i}$ is the results of the airflow network model.

$\dot{Q}_{i,\text{LGrad}}(\text{W})$ is the influence of long-wave radiation between surfaces on zone temperatures. This is calculated as a standard Star network model [116].

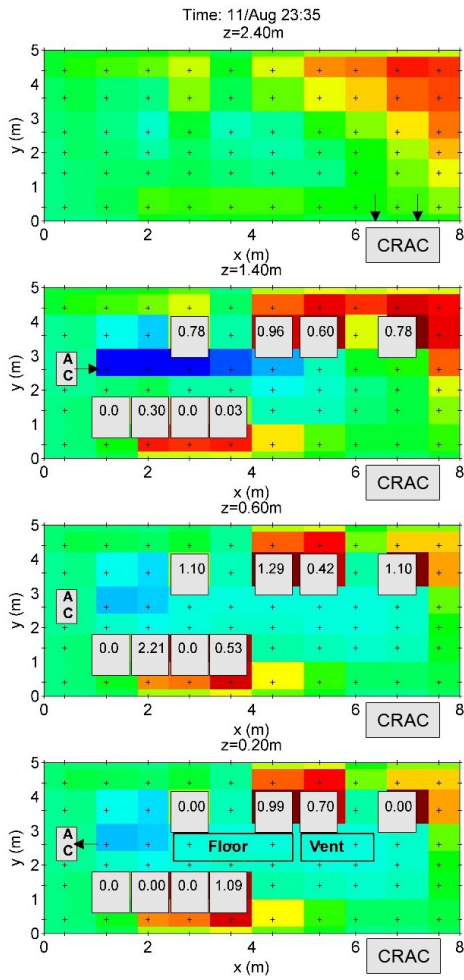
$\dot{Q}_{i,\text{gain}}(\text{W}) \sim \dot{P}_{\text{act,eq}}$ is the internal heat gain for zone i . In the case of a DC, a large majority of heat gain comes from the heat dissipation related to computational processes. This heat flux is applicable only for the rack (box) zones. The internal heat gains are simulated by the ITE model described above.

$\dot{Q}_{i,\text{cool}}(\text{W}) = \rho \dot{V}_{\text{CRAC}} c_{p,\text{air}} \Delta t_{\text{CRAC}-i}$ is heat flux from cooling devices. Where \dot{V}_{CRAC} and t_{CRAC} are the settings of the CRAC unit, and t_i is node of return air temperature. This heat flux is applicable only to zones that are influenced by the CRAC unit and is calculated by the cooling devices model. The inlet temperature and airflow are simulated by the cooling devices model, which is described in the following section.

Equation 4.6 is not complete. Additional heat fluxes can be taken into account according to current conditions, (e.g. direct short-wave radiation entering through windows, if applicable). However, the heat fluxes previously mentioned are most common for the DC case.

An example of the results generated by the DC space and embedded ITE models with a high level of resolution is shown in Figure 4-9. This figure shows a DC layout for four height levels (0.2, 0.6, 1.4, 2.4m) before and after post-processing of the results. The post-processing applies 3-D linear interpolation to represent the temperature gradients between nodes in the DC space. It should be noted that the interpolation is used in this thesis only for visualization purposes. The computational nodes used for evaluation of results are still indicated by black dots.

(a) Real level of resolution



(b) Linear resolution

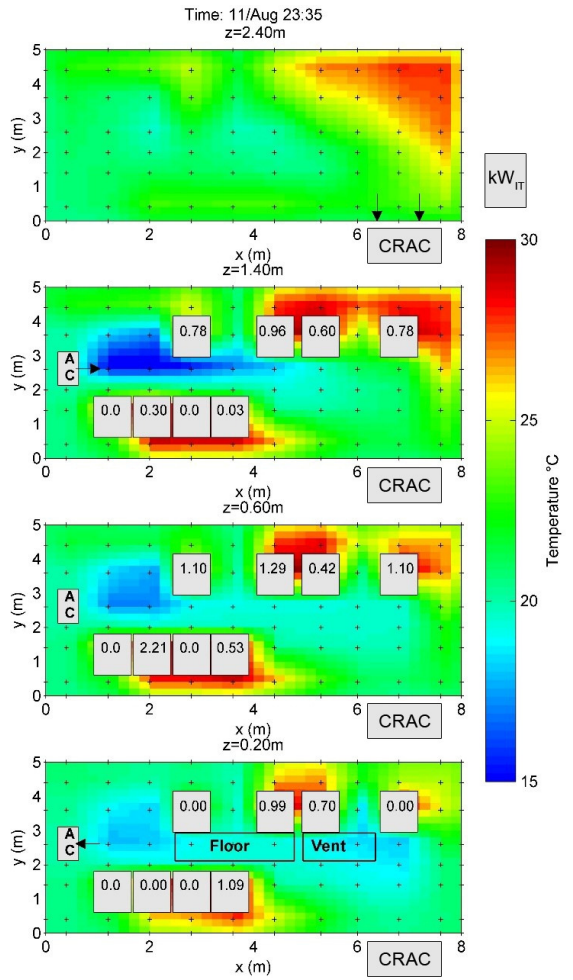


Figure 4-9 Multi-nodal airflow network level of resolution. (a) Real level of resolution
(b) Interpolated results (3D linear interpolation)

4.2.4 Cooling system modelling

While the ITE model and DC space model are relatively new for the BES community, cooling device modelling is similar to existing HVAC system models. An example cooling devices model is depicted in Figure 4-10 and Figure 4-11. The cooling system can be configured based on the technical specification of a real cooling system. The mathematical reference of the individual models is derived from related literature [117].

The components used to model the cooling system, which are described in this section, are grouped into two categories: air-side acting at room scale and water-side acting at building scale.

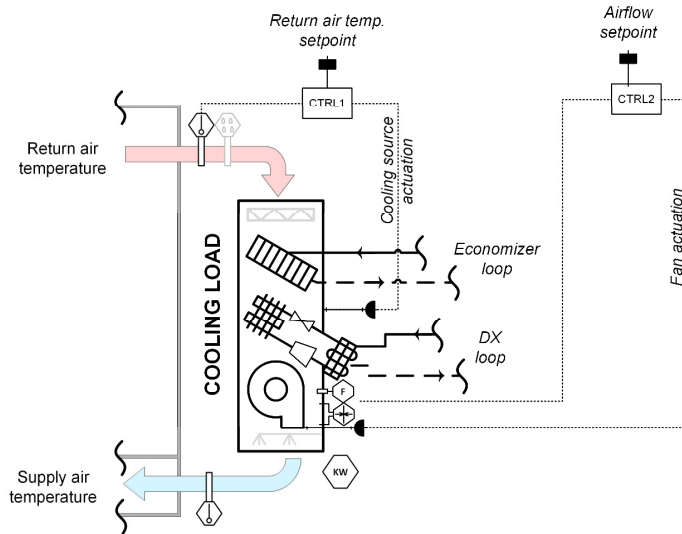


Figure 4-10 Scheme of the model of a cooling system (air-side)

Modelling of the air-side section

The supply air coming from the CRAC unit flows underneath the raised floor and enters the DC space through perforated floor tiles situated in the cold aisle between the two rows of racks. The air moves from the cold aisle through the racks, cooling them down. The used air is rejected into the hot aisle. Finally,

the used air from hot aisle returns to the CRAC unit. The CRAC unit draws the used air from the DC space from just under the ceiling. The air is conditioned (i.e. cooling) in the evaporator coil of the direct expansion (DX) unit and is then supplied back to the DC space.

Modelling of the water-side section

The condenser of the DX unit is cooled by a mix of water (80%) and glycol (20%) circulating in the cooling circuit. This cooling water has the potential to be used for heat recovery in order to supply the DC's waste heat to a nearby heating load (e.g. an adjacent office space). The roof-mounted drycooler ensures that the water entering the CRAC unit is at the required temperature by rejecting heat from the cooling water to the environment, if necessary. The components illustrated in Figure 4-10 and Figure 4-11 are listed and described in following tables. The mathematical description of the sub-models can be found in the mentioned literature based on the component identification number, which in the software is called "type".

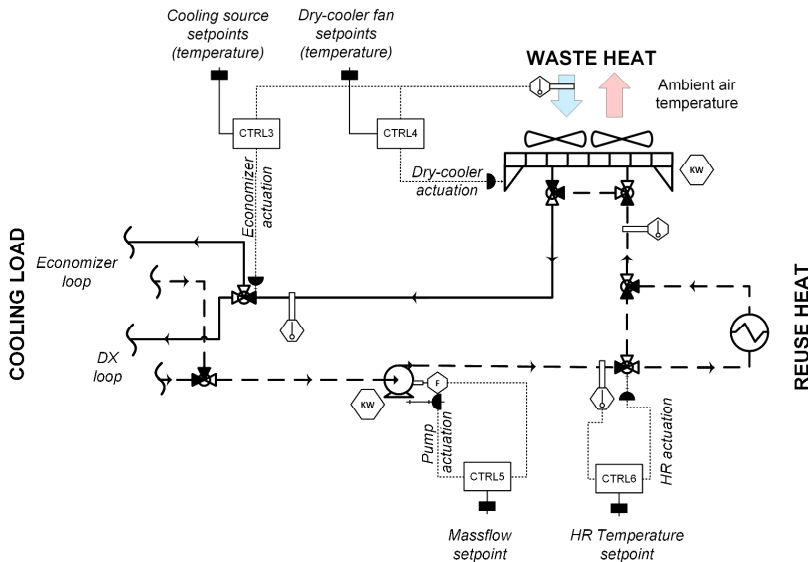
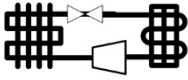


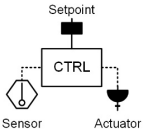
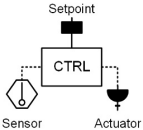


Figure 4-11: Scheme of the model of a cooling system (water-side)

Table 4-2 sub-model's description of the cooling system model (air-side)

component	description	component ID [117],[118]
<p>CRAC DX unit</p> 	<p>This component represents a liquid source refrigerant unit (i.e. heat pump and mechanical cooling). This model conditions warm and moist return air by rejecting the heat to a liquid stream. This model works based on a user-supplied data sheet containing catalogue data for (i) the normalized total and sensible capacity, and (ii) normalized power supply of the DX unit based on the entering cooling water temperature, water flow and air flow rates. The model requires parameters such as rated cooling capacity, power, mass flow rates, etc. The thermal and power output is calculated based on inlet conditions and user-defined data sheet.</p>	<p>multiple-stage Type – 919 single stage Type – 1247 [118]</p>
<p>CRAC Economizer coil</p> 	<p>This component represents a fin-tube heat exchanger (air–water). The inlet air is conditioned by rejecting the heat to the liquid stream. The simplified model uses a fixed value of the overall heat transfer coefficient to calculate the coil effectiveness.</p> <p>The detailed model outlined by Braun [119] states the coil effectiveness based on the NTU method [120] and the specification of the coil geometry.</p> <p>Since modelling of humidity control is not in the scope of this study, the simplified model of humidifier is used for most of the applications</p>	<p>Type – 5 Type – 52 [117]</p>
<p>CRAC fan</p> 	<p>This component represents a variable speed fan. The mass flow rate is linearly related to the control signal. Therefore, the required power for the given mass flow rate can be defined as any polynomial expression of the control signal.</p>	<p>Type – 111 [117]</p>
<p>control 1: cooling source actuation</p> 	<p>This component represents local control of a cooling source (DX unit or economizer) and is an N – stage (ON/OFF) controller. The cooling source is actuated based on sensing return air temperature and defined setpoints. A baseline control is represented by constant temperature setpoint.</p>	<p>N-stage Type – 1503 [118] 2-stage Type – 2 [117]</p>
<p>control 2: fan actuation</p> 	<p>This component represents a baseline control of the CRAC fan that provides a constant control signal to the fan actuator (fan component). The control signal can be further modulated by a higher level- management (e.g, N-stage or PI controller) based on IT inlet temperature.</p>	<p>N-stage Type – 1503 [118] 2-stage Type – 2 [117]</p>

. Table 4-3 sub-model's description the cooling system model (water-side): part I






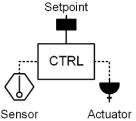
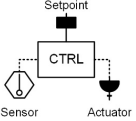
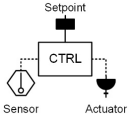
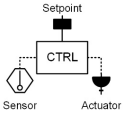
component	description	component ID [117],[118]
<p>pump</p> 	<p>This component represents a variable speed pump. The mass flow rate is linearly related to the control signal. Therefore, the required power for the given mass flow rate can be defined as any polynomial expression of the control signal.</p>	<p>Type – 110 [117]</p>
<p>dry-cooler fan</p> 	<p>This component represents a variable speed fan. The mass flow rate is linearly related to the control signal. The required power for the given mass flow rate can be defined as any polynomial expression of the control signal.</p>	<p>Type – 111 [117]</p>
<p>dry-cooler coil</p> 	<p>This component represents a generic crossflow coil model. This simplified model uses the fixed value of the overall heat transfer coefficient to calculate the coil effectiveness.</p>	<p>Type – 5 [117]</p>
<p>diversion and mixing valve</p> 	<p>This component represents the mixing and diverting of the fluid flow. The diverter is controllable.</p>	<p>Type – 11 [117]</p>
<p>heat recovery heat exchanger</p> 	<p>A heat recovery potential is estimated only for certain conditions given by heat recovery control (see below). The return temperature is cooled down in the heat exchanger, which separates the DC cooling circuit and a reuse heat circuit. Since the demand for reusable heat is unknown, the heat exchange is represented by an “auxiliary cooling unit”. This component calculates the potentially reusable heat for given conditions at DC site.</p>	<p>Type – 99 [117]</p>
<p>control 3: cooling source mode</p> 	<p>The 2-stage controller is used to switch between DX and economizer mode. The mode is switched based on ambient temperature. A baseline control is defined for constant setpoints (e.g. 10°C).</p>	<p>N-stage, Type – 1503 [118] 2-stage , Type – 2 [117]</p>
<p>control 4: dry-cooler actuation</p> 	<p>The local control of a dry-cooler fan is defined as an N – stage controller (3-stage). The controller sets 3 levels of airflow based on ambient temperature bounds. The ambient temperature bounds change with respect to the cooling source mode.</p>	<p>Type – 1503 [118]</p>

Table 4-4: sub-model's description of the cooling system (water-side): part II

component	description	component ID [117],[118]
<p>control 5: pump actuation</p> 	<p>A baseline control of the pump provides a constant control signal to the pump actuator. The control signal can be further modulated by a higher level- management or (e.g. N-stage or PI controller) based on supply/return water temperature.</p>	<p>N-stage, Type – 1503 [118] 2-stage , Type – 2 PID. Type – 23 [117]</p>
<p>control 6: heat recovery actuation</p> 	<p>The heat recovery system is triggered only if the return temperature reaches a certain temperature level (e.g. 45°C). This limit is defined based on the heat recovery system.</p>	<p>2-stage , Type – 2 [117]</p>

To summarize, the modelling of the DC system is specific for each different type of economizer, which is described in chapter 2. Attention should be paid not only to the representation of the system components, but also to the definition of the internal control of the cooling system, which switches between mechanical cooling and economizer mode. Indeed, the economizer mode, which bypasses the energy-hungry mechanical cooling, can save 50 to 90% of the cooling demand throughout the year. The energy consumption performance of mechanical cooling and economizer cooling vary significantly. Therefore, the internal control of this process is equally important as the modelling of the compressor unit or the economizer heat exchanger.

4.2.5 Power systems modelling

Power delivery modelling

The typical power delivery scheme is depicted in Figure 4-12. The power delivery line is decomposed into the individual components which represent

the power delivery losses (e.g. Power Supply Unit (PSU), Power Delivery Unit (PDU) and uninterrupted power supply (UPS)).

The individual component models are part of the Green Data Center Library developed by the RenewIT project [121]. As mentioned in chapter 2, the power delivery system cannot be controlled in a manner similar to the cooling system. In the overall virtual DC environment, the power delivery model captures power losses related with energy transmission and other power manipulation.

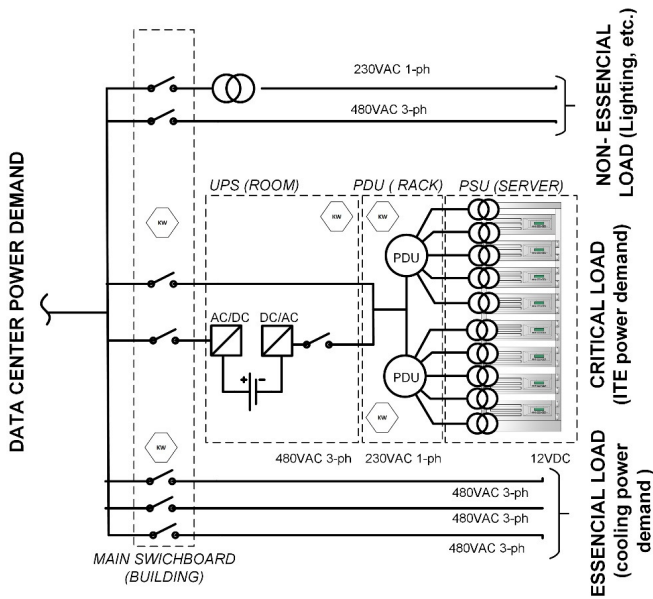


Figure 4-12 Scheme of the model of a power delivery system

The components illustrated in Figure 4-12 are listed and described in Table 4-5. The mathematical description of the sub-models can be found in the mentioned literature based on the component identification number, which in the software is called “type”.

Table 4-5 components description of power delivery system: part I

component	description	component ID [117],[118]
PSU	This model represents power losses at the PSU. The power losses depend on user-defined characteristics of PSU efficiency versus utilization of nameplate power output. The characteristic can be modelled as a polynomial expression of the inputted power load.	Type - 4012 [88]
PDU	This model represents power losses at the PDU. The PDU losses are simulated in a manner similar to those of the PSU	Type - 4002 [88]
UPS	This model represents power losses at UPS. The UPS losses are simulated in a manner similar to those of the PSU	Type - 4001 [88]
main switchboard	This model represents power losses at the main switchboard. The switchboard losses are simulated in a manner similar to those of the PSU	Type - 4004 [88]
grid transformer	This model represents power losses at the main building transformer connecting the DC with the grid. The Grid transformer losses are simulated in a manner similar to those of the PSU	Type - 4008 [88]

The efficiency of the system depends on the typology of the delivery time and is strongly related with the utilization of the nominal (nameplate) power output of the system. The example efficiency curves are shown in Figure 4-13. The typical part-load efficiency can vary from 35% to 84% for given levels of the part-load utilization range. Also, the performance of each power delivery system varies with respect to the applied technology. Thus, each power delivery system performs with its own part-load efficiency characteristic. For instance, assuming the constant level of part-load utilization of 75%, the efficiency levels can vary in the range of 71% - 84% depending on the used power delivery system [122]. To reiterate, the typology of power delivery system was modelled by using a combination of various components from the renewIT library [88]. The final characteristic for the model of the power delivery system is plotted in Figure 4-13.

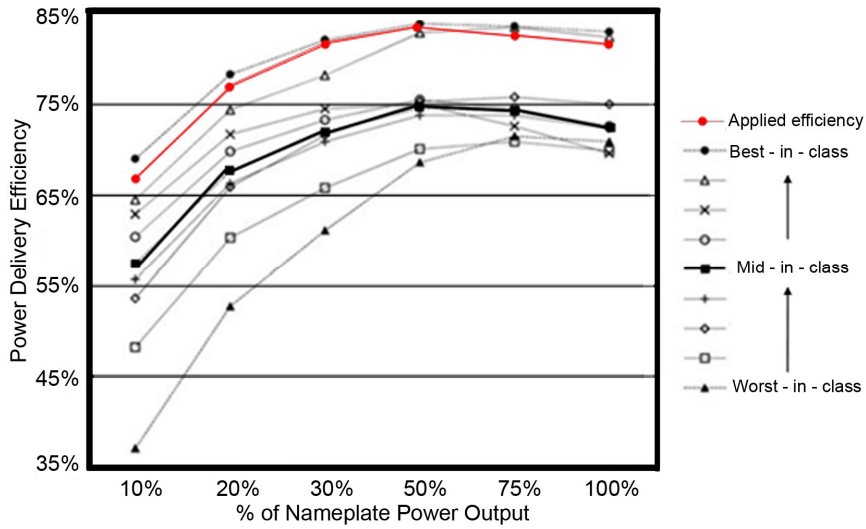


Figure 4-13 Typical and modelled part-load characteristics of power delivery system
adapted from [122]

Power supply modelling

The power supply and storage system depicted in Figure 4-14 was developed at Acciona Technological Research Center in Alcobendas (Madrid, Spain). The configuration of this model follows the specification of the real renewable energy source (RES) laboratory located in Madrid. The model can be configured according to the given technical specifications of the system. The components illustrated in Figure 4-14 are listed and described in Table 4-6. The mathematical description of the sub-models can be found in the mentioned literature based on the component identification, which in the software is called “type”.

The power supply and delivery models represent not only the power generation plant (PV, wind etc.) and power delivery losses, but it is also responsible for the simulation of energy storage and grid demand. The model collects power outputs from other models and calculates the overall DC electricity fluxes, which are shown in equation 4.6. The fluxes terms in the equation are denoted

with a positive or negative sign in brackets according to their relationship with the modelled system. A positive sign denotes energy production and a negative sign denotes energy consumption.

$$(4.6) \quad (-)Total\ DC\ demand + (+) On-site\ RES\ production + (\pm) Batt\ dis/charge + (\pm) Grid = 0$$

Total DC demand consists of IT demand, cooling power demand and power delivery losses. On-site RES production consists of photovoltaic (PV), wind and the biomass plant. The battery and grid can act as power production (energy import/discharge) or power demand (energy export/charge) according to the energy matching.

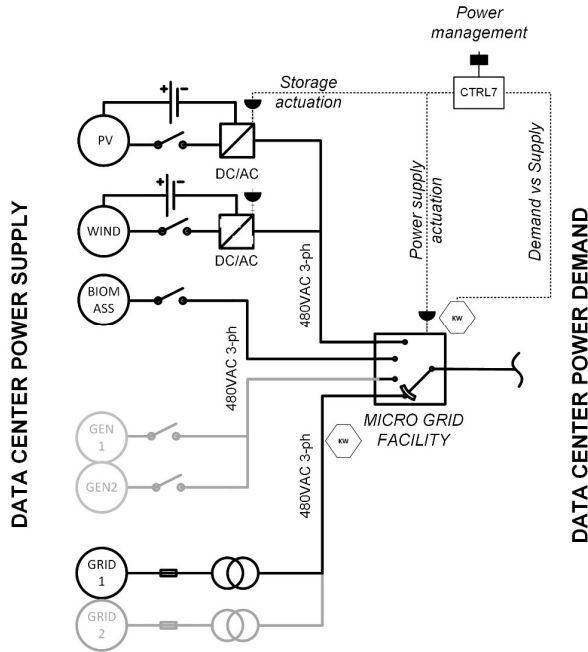


Figure 4-14 Scheme of the model of a power supply system

Table 4-6 sub-model's description of power supply system

denomination	description	component ID [117], [88]
photovoltaic array	The model represents the electrical performance of a photovoltaic array based on an empirical equation for an empirical equivalent circuit model to predict the current-voltage characteristics of a single PV module. The simulated performance depends on ambient temperature, level of solar radiation (total, direct, diffuse), angle of incidence, etc.	Type – 94 [117]
wind turbine	The model represents the electrical performance of a wind turbine based on a model for a wind energy conversion system (WECS) [123, Ch. 6] The simulated performance depends on user-defined characteristics of power generation versus wind velocity. The outcome is further corrected based on hub height, site shear exponent, turbine power losses etc.	Type – 90 [117]
battery array	This model represents electricity storage with defined capacity, charge/discharge load and efficiency. The electrical performance is corrected via empirical characteristics for two types of batteries (Lead-Acid and Li-Ion). This model follows the assumptions and limitations of the model developed by Tremblay, O. et al. [124] The storage level is controllable based on desired state of charge.	Type4015 [88]
inverter	The invertors of the direct to alternative current and alternative to direct current are calculated as electrical transformation with constant power efficiency	user-defined calculation
biomass	The biomass generation represents controllable power generation with no dynamic modelling of the combustion. The desired power (within a user-specified range) is assumed to be delivered into the system. Related environmental and economic impacts are specified as constant based on type of system used.	user-defined calculation
control 7: power supply and storage management	The control logic uses all uncontrollable generation (PV and Wind) first to cover the DC demand. The rest of the DC power demand is met by the controllable generation and then the grid if necessary. A baseline control of storage is based on balance of supply versus demand. If surplus occurs, storage is charged, otherwise it is discharged. The logic can be overruled by higher-level management.	user-defined logic

Since the power supply and delivery model gathers all electricity fluxes in the DC system, this model, if desired, can also carry out calculations of most of the performance indicators such as PUE, CO₂ emissions and operational energy cost etc.

4.3 Definition of boundary conditions

This section describes the boundary conditions considered for the virtual DC environment. The computational experiments require consistent definition of the boundary conditions for each experiment in order to ensure the comparability of the results. The boundary conditions of the virtual DC environment include requested virtual machines (VMs) representing IT workload demand, electrical grid data, weather data and the DC operator strategy.

Requested VMs represent the IT workload demand. The VM traces are related to the type of services and end-user behaviour.

The sample profile of the incoming end-user workload is used as a boundary condition for most of the experiments. It is important to understand that the end-user workload traces are not direct boundary conditions of the virtual DC environment. The workload traces are processed by workload management and the workload management then provides the required input in the form of the server utilization or workload power demand. Two types of workload profiles are Available:

- *VM workload traces from real data centres* - these traces were collected at a production data centre and reflect the workload seen in a private cloud. In more detail, the traces comprise 132 servers, hosting approximately 2400 different VMs over a period of 30 days. Not all of these VMs are active over the entire time period.

- *Synthetic workload traces* - these traces reflect the resource usages of a multi-tier web service. These traces are based on Mediawiki [125], the collaborative editing software used to run the Wikipedia website in a large-sized DC. The monitored resource utilizations were used to create the resource utilization traces and then scaled to the size of the case-study of the small-sized DC. These traces exhibit the characteristic day/night and week-/weekend-day patterns observed in web services. Furthermore, these traces can also be adjusted to define extreme boundary conditions.

Electrical grid data is related to the electricity market price and the percentage share of RES in the grid (i.e. grid CO₂ emission intensity). A sample historical data-set is used for the computational experimentation. As an example, the historical data can be downloaded from the Irish Single Electricity Market Operator (SEMO) [126].

The CO₂ factor of the grid is estimated based on data from the International Energy Agency for each country [127]. Nowadays, some of the smart-grid operators can offer real-time (hourly) monitoring of the grid status (e.g. CO₂ intensity). This data may be recorded and available as input for the model. (e.g. eirGrid [128]). The variable CO₂ intensity can represent the actual share of RES in a grid during the time. However, such data are not yet commonly available for all locations.

Weather conditions are specific to the DC location. Since the typical DC envelope rarely includes glazing, the DC space and cooling system is mainly influenced by outside air temperature and humidity. The other factors such as solar irradiation and wind speed mainly influence the power supply systems including on-site RES. Standard typical meteorological year data (TMY2) [129] are available for many locations around the world.

DC operator strategy is defined by setpoints for individual systems and components. The evaluation of different operation strategies, which vary with

these setpoints, is the main goal of this research. In order to enable the proposed closed-loop testing, the virtual DC environment must ensure an interface for the tested external algorithm, which allows dynamic (step-by-step) access to both the virtual actuators and the virtual monitoring.

4.4 Integration of the virtual data centre environment

To reiterate, the virtual DC environment is meant for the testing of external algorithms. This task requires a reliable connection between the virtual DC environment and the external algorithms. It is rarely feasible for the testing algorithm to be delivered in the form of an executable package and embedded into the testing environment of the virtual DC. The main barriers are usually intellectual property issues and technical feasibility. The technical solution of communication between the virtual DC and external control algorithms should support geographically spread services and a combination of various programming languages. This task requires a sophisticated communication framework that can cope with all requirements. The technical solution of the communication framework is not part of this thesis because it requires a computer science background and goes beyond energy modelling expertise. The communication framework has been developed at the consortium level of the Genic project. The integration work related with the virtual DC environment is conducted to support the given communication interface to satisfy I/O requirements of other partners. To understand the main function of the virtual DC environment as a testing environment of external algorithms, it is important to conceptually explain the communication framework. The role of the virtual DC environment in the larger communication framework is discussed further below.

The communication framework is one of the important aspects of the design of the Genic project architecture. All components from different developers

communicate through the middleware. This allows the control algorithms of every component to remain, if desired, private to the developer. It also allows a system integrator to use solutions from different manufacturers using various programming languages and integrate them into either a real or virtual DC system. As long as the interfaces are active and data formats are specified, the communication framework can ensure the communication of data. Moreover, if the virtual DC system follows the data formats of the real DC system, the tested algorithm can be easily switched from one environment to the other.

4.4.1 Description of the communication framework

Specifically, the RabbitMQ messaging system [62] was used as the basis of the communication framework. All modules of the control platform, most of which are briefly explained in section 2.3, are connected via this message-oriented middleware. The middleware allows the following:

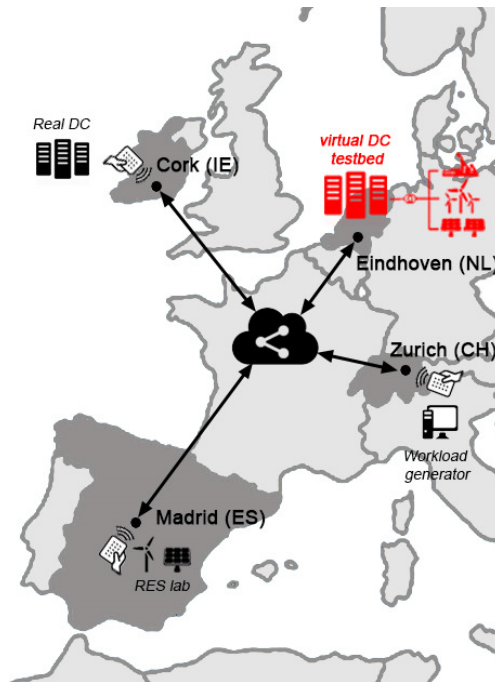


Figure 4-15 Communication framework of the Genic project

Geographical distribution of connected modules

The project partners are allowed to deploy their software components in a distributed manner connecting all geographically distributed services through the communication middleware. In the scope of the Genic project the main demo site is located in Cork, Ireland where the communication, resource management and monitoring components (due to latency) are deployed. The RES demo sites are located in Seville and Madrid in Spain, while the virtual DC environment is located in Eindhoven, Netherlands as is shown in Figure 4-15

Multi-clients and multi-protocol support

The platform requires support for multiple programming languages and protocols due to the variety of expertise of each partner. The communication middleware supports numerous clients, adaptors and tools for different programming languages such as JAVA, Ruby, Python, .NET, Perl, C++, and Matlab, etc.

Robustness and reliability

The communication middleware offers a variety of features to enable tradeoff between performance and reliability. These features include persistence, delivery acknowledgments, publisher confirmations and also the high availability of the services.

Supporting of different communication patterns

Two types of communications patterns are used in the communication framework: (i) an event-based pattern (publish-subscribe), where the software components publish information when it is available and the subscriber consumes the data as soon as it is available, (ii) a time-based pattern, where a module requires data from another module in a given time periodicity.

Ability of adding and removing data providers

Due to the distributed architecture communicating via the middleware, the control modules can be updated or substituted for competitive modules of

other developers at any point in the development. The plug & play manipulation with the modules is satisfied as long as the modules provide the predefined input and output formats including the refresh periodicity of the previous module.

4.4.2 The virtual data center environment within the communication framework

To reiterate, from the perspective of the virtual DC environment, the messaging occurs every computational timestep of the simulation in order to test external algorithms in a closed-loop fashion. The closed-loop fashion requires inputs/outputs to be received/sent every computational timestep. The interface with the middleware client must be designed to be embedded into the BES model structure. Specifically, the virtual DC environment is interfaced with the communication middleware by a script written in the Matlab software [130]. The dynamic (step-by-step) communication is enabled by TRNSYS type 155 (described in [117]). The script collects all outputs from the virtual DC environment, built primarily in TRNSYS [93], and delivers them to the middleware client. At the same time, the Matlab script collects all inputs from the middleware client and prepares these inputs to be applied in the simulation for the next computational timestep.

Examples of the input and output formats are listed in Appendix A as candidates for monitoring and local control. It is important in computational experiments that all modules involved in the testing are synchronized in terms of boundary conditions and time. As part of a computational experiment, the boundary conditions discussed in section 4.3 above are sampled and provided by the modules of the virtual DC environment and workload generator for all other modules in the middleware. After the testing, when the control platform is deployed, the sample boundary condition data are substituted by monitoring (e.g. measurements of outside conditions at the real DC site, incoming

workload) or external services from 3rd parties (e.g. meteorological service or smart-grid service). The time synchronization is addressed by the ‘simulation time’ message published by the Virtual DC environment. A schematic of the synchronization process can be seen in Figure 4-16.

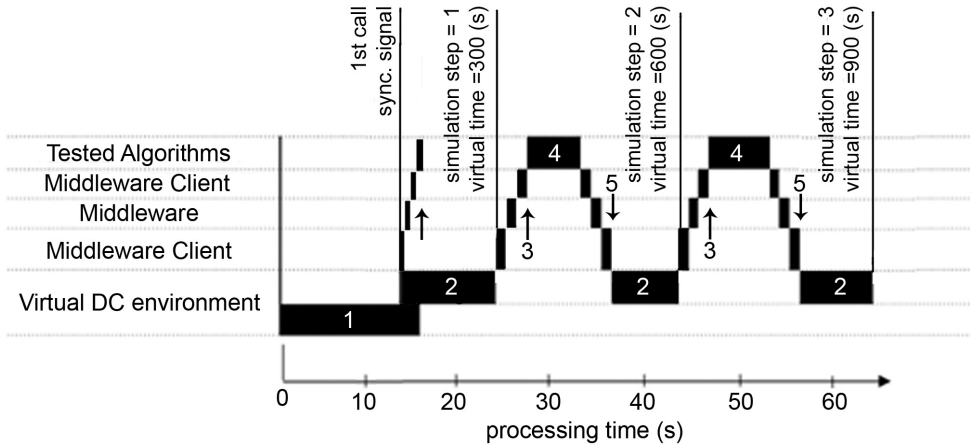


Figure 4-16 Interactive communication process of the simulation-based assessment

This process can be divided into 5 stages; 1 preparation stage and 4 subsequent stages that are repeated until the end of the defined simulation period.

1. Preparation/Initialization
 - a. Design of experiment (location, required VMs profile, weather data, grid data, baseline control strategy, etc.)
 - b. Initialization process of the simulation. At the end of this stage the synchronization time is published to allow the initialization of all modules within the closed loop.
2. Calculation of virtual monitoring data for the first simulation step $k=1$ (default inputs are used). After publishing, the Virtual DC environment awaits the new set points to proceed with the calculation of the following timestep

3. The Middleware client collects the synchronization virtual timestamp for the first simulation step and all the virtual monitoring data and publishes them in the middleware
4. All modules in the testing loop receive a synchronization virtual time stamp and required virtual monitoring data from Virtual DC environment. Based on virtual monitoring data, the optimal set points are calculated for next simulation step
5. New set points are published to the middleware from tested components. The Virtual DC environment receives all the subscribed inputs necessary for the calculation of the next timestep.

Return to point 2 and continue with the calculation of virtual monitoring data for the following simulation step $k=n$. After publishing, the Virtual DC environment awaits the new setpoints to proceed with the calculation of the following timestep. Steps 2 - 5 are repeated until the end of the predefined simulation period.

This iterative process is similar to the one that takes place between the control platform and the physical DC. The simulation - based assessment acts as the last quality control test prior to the full platform deployment in the real DC. This approach can also be used by designers of future DC energy management systems regardless of whether they comply with the Genic architecture or not. The virtual DC environment publishes the virtual time stamp for all of the modules that are involved in the computational experiments to be synchronized. All time-dependent modules in the testing loop are subscribed to this 'SimulationTime' topic and execute their calculations based on synchronization time. This topic allows computational experiments to be significantly faster than would be possible following real-time. For instance, a 1-day simulation including processing time of testing control modules in the loop may take around 2.5 hours, considering that the prototype of the virtual

DC environment is installed on a typical personal computer with the following parameters: processor 3.40(GHz), RAM 8 (GB) and 64bit operating system. Simulation time can also vary with respect to the number of testing components in the testing loop.

In summary, when the virtual DC environment using BES was successfully integrated into the wider simulation tool-chain, this proper integration enabled the close-loop testing of the external algorithms within the wider simulation tool-chain.

4.5 Concluding remarks

The conceptual model, which satisfied the purpose of testing of external algorithms, required large modelling scope, meaning that multiple systems were required to interact with each other. Due to the large modelling scope, careful determination was required of the level of resolution for each individual sub-model in order to keep the overall complexity at a feasible level.

In general, BES tools were found to be suitable tools to support the current holistic vision of DC modelling. This chapter explained the model selection and development. In addition, the selected modelling approach offered sufficient connectivity with the wider simulation and communication tool-chains, which ultimately enables the closed-loop testing of external control algorithms. Based on our experience in the Genic project, it can be recommended that besides the virtual monitoring data, the virtual testbed should also provide a synchronization signal and common boundary conditions for all tested algorithms within the wider simulation and communication tool-chain.

5 Validation and demonstration of the virtual data centre environment

Chapter 5 presents the first set of computational experiments using the virtual data centre (DC) environment. The presented experiments aim to validate and demonstrate the capability of the selected modelling approaches to realistically capture the multi-domain DC processes acting at several scales. The validation and demonstration studies are an important step in the modelling process. These studies provide a level of confidence for the energy modeller and assurance for the external control algorithm developer. Therefore, these experiments were necessarily performed prior to the integration of the virtual DC environment into the wider simulation tool-chain, which enables the testing of the external algorithms. In this type of computational experiment, the virtual DC environment was configured to represent the given DC and renewable energy source (RES) system under default control strategies.

5.1 Technical specification of the case-study

The case-study conducted for the current research includes a virtual DC environment, which represents a university DC of Cork Institute of Technology (CIT) located in Ireland and a RES laboratory of ACCIONA Company located in Spain. These infrastructures were selected as demonstration sites of the Genic project, because they were available for real experimentation.

5.1.1 The university data centre

The bespoke data centre has approximately 40 m² of floor area, and is laid out in a cold and hot aisle arrangement without containments, or in other words, these aisles are not separated by any physical barriers. The geometry of the room is 5 x 8 x 3 m, which includes the raised floor space with underfloor air supply. The nominal load of IT equipment, housed in eight normalized racks, is estimated at 30kW. The racks are largely occupied by communications equipment for the CIT campus and the main e-mail and DNS servers, serving the entire campus community of circa 17,000 users. The layout of the demonstration DC is shown in Figure 5-1.

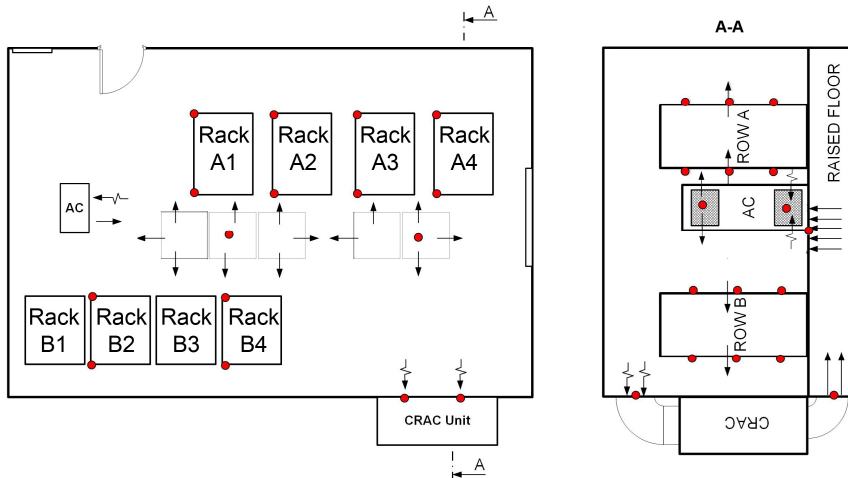


Figure 5-1 Layout and section of the demonstration DC

Table 5-1 shows the sum of the nominal IT power load for each 1/3rd of rack within the DC space. The nominal load is equivalent to the maximal heat dissipation in the DC space. On average, the racks are occupied with servers demanding 5kW per rack (excluding racks B1 and B3). The racks B1 and B3 house network equipment such as switchers or routers with negligible power

demand and related heat dissipation. The highest nominal power demand, at 10,9 kW per rack, can be observed in rack A3.

Table 5-1 Distribution of nominal IT power load (W) within the demonstration DC

POWER LOAD (W)	A1	A2	A3	A4	B1	B2	B3	B4
TOP	1460	870	1970	702	0	760	0	0
MID	4160	457	3790	1640	0	4000	0	1413
BOT	0	457	5160	2498	0	0	0	778
TOTAL	5620	1784	10920	4840	0	4760	0	2191

Concerning cooling of the space, the conditioned supply air is distributed through the space below the raised doubled floor. The height of the underfloor plenum is 0.3 m. The supply air enters the DC space through perforated floor tiles in front of the IT equipment (ITE) in the cold aisle region. From there, most of the air is forced into the ITE by internal fans. The conditioned air is used for the removal of the dissipated heat from the computational processes. The warm air is rejected from the ITE to the hot aisle region of the DC space. Since no containment of the cold or hot aisles is applied in this DC, recirculation and bypass phenomena described in section 2.2 may occur. The air returned to the Computer Room Air-conditioning (CRAC) unit is taken from the mix of return (i.e. used) and supply (i.e. conditioned) air under the ceiling.

In the physical DC, a monitoring sensor network captures the thermal and power processes. The DC space is monitored at 3 height levels as recommended by ASHRAE TC 9.9 [40]. The visualization of the temperature monitoring of the DC space is shown Figure 5-2. The temperature monitoring is visualized for 2 periods before and after application of the tested control algorithms.

(a) average temperatures from
period 6-12/8/2015

(b) average temperatures from
period 6-7/1/2016

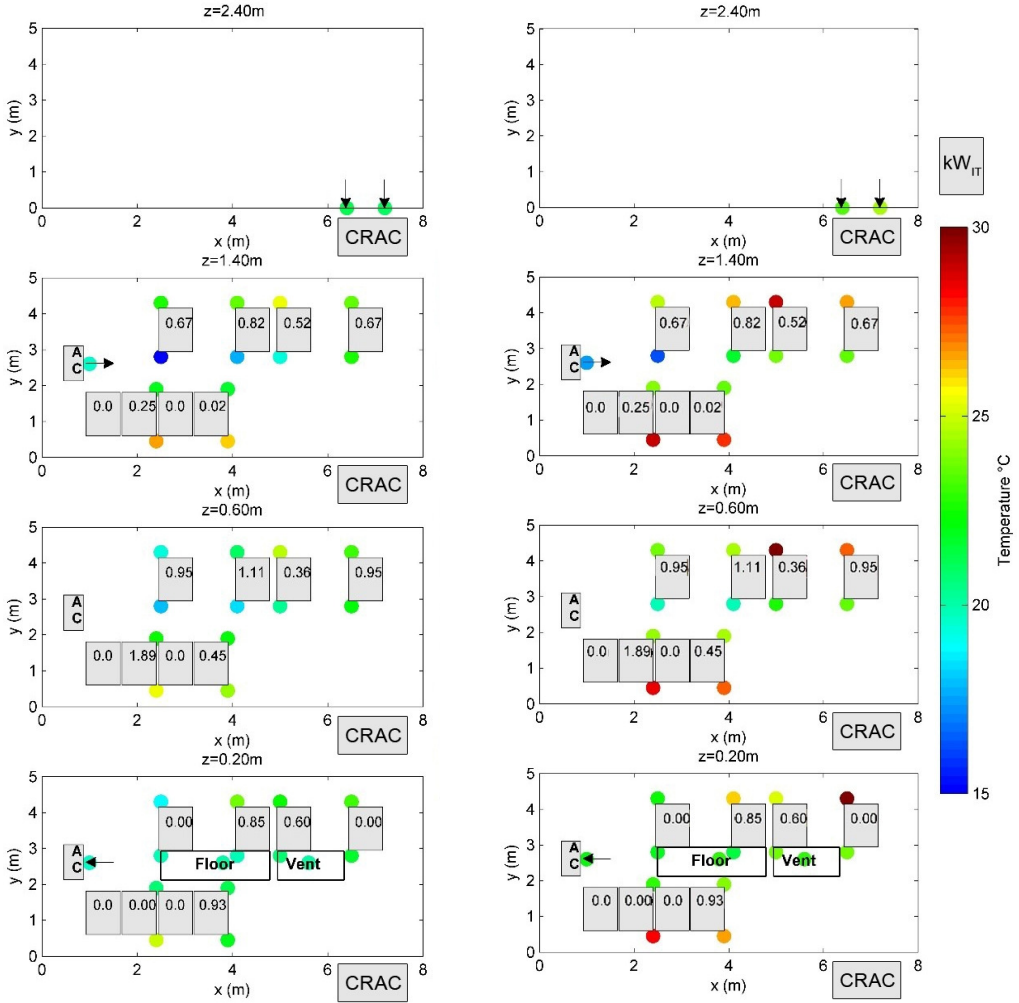


Figure 5-2 Monitoring of DC space – average temperature from periods (a) 6-12/8/2015 and
(b) 1-7/1/2016

The cooling system consists of a single modular CRAC unit with a nominal cooling capacity of 40 kW. (model number: EDPAC DG40BSES [131]). The unit is located in an adjacent room and the conditioned air is supplied via the previously described underfloor air distribution. The return air is taken from under the ceiling via ventilation grills in the wall. In order to condition the air, the CRAC unit exploits a parallel arrangement of a direct expansion (DX) unit and a water economizer. The parallel economizer bypasses the DX unit in periods when the outside air temperature is lower than the indoor air temperature. In both modes, the heat from the CRAC unit is removed by a water circuit that connects the CRAC unit to a roof mounted drycooler, where the heat is released to the outdoor environment. Alternatively, If the temperature potential of waste heat is sufficient, the waste heat can be stored and reused in a neighbouring space or building. A schema of the CRAC cooling system is shown in Figure 5-3.

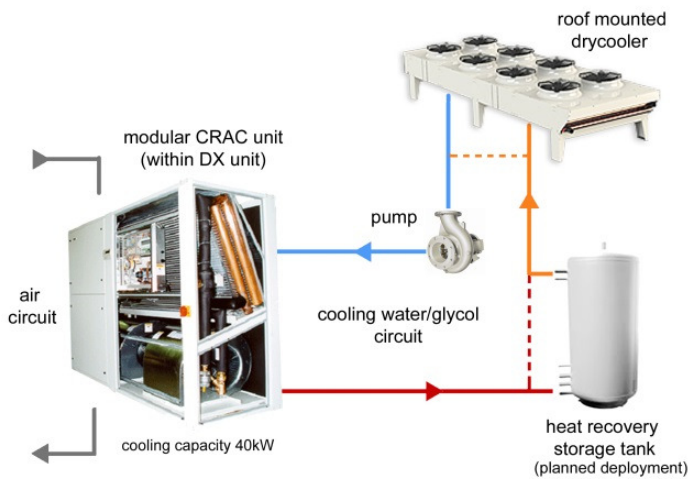


Figure 5-3 Schema of the main DC cooling system (EDPAC unit)

The DC space is also equipped with an air conditioning (AC) system. This is a small split-system with 12.3 kW cooling capacity acting as a backup unit (model

number: Mitsubishi PSA – RP125GA [132]). This unit is located in the DC space and does not provide supply air via the underfloor air distribution system. Supply air from this unit is provided directly to the DC space from the top of the unit with return air entering the unit near the floor (at the bottom of the unit). A schema of the AC cooling system is shown in Figure 5-4.

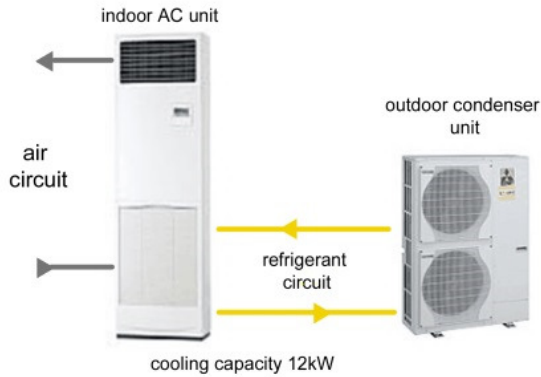


Figure 5-4 Schema of the backup DC cooling system (Mitsubishi unit)

The monitoring of the cooling systems includes the supply and return temperatures measured within the overall wireless sensor network (WSN) of the DC space, and the overall electricity consumption measured at the main switchboard. A sample of the supply and return temperature data for the CRAC unit are shown Figure 5-5.

Since the main system of interest is the CRAC unit, the temperatures are plotted for a period of three days (9/7/ -11/7/2015) when the performance of the CRAC unit was not influenced by the operation of the backup unit. The temperature fluctuation of the supply temperature is caused by the internal ON/OFF controller of the unit. The setpoint of the internal controller, which regulates the return air temperature, is set at 21°C.

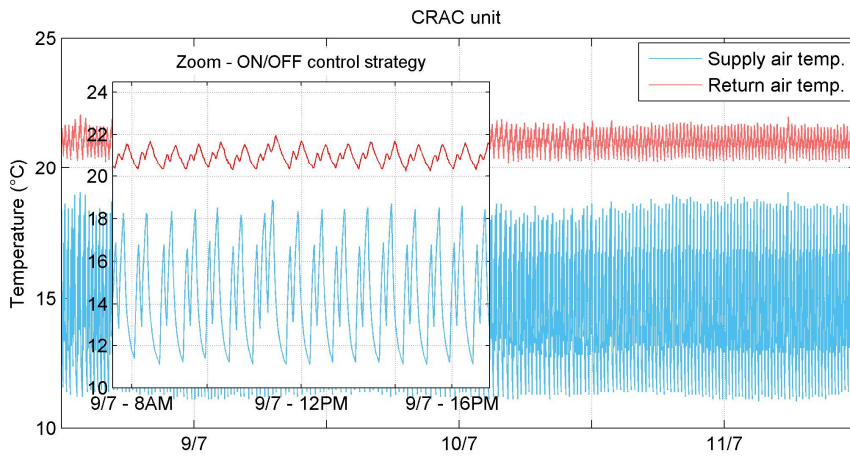


Figure 5-5 Supply and return temperature profile of main CRAC unit for 9/7/2015 – 11/7/2015

The overall DC consumption was captured during the initial energy audit for the period of 22/7/2014 – 31/7/2014. Figure 5-6 shows the breakdown of electricity consumption of the individual domains: IT power, cooling power and power supply losses.

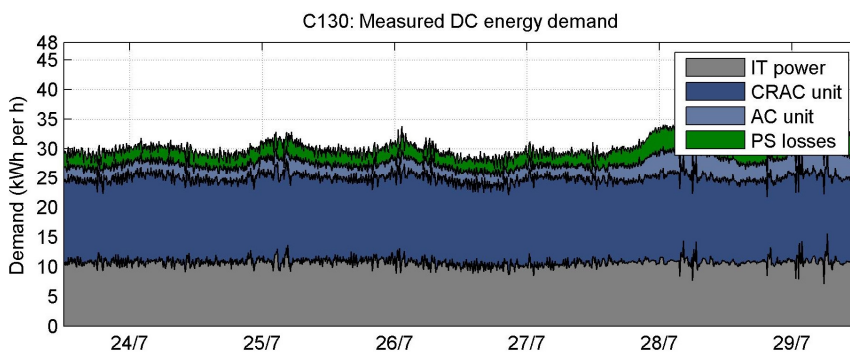


Figure 5-6 Results of energy audit performed in period 22/7/2014 – 31/7/2014

5.1.2 The laboratory of renewable systems

This section describes the renewable energy test facility sites used for the RES demonstration in the Genic project. It gives an overview of the experimental plants connected by micro grid facility, which were available for testing. The testing facility can physically emulate a predefined electricity load (e.g. total load of the DC) and thus test the combination of DC and RES systems. However, this testing facility can only support the power management domain. The testing of the overall “holistic” platform is not possible. More details regarding the RES laboratory are publicly available in project deliverable D5.2 [133].

The micro grid, located at the ACCIONA Technological Research Center in Alcobendas (Madrid), is a 100% renewables based power generation plant. The laboratory facilities can work as an isolated system, providing off-grid generation based on renewable energy sources using batteries for storage, and can also be connected to the electricity grid.

The systems that form part of the installation are:

- Renewable Energy Generation Systems (photovoltaic (PV) and wind emulator)
- Energy Storage System (battery bank)
- Power Converters (charger module, wind module, photovoltaic module and inverter module)
- Communication and Monitoring System (with custom user interface).

The micro grid facility is a modular system that has the ability to adapt to the different requirements of a given installation. Renewable energy systems and power storage systems are directly connected to a direct current bus, and the current inverter module turns it into a pure sine three-phase current. This inverter module is reversible, which means that it is also able to rectify from alternative current to direct current (i.e. the current provided by an extra generator), and use this rectified signal to charge the batteries under specific conditions.

The battery module is responsible for managing the charging and discharging of the battery bank. An installation must have at least one main battery charger module and, optionally, up to three secondary modules. The battery array has a capacity of 10 kWh_{el} with nominal charge and discharge rates of 5 kW_{el}.

The inverter module generates a pure sine wave three phase voltage, with constant amplitude and frequency, adapting the output power to that demanded by the installed loads.

The installed power can be increased by connecting up to a total of four inverter modules in parallel.

The photovoltaic module manages three 15 kW_{el} PV inputs, with an independent control. These inputs can be configured to operate in parallel, thereby obtaining a single input with a maximum power of 45 kW_{el}. The total panel area of this setup is around 84 m².

The wind turbine module works as a converter to manage three 15 kW wind power inputs. These inputs can be configured to operate in parallel with two options: (i) the three inputs in parallel forming a single input with a maximum power of 45 kW, (ii) inputs 1 and 2 in parallel forming a 30 kW input and a 3rd independent input of 15 kW.

The biomass plant using an Organic Rankine Cycle (ORC) is used to support the solar system. The boiler has a capacity of approximately 100 kW_{th}, and allows a maximum temperature output of 203°C. The biomass pellets come from a silo or storage pit that feeds the boiler. In order to increase the efficiency of the system, the pilot plant has an ORC unit that is fed with the high temperature output of the biomass boiler. The ORC is a thermodynamic cycle that uses a working organic fluid (instead of water vapor) to produce electricity. The unit requires an input heat of approximately 80 kW_{th} with a temperature range of 130 -160°C. The nominal electricity output is 7.5 kW_{el}. This system is primarily designed as a heat generator, the electricity outcome,

used in the DC, is considered here as a by-product of the renewable heat generation.

The operating principle of the system is designed to generate alternative current voltage from renewable energy sources. The battery charge and discharge status and the backup generator connection and disconnection will depend on the energy generated by the renewable sources and the demand of the DC. The baseline control strategy aims to store the surplus of the RES system. When the RES production is greater than DC demand, the surplus energy is stored in the batteries. Once the battery bank is fully charged, it is maintained in float status and the power generated is adjusted to meet the demand.

5.2 Measurement uncertainties in model validation and demonstration

All measured data were obtained during regular DC operation. In contrast to laboratory conditions, a DC in regular operation presents certain limitations and uncertainties in terms of achieving measurements. Since measured data are the main input for the validation and demonstration studies, the limitations and uncertainties must be known before any experimentation. This section describes the limitations and uncertainties of the monitoring data gathered during the regular DC operation with additional commentary related to their numerical representation. The limitations and uncertainties can be categorised as follows: (i) availability of measured data (ii) uncertainty of the instruments (iii) representation of sensor data. It should be noted that the following analysis is conducted from the point of view of a building energy modeller. Thus, this section does not include a full description of the sensor network configuration since this would go beyond the reasonable scope of the current PhD thesis. The planning, deployment and management of such a sensor network is a non-

trivial task that requires expert knowledge and experience that cannot be expected from a building energy modeller.

5.2.1 Availability of measured data

The multi-domain “holistic” monitoring faces a challenge similar to that of the modelling of such a complex system as a DC. The “holistic” monitoring in regular operation is confronted with the large complexity of the measured system as well as significant financial and technical constraints. The new control strategies as well as the validation study of the models must be developed in consideration of the limited number of sensors and limited access for instrument installation. Monitoring of all possible processes, which would be necessary in an ideal “laboratory case”, is rarely possible. Moreover, considering the number of involved systems, the construction of such a laboratory is not feasible. These technical constraints are discussed below.

Firstly, there is limited access to some components (hardware accessibility) or monitoring data from a system interface (software accessibility). In some cases, the monitoring cannot support the required level of resolution. In such cases, this means that some components or their corresponding physical states cannot be directly measured at all. In other cases, measurements are not accessible without unauthorized intrusion to the system or its interface (e.g. temperature monitoring of the water circuit of the cooling system).

Secondly, although many of the measured data of interest can be monitored, data loss during the monitoring can occur due to a sensor or a component failure. The DC operator or an automatic fault detection system can handle such a situation. However, such a dataset is devalued for validation purposes, since the validation assumes regular operating conditions. As an example, Figure 5-7 shows the monitoring of airflow of cooling units as an indicator of unit operation over a period of circa 1.5 months. As can be seen, using the DC facility as a living laboratory cannot provide the same quality and reliability as

laboratory measurements. During everyday operation, a real DC may experience outages of individual components or intermittency of sensing (e.g. data loss at 5-8-2015). Although, the DC facility is equipped with back-up systems, which can handle most of the emergency situations, collection of suitable data for scientific purposes is relatively challenging as demonstrated in Figure 5-7.

Another limitation can be identified in sensor placement. An example of this limitation is that the placement of the air temperature sensors within the DC space must again respect the regular operating conditions even though a location in the middle of the space would be more representative for the validation study. However, the everyday access requirements of the ITE do not allow for such a location. The effect of sensor placement on the sensor's reliability is further discussed below in section 5.2.3.

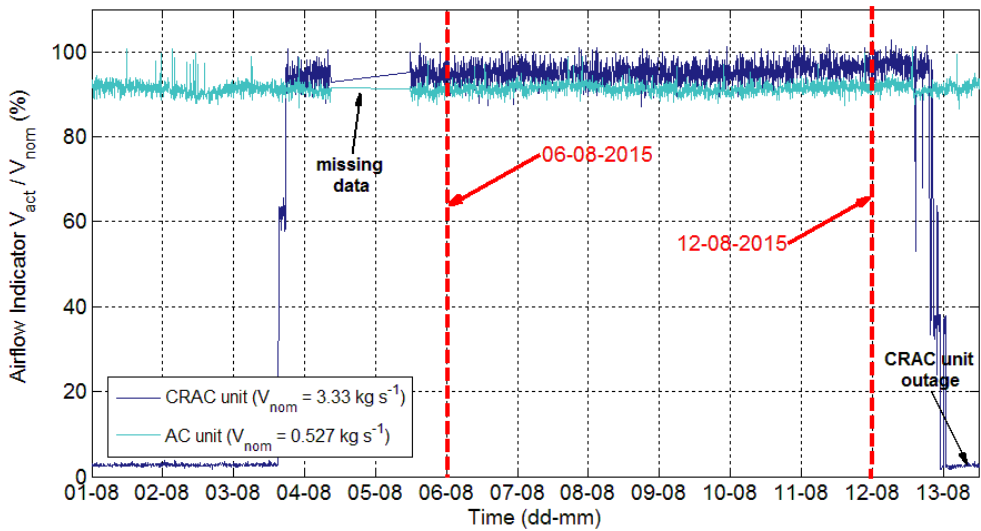


Figure 5-7 Airflow measurements of the CRAC and back up AC unit of the DC demo site

Current research must also consider that the demonstration RES system is not located at the same place as the demonstration DC. Generally, DC systems are not yet commonly equipped with a RES system. In fact, this is a great opportunity for the application of simulation techniques, which can emulate the RES system as if it were an on-site facility. At this stage of the holistic platform development, the virtual combining of these systems is the only affordable and feasible way to test the co-operation of these systems.

From the perspective of RES model validation, the RES model is validated based on the available data from the RES site (located in Spain), then the RES model is virtually transposed to the same location as the DC site (located in Ireland) by changing the boundary conditions of this model. Since Building Energy Simulation (BES) models were usually physics-based models, the missing data can be partially substituted by technical specifications of individual components. As such, the level of confidence can be partially reached by comparison with relevant standards. Standards offer a constant benchmark for quality assessment.

5.2.2 Sensor instrumentation uncertainties

The sensors can be grouped based on scales, domains, or measured physical phenomena states according to their usage. The specific candidates for monitoring are described in Appendix A. Basically, the DC processes are characterized by power metering, temperature, mass flow, velocity and/or humidity monitoring. As is discussed later in this chapter, the complexity and the previously mentioned technical constraints do not allow for the validation of the virtual DC environment as a whole. Therefore, the quality of the virtual data centre environment is separately evaluated using individual sub-models.

If the measurements are available, the individual sub-models are fed relevant measured inputs and simulated outputs are then compared with measurements. In fact, the measured data and monitoring uncertainties play a considerable role

in the validation study. The uncertainties need to be considered for measurements which are used as input for the sub-models as well as for measurements which are used as reference for simulated data. Therefore, the sensors utilized are briefly introduced in Table 5-2. The uncertainties of the measurements listed in this table are used later in the validation study.

Table 5-2 Description of applied measurement instruments

measured state	application, referenced manufacturer	assumed overall uncertainty	sampling Interval
power metering	monitoring of DC power consumption at building scale with division of individual domains, Power Meter Diris A20 [134]	+/- 15%	15 min
power metering	monitoring of IT power consumption at room scale (1/3 rd of rack), APC PDU AP-8853 [135]	+/- 10%	5 min
temperature monitoring	monitoring of the DC space including supply and return air of cooling devices at room scale (1/3 rd of rack), Amethern PANE 103395-410 thermistor [136], SHT11 sensor chip [137]	+/-0,5 °C	0,5 min
humidity sensors	not used, humidifier control is neglected in the “holistic” approach and for this type of system. SHT11 sensor chip [137]	+/- 3,0%RH	1 min
air velocity	monitoring of supply and return air velocity at specific areas of the cooling devices inlet/outlet duct EE575-V2B1 and EE671-V2XDKD [138]	per sensor +/- (0.3m/s +4%) assumed for mass flow +/- 10%	1min

5.2.3 Sensor data representation

This section discusses sensor representation versus computational node representation. This mismatch of the representations was mainly experienced in monitoring of DC space temperatures. The fundamental mismatch here is that the sensors always represent only a particular spot in the DC space, while the computational node of the applied method of a multi-nodal airflow network represents a zone of well-mixed air with a volume of circa 1m³. As discussed in chapter 4, the high-resolution model, which can represent any spot in the DC room, is not applicable in our case because resolution must be compromised due to the large scope and the requirement of dynamic response

within a limited time. The representation mismatch can be minimized by the sensor location. The placement of the sensors can significantly influence the representation of the sensed information.

The space measurements can be divided into three categories according to the importance of the representation for control purposes: (i) supply and return air temperature of the cooling devices, (ii) IT inlet temperature, and (iii) IT outlet temperature.



(a)



(b)

Figure 5-8 Return air temperature monitoring of (a) main cooling system (b) backup cooling system

The first category concerns the supply and return temperatures of the cooling devices. The representation of these temperatures are crucial nodes for thermal control of the DC space and management of the overall cooling system. Therefore, these temperatures are represented by several sensing nodes, as shown in Figure 5-8. Specifically, the supply air of the main CRAC unit is measured by three nodes located in the supply duct and in the space under the perforated tiles. The return air of the main CRAC unit is measured by two nodes located in front of the return duct. The backup AC unit is monitored by

only one node for supply and one node for return. Generally, it can be stated that the air side of the cooling units are measured by a sufficient number of nodes, especially the main CRAC unit, which is equipped with multiple nodes. The computational nodes of this category are comparable with the sensing nodes.

The other two categories deal with DC space temperatures related with the inlet and outlet of the IT equipment. The sensing nodes are attached to each door of racks at a height of 0.3, 0.7 and 1.4m from both sides of the racks, as can be seen in Figure 5-9. These nodes measure DC space air temperatures with a granularity of 1/3rd of rack. This deployment is recommended by ASHRAE [40]. The second category accounts for all IT inlet temperatures with the desired resolution of 1/3rd of rack. These temperature nodes are used for thermal control of the DC space and as an indicator of the temperature distribution on the IT inlet side. These sensors can be used for more advanced thermal strategies such as the thermal-aware computation described in section 2.3.

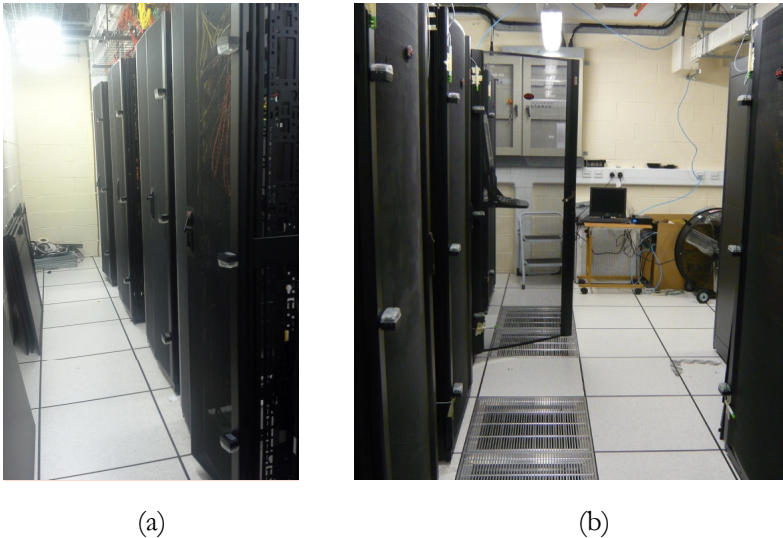


Figure 5-9 Measurement setup of (a) hot aisle zone and (b) cold aisle zone

In this second category, the computational nodes of the multi-nodal airflow network do not truly represent the spot measurements at the rack doors. The computational nodes represent the bulk volume of the air in front of the racks. However, the spot measurements represent just one or two spots at the edge of the overall zone. The mismatch in the representation of the computational node is demonstrated in Figure 5-10, where the local effects such as stream barriers or attached thermal mass of the servers influence the dynamics of the monitored signal.

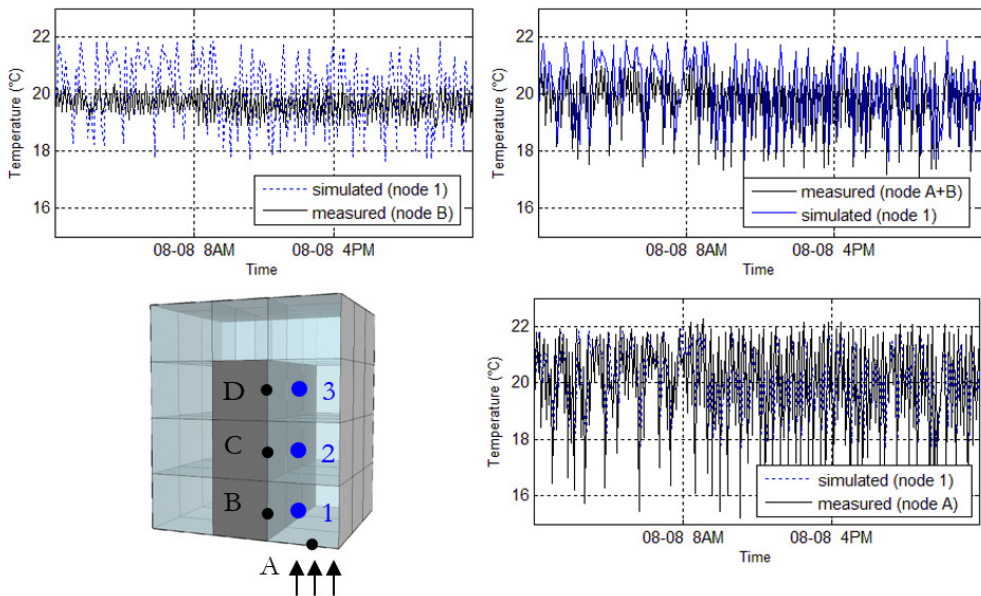


Figure 5-10 Comparison of measured and simulated data for 2 spot measurements,
Inlet of rack A2- bottom

Figure 5-10 shows measurements of inlet air for the bottom section of one of the racks, specifically rack “A2” indicated earlier in Figure 5-1. This particular area is special because the two measured spots (A and B in Figure 5-10) are attached to the area, which is represented by one computational node (node 1 in Figure 5-10). The measurements of spot “A” are strongly influenced by the

fluctuation of supply air coming from the CRAC unit. While the measurements of spot B, which are gathered just a few centimetres from spot A, do not fluctuate with such an intensity as spot A. This discrepancy between spot A and B well demonstrates the effect of stream barriers of supply air and the influence of the additional mass of rack doors, where the sensor is attached. However, the computational air node (node 1) represents the bulk volume of well-mixed air in the zone in front of the rack. This bulk of the well-mixed air can be theoretically represented by averaging the measurements at spots A and B. This premise was confirmed by comparison of these averaged measurements at spots A and B (A+B in Figure 5-10) with computational node 1, as shown in the Figure 5-10.

The measurements at other height levels of this rack are measured only by a single sensor, which seemingly cannot provide complete information about the represented zone. However, all sensors on the inlet side are under a strong influence of the enormous air change driven by the main CRAC unit. The air is released to the DC space at a low air speed from a relatively large number of perforated floor tiles. Here, a relatively uniform air distribution can be assumed.

Moreover, the sensors are located at the inlet side of the IT equipment. As known, the air exhaust is not accompanied by stream fluctuation and temperature changes as it is in the case of air “blowing”. Therefore, these measurements provide relatively good agreement with single spot measurements, as is demonstrated in Figure 5-11 by a comparison of simulated nodes 2 and 3 with measured spots C and D of the selected rack “A2”.

In conclusion, the computational nodes at the inlet can adequately represent the spot temperature measurements. The simulated data and computational nodes are comparable with spot measurements, which are influenced by the main cooling devices.

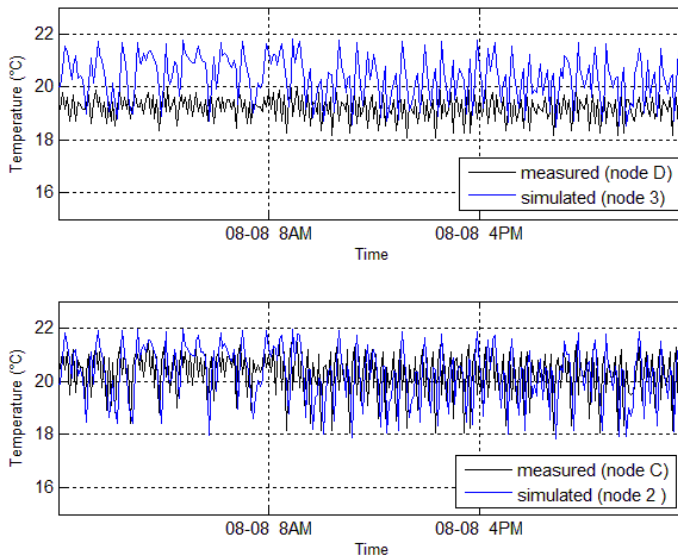


Figure 5-11 Comparison of measured and simulated data for 1 spot measurements,
Inlet of rack A2- middle, top

The third category accounts for all IT outlet temperatures with a resolution of 1/3rd of rack. These temperature nodes are not used for control purposes. They are used mainly for monitoring, visualization and possibly for fault detection. Therefore, the representation of these temperatures is less crucial.

Even though these temperatures are not very relevant for control purposes, the computational method must consider the entire volume of the DC space and therefore must also represent these temperatures to reach overall convergence. However, just as with the inlet side, the zonal representation cannot directly represent the spot measurements. While the temperature nodes at the front are strongly influenced by the enormous air change and uniform air distribution driven by the cooling unit, the temperature spots at the back are under the influence of localized and fluctuating air (with different temperature) blowing from the internal IT fans. Many local stream sources, stream blockage by cables and cold air leakages around the racks (illustrated in

Figure 5-12) generate highly non-uniform air distribution. Such non-uniform air distribution cannot be truly represented by single sensor measurement for the entire zone.

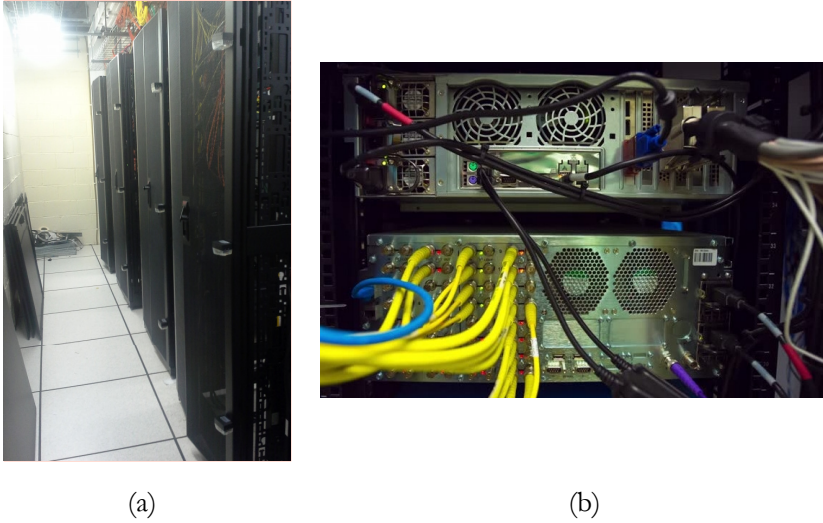


Figure 5-12 (a) spot measurements of hot aisle zone, (b) detailed view of server outlet conditions

Thus, heterogeneous air distribution and inconsistency of representation of computational and measured nodes can be expected. The inconsistency of the representation is demonstrated in Figure 5-13, which shows the largest inconsistency between measured and simulated data observed in the DC space. This area was found in the middle section of rack “A1” (indicated in Figure 5-1) and, because of the large inconsistency, this area was chosen as an example. The IT power and related heat dissipation of this IT box is 0.95 kW_{el} . Demonstrating that the measurements are not fully representative can be done simply by applying the calorimetry equation [120]; with the measured temperature difference of circa 1°C , the theoretical air flow through this IT box would be 3400 kg h^{-1} , which is unrealistic.

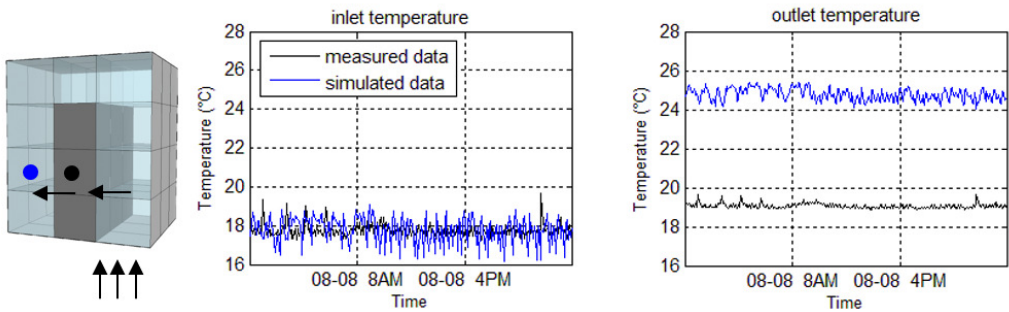


Figure 5-13 Comparison of measured and simulated data for inlet and outlet temperature of rack A1 – middle

Looking at the location of the spot measurements, this outlet temperature is measured at the edge of the rack, where the outlet air is likely blocked by some barrier. Moreover, this specific location is in front of the backup unit in operation, and thus there is strong probability of cold air leakage. As such, the spot measurements cannot be representative of the bulk volume behind the rack.

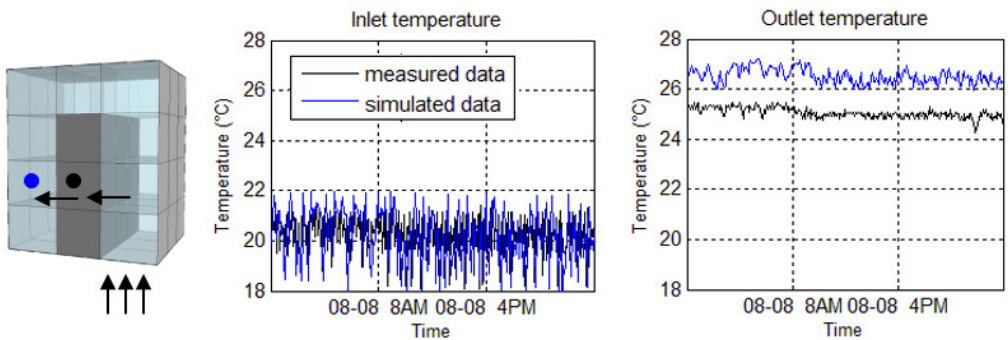


Figure 5-14 Comparison of measured and simulated data for inlet and outlet temperature of rack A3 – middle

Typically, the difference between simulated and measured data is not that significant, which means that these measurements are less influenced by the mentioned negative effects, especially cold air leakage. The typical

representation is demonstrated in Figure 5-14 by the middle section of rack A3, where the values are in relatively good agreement. The IT power related with this IT box is 0.52 kW_{el}.

Besides the inconsistency of the temperature representation, Figure 5-13 and Figure 5-14 also demonstrate the effect of the additional thermal mass of the IT equipment. While the inlet temperature fluctuates considerably, this fluctuation is significantly reduced at the outlet side, where the air exits the zone of the IT box.

To summarize, there exists a risk that the spot measurements at the back of the rack cannot always represent the bulk volume of air behind the racks. In other words, such spot measurements do not fully support the computational resolution of the applied method. In order to improve the validation study, multiple spot measurements in the free space (e.g. attached on temporary stands) would be required. However, such a measurement setup was not compatible with the regular operational conditions of the DC. Even though the temperatures at the back of the rack cannot be fully validated due to limited measurement placement, the simulated temperatures are still provided to the wider tool-chain, mainly for visualization purposes.

Apart from the validation study, the comparison can be still valuable in order to give a recommendation for sensor placement. Since these temperature nodes are not used by the control algorithms and the representation of the spot measurements is questionable, reduction of the temperature nodes of this category can be recommended. The hot aisle region can be monitored via temperature sensors located at the top position and located at the middle of the rack (not at the edge) in order to avoid possible leakage from the cold aisle. Preferably, sensors can be attached in such a way to allow them to reach a larger distance from the rack's door to the free space of the hot aisle in order to reduce the effect of the local streams and blockages. Such a location should

better represent the average temperature of the relevant hot aisle section, while satisfying the regular operating conditions such as easy manipulation of the housed IT. Therefore, the resolution of 1/3rd rack recommended by ASHRAE seems overly conservative for the hot aisle monitoring.

5.3 Validation and demonstration studies

Before the virtual DC environment is applied in the wider simulation-tool chain, the simulation models are configured based on the demonstration case study, and then a series of stand-alone tests is performed to demonstrate the capability of the model. While standards do exist that offer recommendations regarding the common level of acceptance of a model, for example see Coakley, et.al [139], in general, the level of acceptance and criteria of confidence are always related to the simulation purpose. As such, ultimately, there is no uniform guideline for the validation and demonstration of simulation models and these criteria are highly case-dependent.

In our case the criteria of confidence of the virtual DC environment must be agreed at the greater consortium level. The confidence criteria for our application are not only given by an absolute fit to measured data, as is usually the case for prediction models used in model-based control algorithms of individual components or single domains; the virtual DC as a multi-domain testing environment should also ensure that the following three conditions can be met: (i) the model results are still realistic for the expected range of inputs (not only for the measured dataset); (ii) the virtual DC environment represents the real monitoring format; and (iii) the virtual DC environment is able to realistically represent different configurations of the DC to allow different variations of testing (e.g. representation of full occupancy of the racks or representation of DC and RES system at the same location, etc.). The

validation and demonstration studies are important for the communication with external algorithm developers.

Naturally, the validation of the entire virtual DC system as a whole is not feasible due to its large complexity and to the limitations and uncertainties discussed in the previous section. The validation and demonstration study is decomposed according to individual sub models acting at related scales. Specifically, the individual models are manually calibrated and compared with available monitoring data from demonstration sites, or at least compared with relevant standards or technical documentation of modelled systems. The automated calibration, which would likely improve the overall fit, was not feasible due to the given time constraints originating from the planning of the overall Genic project.

This section is divided into validation and demonstration of the DC space model at the room/rack scale (section 5.3.1), DC infrastructure model as an electricity demand at the building scale (section 5.3.2), and demonstration of integrated RES model as part of on-site DC infrastructure (section 5.3.3). The validation and demonstration studies address the processes from scales of rack/room to building/district. Special interest is paid to DC space modelling at the mid-level of resolution, since this topic is a new addition for the BES community.

5.3.1 Validation and demonstration studies at rack/room scales

The validation and demonstration study of the DC space and IT model at room and rack level aim to capture the air temperature distribution within the DC space and provide a full representation of the sensor network shown in Figure 5-2 above. This validation and demonstration study contains three main steps: (i) evaluation of the model performance, (ii) demonstration of the capability to represent the required format of real temperature sensor network, and (iii) demonstration of the DC space model.

Input data for validation and demonstration

The validation and demonstration studies are supported by two different measured datasets of a 6-day period. The datasets are denoted as the “calibration” dataset, which is used for manual calibration, and the “validation” dataset, used for a cross-check of the model performance. The calibration dataset was measured in the period from 6-8-2015 to 12-8-2015 and the validation dataset from 1-1-2016 to 7-1-2016.

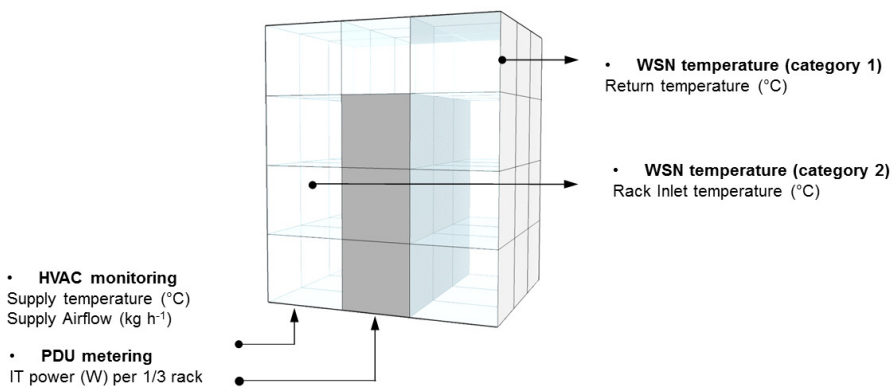


Figure 5-15 Schema of the monitoring of the DC space

The measured data consists of (i) IT power metering per 1/3rd of rack, (ii) temperature sensor network monitoring of the DC space including air side of cooling devices and (iii) airflow (multiple air velocity nodes) measurements of cooling devices. The schema of the process of the DC space model validation is shown in Figure 5-15. The input variables to the model are CRAC and AC supply temperature and total IT power load, shown in Figure 5-16 for both

datasets. The uncertainties of the measurements listed in Table 5-2 in section 5.2.2 are depicted as grey areas around the measured data.

(a) calibration dataset

(b) validation dataset

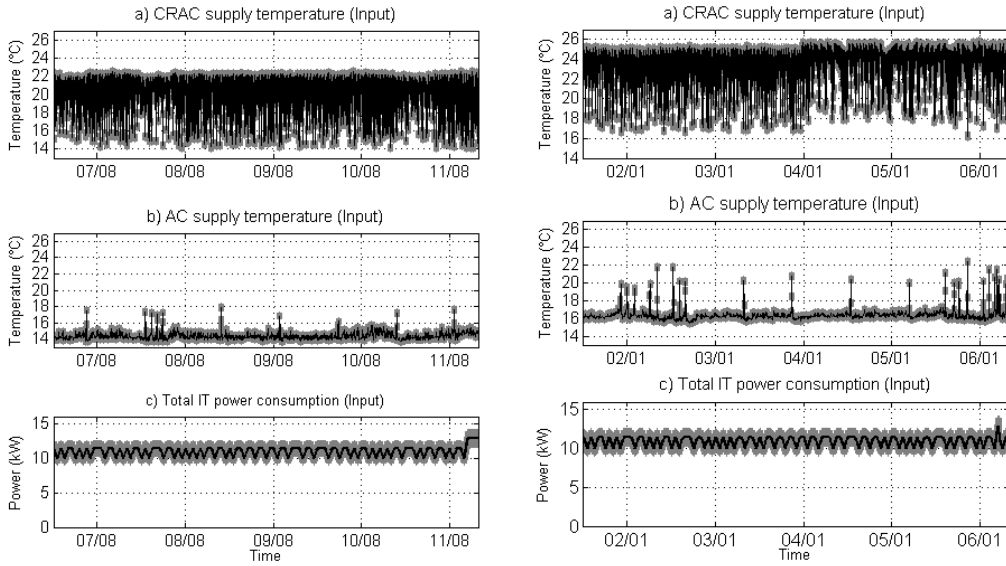


Figure 5-16 Model input for (a) calibration and (b) validation dataset

It should be noted that the validation dataset was gathered during a period of experimentation in thermal management, when the DC environment was operated with setpoints for return air temperature that were 3°C higher than previous operational conditions. In fact, having these two slightly different datasets serves to strengthen the validation process since the validation can be carried out for more than one condition. The cooling devices provides constant airflow during their operational hours. The airflow has been measured and can be approximated at $12000\text{ m}^3\text{ h}^{-1}$ for the CRAC unit and $2900\text{ m}^3\text{ h}^{-1}$. These values are also in agreement with the technical specification sheets of these units [131], [132].

The higher-level resolution model of the DC space requires the IT power with a granularity of 1/3rd of a rack. The measurements are provided with the required granularity. The measured IT power distribution per 1/3rd of rack is shown in Figure 5-17. This distribution is fairly constant during both of the measured periods.

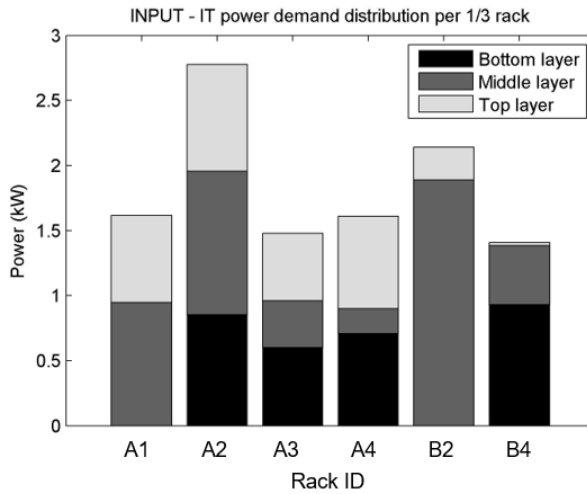


Figure 5-17 Input: IT power distribution per 1/3rd rack

Validation of the DC space model at higher mid-resolution

The DC space model including ITE models are validated by qualitative comparison of the measured and simulated data, while the measured supply temperatures, airflows and IT power metering are input to the DC space model as substitution of the inputs from the cooling and the power supply sub-models. The data from the temperature sensor network are compared with simulated data and the error is quantified. In this validation and demonstration study, absolute and relative errors are used to assess the performance of the model. The absolute error is defined as the difference between the measured and simulated data. The relative error is represented by the coefficient of the variance of the root mean square error. This metric was selected as suitable

based on a review conducted by Coakley et al. [139]. The coefficient of the variance of the root mean square error (RMSE) is defined in equation 5.1.

$$(5.1) \quad CV(RMSE) = \frac{\sqrt{\frac{\sum_{i=1}^{nr} (x_{ref} - x_{sim})^2}{nr}}}{\bar{x}_{ref}}$$

Firstly, the calibration dataset was used for the calibration process. The calibration aims to reduce the error primarily for the return air temperature of the cooling devices while also taking all inlet IT temperatures into account. Thus, two categories of outputs were defined as subjects of the calibration:

- Category 1.- Cooling devices (i.e. CRAC & AC units) return air temperature, higher priority
- Category 2.- Racks inlet air temperature, lower priority

Also, the IT outlet air temperatures, previously denoted as category 3, are shown in the results, even though it was found that there was a risk that the measurements are not representative for these computational nodes. These temperature nodes are still analysed for model demonstration. Regarding calibration, the following parameters were manually tuned in order to maximise the efficacy of the model in terms of temperatures of categories 1 and 2:

- Effective thermal capacity of the zones (time-response)
- Airflow through IT boxes (1/3rd of rack) in a realistic range (100-300m³h⁻¹kW_{IT}⁻¹ per server) [20, Ch. 2], [95]
- Setting of boundary conditions of the associated zone with the AC unit (pressure coefficient of the power law) in order to characterize the stream effect of the atypical air distribution.

Secondly, after the iterative process of the manual calibration, the performance of the calibrated model was cross-checked against the validation dataset.

The measured and simulated data were compared and the absolute and relative error (coefficient of variance) was evaluated. The results of the validation study depict the performance of the calibrated model for both calibration and validation datasets. The comparison of simulated results from the calibrated model against the monitored data extracted from the demonstration DC are shown in Figure 5-18. Specifically, this figure shows a comparison of return air temperature of cooling devices i.e. CRAC and AC units (category 1) including the uncertainty range related with measurements. The detailed overlook of this comparison is also shown in Appendix C.

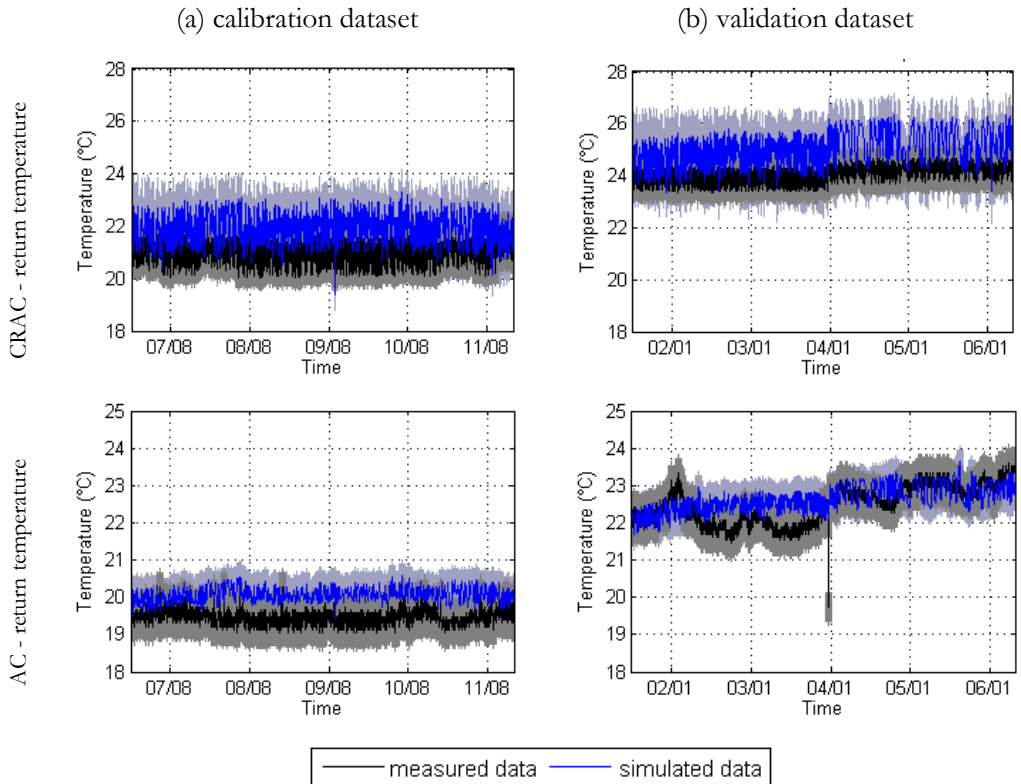


Figure 5-18 Comparison of measured and simulated return air temperature of cooling units (CRAC and AC unit) for calibration and validation dataset including uncertainty range of the measurement instrumentation

This figure shows good agreement in terms of dynamic response of return air temperature. The shown temperature variation reacts very similarly to the heavy fluctuation of input supply air temperature. An average bias of up to 1°C can be observed from the measured data. Considering the uncertainties arising from the sensing of measured inputs and from the sensing of referenced data, there is an overlap of the uncertainty regions and the error cannot be stated with certainty.

(a) calibration dataset

(b) validation dataset

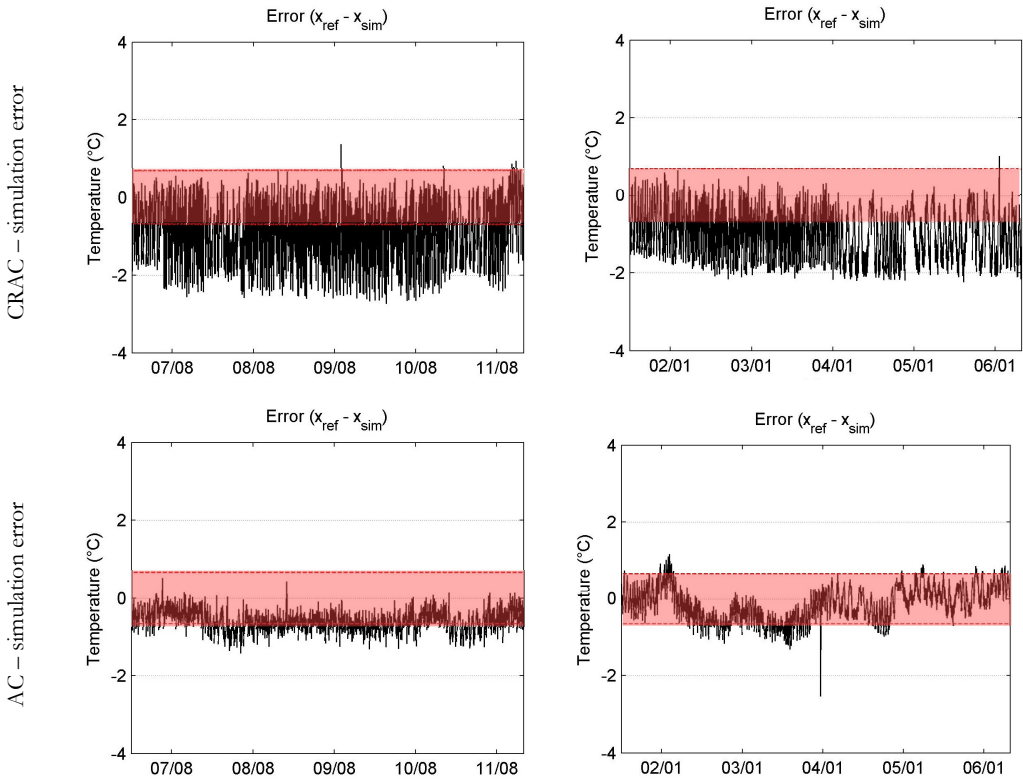


Figure 5-19 Absolute error of simulated return air temperature of cooling units (CRAC and AC unit) for (a) calibration and (b) validation datasets including uncertainty range of the measurement instrumentation

Thus, Figure 5-19 shows the absolute error ($x_{\text{ref}} - x_{\text{sim}}$) between monitored (x_{ref}) and simulated (x_{sim}), including the range of uncertainty, indicated by the red regions, combined from both sources of sensing. The error line indicates the absolute fit of the model. There is a visible mismatch, which is likely due to different initialization conditions of the model. The initialization setting for all temperature nodes is 20°C.

This process is repeated for all temperature nodes in the DC space for both training and validation periods. An example of a detailed comparison of selected nodes was already shown in section 5.2 above. To recall the conclusion from that study, the velocity and temperature distribution is not modelled in detail and the resolution of the DC space model is compromised due to the desired holistic purpose. The temperature distribution within the relatively large computational zones cannot always be assumed to be uniform. Thus, some validation results depend on sensor positioning, which may not necessarily represent the computational zone.

A complete evaluation of the error for all nodes is shown in Figure 5-20. The same analysis of temperature errors was repeated for the validation dataset. The evaluation of error for the validation period is shown in Figure 5-21, where absolute and relative error (coefficient of variance) are depicted. The results include the uncertainties related with measurement instrumentation represented by the error bars. The same analysis of temperature errors was repeated for the validation dataset. The evaluation of error for the validation period is shown in Figure 5-21. It transpired that the calibrated DC space model performed similarly for the validation dataset, where the input supply temperature of the CRAC unit was higher by 4°C due to a change of the return air temperature setpoint from 21°C to 25°C. Also, the backup AC unit supply temperature setpoint was increased from 14°C to 16°C.

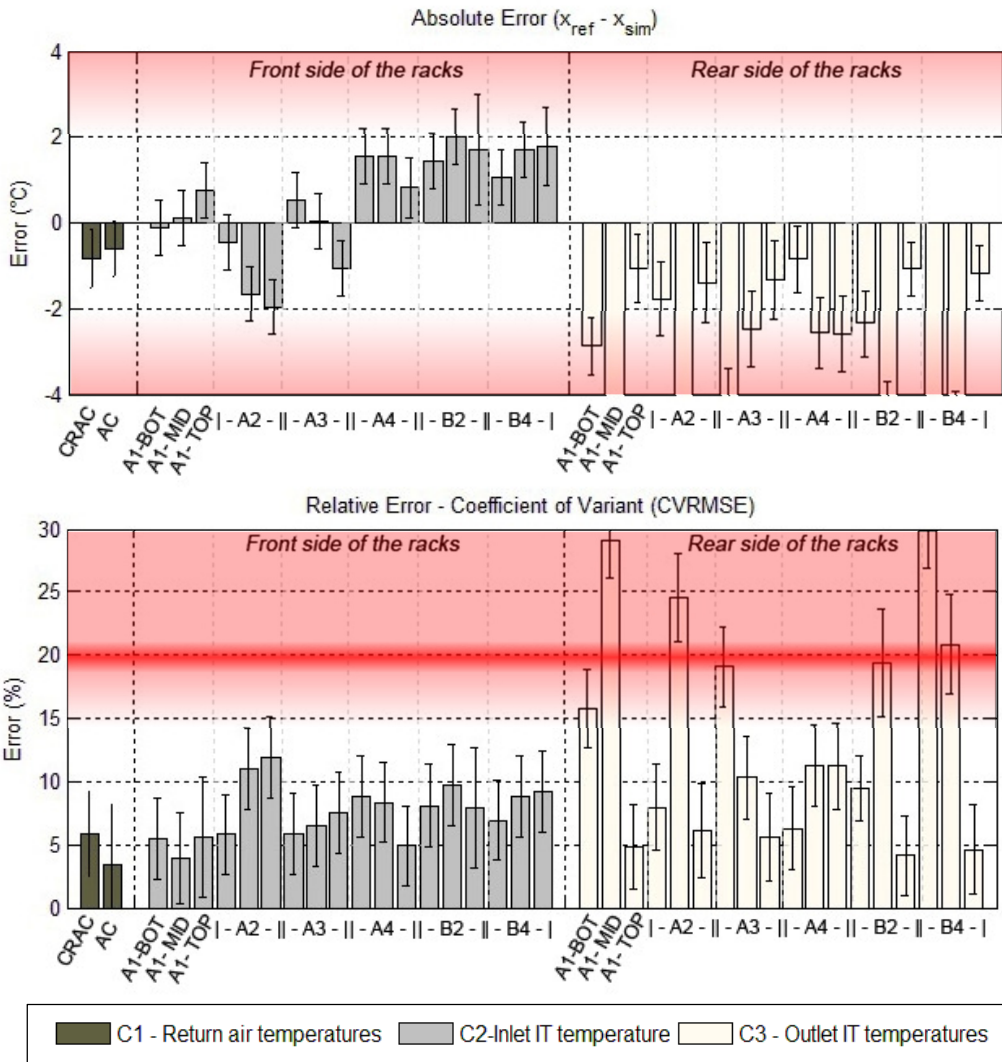


Figure 5-20 Evaluation of absolute and temperature error of the DC space model, calibration period

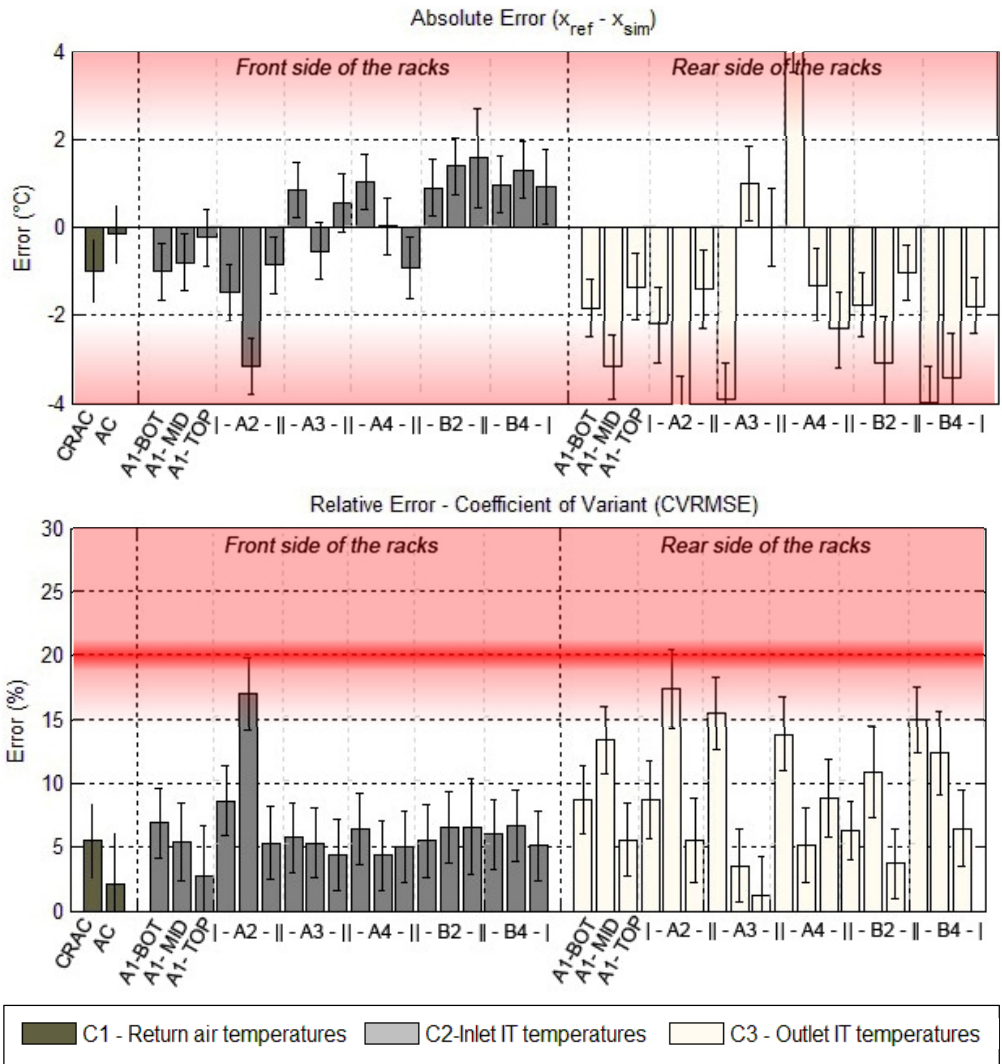


Figure 5-21 Evaluation of absolute and temperature error of the DC space model, validation period

The problem of modelling the local air of the AC unit remains. In fact, this problem can be observed in the high error of the mid inlet node of the rack A2. The relatively high error can be explained due to the temperature at this node being underestimated because of buoyancy effects. The measured data provides evidence that the cold air released from the backup AC unit at the top level loses momentum around this spot and it has a tendency to descend to the mid-level. These effects cannot be truly captured at the selected level of modelling resolution.

However, the overall error evaluation still shows that the model performs well, and it can be concluded that the DC space model is able to represent the real DC space (even including uncommon arrangements of the AC unit) with acceptable relative errors according to published standards.

Demonstration of the DC space model at higher mid-resolution

As introduced in the beginning of this chapter, the absolute fit is not the only criteria of confidence. An important part of the confidence criteria is the ability to represent the data format of the sensor network. This capability of the model is demonstrated in Figure 5-22. The measured data (shown also in Figure 5-2) and interpolated visually between the computational nodes are plotted in a single figure for bottom, mid and top level, and also for plenum level where the air is returned to the CRAC unit. The measured nodes are denoted by coloured dots that relate to spot temperature measurements. The computational nodes are denoted by black crosses in the computed visualization of temperature distribution for the calibration and validation datasets.

The detailed model demonstration, performed for various settings of cooling device and workload, can be found in Appendix C. This study indicates that workload utilization can have an equal influence on the thermal behaviour of the DC space as the control aspects of the cooling system (i.e. supply air

temperature and supply airflow levels). Therefore, the workload level and cooling settings should be carefully balanced in order to achieve the optimal performance.

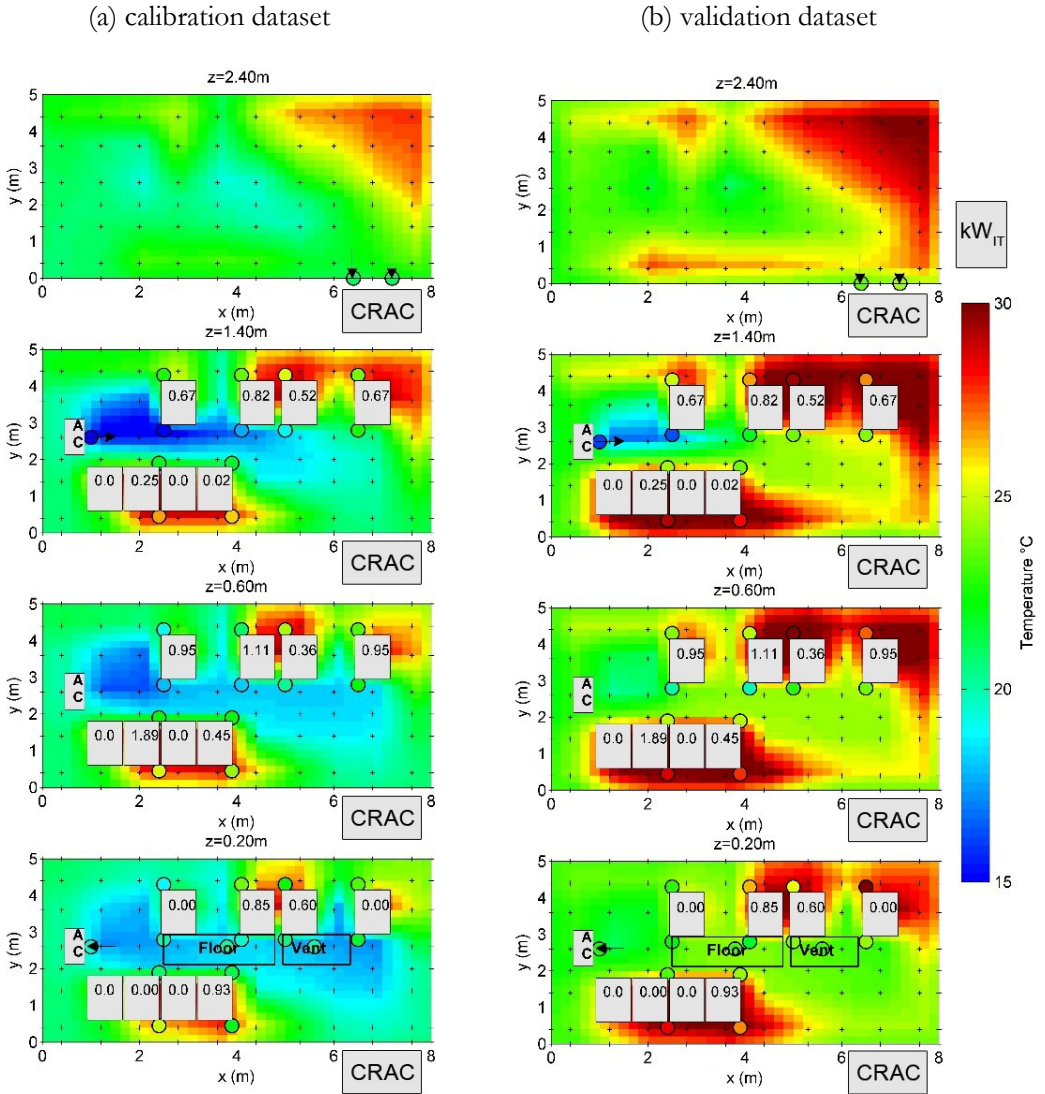


Figure 5-22 Measured nodes versus simulated and interpolated temperature distribution

5.3.1 Validation and demonstration studies at building scale

The validation and demonstration studies at the building level are focused on the lower-resolution space model and cooling system.

Validation of the DC space model at lower mid-resolution

The validation of the lower resolution model is briefly discussed. To reiterate, the model consists of five zones: Underfloor, Cold aisle, Rack, Hot aisle and Upper plenum zone. These zones represent the whole DC space. This model was not selected for application in the wider simulation tool chain, because it does not satisfy the resolution requirements of modern thermal management. In our case, this model was used for yearly evaluation of the HVAC and RES systems acting at building scale. This model is more convenient for such a demonstration due to its low computational demand. Since this model is therefore of less significance, the validation study is only briefly elaborated.

This model is designed mainly for representation of the DC including the underfloor air distribution. Therefore, a period when only the main CRAC unit was in operation was chosen for the validation study. Based on the airflow measurements of the CRAC and back-up AC unit of the DC demo site, shown in Figure 5-7, this period occurred on 9-7-2015. This period was selected for the validation study.

This model requires the definition of constant air distribution efficiency of the DC environment. In our case the air distribution efficiency is represented by the SHI [140], which needs to be obtained from measurements of the space or from the high-resolution model. The model was calibrated in terms of (1) effective thermal capacity of the zones (time-response), and (2) airflow through IT boxes (1/3rd of a rack) in a realistic range ($100\text{-}300\text{m}^3\text{h}^{-1}\text{kW}_{\text{IT},\text{cl}}^{-1}$ per server) [20, Ch. 2], [95].

The input data for this validation study are temperature, measured airflow and measured power consumption of the IT equipment. As we could see in the

previous validation study, the airflow and IT power are fairly constant. Similar results were observed for this period. The airflow was stated at 12 000 kg h⁻¹ and IT load fluctuated in the range of 9 to 11 kW. The input supply temperature is shown in Figure 5-23 together with measurements of the underfloor space and CRAC return temperature. Figure 5-23 also shows the simulated temperatures for the underfloor zone and upper plenum zone.

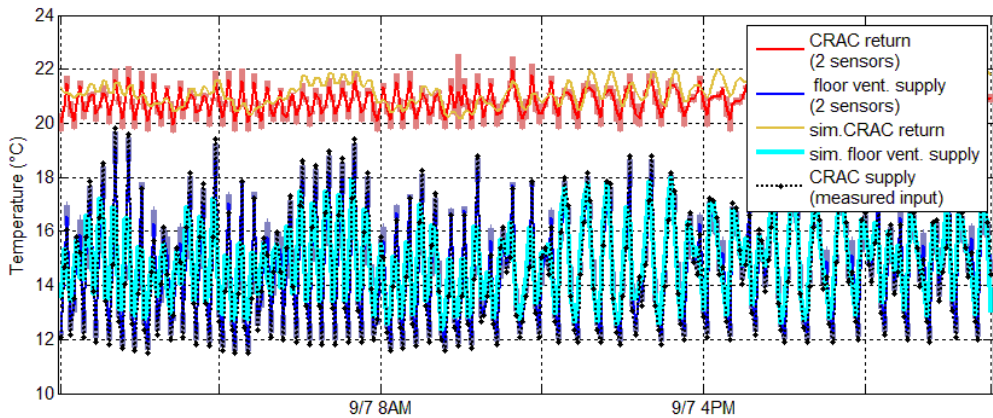


Figure 5-23 Comparison of measured and simulated supply and return temperature

In this case of the low-resolution model, the computational nodes represent numerous measured spots. The range of measured temperatures assigned to the particular computational node can be understood as the uncertainty of the representation. Similarly, as in the previous section, the uncertainties of representative temperature for individual zones are visualized as areas around the plotted curves. The uncertainties are more noticeable for the measurements of cold and hot aisle depicted in Figure 5-24. These regions are measured by 18 sensors. The measurements show that a single zone is represented by a large spread of temperatures. Figure 5-24 shows the average temperature of the cold and hot aisle region and their simulated equivalents.

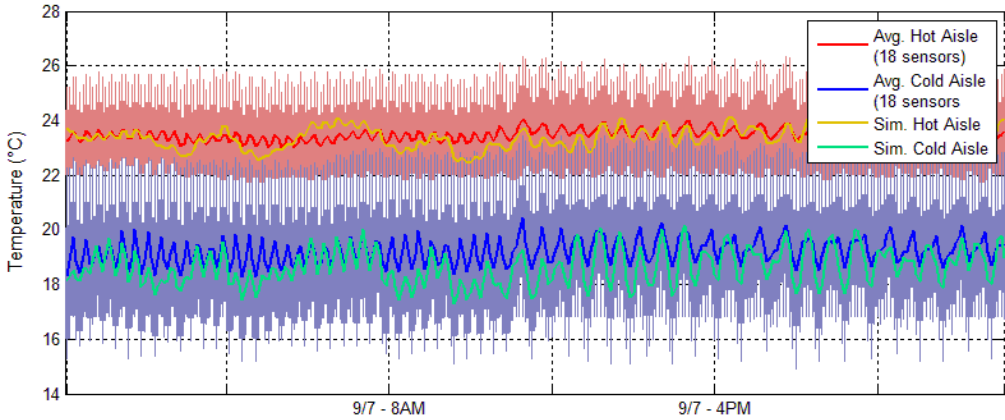


Figure 5-24 Comparison of measured and simulated cold and Hot Aisle temperatures

The absolute and relative errors between measured and simulated temperatures are depicted in Figure 5-25. It is worth noting that although the overall error is relatively small, the uncertainties of the representation are large, especially for cold and hot aisle regions. This representation is given by heterogeneous air distribution of cold and hot aisle regions, where each computational node represents the average of measurements obtained from numerous temperature sensors.

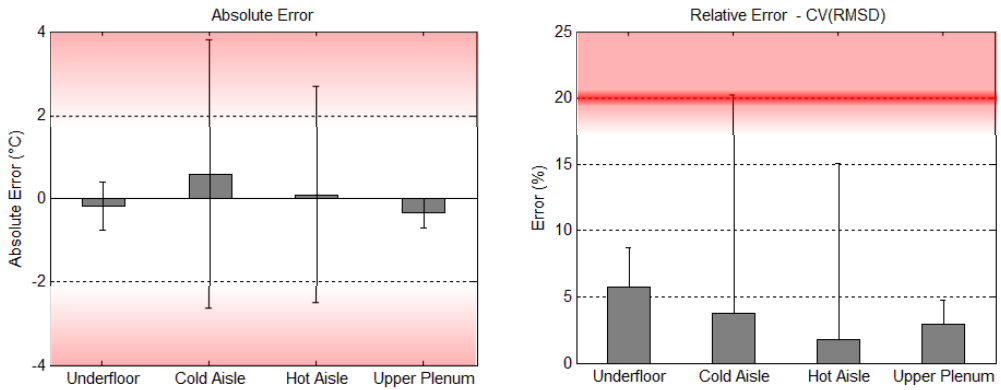


Figure 5-25 Average of absolute and relative error of the lower resolution model

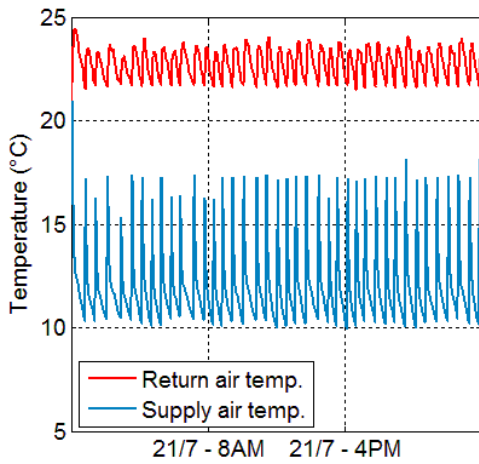
To conclude, the lower resolution model can sufficiently represent the return air temperature for any analysis at building level (e.g. cooling device or power delivery model). The advantages of this model are that it is easy to manipulate and is resizable. The lower resolution comes with less computational demand, which is suitable for long-term (e.g. yearly) analysis. Obviously, the lower resolution does not allow for the analysis of the DC space. The other disadvantage is that the fine calibration of the model requires the support of the high-resolution model in order to define the air distribution efficiency. Otherwise, this factor can also be estimated based on literature (e.g. Fakhim et al. [141]).

Validation and demonstration studies of the cooling and power delivery models

The cooling system and power delivery system is supported with fewer measurements than the previously studied DC space due to the discussed issue of data availability. The validation and demonstration study is supported by temperatures gathered from the already mentioned DC space measurements and the energy audit performed between 22/7/2014 – 31/7/2014. The energy audit provides measurements of the total DC electricity, which are broken down according to the individual items. The validation and demonstration study could not be performed to the same extent as in the previous case, mainly due to limited access to data from the cooling system (e.g. rejecting circuit and drycooler). The model was set based on the technical specification sheet of the individual unit [131], [132]. The thermal performance of the cooling system for the air and water sections is demonstrated for a typical summer and winter day in Figure 5-26 and Figure 5-27.

The simulation for a typical summer day demonstrates the identical on-off behaviour, which was observed in the DC site measurements (Figure 5-5, section 5.1.1).

(a) Typical summer day



(b) Typical winter day

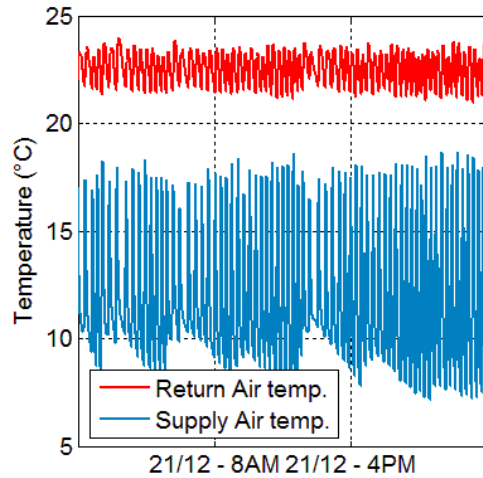
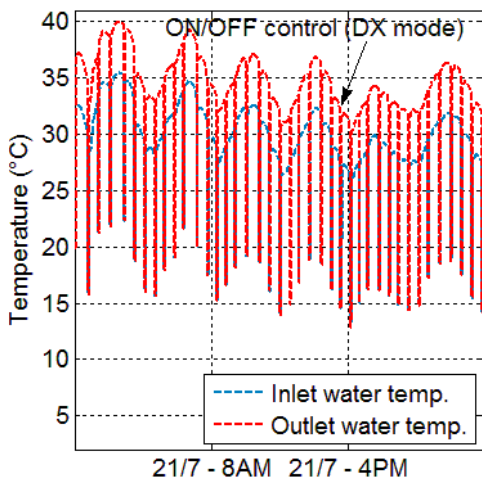


Figure 5-26 demonstration of return and supply air temperatures of the CRAC unit for typical (a) summer and (b) winter day

(a) Typical summer day



(b) Typical winter day

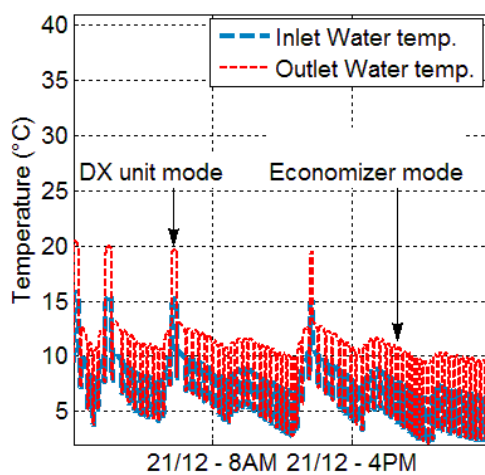


Figure 5-27 demonstration of inlet and outlet water temperatures of the CRAC unit for typical (a) summer and (b) winter day

The internal on-off control of the compressor unit affects temperatures in the heat rejecting circuit at the water side of the unit, which is in the expected range of 35-40 °C. The typical winter day, in which the compressor unit is bypassed, demonstrates the activation of the economizer mode. The variation of temperatures of the heat rejecting circuit, in the range of 3-10°C, are caused by weather conditions at the drycooler. Like the compressor unit, the economizer is controlled in an on-off fashion.

The performance of the electricity demand is supported by the energy audit data. Examining the energy audit in more detail, a comparison of the energy demand measured [133] and the simulated results is shown in Figure 5-28. The measured data corresponds to the period between 23/7/2014 and 29/7/2014. Overall, as can be seen from the figure above, the simulated results are proportionally in agreement with the measured data extracted from the audit.

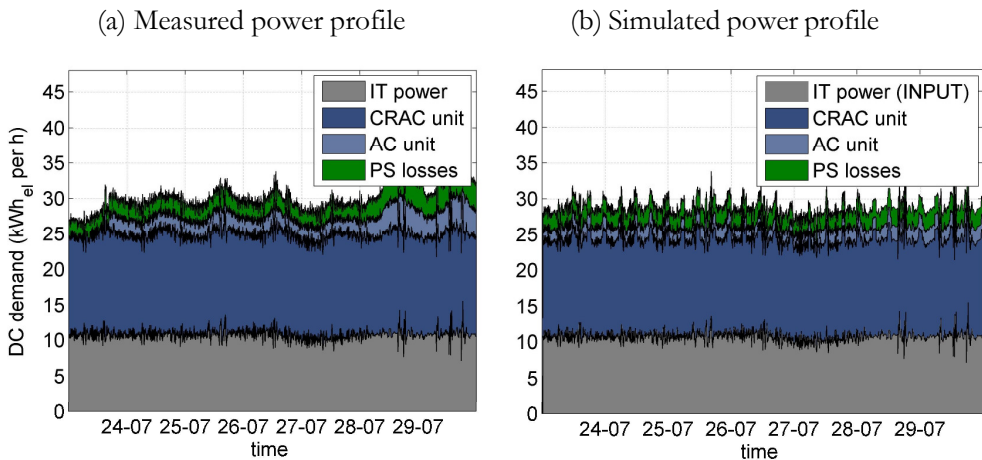


Figure 5-28: Breakdown of Energy demand for C130 DC, (a)measured and (b) simulated

The study is strengthened by a comparison between the power usage effectiveness (PUE) indicator of measured and simulated data for the demo

DC for a ten-day period of the energy audit. This comparison is presented in Figure 5-29. The figure gives an important indication regarding DC utilization and the design and efficiency of the operational infrastructure. The DC utilization during the observed period was mostly in the range of 30% or 9 kW (lower boundary) to 44% or 13 kW (upper boundary). For these values, the PUE for measured data ranged from 2.15 – 3.11 and, for simulated data, from 2.51 – 3.11. It is also important to highlight that under design conditions and 100% or 30 kW of utilization, the PUE of the demo DC should be 1.6.

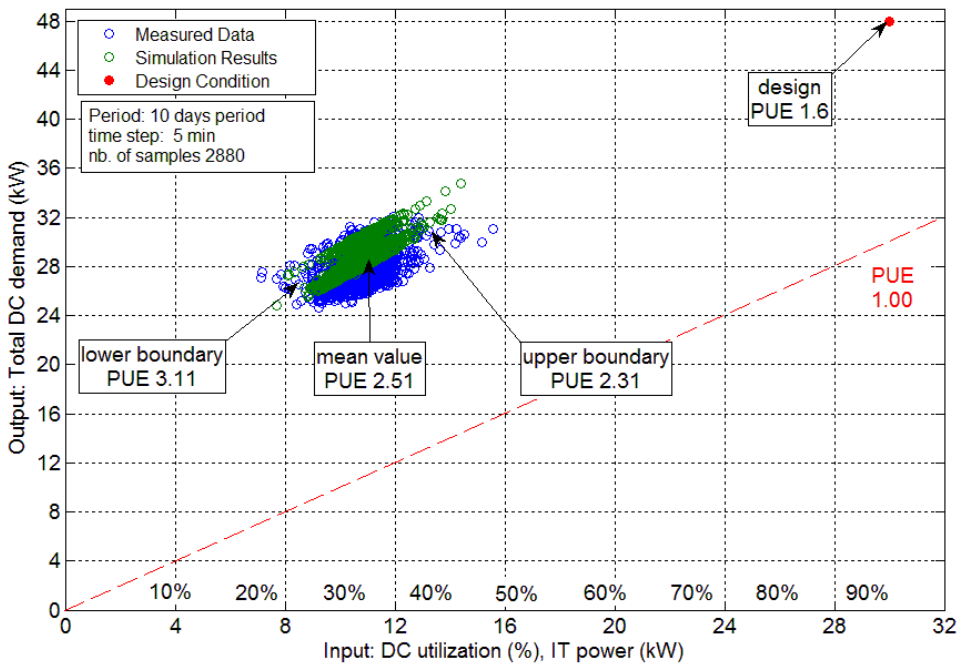


Figure 5-29: Power usage effectiveness based on measured and simulated data for a measured period

Although the agreement between simulated and measured results is clear, the measured values still have a larger spread than the simulated results. This might be due to the operation of the small AC unit. This unit has a nominal power

of 2 kW. While it was assumed to be in continuous operation in the model, it was found that this was not always the case. The difference can be also explained by differences of the outside temperature, where weather data of a typical year were used for the simulation.

5.3.1 Demonstration study at the building/district scale

This study demonstrates the performance of the presented RES model as on-site facility of the DC model. The RES model was developed and validated in the RES lab by an external expert (Acciona). The validated model was then integrated into the internal structure of the overall virtual DC environment.

To reiterate, the case-study facilities, of which the university DC is located in Ireland and the RES laboratory in Spain, were modeled to form the virtual DC environment. While, in reality, they are not physically connected, assessments of the DC energy demand versus RES supply are possible through simulation tests. The performance indicators of interest are the on-site energy fraction (OEF) and on-site energy matching (OEM) indicators [142]. OEF indicates the proportion of the load covered by on-site generated renewable energy, while OEM indicates the matched proportion of on-site generated renewable energy that is used in the load rather than being exported to the grid. These two basic indices are selected to analyse the mismatch between the energy demand and supply sides

To demonstrate the functionality of the virtual DC environment and to assess the performance of on-site energy, a scenario, which represents the real power supply system for both locations in Spain and Ireland (as on-site facility) is considered. This scenario is presented for January (typical winter month), July (typical summer month) and annual evaluation using OEF and OEM factors

This scenario analyses the on-site energy supplied by the demonstration sites of project Genic. The power supply model included in the wider structure of the virtual DC environment was simulated with typical meteorological data for

Cork, Ireland and from Seville, Spain. The power supply system acts as it was integrated on-site of the demonstration DC. Such a setup is used later in the computational experiments presented in Chapter 6.

(a) Situated in Cork

(b) Situated in Seville

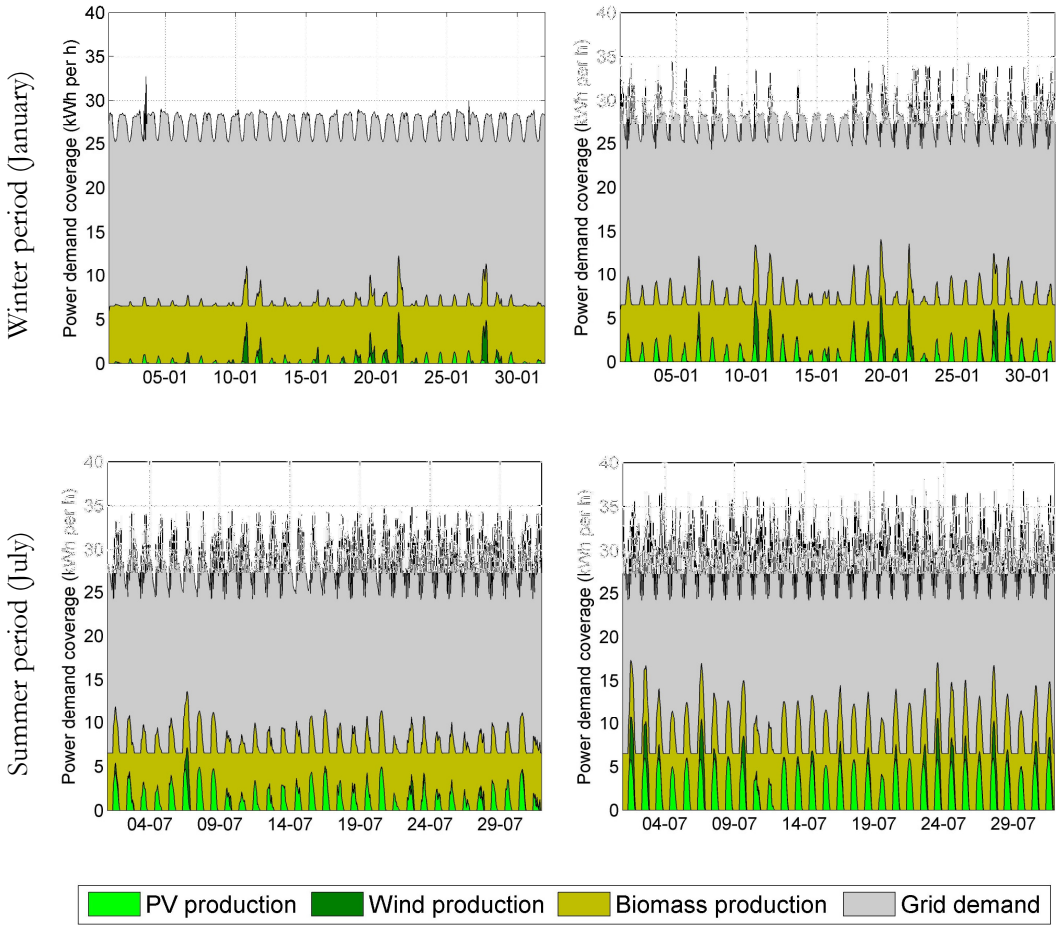


Figure 5-30 Power demand coverage using bespoke RES system for summer and winter period situated (a) Cork, Ireland (b) Spain, Seville,

Figure 5-30 shows typical power demand coverage using bespoke RES systems (PV, Wind, and Biomass production) for winter and summer periods. The left

side demonstrates the situation in Cork, Ireland, while the right side demonstrates the situation in Seville, Spain. The yearly evaluation of OEF reveals that the bespoke RES system can cover only 25,7% and 27,9% of the DC demand for Cork and Seville, respectively. From which, most of the on-site RES production is supplied by the biomass plant. Considering only PV and wind, the demand coverage is 2,4% and 5,3% for Cork and Seville, respectively. Since the fraction of the on-site RES production is relatively low, all energy production is used on-site to cover the DC demand, and thus OEM is always 100%. The monthly evaluation of OEF and OEM is shown in Figure 5-31.

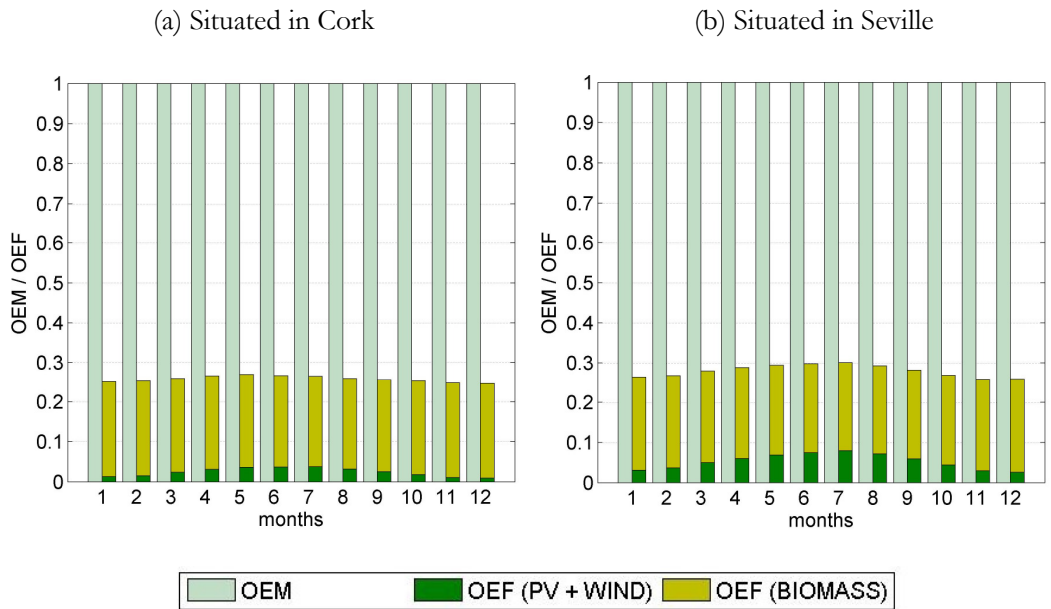


Figure 5-31 Monthly evaluation of power demand coverage using bespoke RES system situated (a) Ireland, Cork (b) Seville, Spain

In summary, the RES model was modelled and validated based on the RES lab in Spain by an external partner. This model was successfully integrated into the wider framework of the virtual DC environment. The performance of the

system was demonstrated through yearly evaluation of the onsite energy fraction and the onsite energy matching for the given case study.

In general, it can be concluded that there is an essential mismatch of power density between demand and generation. With the given configuration and the location in Ireland, the relatively large on-site RES system (e.i. 84m² of PV area, small-scale wind turbine and biomass power plant) could only satisfy 25,7% of the concentrated DC demand (e.i DC floor area of 40m²), of which only 2,4% were satisfied by PV array and small-scale wind turbine. The rest is covered by the biomass power plant.

5.4 Concluding remarks

The main aim of this chapter was to validate and demonstrate the virtual DC environment. To this end, a case study was conducted in which a virtual DC environment was used to represent a real bespoke DC located in Ireland and a real RES laboratory located in Spain. This virtual DC environment was able to represent different configurations within the DC, which in turn allowed for variation in testing of the key variables and performance indicators of interest. Ultimately, it was essential here to determine if the generated results were realistic for the expected range of inputs. In terms of analysing the results, the results generated from the virtual DC environment were compared with measurements taken during the regular operation of a real DC. Therefore, the first step in the analysis was to determine whether there were any limitations in terms of the measurements taken. In order to do so, the monitoring data from the real DC were analysed. The sensors were placed wherever possible in the DC to measure power usage, temperature and massflow. These measurements were used in comparison with the generated results from the virtual DC environment. The following three limitations regarding measurements were identified:

- It was discovered that some of the spot measurements regarding DC space and ITE modelling were not fully representative of the computational nodes. This was particularly evident for the nodes at the temperature measurements of the outlet side of the racks. In brief, the main reason for this finding was the identified mismatch between spot measurements, which are affected by local stream sources and blockages, and computational nodes, which represent larger volumes of the DC space. However, it was ultimately discovered during the development process that the tested management strategies do not require this information for any control purposes. The temperatures at the inlet sides of racks and at the return to the CRAC unit are affected by massive air-change of the CRAC unit. In fact, these spots were found to be generally less sensitive to sensor placement and could represent larger volumes of space. Therefore, it was concluded that the computational nodes can suitably represent the spot measurements.
- In terms of the cooling and power delivery system models, it was found that the number of sensors that it was possible to place in the real DC was insufficient for validation. The available sensors did not provide measurements at the required resolution. Therefore, numerical comparison could not be used to demonstrate all of the model outcomes. While the measurements did support numerical comparison at the building level in terms of total electricity demand of individual domains, other outcomes could only be demonstrated based on standard ranges and common sense.
- Technically, one limitation regarding the power supply model is that it was not possible to access the underlying data due to the confidentiality restrictions of the specialist project partner. However, the given power supply model was accompanied by a validation study [143] that provided

the RES measurements derived from a real lab in Spain. As such, the model can be integrated into the overall structure of the virtual DC environment with confidence.

After considering the above limitations, next the focus turned to the validation and demonstration of the virtual DC performance through the comparison of results. It is important to note here that the quality assurance was complicated by two key factors: (1) the large scope of the modelling; and (2) measurements were taken during regular DC operation, which means that the modelling resolution was compromised, and that the availability of data monitoring was not ideal with respect to regular operation. Therefore, the validation and demonstration of the virtual DC environment had to be decomposed and a number of sub-models had to be assessed in order to facilitate the validation of the results. The results of particular interest relate to the following three groups of sub-models: DC space and ITE model; cooling and power delivery model; and, power supply model.

In order to be able to cover a wide range of testing possibilities, two models for the DC space and ITE were developed and validated. These are denoted as the high-complexity and low-complexity models. For both of these models, errors, including the uncertainties of the sensor measurements, were quantified between the generated results and the measurements from two DC datasets: one for summer and one for winter.

- The high-complexity model represented the DC space by using 240 computational nodes, of which 38 represented the spot measurements of the real temperature sensor network. The errors of the temperatures at the return to the cooling units (2 nodes) were quantified as falling in the range of 0.3 to 1°C with an uncertainty of +/- 0.5°C, which translates to a relative error (CVRMSE) of approximately 5%. The errors of the temperatures at the inlet of the racks (18 nodes) were quantified as falling in the range of

1-3°C with an uncertainty of +/- 0.7°C, which translates to a relative error (CV(RMSE)) of approximately 11%. The errors of the temperatures at the outlet of the racks (18 nodes) were quantified as falling in the range of 1-6°C with an uncertainty of +/- 0.7°C. It is important to note that for some nodes, the relative error exceeded 20%. The results of the first two categories can be viewed positively, since they are in accordance with industry standards [144], [145]. In the third category, the comparison with the measured data is limited due to the aforementioned misrepresentation of spot measurements and computational nodes.

In conclusion, the high-complexity model of DC space satisfied the requirements of resolution of other external partners because it enabled thermal analysis at rack level, which was not possible with the presented low-complexity model. Furthermore, the quality of the generated results was deemed sufficient by the external partners.

- The cooling and power delivery model is validated in terms of total cooling electricity demand. The performance of the model was in agreement with the performance of the real DC. This agreement was evident since both the measured and simulated data for the PUE were in the range of 2.15 to 3.11. In contrast to the DC space model validation, the detailed numerical comparison with measured data was not feasible for the cooling and power delivery system due to limited possibility of measurements at the component level. For instance, the quality assurance of the thermal behaviour of the cooling system relied largely on demonstration of the cooling system because access to measured data was limited. Nevertheless, the simulated data were in the expected range given by standards and technical sheets [94], [131], [132]. It can be concluded that the presented physics-based model, built mainly based on technical sheets, demonstrated realistic energy behaviour

Finally, this chapter provided a demonstration of one way of approaching validation and demonstration as one step within the proposed testing workflow. Wherever possible, measurements were taken and errors in the simulated results of the virtual DC environment were quantified. Where it was not possible to gather all required measurements, the performance of the virtual DC environment was demonstrated by determining that the simulated results fell within expected ranges that were derived from known standards and regulations.

Despite the small gaps in measured data, due to the large scope of the study the quality of the virtual DC environment was found to be satisfactory and capable of achieving its given purpose. The presented validation study was reviewed and verified by external partners from practice and academia within the Genic project. Finally, it was agreed by all involved parties that the virtual DC environment can be used for testing prior to the installation of the control platform in the real DC. It is important to note that the virtual DC environment is never meant to control the real DC processes. It is simply meant to emulate these processes for testing purposes.

6 Execution of computational experimentation for commissioning of holistic data centre operation

Chapter 6 demonstrates the usability of the virtual data centre (DC) environment for the given application, where the virtual DC is used for testing of externally developed algorithms. Thus, in the second set of computational experiments, the virtual DC environment, which was validated and is discussed in the previous chapter, is connected to the wider simulation tool-chain to enable the interactive communication with the external algorithms. The simulated outputs are provided as “virtual monitoring”. This virtual monitoring is subject to the same “monitoring uncertainty” as the real measurement instruments. While the tested multi-domain algorithms operate the virtual DC environment, the simulated performance data from the virtual DC environment are collected. The recorded results from these experiments are analysed and discussed. The impact of the external control algorithms on the DC energy use is always compared with the simulated baseline, characterised by conventional DC management.

6.1 Computational experiment definition

6.1.1 Testing process of the external algorithms

To reiterate, the virtual DC environment, developed and validated in this research, is integrated into the wider simulation & communication tool-chain developed within the framework of the Genic project. The simulation & communication tool-chain allows the dynamic communication between

various entities, individual control algorithms and development support tools, and also acts as an interface for physical devices in real experiments.

All results presented hereunder were gathered from the interactive closed-loop testing of external control algorithms. The presented testing was performed for typical summer and winter seasons with a simulation period of 14 days. The control process was recorded, analysed and evaluated based on data generated by the virtual DC environment. It is important to understand that Building Energy Simulation (BES) specialists, which are in the role of testers here, often have very limited understanding of the internal workings of the tested algorithm due to a lack of knowledge in a particular field or to a developer's confidentiality. By using the mentioned communication framework, no internal information is generally required since the I/O specification is sufficient for any testing. Amongst other things, the communication framework allows the closed-loop testing using the virtual DC environment as a tool to support development.

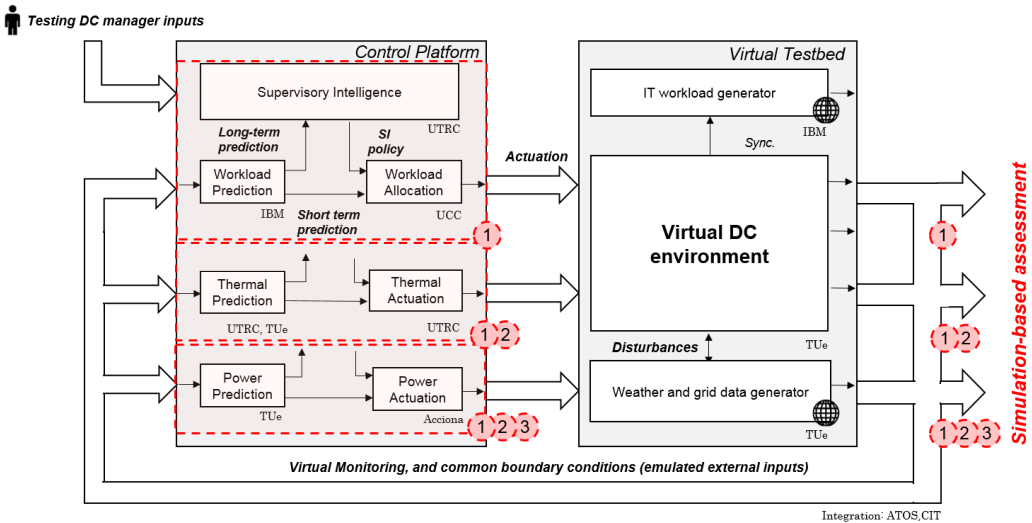


Figure 6-1 Simulation & communication tool-chain for the simulation-based closed-loop testing: tested modules and virtual testbed

The virtual DC environment provides virtual monitoring feedback and evaluates performance of the tested algorithms under conditions very similar to those used in real operation. Since the understanding of the tested algorithm may be limited, the design of computational experiments and discussion of subsequent results should always be conducted in consultation with the algorithm developers.

The closed-loop testing configuration of the computational experiments including relevant developers are shown in Figure 6-1. In this chapter, the testing procedure of individual modules is presented in stages relating to those shown in Figure 6-1. First, the results regarding workload management are presented followed by the results of the combined workload and thermal management, and finally the results of power supply management considering the performance of other previously tested management blocks.

The involved platform modules:

In these experiments, the external modules involved in the testing are a subset of modules required for regular operation, which are workload management, thermal management, power supply management and supervisory management. The supervisory management operates at a higher level of the control platform architecture and it does not directly communicate with either the real or virtual DC environment.

- The workload management encompasses a subset of modules such as workload allocation, short-term workload prediction and server configuration service.
- The thermal management encompasses a subset of modules such as thermal actuation and short-term thermal prediction
- The power management encompasses a subset of modules such as power supply actuation and short-term power prediction (if applicable)

- The supervisory management, which is mainly responsible for demand versus supply energy matching and related economic and ecological outcomes of the DC, encompasses a subset of modules such as supervisory intelligence module, long-term power and thermal and workload predictions.
- The virtual DC environment, weather, grid data and workload generators represent the testing environment.

For more detailed information on the characteristics and functions of these modules refer to related published material [60], [146]. Table 6-1 shows the tested configurations of multiple external algorithms. The computational experimentation is further focused on individual workload management, thermal management and power supply management developed by external partners and briefly described hereunder.

Table 6-1 Settings of platform configuration for all presented computational experiments

setting ID.:	workload management	thermal management	power supply management
{1}	no consolidation	constant setpoints (21°C)	no on-site RES
{2}	consolidation: ITE consumption priorities	constant setpoints (21°C)	no on-site RES
{3}	consolidation: thermal priorities	variable setpoint (18-25°C) (room level control)	no on-site RES
{4}	consolidation: ITE consumption priorities	variable system setpoints (system level control)	no on-site RES
{C1}	consolidation: ITE consumption priorities	constant setpoints (25°C)	no on-site RES
{C2}	consolidation: ITE consumption priorities	cold aisle containment constant setpoints (21°C)	no on-site RES
{5}	consolidation: thermal priorities	variable setpoint (18-25°C) (room level control)	on-site RES; surplus
{6}	consolidation: thermal priorities	variable setpoint (18-25°C) (room level control)	on-site RES; supervisory strategy

Workload management experiments

The tested workload management manipulates IT workload, represented by virtual machines (VMs), in order to firstly ensure service-level agreements (SLAs) and secondly to reduce the IT equipment (ITE) power demand. The reduction of ITE power demand is achieved through a process in which the workload is consolidated and migrated to the preferable ITE within the ITE cluster. The energy savings mainly result from setting unused servers to standby mode. Thus, the idle power of ITE is saved.

The aim of the computational experiments presented here is the testing of the workload allocation algorithm with the following settings:

- Workload Allocation without the migration of VMs (baseline)
- Workload Allocation with the migration of VMs to minimize ITE power
- Workload Allocation with migration of VMs according to thermal preferences

The first setting of workload allocation is the baseline setting of workload allocation without any possibility of dynamic VM migration. Such a workload management is currently used in most DCs [27],[147]. Using this setting, the IT tasks are allocated to the ITE according to the available computational capacity at the time of arrival of each IT task. Each IT task is processed by the same ITE, which is initially allocated until the task is fully processed.

The second setting of workload allocation is the advanced setting of the algorithm, where a predefined number of migrations of VMs are enabled in each timestep; for example, every ten minutes. The IT task can be consolidated and migrated to the most efficient ITE, and the unutilized ITE can be deactivated and put into standby mode. This setting requires mapping of ITE performance within the ITE cluster and short-term prediction of incoming IT

workload in order to reactivate the ITE in advance of a peak, thereby ensuring the SLAs.

The third setting of workload allocation is the advanced setting of the algorithm, when the thermal management provides thermal preferences for each ITE. The IT workload is then allocated to the thermally preferred ITE first, regardless of the ITE's efficiency. Thus, this setting requires the mapping of ITE thermal preferences within the ITE cluster, short-term prediction of incoming IT workload and prediction of the thermal environment.

These settings are compared against each other. This comparison is assessed based on total energy use per domain, and indicators such as IT productivity and power usage efficiency. All relevant indicators are described below in section 6.1.2.

Testing process:

The testing of experiments for the Workload management was executed via the following steps:

- The virtual DC environment publishes the virtual time that will serve for the different modules in the testing loop to synchronise their actions.
- The workload generator module publishes the VM profiles for the current time step.
- The workload allocation receives all necessary inputs (predictions, server mapping, thermal preferences etc.) and then optimizes the allocation for the given arrangement in the virtual C130 DC presented below in section 0. The workload allocation is able to consider thermal priority for each box (1/3rd of a rack).
- The server configuration component translates VM allocation to power consumption per box (1/3rd of a rack) and provides this information to the virtual DC environment

During this iterative process for further analysis and post-processing, the virtual DC environment captures the entire testing process, which includes all electric and thermal energy fluxes, temperature traces, massflows, etc.

Thermal management experiments

The tested thermal management can be configured either for room level only, or for alternative system level actuation. The room level actuation manipulates return temperature set points of the Computer Room Air-conditioning (CRAC) unit in order to obtain the desired inlet ITE temperature in the DC space. In the system level actuation, both the return temperature setpoints and airflow of the CRAC unit are manipulated, as well as the massflow rate of the pump in the heat rejection circuit, drycooler airflow and economizer setpoints. The tested thermal management requires virtual monitoring of the DC space, virtual monitoring of the cooling system and short-term predictions of this monitoring, and prediction of ITE power provided by workload management. The aim of presented computational experiments is the testing of the thermal actuation algorithms with the following settings:

- Constant setpoints (baseline)
- Thermal actuation at room level
- Thermal actuation at system level

The first setting of the thermal management represents the strategy currently used in real DCs. The thermal actuation relies on embedded local control with constant setpoints. The return temperature setpoint is fixed at 21°C and the airflow setpoint is fixed at 3,3 m³s⁻¹.

The second setting of the thermal management is room-level actuation, where the thermal management manipulates return air temperature setpoints in order to reach the desired inlet ITE temperature. This configuration can be deployed and tested at a real demonstration DC.

The third setting of the thermal management refers to system-level actuation, where thermal management manipulates the complete cooling system in order to reach higher level objectives such as minimized energy use or maximized waste heat utilization. In the context of the current research case study, this configuration could only be deployed and tested using a virtual DC environment.

These experiments are compared against each other and against the baseline, which is currently used in the real DC. In addition, two competitive strategies are simulated. These strategies are

- Higher constant setpoint of return air temperature at 25°C
- Cold aisle containment and constant setpoint of cold aisle air at 21°C

These settings are compared against each other. This comparison is assessed based on total energy use per domain, and on violation of the operational temperature range for ITE and power usage efficiency. All relevant indicators are described below in section 6.1.2.

Testing process

The testing of experiments for the thermal management follows these steps:

- For each given time step, a number of variables are published. These are virtual synchronization time, current thermal and electric energy fluxes, massflows, temperature of the DC environment and of the cooling system
- The workload generator module publishes the VMs profile for the current time step
- The short-term predictions predict the ITE power and thermal states for the next hour. This prediction supports the decision making that takes place in the thermal actuation modules
- Optimal temperature set points for the cooling system for the next timestep are sent back to the virtual DC environment

The virtual DC environment captures all electric and thermal energy fluxes, temperature traces, massflows, etc. during this iterative process for further analysis and post-processing.

Power supply and supervisory management experiments

The power supply management is supported by decision making at the supervisory level. The power supply management is responsible for continuous control of the power supply components following the supervisory policies given by supervisory intelligence modules. The supervisory intelligence modules provide hourly policies for controllable renewable energy source (RES) and storage management considering grid, fuel prices or related CO₂ emission equivalent. The supervisory intelligence module was tested in the mode designed to minimize operational cost.

The aim of the computational experiments presented here is the testing of the thermal actuation algorithms with the following settings:

- Power supply strategy based on surplus (baseline) with the RES system
- Power supply strategy with Supervisory Intelligence policies with the RES

The first two settings of power supply management manipulate the controllable RES and batteries according to the on-site RES surplus. Once the supply from on-site RES exceeds the DC demand, the surplus is stored in the batteries. The batteries are discharged once the on-site RES fall below the DC demand. The two settings differ in scale of the applied RES system.

The last two settings of power supply management manipulate the controllable RES and storage status according to the supervisory intelligence policies. The supervisory policies are provided hourly and are calculated based on predicted matching of uncontrollable on-site RES with DC demand and day-ahead market prices.

Testing process

The testing of experiments for the power management and supervisory management follows these steps:

- Virtual synchronization time and current thermal and electric energy fluxes, massflows and temperature of DC environment and cooling system are published for the given timestep.
- The workload generator module publishes the VMs profile for the current time step
- The long-term predictions predict power demand and power supply on an hourly basis for the decision making of supervisory intelligence. (If applicable)
- The supervisory intelligence module provides policies to workload, thermal and power supply management on an hourly basis. (If applicable)
- The power supply management provides commands for on-site RES and storage system (to the virtual DC environment for next time step.)

The virtual DC environment captures all electric and thermal energy fluxes, temperature traces, massflows etc. during this iterative process for further analysis and post-processing.

6.1.2 Key performance indicators

This simulation-based assessment carries out an evaluation of IT workload management, thermal management, power supply management and their combination facilitated by supervisory management. Therefore, the key performance indicators must address multiple criteria in order to realise the evaluation of the desired holistic approach. The key performance indicators (KPIs) selected to address the performance of individual domains and the overall DC are discussed below.

IT productivity

The IT productivity and normalized IT productivity characterize the performance of IT processing. This IT productivity indicator is used to assess IT workload management. The definition of IT productivity is given by Equation 6.1 as a ratio of useful work to ITE power demand. In our case, useful work is defined as number of CPU cycles for the processing of given IT tasks. In order to present the results in a range of 0 to 1, the IT productivity indicator is normalized by rated IT productivity. The normalized IT productivity is then divided by maximal (rated) IT productivity, which is stated for maximal work that can be done by IT and related nominal power demand of IT (Equation 6.2).

$$IT \text{ productivity} = \frac{\text{Useful work (CPU cycles)}}{IT \text{ demand (kWh)}} \quad (6.1)$$

$$\text{normalized IT productivity} = \frac{\text{Actual IT productivity}}{\text{Rated IT productivity}} = \frac{\frac{\text{Useful work}}{\text{Actual IT demand}}}{\frac{\text{Maximal work}}{\text{Rated IT demand}}} \quad (6.2)$$

The presented CPU cycles may not always be representative of useful work for each IT task, and sometimes additional computational parameters need to be taken into account to characterize useful work (e.g. RAM or data storage access). In practice, however, there is often an issue with this performance indicator because the non-uniform definition of useful work is highly dependent on the character of the IT task and type of server (e.g. storage, web-service, high performance computation). Nevertheless, according to the IT experts of the higher-level consortium, the CPU cycles were agreed as a suitable performance indicator for the given case of the demonstration DC.

Power Usage Efficiency

One of the popular indicators of DC energy efficiency is Power Usage Efficiency (PUE) or the analogous Data Centre Infrastructure Efficiency

(DCiE) introduced by Green Grid [148]. Both PUE and DCiE indicators characterize the performance of DC infrastructure such as efficiency of cooling power delivery systems. This indicator is mainly used to assess thermal management.

The more popular PUE is defined by Equation 6.3 as the ratio of total DC power demand to IT power demand. In order to state the DC energy efficiency in the range of 0 to 1, the DCiE indicator can be used.

$$(6.3) \quad PUE = \frac{\text{Total DC demand (kWh)}}{\text{ITE demand (kWh)}}$$

$$(6.4) \quad DCiE = \frac{\text{ITE demand (kWh)}}{\text{Total DC demand (kWh)}}$$

Thermal Environment indicator - Inlet Air Temperature violation

The thermal environment is indicated by violation of ITE inlet air temperature. As a reminder, ASHRAE TC9.9 introduced recommended operational conditions for the standardized classes A1-A4 for compute and storage servers in tightly controlled environments. To provide a recommended DC environment, it is necessary to take into account intake dry-bulb air temperature, humidity (or maximum dew point) or maximum temperature rate of change. The recommended environmental range can be summarized by a dry-bulb temperature range from 18 to 27 °C and a relative humidity range from 30% to 60% [47].

The violation of the recommended temperature range increases the probability of IT failure. The intake temperature can still exceed the recommended temperature for a short time, as long as it remains within the allowable operational range. Nevertheless, it is not recommended to run the ITE in this type of environment outside of the allowable range. The allowable range only states extremes of operating conditions.

The inlet air temperature violation is used to assess the management of DC space. The temperature violation is defined as the deviation of intake server temperatures from the lower or higher bounds of the recommended range. Temperature violation can be expressed by Equation 6.5a and 6.5b.

$$\text{Temperature Violation}_{\text{HI}} = t_{\text{server in},i} > 27\text{-high recommended bound} \quad (6.5a)$$

$$\text{Temperature Violation}_{\text{LO}} = t_{\text{server in},i} < 18\text{-low recommended bound} \quad (6.5b)$$

The alternative representation of required conditions is temperature violation hours, for which the time of violated temperature range is summed up over the period of the experiment

Energy, Cost and emissions

A high-level indication of overall DC performance is achieved by considering total DC energy use, operational costs and CO₂ emissions.

Part-load efficiency characteristic

All indicators mentioned above can be post-processed as a part-load efficiency characteristic in order to evaluate the system behaviour during operational conditions. The part-load efficiency analysis is a fundamental analysis for performance assessment in operational conditions for all kinds of energy systems/components such as heating, cooling, ventilation, power supply or power delivery systems. Thus, the part-load efficiency characteristic mentioned in other literature [149]–[151] offers deeper insights into the studied system/component behaviour assessed by a performance indicator of interest. The part-load analysis is often done at component level in certified laboratories as part of the technical specification. However, the part-load characteristic of the entire system is less common due to the limited possibility to ensure reliable “laboratory” conditions at this level of complexity. The system data are usually gathered during the regular operation for a given period, where the common boundary conditions cannot be guaranteed. Certainly, the virtual DC

environment as a virtual laboratory can overcome the technical limitations and offers virtually common boundary conditions and related required monitoring data.

In order to evaluate and compare the tested operational strategies, the performance during the operational conditions must be further analysed. The evaluation at the part-load characteristic at system level may be complicated because the performance can vary for each part-load utilization level. This effect is caused by system dynamics often driven by the cooperation of multiple components (e.g. refrigerant unit versus economizer mode) with independent local controllers (e.g. effect of ON-OFF controller). These effects can be seen in Figure 6-2, where the performance spread is divided into several performance stages. Although the performance spread is usually large, the general trend can often be identified. Commonly, the efficiency of energy systems has a tendency to decrease for utilization levels further from designed conditions (e.g. lower part-load utilization). This trend is partially a result of component construction (e.g. idle demand, level of operability), which can be considered as a design aspect, and partially due to the selected control strategy (e.g. constant control setpoints), which can be considered as an operational aspect. In this study, the design of the system is the same for all tested control strategies, thus any possible improvement in the performance spread can only be caused by changes in the tested control strategy. The comparison of performance spreads caused by two different control strategies is shown in Figure 6-2.

However, the evaluation of performance spreads is not practical, therefore the datasets need to be post-processed to better communicate the results. During this post-processing, depicted in Figure 6-2, the large performance spread is translated to a mean part-load efficiency curve as a key indication of performance during the operational conditions. Additionally, the performance

spread is translated to the occurrence of performance at the defined part-load utilization level for detailed analysis.

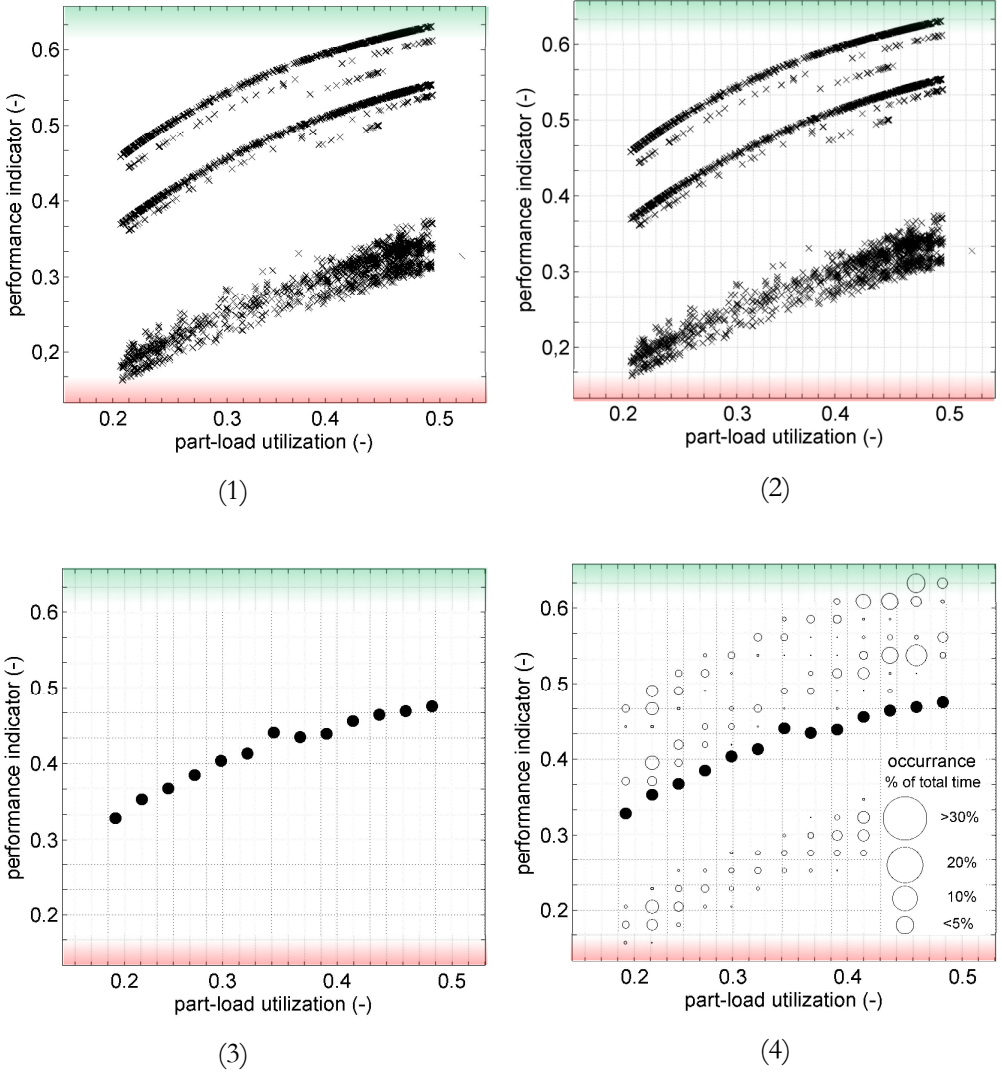


Figure 6-2 Data post-processing – mean part-load efficiency curve and occurrence spread

The mean-part load efficiency indicates an average performance over the part-load utilization range. In theory, the optimally operated system (considering

both design and operational aspects) would provide constantly high efficiency with minimal spread over the entire utilization range. On the other hand, a system with insufficient operability and control strategy would perform with steeply decreasing efficiency with part-load utilization.

The post-processing applied for the results in this chapter can be divided into steps, which are listed below:

1. Find the relationship between DC utilization and the selected KPI, which can be represented as a scatter plot
2. Define the evaluation grid for the KPI and DC utilization
3. Calculate the part-load efficiency curve. The individual points of the curve are the results of averaging of the KPI spread along the DC utilization range given by the evaluation grid. The obtained curve represents the mean part-load efficiency for a given operational strategy
4. Evaluate the spread of the KPI. The spread is evaluated based on the occurrence of the KPI in a given region defined by the evaluation grid. The size of the dot indicates the percentage of time that the system operated at a given part-load and performed with the corresponding efficiency level. The obtained post-processed spread provides additional information about the tested operational strategy, which allows detailed analysis.

This post-processing approach was found to be suitable for the analysis of the impact of the tested control strategy on the given KPI with part-load utilization. As depicted in Figure 6-3, the mean part-load efficiency curve is a practical visualization that can be used for comparison of two control strategies

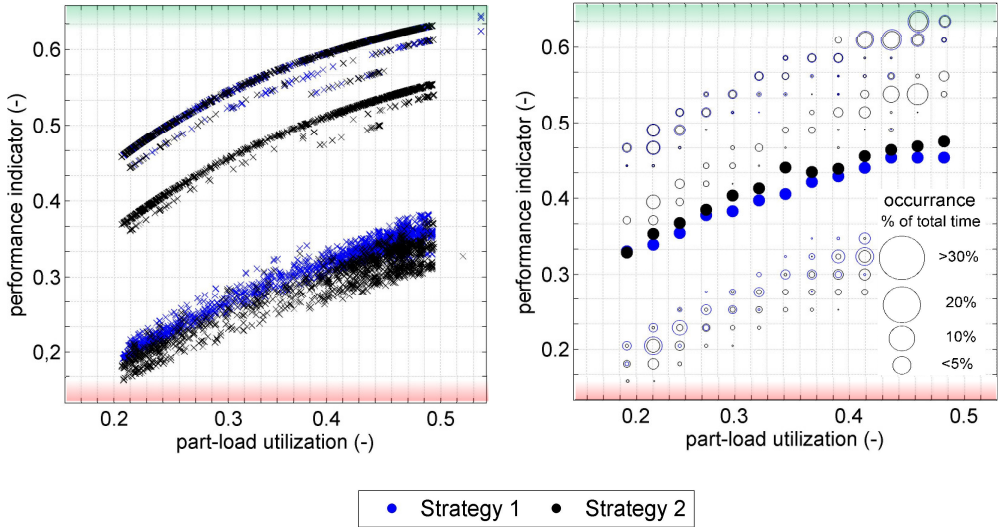


Figure 6-3 Data post-processing – strategies comparison

6.1.3 Model setup for simulation-based assessments

The setup is adjusted from the one reported in the previous chapter in order to enable full control of the overall DC system, which is not possible in the real DC.

The setup for the simulation-based assessment of the external algorithms differs slightly from the one used for the quality assurance study reported in chapter 5. Indeed, the virtual DC environment was configured to simulate the real demonstration sites in order to support commissioning of the tested control platform. However, there is still a serious limitation in terms of executing real experimentation due to the lack of access to the DC infrastructure. Therefore, the virtual DC environment enabled full access to all ITE, cooling and RES components. These minor adjustments are made in order to fully demonstrate the capability of the tested DC management.

Server population for the simulation-based assessment

As depicted in section 5.1.1, the modelled data centre houses 8 racks arranged in two rows (i.e. 6 server racks and 2 communications racks). The room and rack layout is fixed in order to keep the same thermal monitoring specification and thus allow the support of the platform commissioning, where the virtual monitoring is replaced by the real monitoring. In the real DC, most racks are only partially populated and only a few servers are available for real experimentation. In the case of simulation-based assessment, all of the racks are fully populated, but each rack is populated with a number of virtual servers, depending on their size and type. The total number of operable server units, regardless of server type, is a key factor to enable the meaningful demonstration of workload management, which manipulates the IT workload within the server cluster. The server type and server mapping within the room are given design parameters. Thus, the details of the server arrangement for the simulation-based assessment are in Appendix B.

Table 6-2 Distribution of nominal IT power load (W) used in simulation-based assessment.

POWER LOAD (W)	A1	A2	A3	A4	B1	B2	B3	B4
TOP	950	890	1920	1700	0	910	0	1050
MID	1620	1480	1195	1250	0	960	0	1275
BOT	1480	1415	1060	1020	0	2400	0	2000
TOTAL	4050	3785	4175	3970	0	4270	0	4325

Based on the new definition of server population, Table 6-2 shows the final distribution of nominal power load used in the simulation-based assessment. Since one of the features of the tested workload management is to put servers in standby mode to save energy, the servers' power consumption in standby modes are defined as an additional parameter of server's specification (approximately 5% of nominal power). Furthermore, the IT workload

allocation module requires information on the server's resources (CPU and memory capacity).

Cooling system setup and DC arrangement

Since the demonstration DC as a living laboratory works under regular operational conditions, access to the real cooling system was restricted for real testing due to the possible risk of its failure. The DC owner only allowed access to the return air setpoints, and the rest of the cooling system was under embedded local control. With such limited access, the tested thermal algorithm could only address the aspect of thermal environment within the real DC space. The lack of access to the real cooling system limited the ability of the algorithm to fully demonstrate its benefits in terms of achieving energy efficiency.

The virtual DC environment as a virtual laboratory enabled full access to the individual components of the cooling system. Thus, the testing of system-level thermal control was enabled and could be demonstrated. Table 6-3 shows the components that were enabled for system-level control during the simulation-based assessment, which allowed for the inclusion of access to the control of the cooling system.

Table 6-3 Component operability for system-level control

component	operability at demonstration DC	operability at virtual DC environment
CRAC unit – return temperature setpoints	available	available
CRAC unit - fan speed /airflow	not available	available
pump speed/ water flow of heat removal circuit	not available	available
dry cooler settings	not available	available
economizer settings	not available	available

The DC arrangement was also adapted for some of the assessments. There are alternative measures for effective thermal management of the DC space, which can be categorized as DC retrofits. For instance, one of the most popular energy efficiency measures is the implementation of cold aisle containment, which places physical barriers between cold and hot regions of the DC space. The virtual DC system could be readily configured to represent the cold aisle containment. Thus, the tested algorithm could be compared with this competitive management by using the virtual DC environment, which offers additional reference for the tested scenario. To reiterate, the tested algorithms were always compared against the selected simulated baseline, which represents a rather conservative approach to DC management.

RES system

The configuration of the RES system is kept as it was defined in section 5.1.2. The only change is that the modelled RES system is fed by the same boundary conditions (weather and grid data) as those used in the DC. For all experiments, the modelled RES system acts like the on-site RES of the DC located in Ireland.

6.1.4 Boundary conditions for simulation-based assessments

As described in section 4.3, in addition to the tested control signal, the virtual DC energy model also requires external inputs such as requested IT workload demand, grid data and weather conditions. The used inputs for the testing are briefly described in this section.

For visualization purposes, the IT workload is represented by CPU demand normalized by CPU capacity of the housed ITE, where 1 means that full CPU capacity is demanded.

IT workload demand profiles

Figure 6-4 shows a training workload profile with daily peaks, representing the authentic web-service profile. This profile was used for the testing of all tested

algorithms. At the request of the developers of the workload algorithm, the IT workload management was additionally tested with synthetic IT workload profiles, shown in Figure 6-4b. This synthetic profile was prepared in order to test the algorithm over the whole utilization range from minimal load to overloaded scenario, where the capacity of the housed ITE is exceeded. This was deemed important as it allowed for the testing of the workload algorithm's behaviour in extreme conditions. The testing was done for both ascending and descending variations of the same profile, starting from utilization at 10% to 150% of housed ITE capacity.

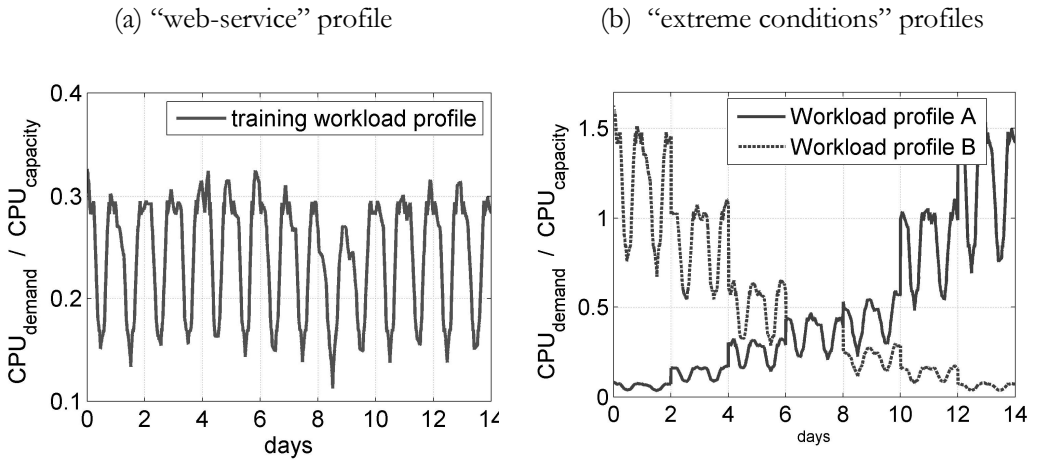


Figure 6-4 IT workload demand profiles; (a) training workload profile “web-service”,
(b) training workload profiles “extreme conditions”

Weather conditions

The virtual DC environment including the modelled on-site RES is (virtually) located in Ireland. The related weather data such as outside air temperature, wind speed and solar radiation profiles are depicted in Figure 6-5.

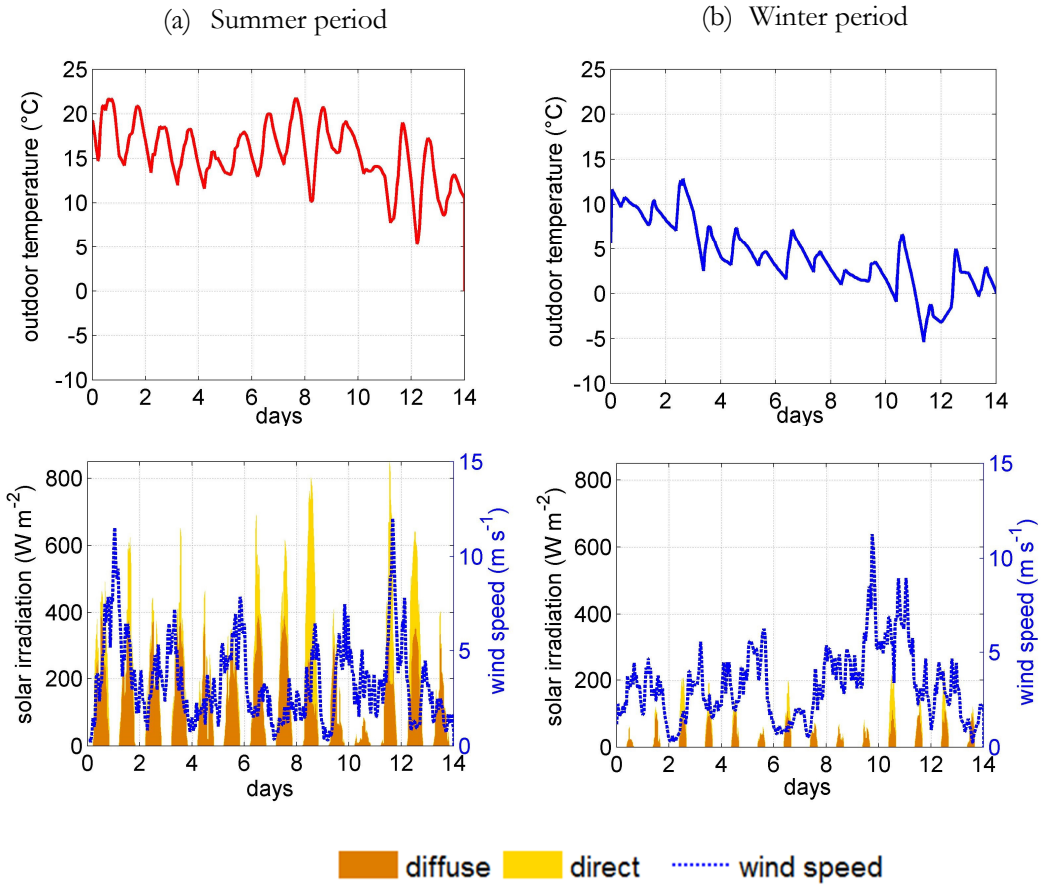


Figure 6-5 Testing weather conditions for Ireland: outside temperature, solar irradiation, wind speed for (a) summer period, (b) winter period

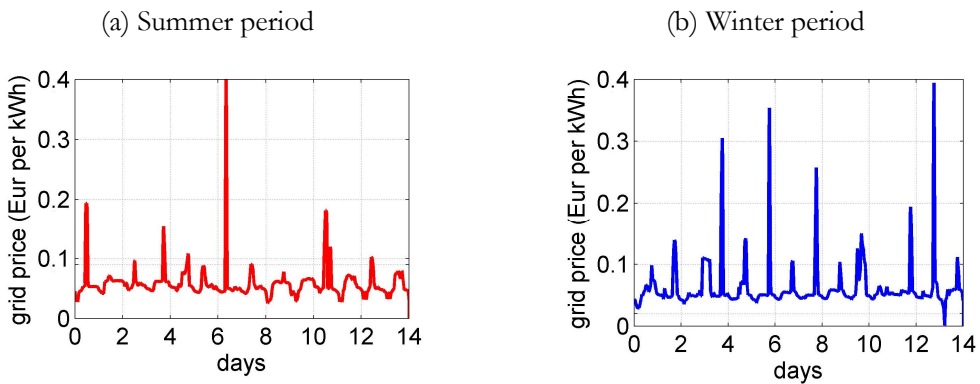


Figure 6-6 Grid price profile; (a) summer period, (b) winter period

Grid data

As mentioned in section 4.3, the historical data of grid prices and grid emission factors were used to characterize the national grid status [126], [127]. The grid price profiles utilized for the summer and winter conditions are provided in Figure 6-6. In the case of Ireland, the grid emission factor was estimated at 456 (gCO₂/kWh) based on annual statistics from the International Energy Agency for the year 2016 [127].

6.2 Computational experiment results

The results presented in this section are the final results from the testing of individual management modules. Before reaching these results, each algorithm was tested individually in order to allow for an extensive debugging procedure, as introduced in Chapter 3. The tested control platform was then deployed and tested in the available infrastructure of the real DC.

To reiterate, the results of the testing are presented in stages by adding individual algorithms to the picture in order to finally archive the results from the overall control platform in operation. The testing begins with the evaluation of IT workload management as this management responsible is for the primary function of the DC. Then, different thermal strategies are tested along with the workload management. Finally, power supply management is added to the virtual operation.

6.2.1 Simulation-based assessment of the IT workload management

The workload management is first tested using the synthetic workload profile covering the full range of utilization. Then, secondly, the variable workload profile representing real web-services is used in order to assess the thermal-aware workload allocation. This variable workload profile is later used for simulation-based assessment of other DC management strategies. Table 6-4 depicts the subset of the tested platform settings in this section.

Table 6-4 Settings of the platform configuration for the presented computational experiments concerning workload management.

setting ID.:	workload management	thermal management	power supply management
{1}	no consolidation	constant setpoints (21°C)	no on-site RES
{2}	consolidation: ITE consumption priorities	constant setpoints (21°C)	no on-site RES
{3}	consolidation: thermal priorities	variable setpoints (18-25°C) (room level control)	no on-site RES

Evaluation of the IT workload management for full utilization range

The results from the testing of workload allocation over the whole utilization range are presented here. Requested CPU capacity for all housed ITE in the virtual DC in this study represents the computational demand from the end-user. This profile is common for all tested workload management strategies. Thus, Figure 6-7 provides a comparison of ITE power demand resulting from manipulation of the housed ITE using the baseline and optimized workload managements to compute the requested CPU capacity of the ascending demand profile shown in Figure 6-4.

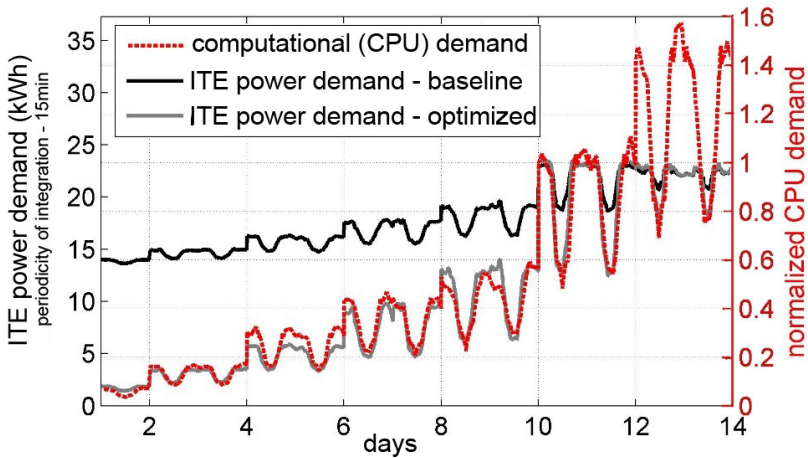


Figure 6-7 ITE power profile resulting from baseline and optimized settings of workload allocation

The workload allocation can greatly influence the ITE power demand. While the baseline strategy keeps all servers active, the advanced strategy optimally consolidates the IT workload, migrates it to the most efficient servers and deactivates the unutilized servers. The advanced workload management eliminates the idle power of the unutilized servers, and therefore, the IT power demand can follow the IT workload demand fairly well.

The ITE power demand and requested CPU capacity is used for part-load efficiency analysis. The normalized IT productivity is used to indicate the performance of the workload allocation algorithm. The part-load efficiency analysis, shown in Figure 6-8, evaluates both descending and ascending profiles. The normalized IT productivity is evaluated in terms of the mean part-load efficiency curve and performance spread for the tested settings.

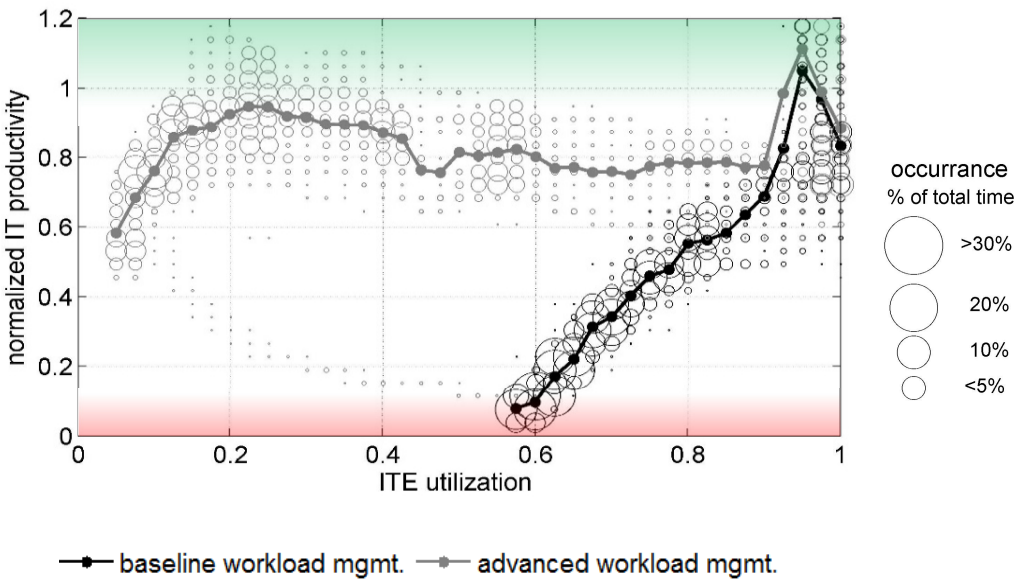


Figure 6-8 Part-load efficiency analysis of normalized IT productivity for baseline and advanced workload management

This analysis reveals that the workload allocation settings can dramatically change the part-load characteristics of IT productivity. While the IT productivity of the baseline strategy decreases heavily with the part-load due to the idle power of unutilized servers (idle power of servers is usually in the range of 30-50% of total server power demand), the advanced strategy is able to trigger the standby regime for unutilized servers (~5% of server power demand). Thus, the IT productivity is kept in the range of 0.8 to 1 over most of the ITE power utilization range. The relatively high productivity can be reached in the range 0.2 to 1 of ITE power utilization. Once the ITE power utilization is lower than 0.2, the IT productivity decreases even for the advanced workload management. The reason for this finding is that the unutilized servers are not completely deactivated. The standby regime still requires minimum power load in order to be able to quickly reactivate the servers. This minimum power load of unutilized servers causes this drop of normalized IT productivity for the lower ITE power utilization.

As the IT workload demand reaches 0.8-0.9 of ITE power capacity, all servers are required, which means that the advanced workload allocation cannot deactivate any servers until the demand drops. The performance of the baseline and advanced workload allocation became almost identical. The DC reaches the design conditions (around 0.95 of the ITE power utilization), where each server works with at maximum efficiency of 95%. After that peak, the IT productivity is reduced again because the ITE capacity is saturated, and as such part of the workload must be suspended.

As long as the cooling system is able to guarantee an allowable temperature in the DC, the IT productivity is not influenced by the outside weather conditions. The weather conditions mainly influence the Power Usage Efficiency (PUE). In order to evaluate the PUE, the total DC power demand needs to be taken into consideration. The total power demand is gathered for

a typical summer and winter period. Figure 6-9 shows the total power and ITE power demand for the baseline workload allocation for the ascending profile.

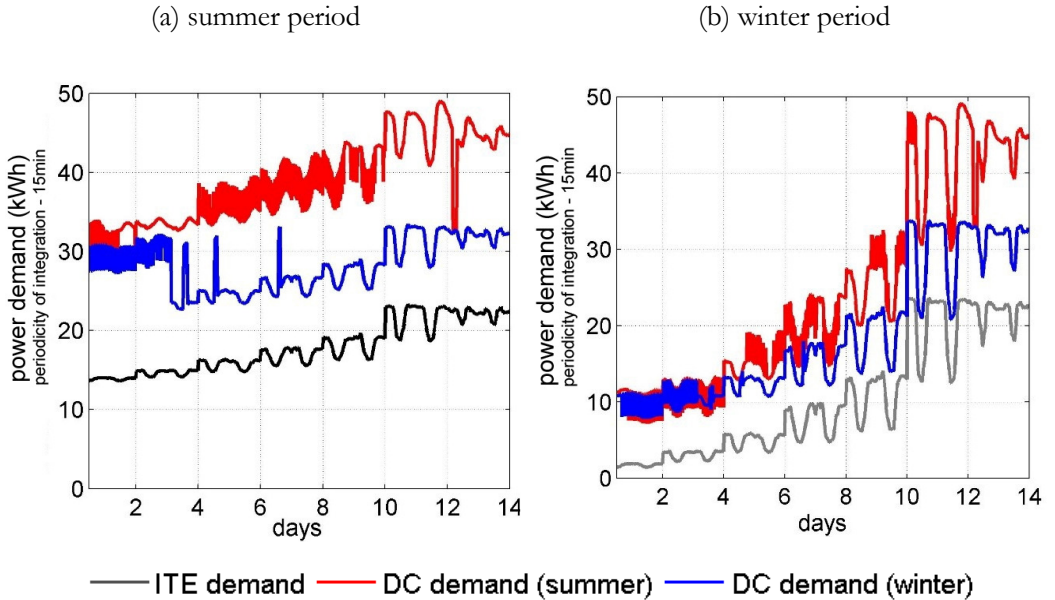


Figure 6-9 Total power and ITE power profile for summer and winter period resulting from (a) baseline and (b) optimized settings of workload allocation

Figure 6-9b shows the total power and ITE power demand for the advanced workload allocation. As for IT productivity, the part-load analysis conducted for PUE evaluates both the ascending and descending IT workload profiles. The mean part-load efficiency curve is drawn separately for summer and winter periods to demonstrate the influence of economizer utilization.

Figure 6-10a highlights the baseline workload allocation results. Figure 6-10b highlights the advanced workload allocation. The mean part-load efficiency curve is projected in both figures in order to compare these settings of the workload allocation. As already demonstrated by the (BISCI) organization [152], the behaviour of the PUE metric follows the hyperbolic trend line within

the part-load utilization. In other words, the DC energy efficiency represented by the PUE metric decreases rapidly with lower ITE utilization.

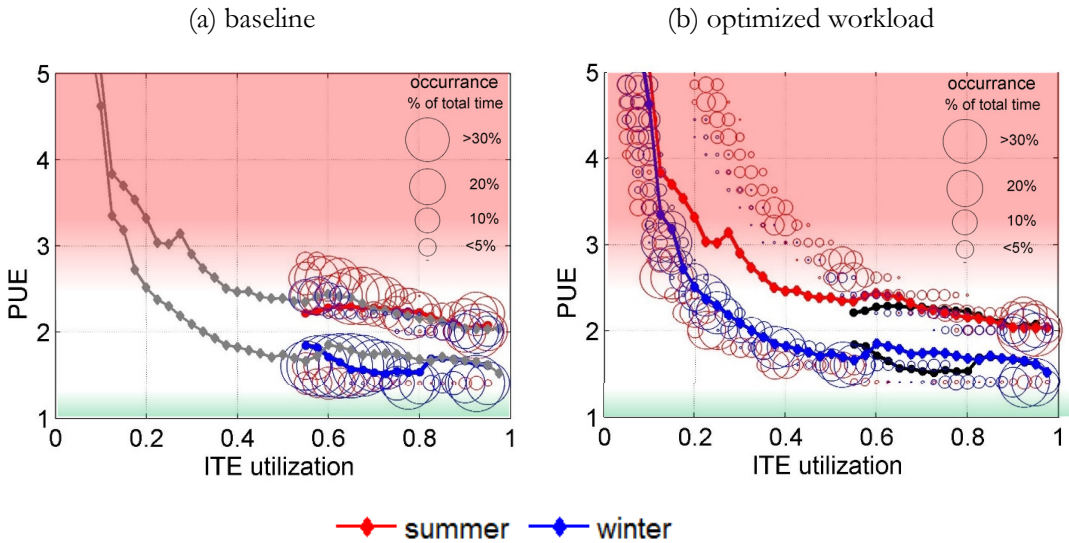


Figure 6-10 Part-load efficiency analysis of PUE for (a) baseline and (b) optimized workload allocation

The DC performs with a similar characteristic regardless of the tested periods. In the winter period, due to higher utilization of the economizer mode of the cooling system, the cooling system provides considerably better efficiency than in the summer period. The performance spread represented by occurrence dots is divided into two efficiency levels for both summer and winter periods. These two levels were partially caused by the ON/OFF internal control of the CRAC unit and partially by switching between mechanical and economizer cooling mode.

Focusing on workload allocation settings, the advanced workload allocation can adapt better to the requested IT workload than the baseline workload allocation. Therefore, the advanced allocation can use a much larger range of the ITE power utilization with the same requested IT workload. However,

since there was no manipulation with systems other than ITE, the PUE logically indicated a similar efficiency of the infrastructure (cooling and power delivery system) in the utilization range, which was common for both workload allocation settings. In fact, the cooling and power delivery system was not able to adapt well to the lower range of the part-load utilization caused by the advanced workload strategy. Thus, the PUE metric indicated a reduction of energy efficiency of these systems when the advanced workload allocation was applied. Table 6-5 summarizes the results of this analysis.

Table 6-5 indicates a conflict between performance indicators using different metrics. While the IT productivity is dramatically increased in the advanced workload allocation setting, the PUE indicates lower efficiency. The absolute numbers reveal that the advanced workload allocation provides an energy saving potential of up to 34% of total energy use.

Table 6-5 Summary of results of the tested summer and winter periods

settings ID	KPI	summer scenario	winter scenario	average	total DC energy demand (MWh per 56 days)	relative savings (%)
{1} - baseline	normalized IT productivity	0.66	0.66	0.66	45.47	ref
	PUE	2.20	1.64	1.92		
{2} - optimized	normalized IT productivity	0.97	0.97	0.97	29.96	34.1%
	PUE	2.79	2.20	2.50		

Evaluation of the IT workload management: thermal-aware allocation

The results from the testing of workload allocation in thermal-aware mode are presented here. This testing is performed only for the training profile representing “web-service”, presented in Figure 6-4. Similar as in previous testing, the IT power profiles resulting from the manipulation of housed ITE using the baseline, ITE power-aware and thermal-aware settings of the workload allocation algorithm are shown in Figure 6-11.

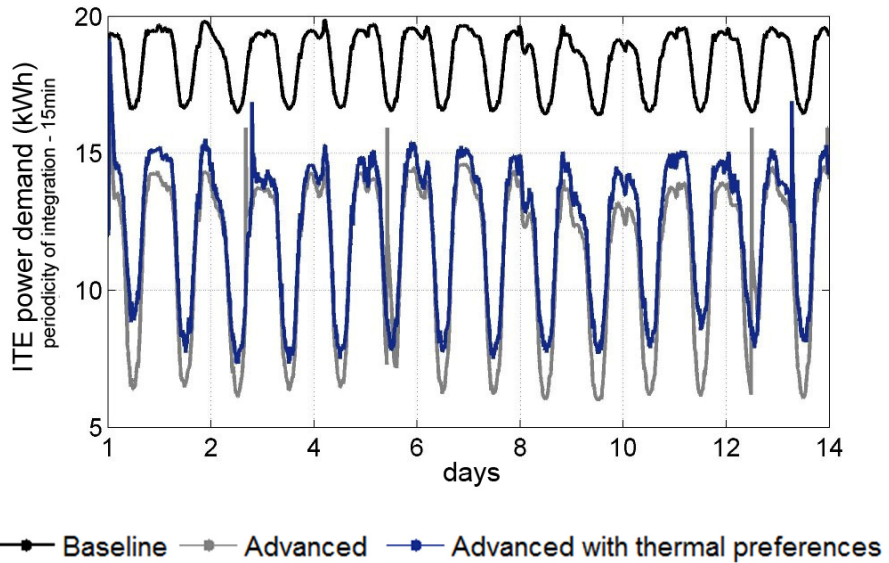


Figure 6-11 ITE power profiles resulting from baseline, ITE power-aware (optimized) and thermal aware settings of the workload allocation

In the case of thermal aware settings, the workload allocation must satisfy the preferences coming from the thermal management. The incoming IT workload is consolidated according to the thermal preferences generated based on the air temperature distribution within the DC room. Thus, the thermal preferences may restrict the utilization of the most efficient servers, which do not necessarily have to be housed in the thermally preferred location. These preferences represent an additional constraint for the workload allocation algorithm resulting in slightly higher ITE power demand and related heat dissipation than the ITE power aware setting.

Again, the normalized IT productivity is assessed for part-load utilization. The mean part-load efficiency curve and performance spread are evaluated for the three settings of workload allocation. This part-load analysis is shown in Figure 6-12.

Since the training “web-service” workload profile captures only part of the utilization range, only some of the previously presented characteristics are visible in this figure. The characteristics of the baseline and advanced settings of the workload allocation were described in the previous analysis. In this study, baseline and advanced settings are used as the benchmark for the thermal-aware setting. For the given case-study, the thermal-aware settings provide similar or slightly lower normalized IT productivity (range of 0.7-0.8) than the settings without thermal awareness. It is worth noting here that the mean part-load efficiency curve is shifted in terms of ITE utilization. This shift shows the increase of the ITE power demand.

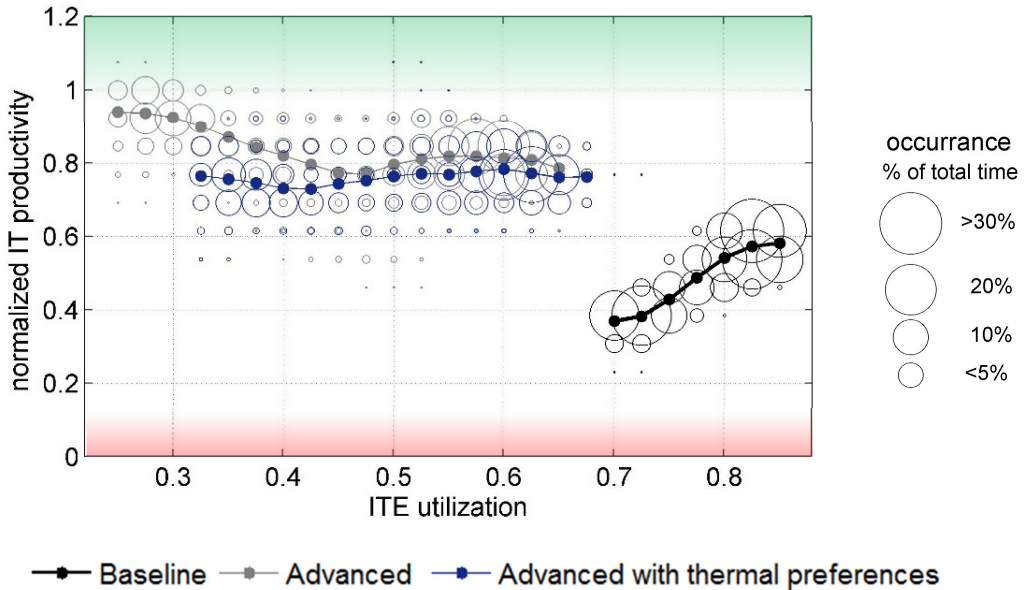


Figure 6-12 Part-load efficiency analysis of IT productivity for presented settings

Since the thermal aware strategy actuates both IT workload and temperature setpoints, the overall power efficiency of the thermal-aware actuation is elaborated later in this chapter as part of the thermal management analysis. In this section, the main point to note is that the workload allocation is able to

listen to the preferences of the thermal management, and that this process leads to a minor decrease of the IT productivity for the given system specification.

6.2.2 Simulation-based assessment of the thermal management

Firstly, results of the thermal management, actuating at room level, are presented. The tested thermal management is compared with both baseline and competitive thermal management strategies. This testing aims at temperature control within the room. Secondly, results of the thermal management actuating at room and building level are presented. This testing aims at energy efficiency of the cooling system. Table 6-6 depicts the subset of the tested platform settings in this section.

Table 6-6 Settings of the platform configuration for the presented computational experiments concerning workload management.

setting ID.:	workload management	thermal management	power supply management
{1}	no consolidation	constant setpoints (21°C)	no on-site RES
{2}	consolidation: ITE consumption priorities	constant setpoints (21°C)	no on-site RES
{3}	consolidation: thermal priorities	variable setpoint (18-25°C) (room level control)	no on-site RES
{4}	consolidation: ITE consumption priorities	variable system setpoints (system level control)	no on-site RES
{C1}	consolidation: ITE consumption priorities	constant setpoints (25°C)	no on-site RES
{C2}	consolidation: ITE consumption priorities	cold aisle containment constant setpoints (21°C)	no on-site RES

Evaluation of the thermal management at room level: temperature conditions

As mentioned earlier, the thermal management has limited operability at room level. Only the temperature setpoint and eventually ITE power distribution, representing heat dissipation, can be controlled. The concept of thermal-aware ITE power distribution was described in the section above.

In this section, the focus lies on the temperature distribution and ability of the tested thermal management to achieve the desired inlet IT temperature. In addition, the tested algorithms are also compared to two competitive strategies in order to offer alternative benchmarks to the baseline strategy, which is a rather conservative approach. Figure 6-15 and Figure 6-17 depicts the visualization of the average temperature distribution considering both the summer and winter testing periods. The temperature distribution is shown for DC layouts in 4 height levels (0.2, 0.6, 1.4 and 2.4m). These layouts are shown for the all tested strategies mentioned in table above.

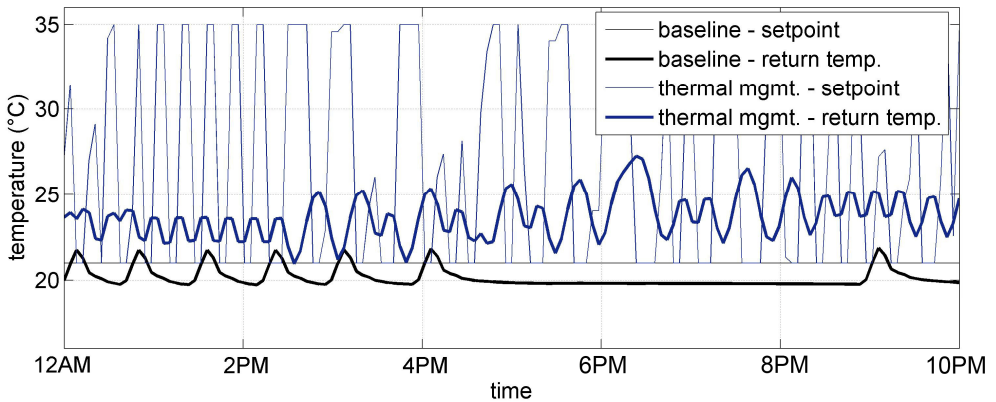


Figure 6-13 Simulated return air temperature and temperature setpoint of baseline thermal management and tested thermal management

The fixed return temperature setpoints at 21°C and the variable return setpoint of the tested thermal management are shown in Figure 6-13. The figure also includes simulated return temperature as a manipulated variable. The essential difference between the baseline and tested algorithm is that in the baseline internal control can only actuate based on the return air temperature. However, the tested algorithm aims to achieve the desired inlet IT temperature based on a temperature sensor network within the DC room. In other words, the tested algorithm receives monitoring data from the DC environment and then varies

the return temperature setpoints of the CRAC unit in order to reach the desired temperatures in front of the housed ITE, where needed. As advised by the algorithm developer, the thermal algorithm must consider the local ON-OFF control of the CRAC unit, which caused additional disturbances in this case. Therefore, the setpoint varied in order to minimize the fluctuation of the inlet temperature ITE.

Comparison with baseline case

The part-load analysis is also performed for the temperature violation of the recommended operational temperatures. This analysis considers all temperature nodes at the front of each rack, and includes both summer and winter periods. The mean part-load efficiency curve and performance spread of the temperature violation are shown in Figure 6-14.

The analysis revealed that the tested thermal algorithm using the variable temperature setpoint could reduce the temperature violation over the entire utilization range regardless of the applied workload allocation. The mean part-load efficiency was constantly below the recommended range by about 0.7°C; however, the performance spread shows that most of the time the ITE inlet temperature remained in the recommended range.

A relatively large performance spread can be observed for all tested settings. Such a spread indicates a fluctuation of the ITE inlet temperatures. This temperature fluctuation is caused by the embedded ON-OFF internal control of the cooling source, which was always present for all cases.

Focusing on the mean part-load efficiency curve of the strategy with the fixed setpoint, this strategy caused the lower bound of the recommended range to be exceeded by 2-6°C. The DC was overcooled for most of the utilization range, which correlated with observations of the real monitoring system. For the majority of the time, the inlet ITE temperature is within or even below the allowable bound for class A1 (the most delicate ITE).

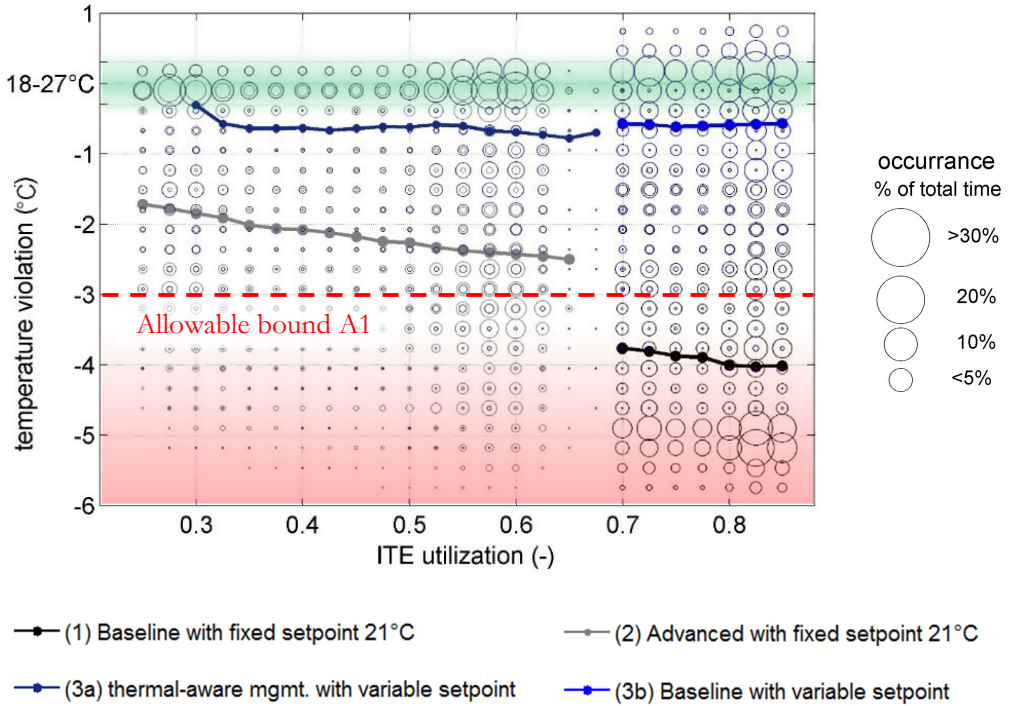


Figure 6-14 Part-load efficiency analysis of temperature violation for the presented settings

The overcooling issue is caused by the slightly oversized cooling system and the conservative selection of the return air setpoint. The overcooling effect resulting from the fixed setpoint is lower for the lower utilization range. The explanation here is that less IT demand naturally leads to less dissipated heat. Thus, with lower utilization, the controlled return air temperature is closer to the evaluated ITE inlet temperature. Therefore, the embedded internal control performed better for lower utilization in terms of temperature violation.

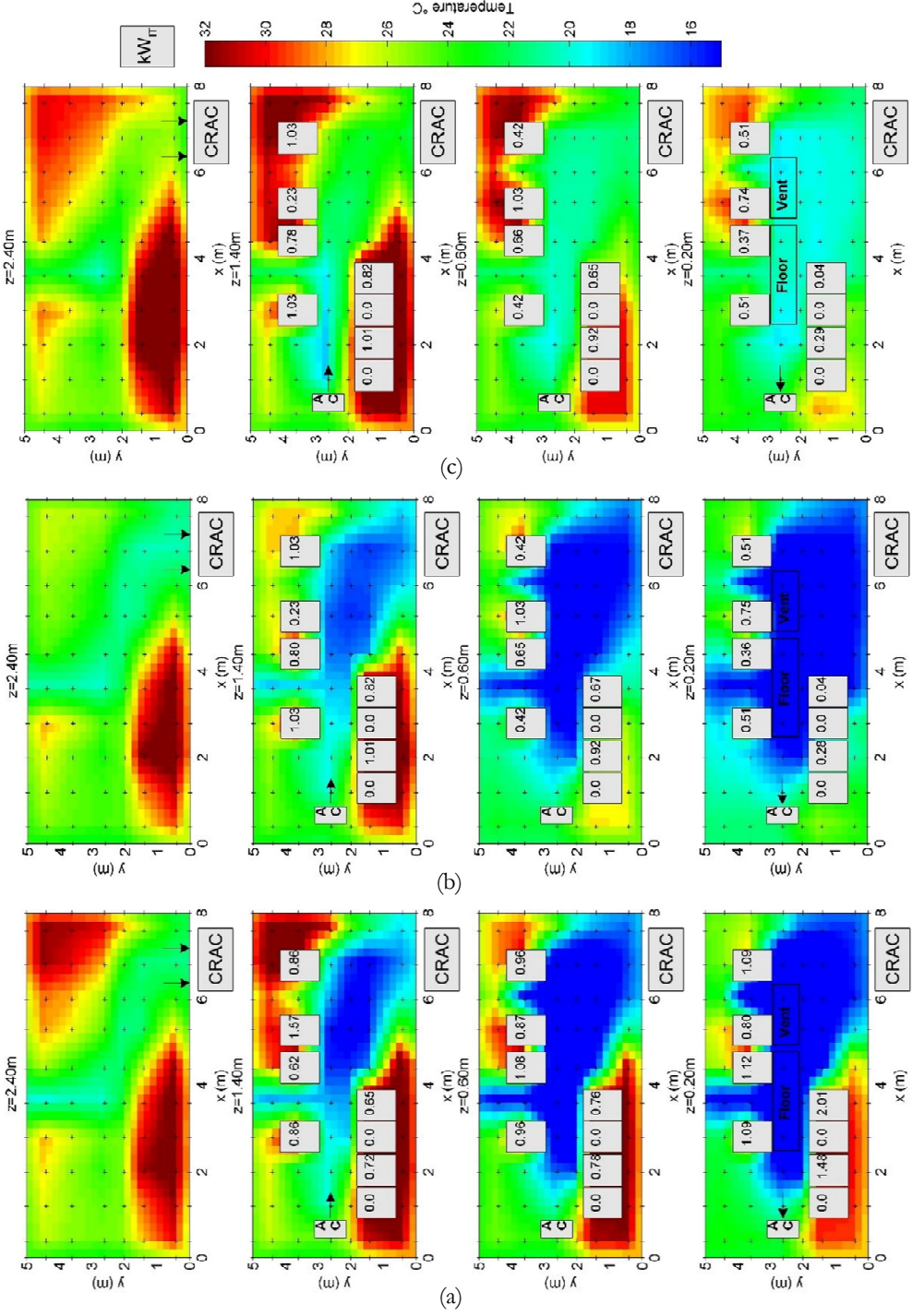


Figure 6-15 Average temperature distribution for tested settings (a) baseline, (b) advanced workload allocation, (c) thermal aware workload management, variable setpoints

Comparison with competitive managements

The tested thermal algorithm is also compared with the competitive thermal management strategies, such as fixed return temperature setpoint of 25°C and cold aisle containmnets with a fixed cold aisle temperature of 21°C. All thermal management strategies were tested for optimized workload allocation. The part-load analysis of the competitive thermal management is shown in Figure 6-16

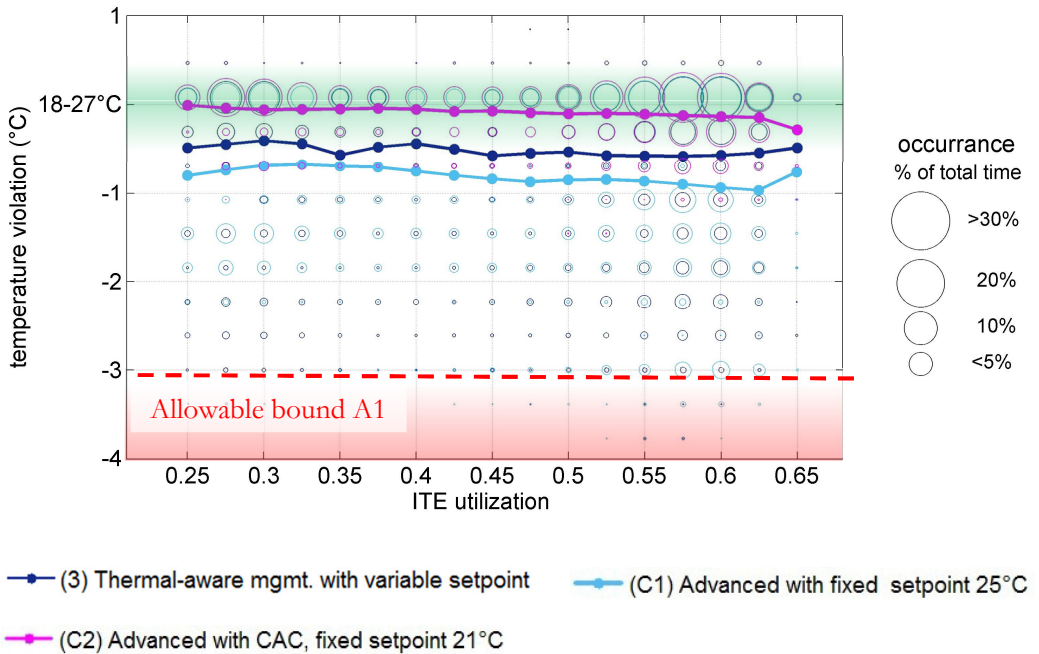


Figure 6-16 Part-load efficiency analysis of temperature violation for presented settings

The tested algorithm performed in line with the selected competitive management strategies in terms of temperature violation. The noticeable shift of the mean part-load efficiency curve denotes the change in ITE utilization caused by the aforementioned effect of the thermal-aware workload allocation.

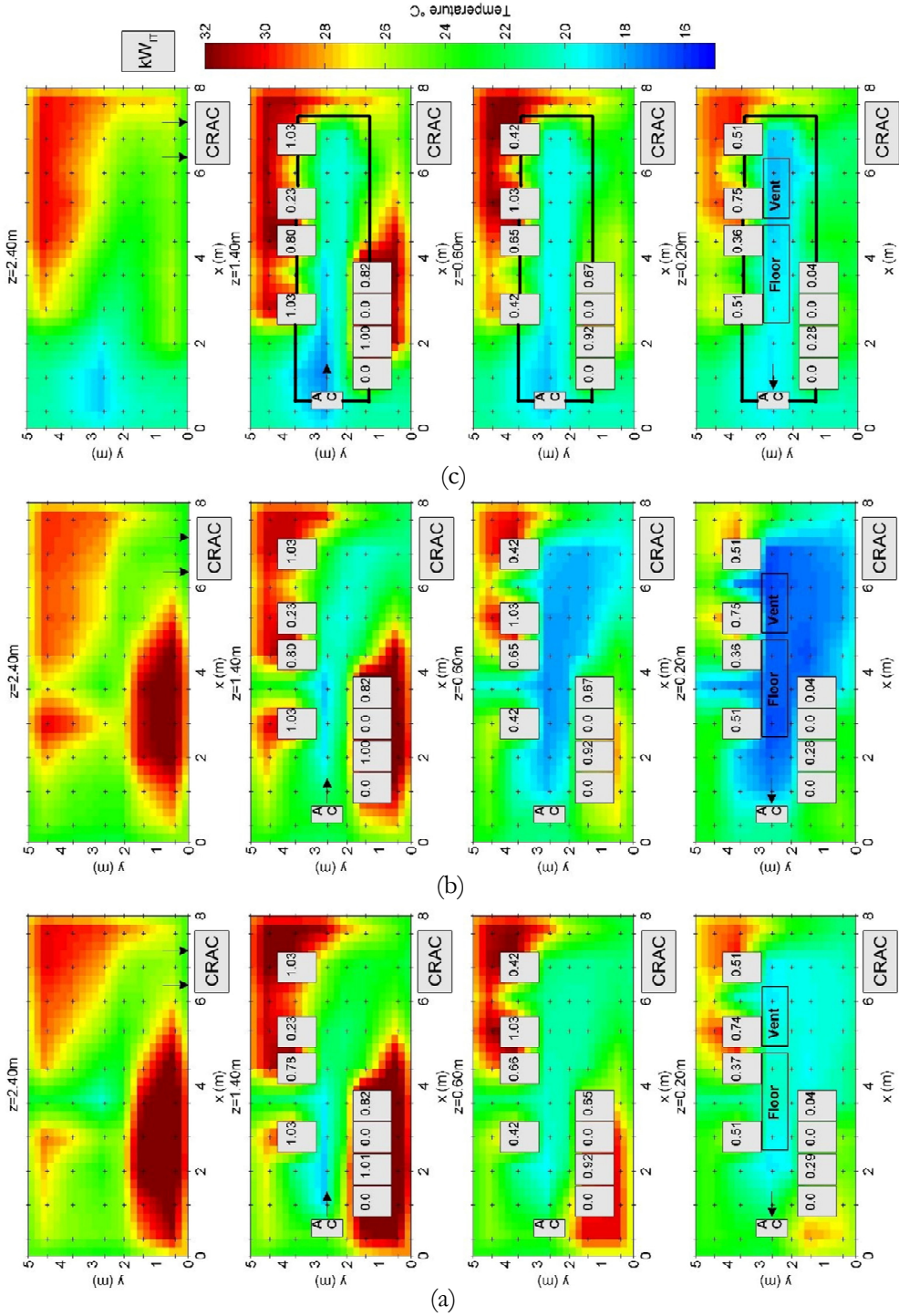


Figure 6-17 Average temperature distribution for tested settings (a) thermal aware workload management, variable setpoints, (b) competitive management C1, (c) competitive management C2

Evaluation of thermal management at system level: total DC energy efficiency

This section discusses the previously introduced settings of workload allocation and thermal actuation, which mainly target temperature control at the room level. In addition, the setting of the thermal management targeting control of the entire cooling system (variable setpoints of return air, fan speed, pump speed, economizer settings etc.) is introduced.

The system-level thermal actuation can actuate all components of the cooling system. These components listen to the variable setpoints of the tested system-level actuation. The setpoints for individual system components are generated based on thermal prediction of the entire system. During the operation, the setpoints can vary within a specified range of operability in order to reach the best possible power outcome of the cooling system. The bounds of the range are set by the algorithm developer. The actuated components and the range of operability are shown in Table 6-7.

Table 6-7 Ranges of operability for individual components within the cooling system

component	controlled variable	range
CRAC temperature sp	the sp for CRAC return temperature	20 to 28°C and 35°C ~ DX unit OFF
CRAC fan speed sp	the percentage of the maximum airflow	0.4 to 1
pump speed sp	the percentage of the maximum water flow	0.4 to 1
economizer sp	economizer is ON if outside temperature is below the sp	-30 °C ~economizer is not used, 10°C~low 15°C~high
dry cooler sp	the percentage of the maximum airflow	0.4 to 1

Again, the part-load analysis is performed. All previously presented settings in Table 6-6 (including system-level thermal actuation) are compared in terms of DC energy efficiency, represented by PUE. This analysis evaluates both summer and winter testing periods together. The four settings of the tested

platform and two competitive thermal strategies are compared and presented in Figure 6-18

This general trend of efficiency reduction corresponds to the idle power of the cooling system and the lower efficiency of the power delivery for part-load utilization, as depicted in Figure 6-18. This characteristic trend line also revealed that when the baseline workload settings were in use, the DC operated at a higher utilization level. Since the higher utilization is closer to the design conditions of the entire DC system, a lower PUE is obtained.

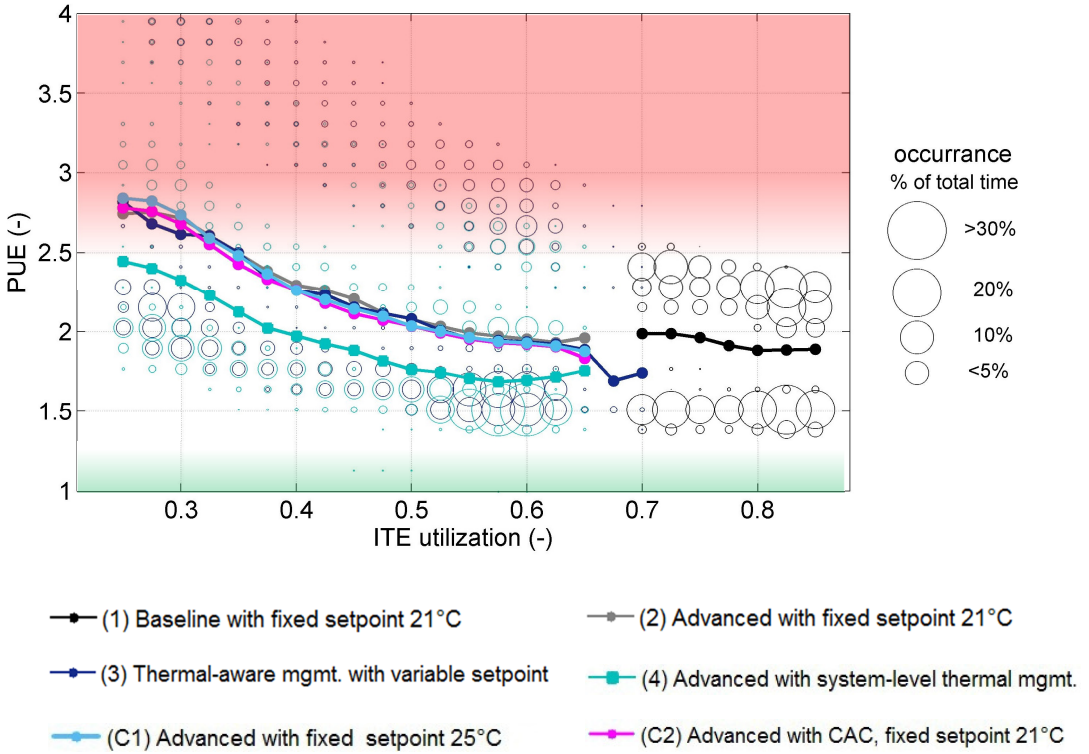


Figure 6-18 Part-load efficiency analysis of PUE for presented settings

Looking at the performance spreads, the performance is clustered in two efficiency levels for all tested settings except for the system-level thermal

actuation. The performance spread for this particular setting indicates that the DC system works with a larger variance of efficiency. To reiterate, the two levels of efficiency are caused by the economizer and also by the embedded ON/OFF control of the CRAC unit. However, for the system-level, thermal actuation manipulated all components in the cooling system and therefore reached various electricity outcomes. In other words, the system-level thermal actuation was better able to adapt to the given ITE part-load utilization. The variance of electricity outcomes explains the difference of the performance spread. Table 6-8 provides a summary of the results of the previously tested settings combining summer and winter scenarios in terms of normalized IT productivity, occurrence of temperature range violation and PUE.

Table 6-8 Summary of testing of workload and thermal management strategies

settings ID.:	{1}	{2}	{3}	{4}	{C1}	{C2}
normalized IT productivity (-)	0.504	0.846	0.767	0.846	0.846	0.846
occurrence of temperature violation (% of time)	99.0	70.9	31.0	31.0	49.8	7.0
PUE (-)	1.917	2.117	2.111	1.825	2.076	2.094
cooling energy use (MWh per 28 days)	8.05	6.19	6.36	4.17	6.03	6.13
total DC energy use (MWh per 28days)	23.66	16.01	16.89	13.84	15.75	15.89
energy savings (%)	-	32.3	28.6	41.5	33.4	32.9

In order to facilitate the easier comparison of results, Table 6-9 presents the obtained results in Table 6-8 as percentages, where 0% represents the worst performance and 100% represents the best performance

Table 6-9 Summary of testing of workload and thermal management strategies, performance representation in range of 0-100%

settings ID.:	{1}	{2}	{3}	{4}	{C1}	{C2}
normalized IT productivity (% of nominal IT productivity)	50.4	84.6	76.7	84.6	84.6	84.6
occurrence of temperature satisfaction (% of time)	1.0	30.1	69.0	69.0	51.2	93.0
DCIE (1/PUE) (%)	52.1	47.22	48.2	54.7	48.1	47.7

6.2.3 Simulation-based assessment of the power management

In this section only some of the results of the supervisory intelligence testing are presented. The full set of results, including, for instance, a study on delaying workload processing based on the supervisory policy, and sensitivity analysis of the supervisory policies to prediction uncertainties, are available in D6.3 [153]. These studies exceed the scope of this thesis.

The main goal of this particular study was to demonstrate the functionality of the testing procedure and operability of the tested algorithms by encompassing the virtual DC environment and tested power and supervisory management. The feasibility or profitability of the given system is not taken into consideration in this study. This particular study assumes that the DC is already equipped with a given on-site RES system.

In this section, the conventional power supply management denoted as the surplus strategy is compared with power supply management supported by supervisory intelligence modules. The demand generated by optimized workload allocation with variable temperature setpoints is used as an input in this study. This demand is partially covered by the RES system defined in section 5.1.2. The studied RES system is virtually located in Ireland as is the on-site RES system of the DC case-study. All six settings of the tested platform are compared. Table 6-10 depicts the subset of the tested platform settings in this section.

Hereunder, the specification of the RES including the controllable, uncontrollable RES systems and storage is briefly recapped.

Table 6-10 Settings of the platform configuration for the presented computational experiments concerning workload, thermal and power management.

setting ID.:	workload management	thermal management	power supply management
{1}	no consolidation	constant setpoints (21°C)	no on-site RES
{2}	consolidation: ITE consumption priorities	constant setpoints (21°C)	no on-site RES
{3}	consolidation: thermal priorities	variable setpoint (18-25°C) (room level control)	no on-site RES
{4}	consolidation: ITE consumption priorities	variable system setpoints (system level control)	no on-site RES
{5}	consolidation: thermal priorities	variable setpoint (18-25°C) (room level control)	on-site RES; surplus
{6}	consolidation: thermal priorities	variable setpoint (18-25°C) (room level control)	on-site RES; supervisory strategy

The controllable renewable generation is represented by an organic Rankine Cycle (ORC) generator. This system can provide both electricity and heat energy. In the test scenarios evaluated here, different fuel prices are assigned for winter and summer seasons. It is assumed that heat is used as a by-product during the winter period and thus the equivalent fuel price is assigned at 0.02 Eur/kWh_{el}. In the summer season, the equivalent fuel price is assigned at 0.09 Eur/kWh_{el}. The emission factor of biomass combustion was assumed, based on literature, to be 150gCO₂/kWh [154]. Additionally, the algorithm developer assumed that a unit can only perform efficiently with uninterrupted operation lasting for at least six hours. During this operation, the power can vary between the maximum power output of 7 kW_{el} to the minimum power output of 4 kW_{el}.

The uncontrollable renewable generation is represented by photovoltaic (PV) and wind generation units. The power output from these systems is

intermittent and cannot be guaranteed due to their dependency on the weather conditions. The combined maximum output from the wind and PV generators is 13 kW. The power management with the default settings manipulate the system in order to prioritise the direct use of uncontrollable energy whenever possible. In cases of surplus, the generated energy is stored or exported back to the grid.

The electrical storage has a capacity of 10 kWh_{el}. The electrical storage can be charged with a maximum charging power of 5 kW_{el} and discharged with a maximum power of 6kW. The default setting of the storage management charges the battery if the surplus occurs, otherwise it discharges.

The results in Figure 6-19 show the performance of the RES system for default surplus management and advanced management supported by the supervisory intelligence module. The study presents results of demand coverage for both summer and winter seasons. If energy storage is utilized, the manipulation of the energy storage is indicated by either discharge rate when the DC demand is partially covered by stored energy, or charge rate when the DC demand is raised due to storing energy.

Using conventional surplus management for DCs, the storage was rarely utilized. This is related to the issue of high-power density of DCs discussed earlier in section 5.3.1. To recall, even small-sized DCs such as the presented case-study require relatively large RES systems to cover their demand. In the case-study, the given on-site RES system was sufficient to cover only around 30% of DC demand over the year. Thus, the given on-site RES system never reached surplus, and therefore the charging of the storage was rarely triggered. Also, the default management did not consider the cost of the grid and the fuel for RES. Therefore, the power supply management cannot react to fluctuations in DC demand, RES generation, and energy prices.

In contrast, the supervisory intelligence module is supported by long-term IT workload, thermal and power prediction as well as day-ahead market services (e.g SEMO [126]). The storage can be operated more intelligently based on matching of predicted RES supply and DC demand. The results of demand coverage for the summer and winter periods using RES with surplus control and RES with supervisory support are presented in Figure 6-19:

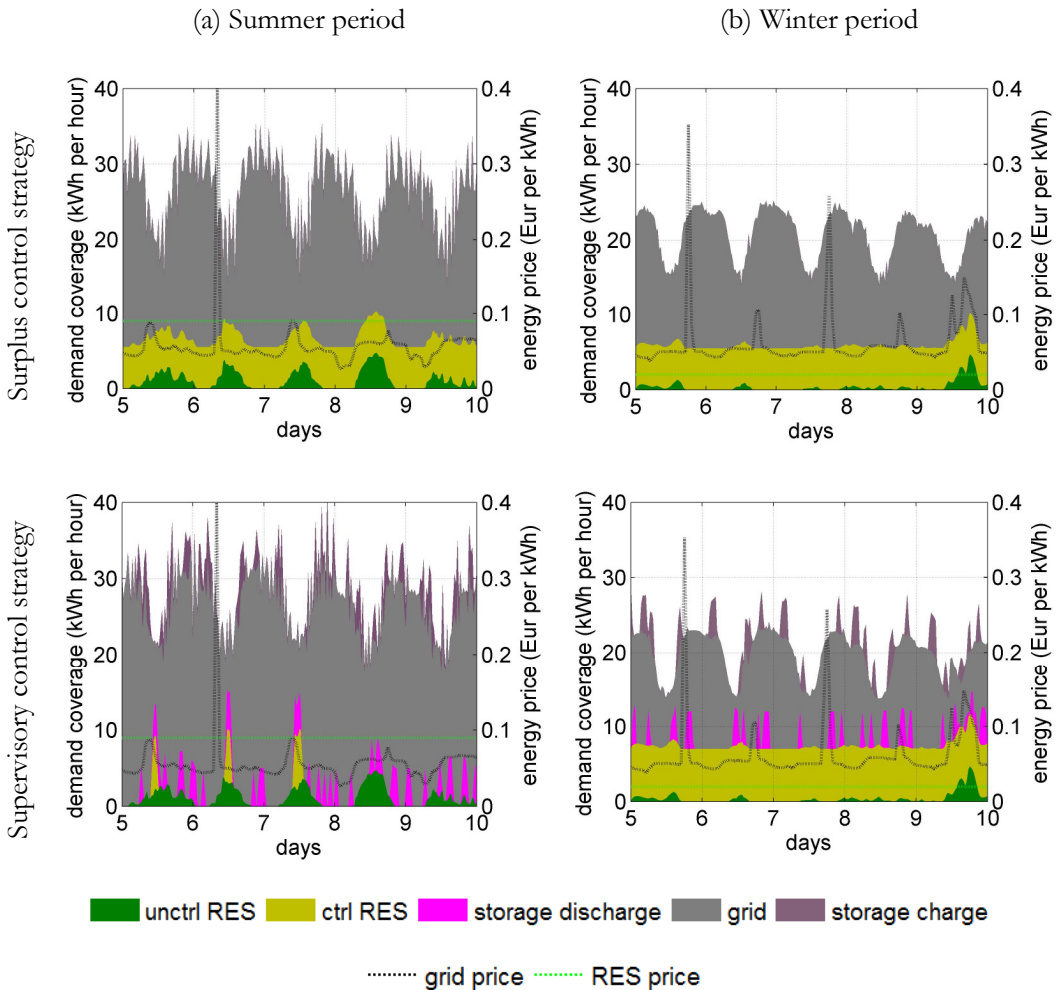


Figure 6-19 Simulation of the power supply system for baseline and tested power management strategy in (a) summer and (b) winter periods

Table 6-11 summarizes all previously presented results including the RES integration in terms of grid demand, energy cost and equivalent CO₂ emissions for the sum of both summer and winter scenarios. It should be noted that the table shows only the partner algorithms within the wider framework of the Genic project. The computational experiments with competitive thermal strategies (C1 and C2), which provided the additional benchmarks for the tested thermal management, are not listed in this table.

Table 6-11 Summary of testing of workload, thermal and power management strategies

settings ID.:	{1}	{2}	{3}	{4}	{5}	{6}
total grid demand (MWh per 28days)	23.658	16.012	16.895	13.847	12.679	12.729
uncontrollable RES generation (MWh per 28days)	NA	NA	NA	NA	0.518	0.518
controllable RES generation (MWh per 28days)	NA	NA	NA	NA	3.694	2.419
storage IN/ OUT (MWh per 28days)	NA	NA	NA	NA	0.00/ 0.00	0.206/ 0.203
total Energy Cost (Eur per 28days)	1398.2	939.9	994.4	813.6	944.9	791.5
equivalent CO ₂ emissions (tons per 28days)	10.78	7.30	7.70	6.31	6.33	6.16

6.3 Concluding remarks

This chapter reported on the testing of the external algorithms in the closed-loop fashion using the virtual DC environment. The virtual DC environment assessed the performance of the tested algorithm for multiple criteria, including ITE productivity, DC infrastructure efficiency, violation of recommended temperature bounds, total DC energy demand, CO₂ emission equivalent, and energy price.

A general conclusion from this chapter is that the testing of the external algorithms using the virtual DC environment supports the decision-making in two key ways. First, it enables the interactive testing and debugging of individual features of control algorithms, which is rarely possible in a real DC environment. Second, the virtual DC environment allows the designing and testing of any desired configurations of the entire DC control platform in a holistic manner. The presented tests were performed prior to the commissioning of the platform for the bespoke DC case-study. More specific conclusions drawn from the generated results are discussed below. To aid the discussion, results are organised and discussed around the following three domains: IT workload management, thermal management and power supply management. The interpretation of the presented results is based on consultation with relevant experts of the Genic project.

IT workload management

The operability of the tested IT workload management, which consists of several modules, was successfully tested in closed-loop fashion. The key results from this testing are discussed below.

- First, the IT workload management was configured to optimize the ITE energy use. From this testing, it can be concluded that of the 41% of energy savings achieved, the workload management was responsible for savings of up to 32% of the total data centre energy consumption. These savings from the workload management were achieved through the consolidation of the workload, the subsequent migration to the most efficient servers, and by triggering the standby mode in unutilized servers. It is worth noting that such a management strategy requires the prediction of IT workload in order to activate the unutilized servers in advance of peaks.

- Second, the IT workload management was configured to follow the thermal priorities of the thermal management in order to provide joint management of both IT workload and the thermal systems to optimize total DC power demand. It can be concluded that when the advanced IT workload management was guided by the thermal priorities, total DC energy use was not optimal. In fact, the results show that the potential to reduce energy use was lower than in the previous setting, which focused only on the ITE energy use. Specifically, the saving potential was simulated at 29% of total DC energy, about 3% less than the previous setting. It can be concluded that the application of the joint strategy did not lead to the anticipated levels of reductions in total DC energy use for the given case-study. The improvement in energy efficiency claimed by other researchers [37], [67], [68] was not observed in the case study presented here.

To elaborate upon this topic, the closed-loop testing revealed a conflicting situation. Thermal management attempted to prioritise its own preferred locations for data processing and related heat dissipation from, so to speak, its own thermal perspective. However, these locations were occupied by servers with lower computational efficiency. As a result, the thermal preferences led to a reduction of the IT efficiency and consequently to higher heat dissipation. For the reported case study, this reduction of IT efficiency outweighed the possible improvement in cooling efficiency. It is worth noting that this strategy was very sensitive to the configuration of housed servers. In theory, if the DC houses ITE with similar efficiency, the negative effect of thermal priorities on the workload allocation would be negligible, which accords with the assumption made in the aforementioned literature.

In conclusion, the dynamic thermal-aware allocation was found to be a very technically complicated concept, and it was concluded that it may not lead to the anticipated level of reductions of total DC energy use if heterogeneous ITE arrangement is considered.

- The next conclusion was drawn from the evaluation of both presented settings of the IT workload management. During these analyses, a contradiction was identified. While the results of IT productivity, which were in agreement with observed energy savings, suggested an increase in efficiency, the PUE results suggested the opposite. However, to correctly interpret this conflicting indication, it should be stated that the lower efficiency indicated by the PUE is solely related with the reduction of efficiency of the cooling and power delivery systems at the lower part-load utilization resulting from the more efficient workload management. Thus, it can be concluded that the improvements achieved by workload management is out of scope of the PUE indicator. Therefore, PUE is not suitable for the assessment of any workload management strategy. The PUE indicator can only capture the efficiency of cooling and power delivery infrastructure.

Thermal management

The operability of the tested thermal management, which consists of several modules, was successfully tested in a closed-loop fashion. The key results from this testing are discussed below.

- First, the assessment of thermal management at room level is discussed. These analyses aimed to assess the temperature distribution within the DC space. The thermal aspect of the joint thermal and workload management strategy was also evaluated in the closed-loop testing. This testing showed that the strategy had the ability to improve the temperature distribution and to prevent hot spots in the DC. This finding is in agreement with the

mentioned studies reported in the literature [37], [67], [68]. While using the baseline strategy, it was discovered that 70% of the time the ITE inlet temperatures fell beyond the recommended temperature range of 18-27°C, and occasionally the temperatures even exceeded the allowable bounds of class A1 (15-32°C). In contrast, the tested thermal management strategy kept the ITE inlet temperatures within the allowable temperature range, while the recommended ITE inlet temperatures were violated much less often (31% of the time). The part-load analysis showed that the allowable temperature range was satisfied regardless of the ITE utilization. These improvements were achieved by varying the temperature setpoints based on the temperature sensor network within the space, and through the application of the thermal-aware workload allocation.

The tested algorithm was compared with the competitive thermal management strategies. Based on this comparison, it was concluded that the tested algorithm was competitive with other thermal management strategies, such as cold aisle containment.

Regarding the temperature distribution assessment, it should be noted that due to the oversized cooling system, the thermal management strategies were mainly tested to determine whether they led to the avoidance of “overcooling”. The undercooling scenario was not studied since it was not applicable for the given case-study.

- Second, the assessment of thermal management strategies at the building level is discussed. These analyses aimed to assess how total energy efficiency was affected by thermal management strategies. The analysis of the building & system level revealed no thermal management strategy operating at room level could achieve significant energy savings for the given DC case-study. The thermal management at room-level only saved up to 3% of the total DC energy. However, when the thermal

management was configured to control the entire cooling system, it achieved energy savings of up to 15% of total DC energy use. It can be concluded then that system-level control of the cooling system is necessary to achieve significant savings.

Power supply management

The operability of the tested power supply management, which consists of several modules, was successfully tested in a closed-loop fashion. The key results from this testing are discussed below.

- As observed in our case-study, the demand of even the small-sized DC considerably exceeded the available generation of the given on-site RES system. It is worth noticing the saving potential of the DC energy efficiency measures versus the potential of the on-site energy generation. When the system-level thermal actuation was applied, the total energy performance was at the same level as when the thermal management was not optimized, and the DC demand was covered by the relatively large RES system. In fact, this finding once again illustrates the mismatch of the power density of demand and generation and the importance of efficient DC management in order to reach a net-zero energy DC.
- Due to the general mismatch resulting from the enormous power density of DC systems, the conventional power supply management strategy, which stores any surplus of on-site RES generation, cannot be deemed to be efficient. In the studied case, this strategy never actually triggered the storage. The supervisory control strategy, which uses energy predictions and the day-ahead market service, was able to react to a larger variety of other trigger points (e.g. energy price level) than only on-site energy surplus. The tested power management improved the CO₂ and energy cost outcomes through better utilization of storage and a controllable on-site RES system.

- Regarding the management of the controllable RES system, it was found that the operational price assigned to this energy generation (e.g. Biomass boiler + ORC unit) can restrict the utilization of such a system. The explanation here is that the power supply management may prioritise supply from the cheaper sources (e.g. grid) in order to reach a better DC outcome in terms of DC energy cost.

Finally, the virtual DC environment developed in this research proved that it is able provide sufficient support for the development of holistic operation within the DC. The tested control algorithms as well as entire control platform developed by external entities were tested in different domains and at various levels of scale. The decision-making is supported by the evaluation of multiple performance indicators for each test, and thus the developer can gain a full picture of the influence of the tested algorithm.

In addition, the achieved results also demonstrate the functionality of the overall simulation and communication-tool chain, where the virtual DC environment was implemented. The interactive communication of multiple entities with the virtual DC environment was successfully executed.

7 Conclusion and future work

7.1 Conclusion

The research reported here is accommodated in the Computational Building Performance Simulation (CBPS) group. This research group aims to expand the modelling and simulation scope to allow the assessment of multi-disciplinary and multi-scale problems. Data centres (DCs) are of great interest since they are a unique building type where several disciplines such as computer science, IT, electrical, mechanical and control engineering must cooperate. As such, DCs represent a good area of study in which skills and expertise in computational simulation could be usefully exploited. Following the logic of previous research by the group, from a broad perspective, the current research aimed to apply Building Energy Simulation (BES) to arrive at comprehensive understanding of the overall DC environment that supports decisions concerning the development and commissioning of novel DC operational strategies.

Another reason that made DCs a particularly interesting object of study was the recent exponential growth in their size and scale and the corresponding growth in the complexity of their management. In brief, this growth is due to the rapid evolution of digital infrastructure, which has seen a general trend of consolidation of data management into ever larger DCs. To understand the scale of growth, DCs are now responsible for approximately 2% of the total world electricity consumption [15], and this figure will likely increase in the future as DCs incorporate more IT equipment to manage the growing amount of data computing for existing and new end-users. In order to be able to manage this trend of expansion, the nature of the DC infrastructure is undergoing change. In particular, modern DCs have recently, or plan in the

near future, to integrate additional energy systems such as renewable energy sources and waste heat utilization systems. Much research attention is currently being devoted to the problem of adequately managing this extended DC infrastructure. The premise of the research at the wider consortium level was that by managing the multi-domain DC infrastructure in a holistic manner, the DC infrastructure can achieve significant reductions in energy use and CO₂ emissions. The holistic operation proposes to coordinate all involved systems to reach the high-level economic and ecological objectives, while at the same time ensuring the required operational conditions in the indoor environment to secure the reliability of their core business activity; data computing.

However, developing new strategies is a problematic and challenging task. The main issue is that the possibility of testing any new strategy, which is necessary for its development, is extremely limited due to the mission critical nature of the DC environment, where any downtime of DC services results in financial penalties and reputation loss. Therefore, the DC community is keen to find novel approaches to the development and testing of new management strategies.

The novel approach proposed in this research was to create a “safe” testing environment to determine the value of new DC management strategies by creating a virtual data centre that could be used for the testing of new strategies without endangering the operation of the real DC. Successful tests in such a safe environment can accelerate the process of implementing new strategies in real DCs.

In order to create this safe testing environment, and in order to verify the results of the research, the following methodological steps were taken. First, the data centre needed to be accurately specified in order to adequately inform the model of the DC that would be used later in the study. Next, a computational model was developed to represent the electrical and thermal

processes within the DC. After its development, it was important to seek quality assurance from relevant experts. As such, the model was accredited by external partners with the relevant expertise from the Genic project. After this accreditation step, the next step was to integrate the computational model into the wider simulation & communication toolchain in order to facilitate the interactive closed-loop testing of the external algorithms. Finally, the results of the testing needed to be analysed in consultation with the algorithm developers. Certain limitations to the described approach are worthy of discussion here. First, it must be noted that as energy modelling specialists, the task of fully understanding the intricacies of DC management was somewhat outside of our building physics and services expertise. In order to achieve the desired holistic management of the DC environment, securing the cooperation of various experts and specialists in disciplines such as IT, thermal management, power management and control theory was essential. Therefore, to deal with the gaps in our expertise and to maximise the potential value of the research, this work was embedded in a multi-domain team, in this case in the framework of the Genic project funded by the European Commission.

Another limitation was identified during the execution of the modelling task. The main limitation of the selected BES modelling approach was found in the thermal representation of DC space at the required levels of server and rack. This representation required higher resolution, which presented the research with an immediate challenge: the modelling of the DC space had to be discretized to a number of computational nodes. However, such a discretization is not typical in BES tools, which typically represent one room with one computational node. It should also be noted that this problem could not be solved by applying high-resolution modelling approaches such as Computational Fluid Dynamics (CFD) due to their long computational time and the lack of ability of co-simulation with other energy models. Thus, in

order to address this issue, a multi-zonal airflow network method was investigated and applied to the overall structure of the virtual DC environment in order to represent the dynamic thermal behaviour of the DC space with the required resolution. Since the application of this method is relatively new for DCs, the method first needed to be validated. This validation for the given case study was executed as part of this research.

The final set of limitations to mention was found when conducting the overall validation and demonstration study. The process was complicated by the large required scope of the modelling and related difficulty of establishing common boundary conditions for the entire DC system, which was necessary to enable the comparison of results of the simulated and real DC. Therefore, the validation and demonstration procedures had to be decomposed into a group of sub-models, and had to be validated and demonstrated separately.

This difficulty was further increased due to the limited ability to gather certain measurements during the regular operation of the real DC. Since the research is situated in the commissioning and regular operational phases, the limited availability of measurements is unsurprising and therefore the modelling approach needed to be selected accordingly to mitigate this issue. The response was to select a BES tool because such a physics-based modelling approach allows for the configuration to be informed by incorporating the technical specifications of the modelled infrastructure. Although the BES tool can provide a trustworthy simulation environment, the quality assurance (i.e. the quantification of simulation error and demonstration of simulated outcomes) of the testing environment remains the main concern of the external algorithm developers since they will ultimately be the end users of the simulation tool.

Ultimately, simulation error is a natural limitation of any modelling process due to the necessary abstraction of reality, and as such it is present in the computational experiment. In order to eliminate the impact of these inherent

errors on the final testing of the external control algorithms, the simulated results must always be compared with a predefined baseline simulated by the same testing environment. Thus, the performance of the tested strategy is evaluated against this simulated baseline. As a result, the simulation error of the model is involved in both the baseline and the experiment, and this error is deducted during the relative comparison. As such, it can be assumed that the assessment of the experiment is only marginally affected by the model error.

The main results achieved from following the key methodological steps outlined above are discussed hereunder. In order to accurately specify the modelled DC infrastructure including the on-site renewable energy source (RES) system, a case study was conducted in which a virtual DC environment was used to represent a real bespoke DC located in Ireland and a real RES laboratory located in Spain. The virtual DC environment demonstrated that the selected modelling approaches did have the ability to represent the desired electric and thermal performance of the bespoke DC.

Next, regarding selection of modelling approaches, the proposed virtual DC environment is compiled from several dynamic control-oriented energy models offering interactive feedback in the form of “virtual monitoring”. The virtual DC environment was able to predict the temperature distribution at the required rack level and, at the same time, predict the overall electrical and thermal performance of the DC across the primary system components. In order to predict the temperature distribution with the required resolution, the multi-zonal airflow network was adopted. Based on the reported results, it can be concluded that the multi-zonal airflow network was able to sufficiently represent the temperatures at the inlet side of the racks and the return air temperature of the studied DC. The temperatures at the outlet side of the racks could not be validated due to the mismatch between the representation of the computational nodes and data regarding the spot measurements.

After the development of the virtual DC environment, its quality had to be assured by relevant experts. As mentioned, the quality assurance had to be decomposed due to the large scope of this study. Also, limitations were found regarding the availability of measured data. Therefore, the simulation errors were quantified wherever possible. Where it was not possible to gather all required measurements, the performance of the virtual DC environment was demonstrated by determining if the simulated results fell within expected ranges. The model was accredited by external partners with the relevant expertise from the Genic project.

After the positive accreditation, the virtual DC environment was integrated into the wider simulation and communication toolchain in order to facilitate the interactive closed-loop testing of the external algorithms. Regarding the simulation error during the closed-loop testing, the simulation error was eliminated by relative comparison with the simulated baseline. Based on our observations, this error could be categorised as reasonable and as such it was not critical for the evaluation of the algorithm's functionality, since the virtual DC environment could realistically emulate the real DC's processes. It should be noted here, however, that larger errors would limit the ability of the model to be used for commissioning support. In such cases, the control platform would need to be re-trained with the most updated monitoring data prior to its deployment in order to successfully adapt to the real DC. However, even if only functionality testing was performed, the development and decision making concerning new management strategies would still be accelerated.

Regarding the testing procedure, different management strategies combining IT, thermal and power management were tested in closed-loop fashion using the virtual DC environment. The simulated results were evaluated by part-load analysis using multiple performance indicators such as IT productivity, PUE and temperature violation. The virtual DC environment allowed for the

simultaneous capture of the electric and thermal DC performance while they were under the influence of the tested external management strategies. It can be concluded that the developed virtual DC environment proved that it is capable of supporting the global evaluation of holistic DC operation. Finally, the results of the test were analysed in consultation with the algorithm developers. The DC algorithm developers involved in the Genic project particularly appreciated a number of aspects of the proposed testing procedure, which are outlined below.

The dynamic feedback of “virtual monitoring” in reasonable time, which enables the acceleration of the closed-loop testing procedure. The capability to replicate tests under identical boundary conditions, which allows the relative comparison of simulated experiments for different configurations of the control platform. Finally, when the virtual monitoring follows the communication format of the real monitoring, the virtual DC environment can be easily substituted by the real DC environment and thus support the commissioning.

In conclusion, this research demonstrated the applicability of BES for the analysis of energy use in a DC and introduced a new application of a BES tool as a testing environment for external control algorithms. The first prototype of such a testing environment was built within this research and its usability was tested. This research is also unique in that the first prototype of the testing environment was subjected to all phases of the proposed testing workflow from development through usability testing to the real-world application, where the initial version of the holistic operation was tested. The final positive evaluation of this work was that the tested control platform was deployed in real operating conditions in a small-sized university DC in Ireland.

7.2 Direction for future work

The presented project achieved the first phase of proof of concept of the testing environment. The wider simulation & communication toolchain, including the first prototype of the virtual DC environment and the first version of the holistic operation, was developed and successfully tested in a closed-loop. In the future, some of the presented studies could be further extended by using the same testing setup. For instance, the deep analysis of different supervisory management strategies such as demand response, including policies for workload and thermal management, could be instrumental in understanding the energy flexibility of DCs. Some initial testing in this area has already been conducted within the Genic project and the results are publicly available in project deliverable D6.3 [153]

Next, the virtual DC environment can also mimic some fault situations within the simulated infrastructure. Fault simulation is beneficial for the development and training of fault detection and diagnostics (FDD) algorithms. Some initial experiments in this area were performed within the Genic project, and the result can be found in deliverable D4.5 [155]. The initial testing revealed promising potential for the virtual DC environment in this area, which could be elaborated. However, these particular results are not publicly available because they are the intellectual property of the FDD algorithm developer.

From the modelling perspective, the virtual DC environment was configured to represent the given case-study of an educational DC in order to be able to support all phases, from the platform development to commissioning and real operation. This approach requires exact DC specification and calibration of the virtual DC environment for every new case. Although modelling the exact DC specification can prolong the preparation phase of the development of algorithms, in the end the comprehensive closed-the-loop testing saves time during commissioning. This research clearly demonstrates that the developed

modelling approach can be feasibly replicated for a wide range of DC configurations.

Alternatively, testing of the different management strategies can be done using the generic representation of DCs. Indeed, the modelling of various generic DC sizes and typologies would greatly extend the applicability of the virtual DC environment within the DC field. However, such testing would provide less support for the commissioning phase. It would be sufficient to support the development of novel strategies in terms of functionality testing. The tested algorithms would need to be largely adapted to the given DC case. In addition, there are serious difficulties associated with validation of the generic DC testbed. The validation requires measurement datasets from various DC sites. Obtaining these datasets from commercial DCs is very complicated due to confidentiality reasons.

The modelling approaches used in the virtual DC environment can also be used to create a stand-alone tool to support purposes other than commissioning and operation, e.g. simulation-aided design. The described modelling approaches have already been applied in several MSc student projects of the CBPS research group. These projects include the simulation-based design of a waste heat utilization system for a data center on a campus [156], simulation-based assessment of technical requirements to power data centres with renewable energy [157] and simulation-based assessment of humidity treatment in a data center cooling system with an air-side economizer [158]. Such projects demonstrate the wide applicability of the presented modelling approaches.

Finally, after its successful testing in the DC, the applicability of the simulation-based closed-loop testing can also be extended to other building types. Essentially, the simulation-based closed-loop testing of new operational strategies can be applied in any building. That said, such a testing approach is particularly beneficial for multi-disciplinary and mission critical environments

(e.g. power plants, factories etc.), where multi-domain energy management is required but real testing is complicated, if not impossible.

Appendix A: Candidates for monitoring and local control in the DC environment

Appendix A provides candidates for DC monitoring and local control in relation to scale and domain (process). The monitoring candidates are listed for IT workload, DC space environment, cooling and power systems.

Table A-1 IT workload monitoring candidates

measured variable	scale	process	description
central processing unit (CPU) usage (Hz)	server	data processing, powering	These measurements are gathered via IT performance management tools using workload virtualization techniques. The data are available via the internet or local network interface. The necessary condition for such measurements is that the IT performance management tool is installed on the server. Thus, the monitoring tool can collect high-resolution monitoring of IT performance metrics including energy of individual serves.
random access memory (RAM) usage (MB)			
hard disk usage (MB)			
network transmitted (bps)			
network received (bps)			
power usage (kWh)			

Table A-2 DC environment monitoring candidates: part I

measured variable	scale	process	description
DC environment temperature <ul style="list-style-type: none"> • <i>IT equipment inlet air temperature</i> • <i>IT equipment outlet air temperature</i> • <i>plenum temperature</i> • <i>under floor temperature</i> 	room, rack	thermal conditioning	ASHRAE recommends measuring the environment temperatures for each one-third of a rack for IT inlet air temperature (cold aisle) and at least one temperature at the top position for IT outlet air temperature to detect recirculation. The temperature measurements of the DC environment can be extended by incorporating spot measurements of plenum or underfloor temperatures. These measurements can be combined with supply and return air temperature to CRAC/CRAH units (table A-) in order to find the representative temperature of the DC environment
DC environment humidity <ul style="list-style-type: none"> • <i>IT equipment inlet humidity</i> • <i>plenum humidity</i> 			The high-resolution measurements of the humidity level are mainly relevant for systems with the direct air economizer, where tight control of humidity is required.

Table A-3 DC environment monitoring candidates: part II

measured variable	scale	process	description
DC environment airstream velocity (m s ⁻¹) <ul style="list-style-type: none"> • supply and return air stream • IT equipment inlet air stream • floor tile air stream 	room, rack	thermal conditioning	The high-resolution measurements of airstream velocity are mainly used for calibration of high-resolution models as one-time “audit measurements” The highly fluctuating behavior of this signal is not suitable for operational purposes
DC environment pressure (pa) <ul style="list-style-type: none"> • hot / cold aisle containment pressure • plenum pressure • under floor plenum pressure 			The speed of the CRAC/CRAH fan can be controlled based on pressure levels in one of the DC environment zones

Table A-4 cooling system monitoring candidates: part I

measured variable	scale	process	description
total cooling demand (kWh)	room	thermal conditioning	The cooling demand represents the dissipated heat into the DC space. This value is estimated as the total power load of housed IT equipment.
total cooling load (kWh)			The cooling load represents the heat rejected from the DC space by the cooling system. It is usually indirectly measured based on a calorimetry equation at CRAC/CRAH/CDU. The heat is given by formula $\dot{Q} = \dot{m} \cdot c \cdot \Delta t$, where \dot{Q} is cooling load, \dot{m} is mass flow, c is specific heat and Δt is temperature difference
total waste heat (kWh)	district, building,		The waste heat represents the heat rejected to the ambient environment. It is indirectly measured at drycooler, cooling tower or other heat rejecting device.
total reuse heat (kWh)			The total reused heat represents the waste heat reused for another purpose (e.g. swimming pool heating). It is indirectly measured at the reuse heat coil.

Table A-4 cooling system monitoring candidates: part II

measured variable	scale	process	description
cooling system temperature monitoring (°C) <ul style="list-style-type: none"> • CRAC/CRAH Return air temperature • CRAC/CRAH Supply air temperature • CRAC/CRAH Inlet liquid temperature • CRAC/CRAH Outlet liquid temperature • condenser temperature* • evaporator temperature* • cooling tower/Drycooler inlet liquid temperature • cooling tower/Drycooler outlet liquid temperature 	building, room	thermal conditioning	These measurements represent important temperatures within the DC cooling system
cooling system mass flow/pressure monitoring (kg h ⁻¹ / Pa) <ul style="list-style-type: none"> • CRAC/CRAH air flow • CRAC/CRAH air pressure drop • pump(s) liquid flow • pump(s) pressure drop • compressor pressure drop*** 	building, room	thermal conditioning	These measurements represent mass flow or pressure level within the DC cooling system *** rarely available for system-based control

Table A-5 Power Monitoring candidates

measured variable	scale	process	description
total DC power demand (kWh)	building	all	The total DC demand represents the sum of the critical, essential, and non-essential loads. It is measured at the main DC switchboard or by micro grid devices when on-site RES generation is present.
total DC grid load (kWh)			The total DC grid load represents the load required from the grid. This value is typically the same as Total DC power demand. The value only differs when on-site RES generation is present. It is measured at the main DC switchboard or by micro grid devices
mission critical power load (kWh) <ul style="list-style-type: none"> total IT power load IT power load per rack IT power load per server 	room, rack, server	powering, data processing	The mission critical power load usually represents the load of IT equipment housed in the DC. It can be measured by UPS devices (Room level), PDU (Rack level) or individual PSU for individual servers (Server level)
essential power load (kWh) <ul style="list-style-type: none"> total cooling system power load CRAC/CRAH power load refrigerant unit power load pumps power load fans power load cooling tower/Dry cooler power load 	building, room	powering, thermal conditioning	The essential power load usually represents the load for all components of the cooling system. It can be measured at the related switchboard or at individual components. It should be noted that some components of the cooling system (e.g. CRAC fans) can be included in a mission critical category and power delivery can be covered by UPS systems.
non-essential power load (kWh) <ul style="list-style-type: none"> lighting safety and security systems 	building	powering	The non-essential power load represents the load related with an auxiliary system of the DC. The non-essential load is measured at the main switchboard. In theory, the total power demand should be the sum of all critical, essential, and non-essential loads. However, there is always some difference between the sum of component measurements and the main switchboard measurement due to power delivery losses.
power generation (kWh) <ul style="list-style-type: none"> PV production wind production 	district, building	powering	The power generation represents energy generation from plants owned by the DC (e.g. PV, Wind or biomass). The power generation is measured at the micro grid device.
battery power charge/ discharge (kWh)	building	powering	The battery charge status is measured at the micro grid device.
battery state of charge (%)			

Table A-6 Local control candidates

measured variable	scale	process	description
IT workload actuation commands	server,	workload	The IT workload management provides optimal setpoints/commands for each VM: Suspend, Migrate. And for each server: Deactivated, Activated in line with supervisory management
<i>HVAC commands</i> <i>CRAC/CRAH setpoints</i> <ul style="list-style-type: none"> • <i>supply air temperature setpoint</i> • <i>air-flowrate setpoints</i> • ... <i>CDU setpoints</i> <ul style="list-style-type: none"> • <i>liquid-flowrate setpoints</i> 	room, rack	thermal conditioning	<p>The Thermal management provides optimal setpoints to individual local controllers for the overall cooling system in line with supervisory management</p> <p>It can be noted that the conventional air-based cooling system (CRAC/CRAH unit) mainly actuates at the building and the room scale. The thermal actuation at rack and server scale is very limited for this type of system</p>
<i>HVAC commands</i> <i>heat rejecting circuit setpoints</i> <ul style="list-style-type: none"> • <i>liquid flowrate set points</i> • <i>dry-cooler/aircooled chiller air-flowrate setpoints</i> • <i>economizer temperature set points</i> • ... 	building		
<i>power supply commands</i> <ul style="list-style-type: none"> • <i>on-site controllable power supply set points</i> • <i>on-site uncontrollable on/off set points</i> • <i>on-site battery charge/discharge signal</i> 	building, district	powering	The power management provides the optimal on-site power supply and power storage management to the local control in line with supervisory management

Appendix B: Server arrangement in the real and simulation setup

Appendix B depicts the server arrangement in both the real and simulation setup and provides the mapping of the power load and related dissipated heat within the DC space. To recall the arrangement of the racks, Figure B-1 shows the layout of the studied DC.

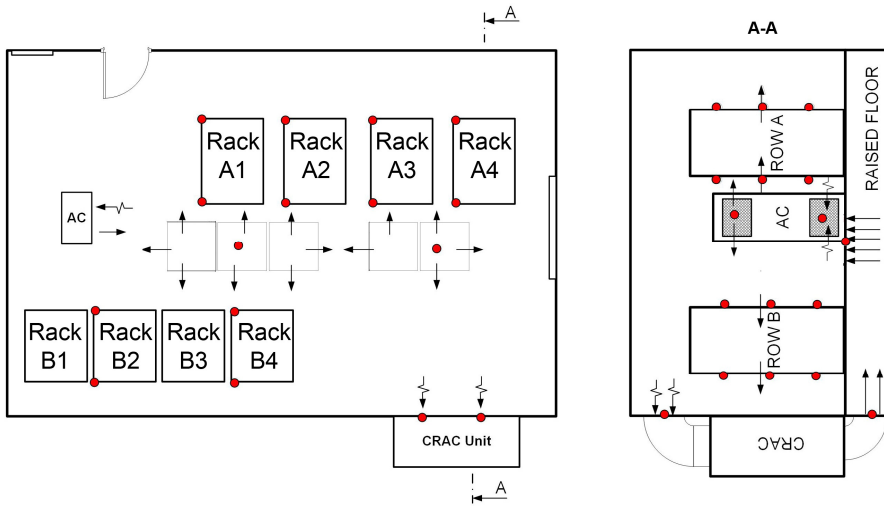


Figure B-1 DC layout and section of the demonstration DC

Arrangement of ITE in the real university DC

Table B-1 shows the maximal IT power load and related heat dissipation for the real university DC at a resolution of 1/3rd of the rack. Table B-2 shows individual server specifications. The ITE arrangement within the individual racks is demonstrated in Figure B-2, where each sever type is indicated by its specific colour code

Table B-1 Distribution of maximal IT power load (W) with the demonstration DC

RACK (W)	A1	A2	A3	A4	B1	B2	B3	B4
TOP	1460	870	1970	702	0	760	0	0
MID	4160	457	3790	1640	0	4000	0	1413
BOT	0	457	5160	2498	0	0	0	778
TOTAL	5620	1784	10920	4840	0	4760	0	2191

Table B-2 Server parameters: chassis size and power consumption.

ID code		server type	chassis size (U)	maximum Power (W)	number of servers
SERVER 1		Cisco 3750 Catalyst	1	160	7
SERVER 2		Cisco 4500 Catalyst	1	276	3
SERVER 3		Cisco 6500 Catalyst	12	4000	1
SERVER 4		Cisco 5548 UP	1	89	6
SERVER 5		Cisco 6248 UP	1	89	7
SERVER 6		Cisco UCS 5108	6	2498	3
SERVER 7		Cisco UCS v2 C220M3	1	650	3
SERVER 8		Dell Power Vault TL4000	2	870	1
SERVER 9		Dell Power Edge R220	1	304	5
SERVER 10		Dell Power Edge R710	2	870	2
SERVER 11		Dell Power Edge R910	4	1100	2
SERVER 12		Dell Power Edge R1950	1	670	2
SERVER 13		Dell Power Edge R2600	4	908	1
SERVER 14		EMC VNX 5300	14	457	2
SERVER 15		Mac OS Xserver 10.6	1	700	4
SERVER 16		HP ProLiant DL 380	1	750	1
OTHER IT		e.g switches, routers etc.	1	<10	5

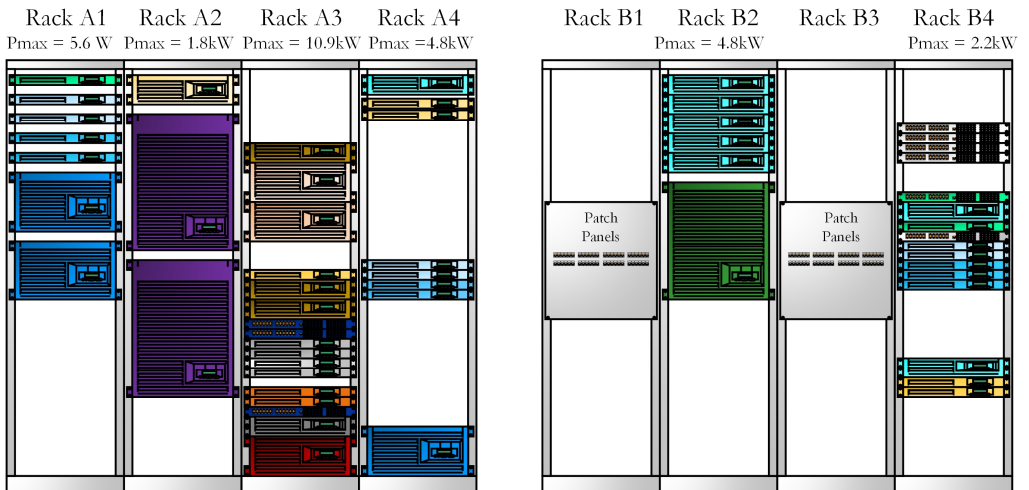


Figure B-2 Server arrangement in the university DC

Arrangement of ITE in the virtual DC environment

Similarly, table B-3 shows the maximal IT power load and related heat dissipation for the virtual DC environment at a resolution of 1/3rd of the rack. Table B-4 and Table B-5 further specify the performance of servers. The ITE arrangement within the individual racks is again demonstrated in Figure B-3, where each sever type is indicated by its specific colour code

Table B-3 distribution of nominal IT power load (W) used in simulation-based assessment.

RACK (W)	A1	A2	A3	A4	B1	B2	B3	B4
TOP	950	890	1920	1700	0	910	0	1050
MID	1620	1480	1195	1250	0	960	0	1275
BOT	1480	1415	1060	1020	0	2400	0	2000
TOTAL	4050	3785	4175	3970	0	4270	0	4325

Table B-4: Server parameters: chassis size and power consumption.

ID code	chassis size (U)	maximum power (W)	idle power (W)	standby power (W)	nominal power (W)
SERVER 1	1	90	30	5	300
SERVER 2	1	95	35	5	300
SERVER 3	1	105	45	5	300
SERVER 4	2	130	70	5	550
SERVER 5	2	140	80	5	550
SERVER 6	2	160	100	5	550
SERVER 7	2	300	140	5	500
SERVER 8	2	400	270	5	600
SERVER 9	2	460	300	5	600

Table B-5: Server parameters: CPU core, CPU speed, and memory.

ID code		CPU size (# physical cores)	CPU size (# virtual cores)	CPU speed (MHz)	memory capacity (GB)	number of servers
SERVER 1		4	8	3200	16	3
SERVER 2		4	8	3200	32	8
SERVER 3		4	8	3200	64	48
SERVER 4		6	12	2000	64	2
SERVER 5		6	12	2000	128	12
SERVER 6		6	12	2000	256	23
SERVER 7		12	24	2700	128	19
SERVER 8		16	32	2000	128	14
SERVER 9		16	32	2900	128	3

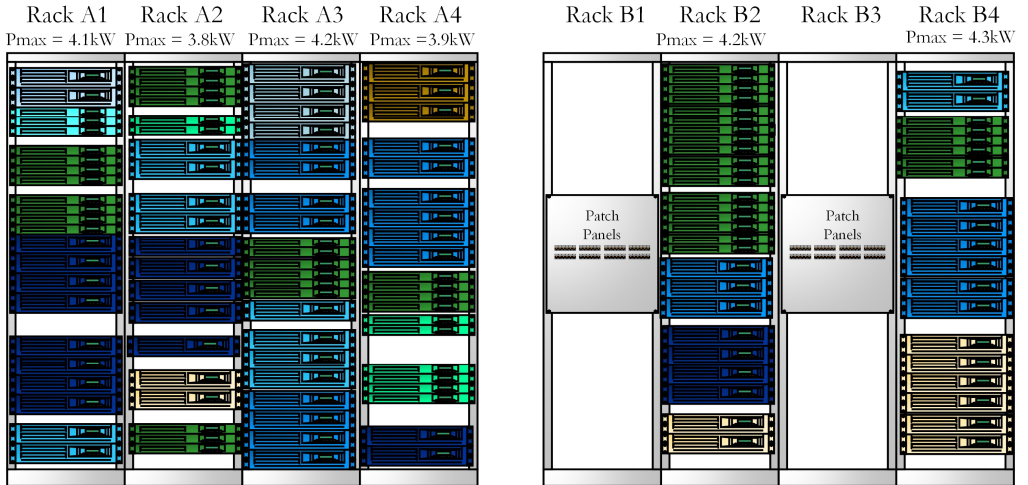


Figure B-3 Server arrangement for simulation-based assessment

Appendix C: Validation and demonstration of the DC space model

Validation of the DC space model

The comparison of measured and simulated temperatures of the first category presented in chapter 5 are shown here again. Figures C-1 and C-2 provide a detailed overview of this comparison, where figure C-1 shows the return air temperature for the CRAC and AC units for the calibration data set, and figure C-2 shows the return air temperature for the CRAC and AC units for the validation data set.

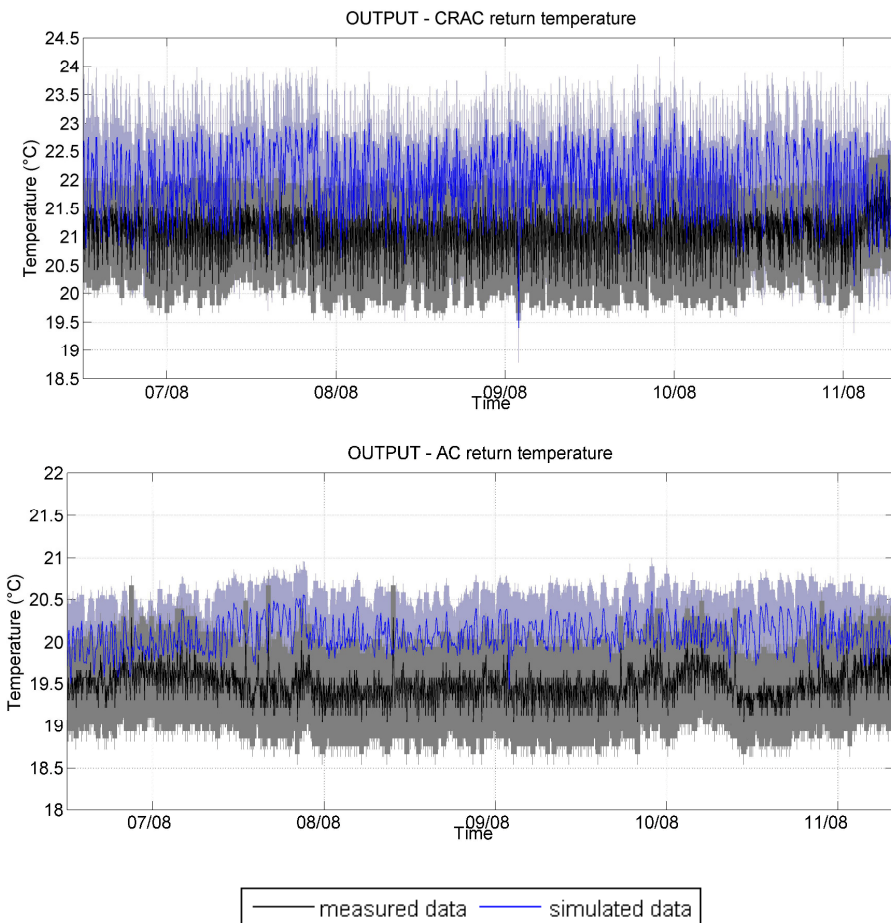


Figure C-7-1 Detailed overview: measured and simulated return air temperature of cooling units (CRAC and AC unit) for the calibration dataset including the uncertainty range of the measurement instrumentation

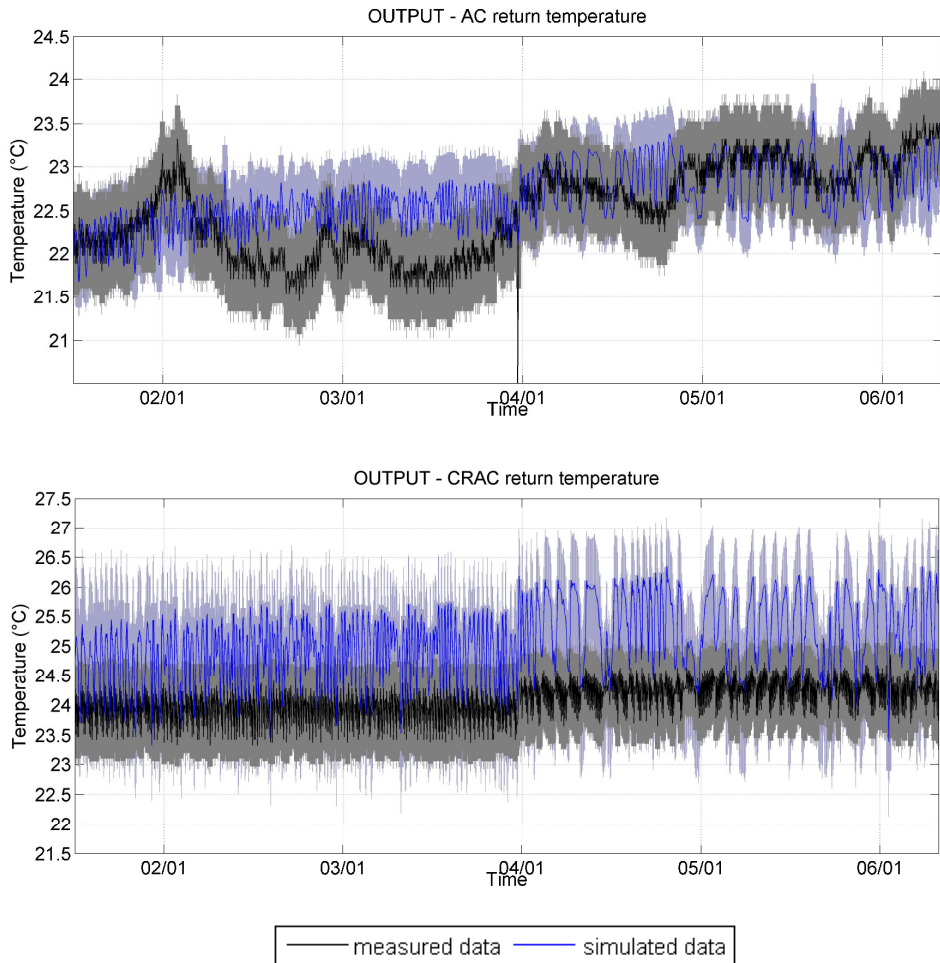


Figure C-2 Detailed overview: comparison of measured and simulated return air temperature of cooling units (CRAC and AC unit) for validation dataset including uncertainty range of the measurement instrumentation

Demonstration of the DC space model

The demonstration of the model is performed for various settings of supply temperature, supply airflow and IT utilization. The results of the computed temperature distribution are shown for 4 high levels of layouts (bottom, mid, top and plenum) and also for 2 sections capturing the CRAC outlet and CRAC inlet including the typical hot aisle and cold arrangement.

Varying temperature setpoints

The influence of the supply air temperature setpoint of the HVAC system is shown in Figure C-3. Three scenarios for low (17°C), medium (21°C) and high (25°C) supply temperature setpoints are

simulated. Workload across IT devices (50%) and HVAC supply airflow (12000kg/h) remain constant. Higher supply temperatures (e.g. 25°C) can create acceptable conditions at the inlet side for most of the servers. There is a minimum difference compared to the scenario with a low supply temperature setpoint (17°C). The analysis of temperatures across the DC space shows that there is significant potential for energy savings by allowing higher setpoint temperatures and provided that there is optimal airflow management (e.g. aisle containments).

Varying airflow setpoints

The influence of the airflow settings in the CRAC unit is shown in Figure C-4. It displays high (12000 kg/h), medium (5500 kg/h) and low (3500 kg/h) ventilation scenarios. Workload across IT devices (50%) and HVAC setpoint temperatures (21°C) remain constant. Visualizing the results, the top layer section in the low ventilation scenario (3500 kg/h) gives a clear indication of the potential risk for hot spots and hence, IT equipment malfunction. On the other hand, the small air conditioning unit (on the left of the picture) is better not used in the high ventilation scenario (12000 kg/h), since its supply and return temperatures are quite similar. Even in this last scenario, it is easy to detect the locations (racks) within the DC space that have greater potential to suffer high temperatures. The potential for hot spots at higher positioned racks is depicted in Figure C-4, which shows a transversal section of the DC.

Influence of workload utilization (%) in the DC

The influence of varying workload levels (%) in the DC can be seen in Figure C-5. It displays high (75%), medium (50%) and low (25%) workload levels scenarios. HVAC setpoint temperature (21°C) and HVAC supply airflow (12000 kg/h) remain constant. These variations in workload, as also shown in Figure C-5, have a significant impact on the temperatures across the DC space and, compared with the previous scenarios, the results indicate that workload has equal influence on the DC space as other control aspects of the HVAC system (i.e. supply air temperature and supply airflow levels). Therefore, the workload level and HVAC settings should to be carefully balanced in order to achieve the optimal performance.

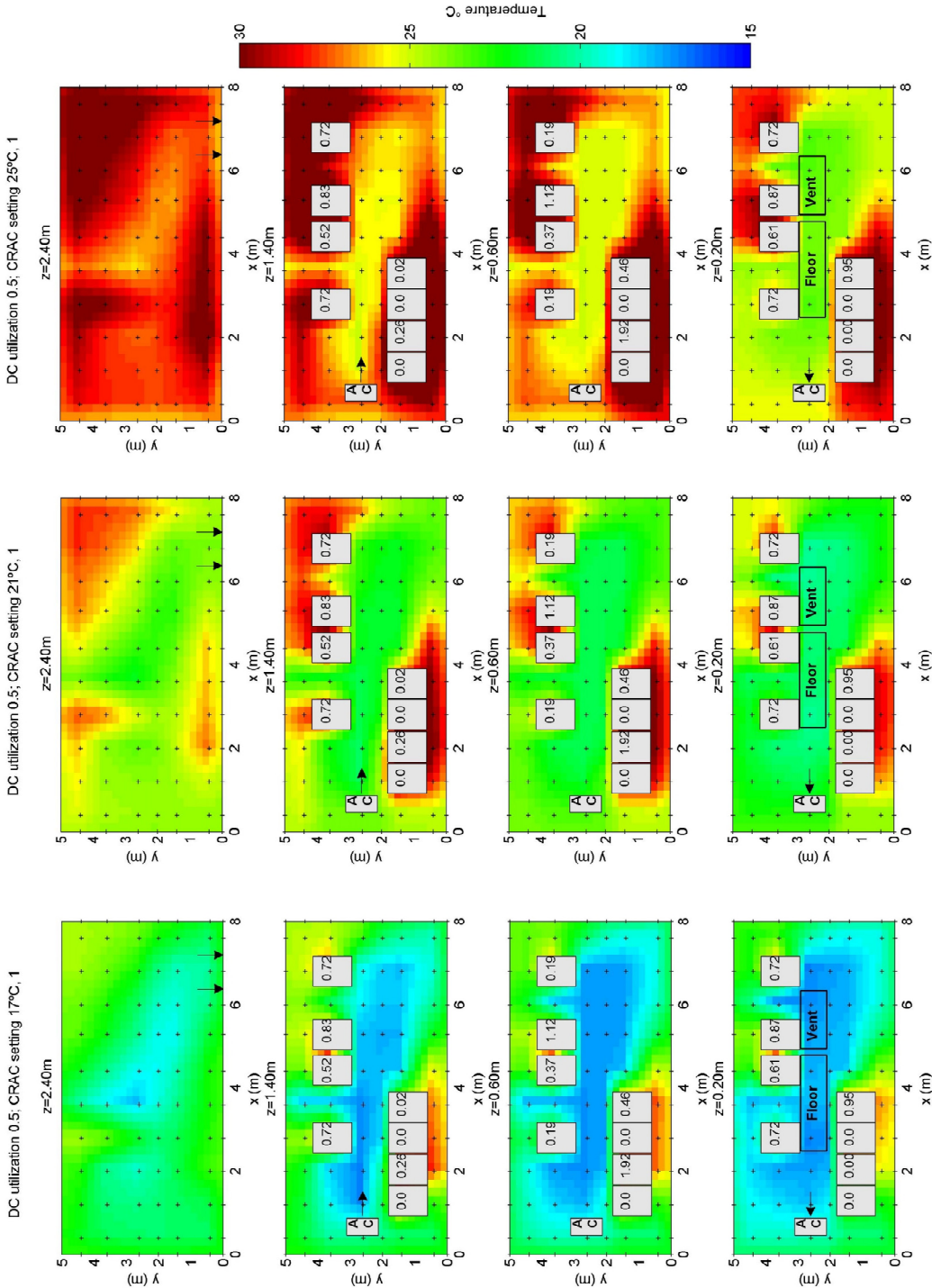


Figure C-3 Demonstration of DC space model: temperature setpoint variant

References

- [1] T. Krüger and T. Kolbe, “Building analysis for urban energy planning using key indicators on virtual 3D city models—the energy atlas of Berlin,” *Int. Arch. Photogramm. Remote Sens. Spat. Inf. Sci.*, vol. 39.(B2), no. September, pp. 145–150, 2012.
- [2] Z. Li, S. J. Quan, and P. P. J. Yang, “Energy performance simulation for planning a low carbon neighborhood urban district: A case study in the city of Macau,” *Habitat Int.*, vol. 53, pp. 206–214, 2016.
- [3] H. Lund and B. V. Mathiesen, “Energy system analysis of 100% renewable energy systems—The case of Denmark in years 2030 and 2050,” *Energy*, vol. 34, no. 5, pp. 524–531, 2009.
- [4] C. J. Hopfe and J. L. M. Hensen, “Uncertainty analysis in building performance simulation for design support,” *Energy Build.*, vol. 43, no. 10, pp. 2798–2805, 2011.
- [5] H. Samuelson, S. Claussnitzer, A. Goyal, Y. Chen, and A. Romo-Castillo, “Parametric energy simulation in early design: High-rise residential buildings in urban contexts,” *Build. Environ.*, vol. 101, pp. 19–31, 2016.
- [6] J. Clarke, *Energy simulation in building design*, 2nd ed. Glasgow: Butterworth Heinemann, 2001.
- [7] R. C. G. M. Loonen, F. Favoino, J. L. M. Hensen, and M. Overend, “Review of current status, requirements and opportunities for building performance simulation of adaptive facades,” *J. J. Build. Perform. Simul.*, vol. 10, no. 2, pp. 1940–1493, 2017.
- [8] P. Hoes, M. Trcka, J. L. M. Hensen, and B. Hoekstra Bonnema, “Investigating the potential of a novel low-energy house concept with hybrid adaptable thermal storage,” *Energy Convers. Manag.*, vol. 52, no. 6, pp. 2442–2447, 2011.
- [9] J. . Clarke, M. Janak, and P. Ruysevelt, “Assessing the overall performance of advanced glazing systems,” *Sol. Energy*, vol. 63, no. 4, pp. 231–241, 1998.

- [10] X. Li and J. Wen, "Review of building energy modeling for control and operation," *Renew. Sustain. Energy Rev.*, vol. 37, pp. 517–537, 2014.
- [11] J. . Clarke *et al.*, "Simulation-assisted control in building energy management systems," *Energy Build.*, vol. 34, no. 9, pp. 933–940, 2002.
- [12] D. E. Claridge, "USING SIMULATION MODELS FOR BUILDING COMMISSIONING."
- [13] C. Lee, "Simulation-based performance assessment of climate adaptive greenhouse shells," Eindhoven University of Technology, 2017.
- [14] Lee. B, "Building Energy Simulation Based Assessment of Industrial Halls for Design Support," Eindhoven University of Technology, 2014.
- [15] A. Shehabi *et al.*, "United States Data Center Energy Usage Report," 2016.
- [16] Emerson, "Understanding the Cost of Data Center Downtime: An Analysis of the Financial Impact on Infrastructure Vulnerability," 2011.
- [17] Consortium Genic, "project GENiC," 2013. [Online]. Available: <http://projectgenic.eu/>.
- [18] European Commission, "European Commission : CORDIS : Projects & Results Service : Globally optimized ENergy efficient data Centres - GENiC." [Online]. Available: http://cordis.europa.eu/project/rcn/110718_en.html. [Accessed: 01-Jul-2017].
- [19] J. A. Sokolowski and C. M. Banks, *MODELING AND SIMULATION FUNDAMENTALS Theoretical Underpinnings and Practical Domains*. John Wiley & Sons, Inc., Hoboken, New Jersey, 2010.
- [20] J. Yogendra and K. Pramod, *Energy Efficient Thermal Management of Data Centres*. London: Springer, 2012.
- [21] E. Masanet and J. Koomey, "How green is the Internet? Summit," 2013. [Online]. Available: <https://www.google.com/events/howgreenistheinternet2013/>.
- [22] D. Paul, "ICT Energy Strategic Research Agenda Executive Summary," 2016.
- [23] International Telecommunication Union, "ICT Facts and Figures 2016," 2016.

- [24] Internet Systems Consortium, “ISC Internet Domain Survey,” 2017. [Online]. Available: <https://www.isc.org/network/survey/>. [Accessed: 01-Jul-2017].
- [25] M. Stansberry, “UPTIME INSTITUTE DATA CENTER INDUSTRY SURVEY 2015 Focus on budgets, planning, metrics, and life safety,” 2015.
- [26] J. Glanz, S. Clara, and C. — Jeff, “Power, Pollution and the Internet,” *The New York Times*, New York, NY, 22-Sep-2012.
- [27] M. Ebbers *et al.*, *Smarter Data Centers Achieving Greater Efficiency*. 2011.
- [28] The Greaves Group, “Virtualization in Education,” *Virtualization View*, no. October, pp. 1–20, 2007.
- [29] L. Strong, B. Taylor, V. Renaud, and I. Seaton, “Top Data Center Trends and Predictions to Watch for in 2016,” *Uptime Technologies*, 2015. [Online]. Available: <http://www.uptime.com/blog/top-data-center-trends-and-predictions-to-watch-for-in-2016/>. [Accessed: 02-Jul-2017].
- [30] P. Mell and T. Grance, “The NIST Definition of Cloud Computing Recommendations of the National Institute of Standards and Technology.”
- [31] X. Sun, N. Ansari, and R. Wang, “Optimizing Resource Utilization of a Data Center,” *IEEE Commun. Surv. Tutorials*, vol. 18, no. 4, pp. 2822–2846, 2016.
- [32] U. Mandal, M. Habib, S. Zhang, B. Mukherjee, and M. Tornatore, “Greening the cloud using renewable-energy-aware service migration,” *IEEE Netw.*, vol. 27, no. 6, pp. 36–43, Nov. 2013.
- [33] K. Ebrahimi, G. F. Jones, and A. S. Fleischer, “A review of data center cooling technology, operating conditions and the corresponding low-grade waste heat recovery opportunities,” *Renew. Sustain. Energy Rev.*, vol. 31, pp. 622–638, Mar. 2014.
- [34] Y. Sverdlik, “How Renewable Energy is Changing the Data Center Market,” 2016. [Online]. Available: <http://www.datacenterknowledge.com/archives/2016/08/11/how-renewable-energy-is-changing-the-data-center-market/>.
- [35] E. SHEME and N. Frashëri, “Implementing Workload Postponing In Cloudsim

- to Maximize Renewable Energy Utilization,” *J. Eng. Res. Appl. www.ijera.com*, vol. 6, no. 83, pp. 2248–962223, 2016.
- [36] R. H. Katz *et al.*, “An information-centric energy infrastructure: The Berkeley view,” *Sustain. Comput. Informatics Syst.*, vol. 1, no. 1, pp. 7–22, 2011.
- [37] Q. Tang, S. K. S. Gupta, and G. Varsamopoulos, “Thermal-aware task scheduling for data centers through minimizing heat recirculation,” *Proc. - IEEE Int. Conf. Clust. Comput. ICC3*, pp. 129–138, 2007.
- [38] Z. Liu *et al.*, “Renewable and Cooling Aware Workload Management for Sustainable Data Centers *,” in *SIGMETRICS’ 12*, 2012.
- [39] T. K. Nielsen and D. Bouley, “How Data Center Infrastructure Management Software Improves Planning and Cuts Operational Costs Revision 3,” 2012.
- [40] ASHRAE TC 9.9, *Design Considerations for Datacom Equipment Centers*. American Society of Heating, Refrigerating, and Air-Conditioning Engineers, 2009.
- [41] Uptime Institute, “Data Center Site Infrastructure Tier Standard: Topology,” 2009.
- [42] NiPS Laboratory, “NiPS Summer School 2016; ICT - Energy: Energy consumption in future ICT devices,” 2016. [Online]. Available: <http://www.nipslab.org/summerschool2016>. [Accessed: 02-Jul-2017].
- [43] L. A. Barroso and U. Hölzle, *The Datacenter as a Computer: An Introduction to the Design of Warehouse-Scale Machines*, vol. 4, no. 1. 2009.
- [44] Consumer Electronics Association, “CEA-310-E design requirements for Cabinets, Panels, Racks and Subracks,” 2005.
- [45] Facebook, “Open Compute Project,” 2011. [Online]. Available: <http://opencompute.org/>. [Accessed: 02-Jul-2017].
- [46] G. Fagas, G. Luca, P. Douglas, and B. Gabriel Abadal, *ICT - Energy - Concepts Towards Zero - Power Information and Communication Technology*, First. InTech, 2014.
- [47] The American Society of Heating Refrigerating and Air-Conditioning Engineers (ASHRAE), *Thermal Guidelines for Data Processing Environments*, 3rd ed. Atlanta: W. Stephen Comstock, 2012.

- [48] B. V. Renaud and M. Mescall, "Uptime Institute Annual Report : Data Center Density," 2012.
- [49] S. Zimmermann, I. Meijer, M. K. Tiwari, S. Paredes, B. Michel, and D. Poulidakos, "Aquasar: A hot water cooled data center with direct energy reuse," *Energy*, vol. 43, no. 1, pp. 237–245, Jul. 2012.
- [50] T. Brunschwiler, B. Smith, E. Ruetsche, and B. Michel, "Toward zero-emission data centers through direct reuse of thermal energy," *IBM J. Res. Dev.*, vol. 53, no. 3, p. 11:1-11:13, May 2009.
- [51] M. Stansberry, "UPTIME INSTITUTE DATA CENTER INDUSTRY SURVEY 2014," 2014. [Online]. Available: <https://journal.uptimeinstitute.com/2014-data-center-industry-survey/>. [Accessed: 02-Jul-2017].
- [52] J. Rambo and Y. Joshi, "Modeling of data center airflow and heat transfer: State of the art and future trends," *Distrib. Parallel Databases*, vol. 21, no. 2–3, pp. 193–225, 2007.
- [53] V. K. Arghode and Y. Joshi, *Air Flow Management in Raised Floor Data Centers*. Springer , 2016.
- [54] H. Zhang, S. Shao, H. Xu, H. Zou, and C. Tian, "Free cooling of data centers: A review," *Renew. Sustain. Energy Rev.*, vol. 35, pp. 171–182, Jul. 2014.
- [55] B. A. Weerts, D. Gallaher, R. Weaver, and O. VanGeet P. E., "Green Data Center Cooling: Achieving 90% Reduction: Airside Economization and Unique Indirect Evaporative Cooling," in *2012 IEEE Green Technologies Conference*, 2012, pp. 1–6.
- [56] H. Jim *et al.*, *Data centres : an introduction to concepts and design*. Norwitch: CIBSE, 2012.
- [57] D. Loucks *et al.*, "POWER EQUIPMENT AND DATA CENTER DESIGN," 2012.
- [58] Google, "Achieving Our 100% Renewable Energy Purchasing Goal and Going Beyond," 2016.

- [59] Consortium Genic, “Deliverable 1.2 Requirements & Draft Architecture,” 2014.
- [60] Consortium Genic, “Deliverable 1.4 Refined Genic Architecture,” 2015.
- [61] PikeResearch, “Green Data Centers,” 2012.
- [62] Pivotal, “RabbitMQ - Messaging that just works,” 2017. [Online]. Available: <https://www.rabbitmq.com/>. [Accessed: 02-Jul-2017].
- [63] The American Society of Heating Refrigerating and Air-Conditioning Engineers (ASHRAE), “BACnet,” 2017. [Online]. Available: <http://www.bacnet.org/>. [Accessed: 02-Jul-2017].
- [64] S. Wang, Z. Ma, and M. Ashrae, “Supervisory and Optimal Control of Building HVAC Systems: A Review,” *HVAC&R Res. JANUARY*, vol. 14, no. 1, 2008.
- [65] D. Grimes *et al.*, “Robust Server Consolidation: Coping with Peak Demand Underestimation,” in *2016 IEEE 24th International Symposium on Modeling, Analysis and Simulation of Computer and Telecommunication Systems (MASCOTS)*, 2016, pp. 271–276.
- [66] C. E. Bash, C. D. Patel, and R. K. Sharma, “Dynamic thermal management of air cooled data centers,” *Therm. Thermomechanical Phenom. Electron. Syst. 2006. ITHERM’06. Tenth Intersoc. Conf.*, pp. 445--452, 2006.
- [67] A. Banerjee, T. Mukherjee, G. Varsamopoulos, and S. K. S. Gupta, “Integrating cooling awareness with thermal aware workload placement for HPC data centers,” *Sustain. Comput. Informatics Syst.*, vol. 1, no. 2, pp. 134–150, 2011.
- [68] J. Wan, X. Gui, R. Zhang, and L. Fu, “Joint Cooling and Server Control in Data Centers: A Cross-Layer Framework for Holistic Energy Minimization,” *IEEE Syst. J.*, pp. 1–12, 2017.
- [69] F. Kong and X. Liu, “A Survey on Green-Energy-Aware Power Management for Datacenters,” *ACM Comput. Surv. Artic.*, vol. 47, no. 30, 2014.
- [70] T. I. Salsbury and S. Ashish, “Control System Commissioning for Enhanced Building Operations,” *Proc. 3rd Int. Conf. Enhanc. Build. Oper. Oct. 13-15*, vol. 1,

no. 414, pp. 1–9, 2003.

- [71] T. U. Darmstadt, “Forschungsprojekt ETA-Fabrik – ETA-Fabrik – Technische Universität Darmstadt,” 2017. [Online]. Available: <http://www.eta-fabrik.tu-darmstadt.de/eta/index.de.jsp>. [Accessed: 02-Jul-2017].
- [72] D. Müller and J. Fütterer, “The E.ON ERC Main Building – a Demonstration Bench for Control Research.”
- [73] D. Cook, “Evolution of Programming Languages and Why a Language is Not Enough to Solve Our Problems,” 1999. [Online]. Available: <http://lsc.fie.umich.mx/~juan/Materias/FIE/Lenguajes/Slides/Papers/Evolution.html>. [Accessed: 03-Jul-2017].
- [74] R. E. Shannon, “INTRODUCTION TO THE ART AND SCIENCE OF SIMULATION.”
- [75] D. K. Pace, “Ideas About Simulation Conceptual Model Development,” *JOHNS HOPKINS APL Tech. Dig.*, vol. 21, no. 3, 2000.
- [76] S. Robinson, “Conceptual modelling for simulation Part I: definition and requirements,” *J. Oper. Res. Soc.*, vol. 59, no. 3, pp. 278–290, Mar. 2008.
- [77] J. L. M. Hensen and R. Lamberts, *Building performance simulation for design and operation*, Abingdon. Spon Press, 2011.
- [78] B. P. Zeigler, H. Praehofer, and T. G. Kim, *Theory of modeling and simulation : integrating discrete event and continuous complex dynamic systems*. Academic Press, 2000.
- [79] J. Banks and R. Gibson, “Don’t Simulate When... 10 Rules for Determining when Simulation Is Not Appropriate-While simulation tools are appropriate for solving many types of problems, in some situations there are quicker,” *IIE Solut.*, vol. 29, no. 9, pp. 30–33, 1997.
- [80] J. Banks and L. Chwif, “Warnings about simulation,” *J. Simul.*, vol. 524, pp. 279–291, 2011.
- [81] S. W. Ham, M. H. Kim, B. N. Choi, and J. W. Jeong, “Simplified server model

- to simulate data center cooling energy consumption,” *Energy Build.*, vol. 86, pp. 328–339, Jan. 2015.
- [82] A. Lie Foucquier, S. Robert, F. Dé, R. Suard, L. Sté Phan, and A. Jay, “State of the art in building modelling and energy performances prediction: A review,” *Renew. Sustain. Energy Rev.*, vol. 23, pp. 272–288, 2013.
- [83] P. Zelenský, J. L. M. Hensen, J. Bynum, V. Zavřel, and M. Barták, “AIR-FLOW MODELLING IN DESIGN AND OPERATION OF DATA CENTERS,” in *IBPSA-CZ 2014*, 2014.
- [84] T. J. Breen, E. J. Walsh, J. Punch, A. J. Shah, and C. E. Bash, “From chip to cooling tower data center modeling: Part I Influence of server inlet temperature and temperature rise across cabinet,” in *Thermal and Thermomechanical Phenomena in Electronic Systems (ITherm), 2010 12th IEEE Intersociety Conference on*, 2010, pp. 1–10.
- [85] E. J. Walsh, T. J. Breen, J. Punch, A. J. Shah, and C. E. Bash, “From chip to cooling tower data center modeling: Part II Influence of chip temperature control philosophy,” in *Thermal and Thermomechanical Phenomena in Electronic Systems (ITherm), 2010 12th IEEE Intersociety Conference on*, 2010, pp. 1–7.
- [86] S. Pelley, D. Meisner, T. F. Wenisch, and J. W. VanGilder, “Understanding and Abstracting Total Data Center Power,” *WEED Work. Energy Effic. Des.*, 2009.
- [87] the National Renewable Energy Laboratory (NREL), “EnergyPlus version 8.3.” 2015.
- [88] RenewIT consortium, “Green Data Centre Library - Renewit,” 2016. [Online]. Available: <http://www.renewit-project.eu/green-data-centre-library/>. [Accessed: 03-Jul-2017].
- [89] L. Phan and C.-X. Lin, “A multi-zone building energy simulation of a data center model with hot and cold aisles,” *Energy Build.*, vol. 77, pp. 364–376, 2014.
- [90] A. Leva, D. Mastrandrea, M. Bonvini, and A. V. Papadopoulos, “Object-Oriented Modelling and Simulation of Air Flow in Data Centres Based on a

Quasi-3D Approach for Energy Optimisation,” in *7th International Conference on Utility and Cloud Computing*, 2014.

- [91] J. Salom, E. Oró, and A. G. S. A. de Besòs, “Dynamic Modelling of Data Centre Whitespaces, Validation with Collected Measurements,” in *Building Simulation 2015, 14th International Conference of the International Building Performance Simulation Association*, 2015.
- [92] E. Oró, V. Depoorter, A. Garcia, and J. Salom, “Energy efficiency and renewable energy integration in data centres. Strategies and modelling review,” *Renew. Sustain. Energy Rev.*, vol. 42, pp. 429–445, 2015.
- [93] Thermal Energy System Specialists, “TRNSYS : Transient System Simulation Tool.” 2012.
- [94] M. S. Owen and H. E. Kennedy, *2009 ASHRAE handbook: fundamentals*. American Society of Heating, Refrigeration, and Air-Conditioning Engineers, 2009.
- [95] N. Rasmussen, “Guidelines for Specification of Data Center Power Density,” 2005.
- [96] ASHRAE TC 9.9, *Data Center Design and Operation - ASHRAE Datacom Series*, 2nd ed. American Society of Heating, Refrigerating and Air-Conditioning Engineers, 2010.
- [97] H. B. Thomas, “ASCE Standard 7-10 Dead and Live Loads,” American Society of Civil Engineers, Reston, VA, Apr. 2011.
- [98] D. Moss and J. H. Bean, “Energy Impact of Increased Server Inlet Temperature,” 2011.
- [99] L. T. Peiró and F. Ardente, “Environmental Footprint and Material Efficiency Support for product policy, analysis of material efficiency requirements of enterprise servers,” 2015.
- [100] E. Rotem, “Temperature measurement in the Intel ® Core TM Duo Processor.”
- [101] J. Niemann, K. Brown, and V. Avelar, “Impact of Hot and Cold Aisle

- Containment on Data Center Temperature and Efficiency,” *APC White Pap.*, vol. 135 Revisi, 2011.
- [102] B. Muralidharan, S. Shrivastava, M. Ibrahim, S. Alkharabsheh, and B. Sammakia, “Impact of Cold Aisle Containment on Thermal Performance of Data Center,” in *ASME 2013 International Electronic Packaging Technical Conference and Exhibition, Volume 2: Thermal Management; Data Centers and Energy Efficient Electronic Systems*, 2013, p. 5.
- [103] M. Tatchell-Evans, N. Kapur, J. Summers, H. Thompson, and D. Oldham, “An experimental and theoretical investigation of the extent of bypass air within data centres employing aisle containment, and its impact on power consumption,” *Appl. Energy*, vol. 186, pp. 457–469, 2017.
- [104] M. M. Toulouse, G. Doljac, V. P. Carey, and C. Bash, “Exploration of a Potential-Flow-Based Compact Model of Air-Flow Transport in Data Centers,” no. 43864. pp. 41–50, 2009.
- [105] J. VanGilder, “Real-Time data center cooling analysis,” *bin Film Thermoelectr. Today Tomorrow*, vol. 14, pp. 14–19, 2011.
- [106] M. Salim and R. Tozer, “Data Center Air Management Metrics-Practical Approach,” in *Thermal and Thermomechanical Phenomena in Electronic Systems (ITherm) 12th IEEE Intersociety Conference*, 2010, pp. 1–8.
- [107] V. Zavr̆el, J. I. Torrens, J. D. Bynum, and J. L. M. Hensen, “Model Development for Simulation Based Global Optimisation of Energy Efficient Data Centres,” in *Building Simulation 2015, 14th International Conference of the International Building Performance Simulation Association*, 2015, p. 8.
- [108] J. W. Axley, “Surface-drag flow relations for zonal modeling,” *Build. Environ.*, vol. 36, no. 7, pp. 843–850, Aug. 2001.
- [109] E. Wurtz, J.-M. Nataf, and F. Winkelmann, “Two- and three natural and mixed convection simulation using modular zonal models in buildings,” *Heat Mass Transfer*, vol. 42, no. 923–940, p. 18, 1999.
- [110] the National Institute of Standards and Technology (NIST), “CONTAM version 3.2.0.2.” 2015.

- [111] S. D. Conte and de C. Boor, *Elementary Numerical Analysis*. New York NY, 1972.
- [112] G. N. Walton, “Airflow network models for element based building airflow modeling,” *ASHRAE Trans.*, vol. 95, no. 2, pp. 611–620, 1989.
- [113] G. N. Walton and W. S. Dols, “CONTAM user guide and program documentation,” 2005.
- [114] S. McAllister, V. P. Carey, A. Shah, C. Bash, and C. Patel, “Strategies for effective use of exergy-based modeling of data center thermal management systems,” *Microelectronics J.*, vol. 39, no. 7, pp. 1023–1029, 2008.
- [115] B. Delcroix, M. Kummert, A. Daoud, and M. D. E. Hiller, “Conduction transfer functions in TRNSYS multizone building model: current implementation, limitations and possible improvements,” *Proc. SimBuild 2012 5th Conf. IBPSA-USA*, pp. 219–226, 2012.
- [116] J. E. Seem, “Modeling of heat transfer in buildings,” University of Wisconsin Madison, 1987.
- [117] the Solar Energy Laboratory, “Trnsys 17 - Volume 4 Mathematical Reference,” Wisconsin-Madison, 2012.
- [118] the Solar Energy Laboratory, “TESSLibs 17 Component Libraries for the TRNSYS Simulation Environment Vol. 1-13,” Wisconsin-Madison, 2012.
- [119] J. E. Braun, “Methodologies for the Design and Control of Chilled Water Systems,” UNIVERSITY OF WISCONSIN - MADISON, 1988.
- [120] F. P. Incropera, D. P. DeWitt, T. L. Bergman, and A. S. Lavine, *Fundamentals of Heat and Mass Transfer*, 6th ed. John Wiley & Sons, 2007.
- [121] J. Salom, “RenewIT.” [Online]. Available: <http://www.renewit-project.eu/>.
- [122] M. Ton and B. Fortenbury, “High Performance Buildings: Data Centers Server Power Supplies Legal Notice,” 2005.
- [123] G. M. Masters, *Renewable and efficient electric power systems*. Wiley - IEEE Press, 2013.
- [124] O. Tremblay and L.-A. Dessaint, “Experimental Validation of a Battery

Dynamic Model for EV Applications Experimental Validation of a Battery Dynamic Model for EV Applications,” *World Electr. Veh. J. V*, vol. 3, no. October, pp. 289–298, 2009.

- [125] MediaWiki, “MediaWiki,” 2015. [Online]. Available: <https://www.mediawiki.org/wiki/MediaWiki>.
- [126] SEMO, “SEMO,” 2015. [Online]. Available: <http://www.sem-o.com/>.
- [127] International Energy Agency, “IEA Statistics.” [Online]. Available: <http://www.iea.org/statistics/>.
- [128] EIRGRID, “EIRGRID GROUP: System Information,” 2015. [Online]. Available: <http://www.eirgridgroup.com/how-the-grid-works/system-information/>. [Accessed: 03-Jul-2017].
- [129] W. Marion and U. Ken, *User’s Manual for TMY2s*. 1995.
- [130] The MathWorks, “MATLAB 2014b.” Natick, 2014.
- [131] EDPAC, “Close Control Modular Range - Engineering Data Manual,” 1992.
- [132] the Mitsubishi Electric, “Product Information PSA-RP125GA,” 2007.
- [133] Consortium Genic, “Deliverable D5.2 Energy Use Cases, Measurement, Methodology & Energy Baseline for the Demonstration Sites,” 2014.
- [134] SOCOMEC, “DIRIS A20 Multifunction meters - PMD,” 2016.
- [135] APC by Schneider Electric, “Rack Power Distribution,” 2012.
- [136] AMETHERM, “Thermistors datasheet PANE 103395-410,” 2008.
- [137] MEMSIC, “TELOSBMOTE PLATFORM datasheet,” 2015.
- [138] ELEKTRONIK E+E, “HVAC Miniature Air Flow Transmitter datasheet,” 2015.
- [139] D. Coakley, P. Raftery, and M. Keane, “A review of methods to match building energy simulation models to measured data,” *Renew. Sustain. Energy Rev.*, vol. 37, pp. 123–141, 2014.
- [140] R. Sharma, C. Bash, and C. Patel, “Dimensionless Parameters for Evaluation of Thermal Design and Performance of Large-scale Data Centers,” *8th*

AIAA/ASME Jt. Thermophys. Heat Transf. Conf., pp. 1–11, 2002.

- [141] B. Fakhim, M. Behnia, S. W. Armfield, and N. Srinarayana, “Cooling solutions in an operational data centre: A case study,” *Appl. Therm. Eng.*, vol. 31, no. 14–15, pp. 2279–2291, 2011.
- [142] S. Cao, A. Hasan, and K. Sirén, “On-site energy matching indices for buildings with energy conversion, storage and hybrid grid connections,” *Energy Build.*, vol. 64, pp. 423–438, Sep. 2013.
- [143] Consortium Genic, “Deliverable 5.5 Verification and validation of GENiC platform,” 2016.
- [144] R. and A.-C. E. American Society of Heating and American National Standards Institute., *ASHRAE guideline 14-2002: measurement of energy and demand savings*. Atlanta: American Society of Heating, Refrigerating and Air-Conditioning Engineers, 2002.
- [145] Efficiency Valuation Organization (EVO), “International Performance Measurement and Verification Protocol Concepts and Options for Determining Energy and Water Savings,” 2012.
- [146] T. Galdiz *et al.*, “The GENiC architecture for integrated data centre energy management,” pp. 7–10, 2015.
- [147] J. O. Iglesias, L. Murphy, M. De Cauwer, D. Mehta, and B. O’Sullivan, “A Methodology for Online Consolidation of Tasks through More Accurate Resource Estimations,” in *2014 IEEE/ACM 7th International Conference on Utility and Cloud Computing*, 2014, pp. 89–98.
- [148] C. (Microsoft) Belady, A. (AMD) Rawson, J. (Dell) Pfleuger, and T. (Spraycool) Cader, “Green Grid Data Center Power Efficiency Metrics : Pue and Dcie Editors :,” *Green Grid*, pp. 1–9, 2008.
- [149] I. Stanford and W. Herbert, *HVAC water chillers and cooling towers: fundamentals, application, and operation*. CRC Press, 2011.
- [150] F. (Fred) Porges and J. Porges, *Handbook of heating, ventilating, and air conditioning*. Butterworths, 1982.

- [151] A. T. Almeida and A. H. Rosenfeld, *Demand-Side Management and Electricity End-Use Efficiency*. Springer Netherlands, 1988.
- [152] D. Bouley, “Understanding PUE Measurement and analysis tools and processes Best practices for improving PUE.” 2009.
- [153] Consortium Genic, “Deliverable 6.3 Energy optimization and control strategies demonstration results,” 2016.
- [154] R. Dones, T. Heck, and S. Hirschberg, “GREENHOUSE GAS EMISSIONS FROM ENERGY SYSTEMS: COMPARISON AND OVERVIEW.”
- [155] Consortium Genic, “Deliverable 4.5 Fault detection and system-level diagnostics decision support services,” 2016.
- [156] V. Dvorak, V. Zavrel, J. I. Torrens, and J. L. M. Hensen, “Simulation-based design of waste heat utilization system for a data center in campus: Reducing university carbon footprint,” Eindhoven University of Technology, 2017.
- [157] A. P. Hernandez, V. Zavrel, J. I. Torrens, and J. L. M. Hensen, “Powering Data Centers with Renewable Energy: Simulation-based design of system for a case study in the university campus,” Eindhoven University of Technology, 2017.
- [158] A. P. Rachman, V. Zavrel, J. I. Torrens, and J. Hensen, “Simulation-Based Assessment of Humidity Treatment in Data Center Cooling System with Air-Side Economizer,” Eindhoven, 2017.

Source of cover image: Timofeev Vladimir, Shutterstock accessed January 2018

Curriculum vitae

Vojtěch Zavřel was born in Prague, Czech Republic, on the 9 of September 1988. He pursued his Master of Science degree at Czech Technical University, Faculty of Mechanical Engineering, Dept. of Environmental Engineering. During this study he developed an interest in building energy systems and their numerical modelling. In 2013, he finished his final master project about thermal modelling of failure of a data center's cooling plant. The thesis was awarded 1st prize of the "Zvoníčková foundation" in the thematic group the Environmental Engineering

In the end of the year 2013, he started a PhD project about building energy modelling to support the testing and commissioning of novel data center operational strategies, supervised by professor Jan L.M. Hensen. The PhD project was part of a multi-disciplinary research embedded in the framework of the Genic project funded by European Union.

.

List of publications

Chapter, Scientific peer reviewed

2017 Pesch, D., Rea, S., Torrens Galdiz, J.I., Zavrel, V., Hensen, J.L.M., Grimes, D., O'Sullivan, B., Scherer, T., Birke, R., Chen, L., Engbersen, T., Lopez, L., Pages, E., Mehta, D., Townley, J. & Tsachouridis, V. (2017). ICT - Energy Concepts for Energy Efficiency and Sustainability. Globally optimised energy-efficient data centres (pp. 187-213). s.l.: Intech open access publisher.

Conference contribution, Scientific peer reviewed

2017 Zavrel, V., Torrens Galdiz, J.I. & Hensen, J.L.M. (2017) Implementation and Demonstration of a Building Simulation Based Testbed for Assessment of Data Centre Multi-domain Control Strategies. Building Simulation 2015 : 15th international conference of IBPSA, December 7-9, 2016, San Francisco, USA IBPSA (submission accepted).

2016 Torrens, J.I., Mehta, D., Zavrel, V., Grimes, D., Scherer, Th., Birke, R., Chen, L., Rea, S., Lopez, L., Pages, E. & Pesch, D. (2016). Integrated energy efficient data centre management for green cloud computing. Integrated Energy Efficient Data Centre Management for Green Cloud Computing (pp. 375-386).

Zavrel, V., Torrens, J.Ignacio & Hensen, J.L.M. (2016). Simulation-based assessment of thermal aware computation of a bespoke data centre. In P.K. Heiselberg (Ed.), CLIMA 2016 : Proceedings of the 12th REHVA World Congress Aalborg: Aalborg University, Department of Civil Engineering.

2015 Pesch, D., McGibney, A., Sobonski, P., Rea, S., Scherer, Th., Chen, L., Engbersen, T., Mehta, D., O'Sullivan, B., Pages, E., Townley, J., Kasinathan, Dh., Torrens, J.I., Zavrel, V. & Hensen, J.L.M. (2015). The GENiC architecture for integrated data centre energy management. Proceedings 2015 IEEE/ACM 8th International Conference on Utility and Cloud Computing (UCC 2015), 7-10 December 2015, Limassol, Cyprus (pp. 540-546). Piscataway: Institute of Electrical and Electronics Engineers Inc..

Van Schie, F.T., Zavrel, V., Torrens Galdiz, J.I., Hundertmark, T.F.W. & Hensen, J.L.M. (2015). Optimizing the total energy consumption and CO₂ emissions by distributing computational workload among worldwide dispersed data centers. Building Simulation 2015 : 14th international conference of IBPSA, December 7-9, 2015, Hyderabad, India (pp. 1118-1125). IBPSA.

Zavrel, V., Torrens Galdiz, J.I., Bynum, J.D. & Hensen, J.L.M. (2015). Model development for simulation based global optimization of energy efficient data centres. Building Simulation 2015 : 14th international conference of IBPSA, December 7-9, 2015, Hyderabad, India (pp. 1079-1086). IBPSA. In Scopus

2014 Zavrel, V., Bartak, M. & Hensen, J.L.M. (2014). Simulation of a data center cooling system in an emergency situation. Proceedings of the 8th IBPSA-CZ conference Simulace Budov a Techniky Prostředí, 6-7 November 2014, Prague, Czech Republic (pp. 57-64). Prague: Česká technika - nakladatelství ČVUT.

Zelensky, P., Hensen, J.L.M., Bynum, J.D., Zavrel, V. & Bartak, M. (2014). Air-flow modeling in design and operation of data centers. Proceedings of the 8th IBPSA-CZ conference Simulace Budov a

Techniky Prostředí, 6-7 November 2014, Prague, Czech Republic (pp. 71-75). Česká technika - nakladatelství ČVUT.

Professional

2017 van de Voort, Tom, Hensen, J.L.M., Torrens Galdiz, J.I. & Zavrel, V. (2017). Analysis of performance metrics for data center efficiency : should the Power Utilization Effectiveness PUE still be used as the main indicator? (Part 2). REHVA Journal, 2017(2), 37-43.

van de Voort, T., Zavrel, V., Torrens Galdiz, J.I. & Hensen, J.L.M. (2017). Analysis of performance metrics for data center efficiency : should the Power Utilization Effectiveness PUE still be used as the main indicator? (Part 1). REHVA Journal, February, 5-11.

2015 Zavrel, V., Bartak, M. & Hensen, J.L.M. (2015). Simulace chladicího systémy datacentra v havarijním stavu. Vytápění, větrání, instalace ; VVI, 2015(4), 160-164.

Bouwstenen is een publikatiereeks van de Faculteit Bouwkunde, Technische Universiteit Eindhoven. Zij presenteert resultaten van onderzoek en andere activiteiten op het vakgebied der Bouwkunde, uitgevoerd in het kader van deze Faculteit.

Bouwstenen zijn telefonisch te bestellen op nummer
040 - 2472383

Kernredactie
MTOZ

Reeds verschenen in de serie

Bouwstenen

nr 1

Elan: A Computer Model for Building Energy Design: Theory and Validation

Martin H. de Wit

H.H. Driessen

R.M.M. van der Velden

nr 2

Kwaliteit, Keuzevrijheid en Kosten: Evaluatie van Experiment Klarendal, Arnhem

J. Smeets

C. le Nobel

M. Broos

J. Frenken

A. v.d. Sanden

nr 3

Crooswijk: Van 'Bijzonder' naar 'Gewoon'

Vincent Smit

Kees Noort

nr 4

Staal in de Woningbouw

Edwin J.F. Delsing

nr 5

Mathematical Theory of Stressed Skin Action in Profiled Sheeting with Various Edge Conditions

Andre W.A.M.J. van den Bogaard

nr 6

Hoe Berekenbaar en Betrouwbaar is de Coëfficiënt k in x -ksigma en x -ks?

K.B. Lub

A.J. Bosch

nr 7

Het Typologisch Gereedschap: Een Verkennende Studie Omtrent Typologie en Omtrent de Aanpak van Typologisch Onderzoek

J.H. Luiten

nr 8

Informatievoorziening en Beheerprocessen

A. Nauta

Jos Smeets (red.)

Helga Fassbinder (projectleider)

Adrie Proveniers

J. v.d. Moosdijk

nr 9

Strukturering en Verwerking van Tijdgegevens voor de Uitvoering van Bouwwerken

ir. W.F. Schaefer

P.A. Erkelens

nr 10

Stedebouw en de Vorming van een Speciale Wetenschap

K. Doevendans

nr 11

Informatica en Ondersteuning van Ruimtelijke Besluitvorming

G.G. van der Meulen

nr 12

Staal in de Woningbouw, Korrosie-Bescherming van de Begane Grondvloer

Edwin J.F. Delsing

nr 13

Een Thermisch Model voor de Berekening van Staalplaatbetonvloeren onder Brandomstandigheden

A.F. Hamerlinck

nr 14

De Wijkgedachte in Nederland: Gemeenschapsstreven in een Stedebouwkundige Context

K. Doevendans

R. Stolzenburg

nr 15

Diaphragm Effect of Trapezoidally Profiled Steel Sheets:

Experimental Research into the Influence of Force Application

Andre W.A.M.J. van den Bogaard

nr 16

Versterken met Spuit-Ferrocement: Het Mechanische Gedrag van met Spuit-Ferrocement Versterkte Gewapend Betonbalken

K.B. Lubir

M.C.G. van Wanroy

nr 17

**De Tractaten van
Jean Nicolas Louis Durand**
G. van Zeyl

nr 18

**Wonen onder een Plat Dak:
Drie Opstellen over Enkele
Vooronderstellingen van de
Stedebouw**
K. Doevendans

nr 19

**Supporting Decision Making Processes:
A Graphical and Interactive Analysis of
Multivariate Data**
W. Adams

nr 20

**Self-Help Building Productivity:
A Method for Improving House Building
by Low-Income Groups Applied to Kenya
1990-2000**
P. A. Erkelens

nr 21

**De Verdeling van Woningen:
Een Kwestie van Onderhandelen**
Vincent Smit

nr 22

**Flexibiliteit en Kosten in het Ontwerpproces:
Een Besluitvormingondersteunend Model**
M. Prins

nr 23

**Spontane Nederzettingen Begeleid:
Voorwaarden en Criteria in Sri Lanka**
Po Hin Thung

nr 24

**Fundamentals of the Design of
Bamboo Structures**
Oscar Arce-Villalobos

nr 25

Concepten van de Bouwkunde
M.F.Th. Bax (red.)
H.M.G.J. Trum (red.)

nr 26

Meaning of the Site
Xiaodong Li

nr 27

**Het Woonmilieu op Begrip Gebracht:
Een Speurtocht naar de Betekenis van het
Begrip 'Woonmilieu'**
Jaap Ketelaar

nr 28

Urban Environment in Developing Countries
editors: Peter A. Erkelens
George G. van der Meulen (red.)

nr 29

**Stategische Plannen voor de Stad:
Onderzoek en Planning in Drie Steden**
prof.dr. H. Fassbinder (red.)
H. Rikhof (red.)

nr 30

Stedebouwkunde en Stadsbestuur
Piet Beekman

nr 31

**De Architectuur van Djenné:
Een Onderzoek naar de Historische Stad**
P.C.M. Maas

nr 32

Conjoint Experiments and Retail Planning
Harmen Oppewal

nr 33

**Strukturformen Indonesischer Bautechnik:
Entwicklung Methodischer Grundlagen
für eine 'Konstruktive Pattern Language'
in Indonesien**

Heinz Frick arch. SIA

nr 34

**Styles of Architectural Designing:
Empirical Research on Working Styles
and Personality Dispositions**
Anton P.M. van Bakel

nr 35

**Conjoint Choice Models for Urban
Tourism Planning and Marketing**
Benedict Dellaert

nr 36

Stedelijke Planvorming als Co-Productie
Helga Fassbinder (red.)

nr 37

Design Research in the Netherlands

editors: R.M. Oxman
M.F.Th. Bax
H.H. Achten

nr 38

Communication in the Building Industry

Bauke de Vries

nr 39

**Optimaal Dimensioneren van
Gelaste Plaatliggers**

J.B.W. Stark
F. van Pelt
L.F.M. van Gorp
B.W.E.M. van Hove

nr 40

Huisvesting en Overwinning van Armoede

P.H. Thung
P. Beekman (red.)

nr 41

**Urban Habitat:
The Environment of Tomorrow**

George G. van der Meulen
Peter A. Erkelens

nr 42

A Typology of Joints

John C.M. Olie

nr 43

**Modeling Constraints-Based Choices
for Leisure Mobility Planning**

Marcus P. Stemerding

nr 44

Activity-Based Travel Demand Modeling

Dick Ettema

nr 45

**Wind-Induced Pressure Fluctuations
on Building Facades**

Chris Geurts

nr 46

Generic Representations

Henri Achten

nr 47

**Johann Santini Aichel:
Architectuur en Ambiguiteit**

Dirk De Meyer

nr 48

**Concrete Behaviour in Multiaxial
Compression**

Erik van Geel

nr 49

Modelling Site Selection

Frank Witlox

nr 50

Ecolemma Model

Ferdinand Beetstra

nr 51

**Conjoint Approaches to Developing
Activity-Based Models**

Donggen Wang

nr 52

On the Effectiveness of Ventilation

Ad Roos

nr 53

**Conjoint Modeling Approaches for
Residential Group preferences**

Eric Molin

nr 54

**Modelling Architectural Design
Information by Features**

Jos van Leeuwen

nr 55

**A Spatial Decision Support System for
the Planning of Retail and Service Facilities**

Theo Arentze

nr 56

Integrated Lighting System Assistant

Ellie de Groot

nr 57

Ontwerpend Leren, Leren Ontwerpen

J.T. Boekholt

nr 58

**Temporal Aspects of Theme Park Choice
Behavior**

Astrid Kemperman

nr 59

**Ontwerp van een Geïndustrialiseerde
Funderingswijze**

Faas Moonen

nr 60

**Merlin: A Decision Support System
for Outdoor Leisure Planning**

Manon van Middelkoop

nr 61

The Aura of Modernity

Jos Bosman

nr 62

Urban Form and Activity-Travel Patterns

Daniëlle Snellen

nr 63

Design Research in the Netherlands 2000

Henri Achten

nr 64

**Computer Aided Dimensional Control in
Building Construction**

Rui Wu

nr 65

Beyond Sustainable Building

editors: Peter A. Erkelens
Sander de Jonge
August A.M. van Vliet

co-editor: Ruth J.G. Verhagen

nr 66

Das Globalrecyclingfähige Haus

Hans Löfflad

nr 67

Cool Schools for Hot Suburbs

René J. Dierkx

nr 68

**A Bamboo Building Design Decision
Support Tool**

Fitri Mardjono

nr 69

Driving Rain on Building Envelopes

Fabien van Mook

nr 70

Heating Monumental Churches

Henk Schellen

nr 71

**Van Woningverhuurder naar
Aanbieder van Woongenot**

Patrick Dogge

nr 72

**Moisture Transfer Properties of
Coated Gypsum**

Emile Goossens

nr 73

Plybamboo Wall-Panels for Housing

Guillermo E. González-Beltrán

nr 74

The Future Site-Proceedings

Ger Maas

Frans van Gassel

nr 75

**Radon transport in
Autoclaved Aerated Concrete**

Michel van der Pal

nr 76

**The Reliability and Validity of Interactive
Virtual Reality Computer Experiments**

Amy Tan

nr 77

**Measuring Housing Preferences Using
Virtual Reality and Belief Networks**

Maciej A. Orzechowski

nr 78

**Computational Representations of Words
and Associations in Architectural Design**

Nicole Segers

nr 79

**Measuring and Predicting Adaptation in
Multidimensional Activity-Travel Patterns**

Chang-Hyeon Joh

nr 80

Strategic Briefing

Fayez Al Hassan

nr 81

Well Being in Hospitals

Simona Di Cicco

nr 82

**Solares Bauen:
Implementierungs- und Umsetzungs-
Aspekte in der Hochschulausbildung
in Österreich**

Gerhard Schuster

nr 83

Supporting Strategic Design of Workplace Environments with Case-Based Reasoning

Shauna Mallory-Hill

nr 84

ACCEL: A Tool for Supporting Concept Generation in the Early Design Phase

Maxim Ivashkov

nr 85

Brick-Mortar Interaction in Masonry under Compression

Ad Vermeltfoort

nr 86

Zelfredzaam Wonen

Guus van Vliet

nr 87

Een Ensemble met Grootstedelijke Allure

Jos Bosman

Hans Schippers

nr 88

On the Computation of Well-Structured Graphic Representations in Architectural Design

Henri Achten

nr 89

De Evolutie van een West-Afrikaanse Vernaculaire Architectuur

Wolf Schijns

nr 90

ROMBO Tactiek

Christoph Maria Ravesloot

nr 91

External Coupling between Building Energy Simulation and Computational Fluid Dynamics

Ery Djunaedy

nr 92

Design Research in the Netherlands 2005

editors: Henri Achten

Kees Dorst

Pieter Jan Stappers

Bauke de Vries

nr 93

Ein Modell zur Baulichen Transformation

Jalil H. Saber Zaimian

nr 94

Human Lighting Demands: Healthy Lighting in an Office Environment

Myriam Aries

nr 95

A Spatial Decision Support System for the Provision and Monitoring of Urban Greenspace

Claudia Pelizaro

nr 96

Leren Creëren

Adri Proveniers

nr 97

Simlandscape

Rob de Waard

nr 98

Design Team Communication

Ad den Otter

nr 99

Humaan-Ecologisch Georiënteerde Woningbouw

Juri Czabanowski

nr 100

Hambase

Martin de Wit

nr 101

Sound Transmission through Pipe Systems and into Building Structures

Susanne Bron-van der Jagt

nr 102

Het Bouwkundig Contrapunt

Jan Francis Boelen

nr 103

A Framework for a Multi-Agent Planning Support System

Dick Saarloos

nr 104

Bracing Steel Frames with Calcium Silicate Element Walls

Bright Mweene Ng'andu

nr 105

Naar een Nieuwe Houtskeletbouw

F.N.G. De Medts

nr 106 and 107
Niet gepubliceerd

nr 108
Geborgenheid
T.E.L. van Pinxteren

nr 109
Modelling Strategic Behaviour in Anticipation of Congestion
Qi Han

nr 110
Reflecties op het Woondomein
Fred Sanders

nr 111
On Assessment of Wind Comfort by Sand Erosion
Gábor Dezsö

nr 112
Bench Heating in Monumental Churches
Dionne Limpens-Neilen

nr 113
RE. Architecture
Ana Pereira Roders

nr 114
Toward Applicable Green Architecture
Usama El Fiky

nr 115
Knowledge Representation under Inherent Uncertainty in a Multi-Agent System for Land Use Planning
Liyang Ma

nr 116
Integrated Heat Air and Moisture Modeling and Simulation
Jos van Schijndel

nr 117
Concrete Behaviour in Multiaxial Compression
J.P.W. Bongers

nr 118
The Image of the Urban Landscape
Ana Moya Pellitero

nr 119
The Self-Organizing City in Vietnam
Stephanie Geertman

nr 120
A Multi-Agent Planning Support System for Assessing Externalities of Urban Form Scenarios
Rachel Katoshevski-Cavari

nr 121
Den Schulbau Neu Denken, Fühlen und Wollen
Urs Christian Maurer-Dietrich

nr 122
Peter Eisenman Theories and Practices
Bernhard Kormoss

nr 123
User Simulation of Space Utilisation
Vincent Tabak

nr 125
In Search of a Complex System Model
Oswald Devisch

nr 126
Lighting at Work: Environmental Study of Direct Effects of Lighting Level and Spectrum on Psycho-Physiological Variables
Grazyna Górnicka

nr 127
Flanking Sound Transmission through Lightweight Framed Double Leaf Walls
Stefan Schoenwald

nr 128
Bounded Rationality and Spatio-Temporal Pedestrian Shopping Behavior
Wei Zhu

nr 129
Travel Information: Impact on Activity Travel Pattern
Zhongwei Sun

nr 130
Co-Simulation for Performance Prediction of Innovative Integrated Mechanical Energy Systems in Buildings
Marija Trčka

nr 131
Niet gepubliceerd

nr 132

Architectural Cue Model in Evacuation Simulation for Underground Space Design

Chengyu Sun

nr 133

Uncertainty and Sensitivity Analysis in Building Performance Simulation for Decision Support and Design Optimization

Christina Hopfe

nr 134

Facilitating Distributed Collaboration in the AEC/FM Sector Using Semantic Web Technologies

Jacob Beetz

nr 135

Circumferentially Adhesive Bonded Glass Panes for Bracing Steel Frame in Façades

Edwin Huveners

nr 136

Influence of Temperature on Concrete Beams Strengthened in Flexure with CFRP

Ernst-Lucas Klamer

nr 137

Sturen op Klantwaarde

Jos Smeets

nr 139

Lateral Behavior of Steel Frames with Discretely Connected Precast Concrete Infill Panels

Paul Teewen

nr 140

Integral Design Method in the Context of Sustainable Building Design

Perica Savanović

nr 141

Household Activity-Travel Behavior: Implementation of Within-Household Interactions

Renni Anggraini

nr 142

Design Research in the Netherlands 2010

Henri Achten

nr 143

Modelling Life Trajectories and Transport Mode Choice Using Bayesian Belief Networks

Marloes Verhoeven

nr 144

Assessing Construction Project Performance in Ghana

William Gyadu-Asiedu

nr 145

Empowering Seniors through Domotic Homes

Masi Mohammadi

nr 146

An Integral Design Concept for Ecological Self-Compacting Concrete

Martin Hunger

nr 147

Governing Multi-Actor Decision Processes in Dutch Industrial Area Redevelopment

Erik Blokhuis

nr 148

A Multifunctional Design Approach for Sustainable Concrete

Götz Hüsken

nr 149

Quality Monitoring in Infrastructural Design-Build Projects

Ruben Favié

nr 150

Assessment Matrix for Conservation of Valuable Timber Structures

Michael Abels

nr 151

Co-simulation of Building Energy Simulation and Computational Fluid Dynamics for Whole-Building Heat, Air and Moisture Engineering

Mohammad Mirsadeghi

nr 152

External Coupling of Building Energy Simulation and Building Element Heat, Air and Moisture Simulation

Daniel Cóstola

nr 153

**Adaptive Decision Making In
Multi-Stakeholder Retail Planning**

Ingrid Janssen

nr 154

Landscape Generator

Kymo Slager

nr 155

Constraint Specification in Architecture

Remco Niemeijer

nr 156

**A Need-Based Approach to
Dynamic Activity Generation**

Linda Nijland

nr 157

**Modeling Office Firm Dynamics in an
Agent-Based Micro Simulation Framework**

Gustavo Garcia Manzato

nr 158

**Lightweight Floor System for
Vibration Comfort**

Sander Zegers

nr 159

Aanpasbaarheid van de Draagstructuur

Roel Gijsbers

nr 160

'Village in the City' in Guangzhou, China

Yanliu Lin

nr 161

Climate Risk Assessment in Museums

Marco Martens

nr 162

Social Activity-Travel Patterns

Pauline van den Berg

nr 163

**Sound Concentration Caused by
Curved Surfaces**

Martijn Vercammen

nr 164

**Design of Environmentally Friendly
Calcium Sulfate-Based Building Materials:
Towards an Improved Indoor Air Quality**

Qingliang Yu

nr 165

**Beyond Uniform Thermal Comfort
on the Effects of Non-Uniformity and
Individual Physiology**

Lisje Schellen

nr 166

Sustainable Residential Districts

Gaby Abdalla

nr 167

**Towards a Performance Assessment
Methodology using Computational
Simulation for Air Distribution System
Designs in Operating Rooms**

Mônica do Amaral Melhado

nr 168

**Strategic Decision Modeling in
Brownfield Redevelopment**

Brano Glumac

nr 169

**Pamela: A Parking Analysis Model
for Predicting Effects in Local Areas**

Peter van der Waerden

nr 170

**A Vision Driven Wayfinding Simulation-System
Based on the Architectural Features Perceived
in the Office Environment**

Qunli Chen

nr 171

**Measuring Mental Representations
Underlying Activity-Travel Choices**

Oliver Horeni

nr 172

**Modelling the Effects of Social Networks
on Activity and Travel Behaviour**

Nicole Ronald

nr 173

**Uncertainty Propagation and Sensitivity
Analysis Techniques in Building Performance
Simulation to Support Conceptual Building
and System Design**

Christian Struck

nr 174

**Numerical Modeling of Micro-Scale
Wind-Induced Pollutant Dispersion
in the Built Environment**

Pierre Gousseau

nr 175

**Modeling Recreation Choices
over the Family Lifecycle**

Anna Beatriz Grigolon

nr 176

**Experimental and Numerical Analysis of
Mixing Ventilation at Laminar, Transitional
and Turbulent Slot Reynolds Numbers**

Twan van Hooff

nr 177

**Collaborative Design Support:
Workshops to Stimulate Interaction and
Knowledge Exchange Between Practitioners**

Emile M.C.J. Quanjel

nr 178

Future-Proof Platforms for Aging-in-Place

Michiel Brink

nr 179

**Motivate:
A Context-Aware Mobile Application for
Physical Activity Promotion**

Yuzhong Lin

nr 180

**Experience the City:
Analysis of Space-Time Behaviour and
Spatial Learning**

Anastasia Moiseeva

nr 181

**Unbonded Post-Tensioned Shear Walls of
Calcium Silicate Element Masonry**

Lex van der Meer

nr 182

**Construction and Demolition Waste
Recycling into Innovative Building Materials
for Sustainable Construction in Tanzania**

Mwita M. Sabai

nr 183

**Durability of Concrete
with Emphasis on Chloride Migration**

Przemysław Spiesz

nr 184

**Computational Modeling of Urban
Wind Flow and Natural Ventilation Potential
of Buildings**

Rubina Ramponi

nr 185

**A Distributed Dynamic Simulation
Mechanism for Buildings Automation
and Control Systems**

Azzedine Yahiaoui

nr 186

**Modeling Cognitive Learning of Urban
Networks in Daily Activity-Travel Behavior**

Şehnaz Cenani Durmazoğlu

nr 187

**Functionality and Adaptability of Design
Solutions for Public Apartment Buildings
in Ghana**

Stephen Agyefi-Mensah

nr 188

**A Construction Waste Generation Model
for Developing Countries**

Lilliana Abarca-Guerrero

nr 189

**Synchronizing Networks:
The Modeling of Supernetworks for
Activity-Travel Behavior**

Feixiong Liao

nr 190

**Time and Money Allocation Decisions
in Out-of-Home Leisure Activity Choices**

Gamze Zeynep Dane

nr 191

**How to Measure Added Value of CRE and
Building Design**

Rianne Appel-Meulenbroek

nr 192

**Secondary Materials in Cement-Based
Products:
Treatment, Modeling and Environmental
Interaction**

Miruna Florea

nr 193

**Concepts for the Robustness Improvement
of Self-Compacting Concrete:
Effects of Admixtures and Mixture
Components on the Rheology and Early
Hydration at Varying Temperatures**

Wolfram Schmidt

nr 194

Modelling and Simulation of Virtual Natural Lighting Solutions in Buildings

Rizki A. Mangkuto

nr 195

Nano-Silica Production at Low Temperatures from the Dissolution of Olivine - Synthesis, Tailoring and Modelling

Alberto Lazaro Garcia

nr 196

Building Energy Simulation Based Assessment of Industrial Halls for Design Support

Bruno Lee

nr 197

Computational Performance Prediction of the Potential of Hybrid Adaptable Thermal Storage Concepts for Lightweight Low-Energy Houses

Pieter-Jan Hoes

nr 198

Application of Nano-Silica in Concrete

George Quercia Bianchi

nr 199

Dynamics of Social Networks and Activity Travel Behaviour

Fariya Sharmeen

nr 200

Building Structural Design Generation and Optimisation including Spatial Modification

Juan Manuel Davila Delgado

nr 201

Hydration and Thermal Decomposition of Cement/Calcium-Sulphate Based Materials

Ariën de Korte

nr 202

Republiek van Beelden: De Politieke Werkingen van het Ontwerp in Regionale Planvorming

Bart de Zwart

nr 203

Effects of Energy Price Increases on Individual Activity-Travel Repertoires and Energy Consumption

Dujuan Yang

nr 204

Geometry and Ventilation: Evaluation of the Leeward Sawtooth Roof Potential in the Natural Ventilation of Buildings

Jorge Isaac Perén Montero

nr 205

Computational Modelling of Evaporative Cooling as a Climate Change Adaptation Measure at the Spatial Scale of Buildings and Streets

Hamid Montazeri

nr 206

Local Buckling of Aluminium Beams in Fire Conditions

Ronald van der Meulen

nr 207

Historic Urban Landscapes: Framing the Integration of Urban and Heritage Planning in Multilevel Governance

Loes Veldpaus

nr 208

Sustainable Transformation of the Cities: Urban Design Pragmatics to Achieve a Sustainable City

Ernesto Antonio Zumelzu Scheel

nr 209

Development of Sustainable Protective Ultra-High Performance Fibre Reinforced Concrete (UHPRC):

Design, Assessment and Modeling

Rui Yu

nr 210

Uncertainty in Modeling Activity-Travel Demand in Complex Urban Systems

Soora Rasouli

nr 211

Simulation-based Performance Assessment of Climate Adaptive Greenhouse Shells

Chul-sung Lee

nr 212

Green Cities: Modelling the Spatial Transformation of the Urban Environment using Renewable Energy Technologies

Saleh Mohammadi

nr 213

A Bounded Rationality Model of Short and Long-Term Dynamics of Activity-Travel Behavior

Ifigeneia Psarra

nr 214

Effects of Pricing Strategies on Dynamic Repertoires of Activity-Travel Behaviour

Elaheh Khademi

nr 215

Handstorm Principles for Creative and Collaborative Working

Frans van Gassel

nr 216

Light Conditions in Nursing Homes: Visual Comfort and Visual Functioning of Residents

Marianne M. Sinoo

nr 217

Woonsporen:

De Sociale en Ruimtelijke Biografie van een Stedelijk Bouwblok in de Amsterdamse Transvaalbuurt

Hüseyin Hüsnü Yegenoglu

nr 218

Studies on User Control in Ambient Intelligent Systems

Berent Willem Meerbeek

nr 219

Daily Livings in a Smart Home: Users' Living Preference Modeling of Smart Homes

Erfaneh Allameh

nr 220

Smart Home Design: Spatial Preference Modeling of Smart Homes

Mohammadali Heidari Jozam

nr 221

Wonen:

Discoursen, Praktijken, Perspectieven

Jos Smeets

nr 222

Personal Control over Indoor Climate in Offices: Impact on Comfort, Health and Productivity

Atze Christiaan Boerstra

nr 223

Personalized Route Finding in Multimodal Transportation Networks

Jianwe Zhang

nr 224

The Design of an Adaptive Healing Room for Stroke Patients

Elke Daemen

nr 225

Experimental and Numerical Analysis of Climate Change Induced Risks to Historic Buildings and Collections

Zara Huijbregts

nr 226

Wind Flow Modeling in Urban Areas Through Experimental and Numerical Techniques

Alessio Ricci

nr 227

Clever Climate Control for Culture: Energy Efficient Indoor Climate Control Strategies for Museums Respecting Collection Preservation and Thermal Comfort of Visitors

Rick Kramer

nr 228

nog niet bekend / gepubliceerd

nr 229

nog niet bekend / gepubliceerd

nr 230

Environmental assessment of Building Integrated Photovoltaics: Numerical and Experimental Carrying Capacity Based Approach

Michiel Ritzen

nr 231

Performance of Admixture and Secondary Minerals in Alkali Activated Concrete: Sustaining a Concrete Future

Arno Keulen

nr 232

nog niet bekend / gepubliceerd

nr 233

Stage Acoustics and Sound Exposure in Performance and Rehearsal Spaces for Orchestras:

Methods for Physical Measurements

Remy Wenmaekers

nr 234

Municipal Solid Waste Incineration (MSWI) Bottom Ash:

From Waste to Value Characterization, Treatments and Application

Pei Tang

nr 235

Large Eddy Simulations Applied to Wind Loading and Pollutant Dispersion

Mattia Ricci

nr 236

Alkali Activated Slag-Fly Ash Binders: Design, Modeling and Application

Xu Gao

nr 237

Sodium Carbonate Activated Slag: Reaction Analysis, Microstructural Modification & Engineering Application

Bo Yuan

nr 238

Shopping Behavior in Malls

Widiyani

nr 239

Smart Grid-Building Energy Interactions: Demand Side Power Flexibility in Office Buildings

Kennedy Otieno Aduda

nr 240

Modeling Taxis Dynamic Behavior in Uncertain Urban Environments

Zheng Zhong

nr 241

Gap-Theoretical Analyses of Residential Satisfaction and Intention to Move

Wen Jiang

nr 242

Travel Satisfaction and Subjective Well-Being: A Behavioral Modeling Perspective

Yanan Gao

nr 000

The Title:

Na de Dubbele Punt the Subtitle

Naam Schrijver

nr 000

nog niet bekend / gepubliceerd

nr 231 **MISSCHIEN NOG NIET DE DEF TITEL**

Design and Performance of Plasticizing

Admixture and Secondary Minerals in

Alkali Activated Concrete:

Sustaining a Concrete Future

Arno Keulen

nr 234

titel nog niet bekend / gepubliceerd

Pei Tang

This research demonstrates the applicability of building energy simulation (BES) for the multi-domain analysis of energy use in data centres (DCs) and introduces a new application of a BES tool as a testing environment for external control algorithms. These external control algorithms are part of “holistic” DC operation, which aims to coordinate and optimize the main DC processes at the system-level. Considering the mission critical nature of the DC environment, where any possible downtime of DC services results in serious financial penalties and reputation loss, any real experiments necessary for the platform development are extremely limited.

However, DC energy modelling and dynamic computational experimentation represent a safe virtual testing environment for novel control strategies. Successful tests in such a safe environment can accelerate the process of implementing new operational strategies in physical DCs. The virtual testing environment using BES is a feasible alternative to assess the potential of tested control strategies.

This research is also unique in that the first prototype of the virtual DC environment was subjected to all phases of the proposed testing workflow from development through usability testing to real-world application, where the initial version of the holistic operation was tested. The usability of this virtual DC environment was endorsed by a wider research consortium of industrial and academic partners in the frame of the Genic project funded by the European Commission.

F A C

B W H

E H U

/ Department of the Built Environment

TU/e

Technische Universiteit
Eindhoven
University of Technology